UNIVERSITY OF CALIFORNIA, SAN DIEGO

Targeting Glycosaminoglycans with Small Molecules: Design, Synthesis, and Applications

A dissertation submitted in partial satisfaction of the requirements for the degree Doctor of Philosophy

in

Chemistry

by

Ryan Joseph Weiss

Committee in Charge:

Professor Yitzhak Tor, Chair
Professor Jeffrey Esko
Professor Thomas Hermann
Professor Clifford Kubiak
Professor James Whitesell

2015

The dissertation of Ryan Joseph Weiss is approved, and it is acceptable in quality and form for publication on microfilm and electronically:

Chair

University of California, San Diego

2015

DEDICATION

To my amazing parents, Glenn & Judy, my brother & bandmate for life, Kevin, and my best friend & love of my life, Kristina.

“I can do all things through Christ who strengthens me.”

Philippians 4:13

TABLE OF CONTENTS

LIST OF FIGURES

LIST OF SCHEMES

LIST OF TABLES

LIST OF SPECTRA

ACKNOWLEDGEMENTS

I would like to acknowledge Professor Yitzhak Tor for his invaluable mentorship, patience, and support over the years towards my development as a scientist and critical thinker. He has always been available to answer scientific questions and discuss my research while also giving me the freedom to explore new research interests and learn new techniques.

I also want to thank the many members of the Tor lab for being so helpful and supportive throughout my graduate career. I thank Drs. Renatus Sinkeldam, Ezequiel Wexselblatt, and Andrea Fin for many intellectual discussions and for guidance while learning new techniques. I would also like to thank Carolyn White for her exceptional effort in helping me complete the photophysical studies.

I would like to thank Professor Jeffrey Esko for being an excellent mentor and for letting me work in his lab. His insight, advice, and collaboration were essential to my success with these projects. I am also very appreciative to the Esko lab for making me feel so welcome and answering all my biological questions. I would like to especially thank Dr. Philip Gordts for his help in completing the *in vivo* mice studies and for always encouraging me in my scientific endeavors. I also thank Patrick Secrest for his help with the mice injections, Dr. Chrissa Dwyer for helping me with the microscopy studies, and Drs. Manuela Schuksz and Beth Wilson for their help with the cell binding assays. I also acknowledge Dr. Ding Xu for providing the soluble RAGE protein for the binding experiments.

I am very grateful to Qiongyu Chen and Dr. Dzung Le (UCSD Murine Hematology, Chemistry and Coagulation Core) for their help with the coagulation assays and for contributing their time, resources, and lab space so I could learn new techniques and complete the heparin reversal and detection projects.

I am grateful to Dr. Yongxuan Su (UCSD MS Facility) for the mass spectrometry measurements, and Drs. Curtis Moore and Arnold Rhinegold (UCSD Chemistry and Biochemistry X-ray Facility) for their help in obtaining crystal structures. I also thank Dr. Anthony Mrse for his availability and assistance with the NMR instruments (UCSD NMR Facility) and for our great musical discussions.

Chapter 1 is in full currently being prepared for submission: Weiss, R. J.; Esko, J. D.; Tor, Y. Targeting Glycosaminoglycans with Small Molecules. The dissertation author is the main author of this work.

Chapter 2 is a full reprint from: Weiss, R. J.; Gordts, P. L.; Le, D.; Esko, J. D.; Tor, Y. Small Molecule Antagonists of Cell-Surface Heparan Sulfate and Heparin–Protein Interactions. *Chemical Science*, in revision. The dissertation author is the main author and researcher of this work.

Chapter 3 is in full currently being prepared for submission: Weiss, R. J.; White, C. M.; Esko, J. D.; Tor, Y. Surfen as a Turn-on Fluorescent Probe for Detecting Heparin in Plasma. The dissertation author is the main author and researcher of this work.

VITA

2006–2008	Teaching Assistant, Point Loma Nazarene University
2008	B.S. in Chemistry, Point Loma Nazarene University, San Diego
2008–2014	Teaching Assistant, University of California, San Diego
2010	M.S. in Chemistry, University of California, San Diego
2015	Ph.D. in Chemistry, University of California, San Diego

PUBLICATIONS

Weiss, R. J.; Gordts, P. L.; Le, D.; Esko, J. D.; Tor, Y. Small Molecule Antagonists of Cell Surface Heparan Sulfate and Heparin–Protein Interactions. *Chemical Science (in revision).*

Weiss, R. J.; White, C. M.; Esko, J. D.; Tor, Y. Surfen as a Turn-on Fluorescent Probe for Detection of Heparin in Plasma. *In Preparation*.

Weiss, R. J.; Esko, J. D.; Tor, Y. Targeting Glycosaminoglycans with Small Molecules. *In Preparation*.

Shellhamer, D. F.; Davenport, K. J.; Jones, R. N.; Thorpe, J. J.; Weiss, R. J.; Heasley, V. L. Reactions of halogens and interhalogens with 1,1,2-trifluorobut-1-en-4-ol and 3-buten-1-ol; a study on the rearrangement of trifluorosubstituted 3-membered halonium ions. *Trends in Organic Chemistry*, **2010**, *14*, 73-77.

Shellhamer, D. F.; Davenport, K. J.; Forberg, H. K.; Herrick, M. P.; Jones, R. N.; Rodriguez, S. J.; Sanabria, S.; Trager, N. N.; Weiss, R. J.; Heasley, V. L; Boatz, J. A. Rearrangement of 3-Membered 1,1,2-Trifluorobromonium and Iodonium Ions and Comparison of Trifluorochloronium to Fluorocarbenium Ions. *Journal of Organic Chemistry*. **2008**, *73*, 4532-4538.

ABSTRACT OF THE DISSERTATION

Targeting Glycosaminoglycans with Small Molecules: Design, Synthesis, and Applications

by

Ryan Joseph Weiss

Doctor of Philosophy in Chemistry

University of California, San Diego, 2015

Professor Yitzhak Tor, Chair

Glycosaminoglycans (GAGs) are a family of long anionic polysaccharides that are found on the surface of all cells and in the extracellular matrix. These complex cell surface carbohydrates are known to regulate important biological processes and have been implicated in certain pathophysiological states. Thus, interest exists in agents controlling GAG–protein interactions as both therapeutics and glycobiology tools. The accessibility and versatility of small

molecules that can antagonize GAG–protein interactions make them particularly attractive as drug candidates. This motivated the work shown here, which addressed the design and preparation of small molecules for targeting and detecting GAGs.

Surfen, *bis*-2-methyl-4-amino-quinolyl-6-carbamide, was previously reported as a small molecule antagonist of heparan sulfate (HS), a key cell surface GAG. To generate structure-activity relationships, a series of rationally designed surfen analogs was synthesized, where its dimeric structure, exocyclic amines, and urea linker region were modified to probe the role of each moiety in recognizing HS. An *in vitro* assay monitoring inhibition of fibroblast growth factor 2 binding to wild-type CHO cells was utilized to quantify interactions with cell surface HS. The dimeric molecular structure of surfen and its aminoquinoline ring systems were essential for its interaction with HS, and certain dimeric analogs displayed higher inhibitory potency than surfen. These molecules were also able to antagonize other HS–protein interactions including the binding of soluble RAGE to HS. Importantly, selected analogs were shown to neutralize heparin and other heparinoids, including the synthetic pentasaccharide fondaparinux, for which no antidote exists, both *in vitro* and *in vivo* in mice. Additional studies were also performed to highlight other potential applications for surfen and its analogs.

Heparin, the most highly sulfated GAG, is used as an anticoagulant in surgery and for the treatment of certain thrombotic diseases. Adverse side effects can occur with heparin administration; therefore, it is necessary to closely monitor heparin plasma levels in patients. Here, we utilize surfen as a selective

turn-on fluorescent probe for the detection of heparin in human plasma samples. A detailed photophysical analysis helped to further elucidate this molecule's unique interaction with heparin and the nature of its turn-on fluorescence features. Surfen demonstrates aggregation-induced emission upon forming a supramolecular complex with heparin in solution and exhibits photophysical sensitivity to its microenvironment.

Chapter 1:

Introduction

1.1 Glycosaminoglycans: Structure and Function in Physiology

The glycocalyx is an intricate network of negatively charged carbohydrates, glycoproteins, and glycolipids found on the external surface of all cells. This dynamic canopy of carbohydrate-rich biomolecules protects the cell surface and facilitates the interactions with a variety of ligands and enzymes that are essential for signalling and development.[1] Due to their key roles in normal cell function and involvement in certain pathophysiological conditions, extensive research has been aimed at studying and targeting these membrane-bound macromolecules.[2-4] A major component of the glycocalyx are glycosaminoglycans (GAGs), which are a family of long linear polysaccharides that provide a diverse array of biological functions in nature. The heterogeneous carbohydrate chains contain repeating sugar units that consist of amino sugars (*N*-acetylglucosamine or *N*-acetylgalactosamine) and uronic sugars (glucuronic or iduronic acid). In most cases, these macromolecules can be heterogeneously sulfated at specific sites to give an overall high negative charge. Due to the diverse structures, charge, and functions of different GAGs, they play key roles in homeostasis, metabolism, cell proliferation, signaling, motility, development, and angiogenesis through their interactions with proteins and growth factors.[5]

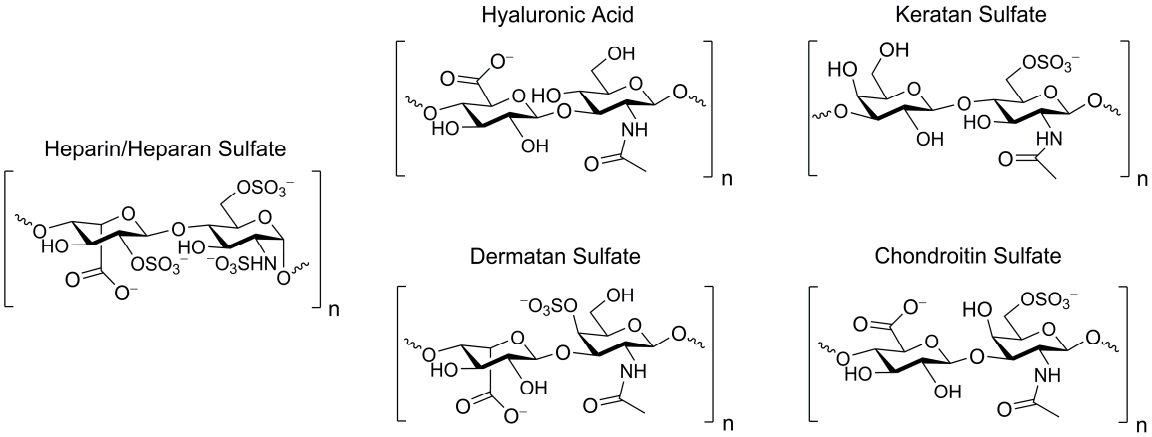

Figure 1.1: Common repeating disaccharide regions of glycosaminoglycans.

Several different families of GAGs exist, and they are separated into four main groups dependent on their sulfation pattern and sugar content: heparin/heparan sulfate, chondroitin sulfate/dermatan sulfate, keratan sulfate, and hyaluronic acid (**Figure 1.1**). These polysaccharides can be found on the cell surface covalently attached to a core protein (known collectively as a proteoglycan), or they can exist freely in the extracellular matrix. Three main families of core proteins, each with their specific function and structure, have been characterized including membrane-bound syndecans,[6] glypicans,[7] and basement membrane proteins called perlecan[8] and agrin.[9] GAG chains are constructed while attached to their core protein. The heterogeneity of GAG polysaccharides can mainly be attributed to their biosynthesis in the cell through specific enzymes. Proteoglycans are assembled by glucosyl transferases in the Golgi apparatus of the cell and can be processed further by endosulphatases, which can remove sulfate groups from specific sugar residues.[10] Hyaluronic acid (HA), a nonsulfated GAG, can be found in the extracellular matrix of neuronal

and connective tissues and exists unattached to a proteoglycan core. HA is an important component of skin and cartilage, and can also be found as a lubricant in the synovial fluid between joints.[11] Sulfated chondroitin/dermatan sulfate proteoglycans are structural components of cartilage and skin involved in wound repair.[12] Keratan sulfate (KS) proteoglycans function in central nervous system injury repair and are specifically found in the cornea, cartilage, and bone.[13]

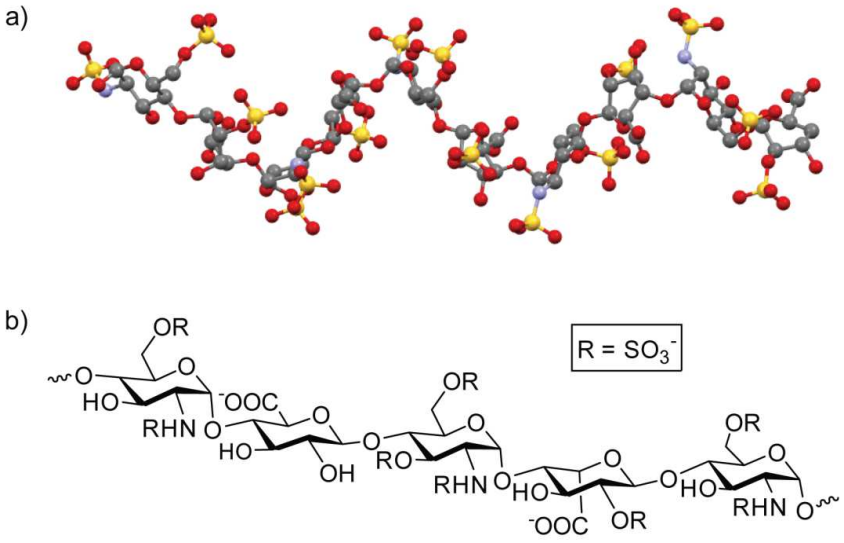

Figure 1.2: a) Heparin X-ray crystal structure (dodecasaccharide, helical form; adapted from PDB: 1E0O) and b) pentasaccharide antithrombin (AT) binding sequence.

Heparin is the most sulfated, heterogeneous GAG with the highest negative charge density of any known biomolecule. Heparin and heparan sulfate (HS) are linear polysaccharides consisting of repeating glucosamine and uronic acid disaccharide units that are heterogeneously *N*- and *O*-sulfated in specific regions. Heparin's structure resembles a more highly sulfated form of the anionic GAG chains of HS proteoglycans (~2.3 sulfate groups per disaccharide

compared to ~0.8 for HS). Heparin was found to exist primarily as a helical structure with L-iduronic acid sugar residues providing it flexibility (**Figure 1.2**).[14] While HS is ubiquitously expressed in all animal cells, heparin is produced and stored in the secretory granules of mast cells in connective tissue. This highly anionic polysaccharide was discovered in 1916 and proved to be a potent blood anticoagulant.[15,16] Later studies found that heparin's anticoagulant activity was based on its interaction with the endogenous serine protease inhibitor antithrombin III (AT), the main inhibitor in the coagulation cascade.[17] Heparin binds to this protease and facilitates a conformational change that accelerates AT's inhibition of coagulation factors such as factor Xa and thrombin (**Figure 1.3**).[18] It was discovered that heparin's interaction with AT was dependent on a distinct pentasaccharide sequence rather than overall molecular charge.[19] Since its discovery, exogenous heparin has been a very important anticoagulant agent in surgery and is used in treatment for certain thrombotic diseases such as venous thromboembolism.[20,21]

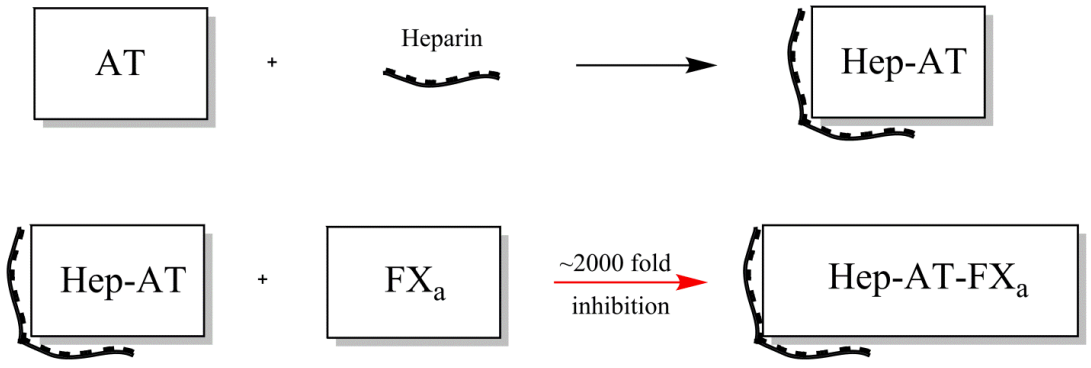

Figure 1.3: Heparin binds to antithrombin (AT) and inhibits FXa in the coagulation cascade.

1.2 Heparan Sulfate: Structure and Biosynthesis

Here, we will mainly be focusing on heparan sulfate (HS), which are highly sulfated GAGs that have been studied extensively over the years for their key roles in animal physiology and pathology. Heparan sulfate proteoglycans (HSPG's) are expressed on virtually all animal cell membranes and in the extracellular matrix. They consist of a core protein with branching HS polysaccharide chains. HS itself is a linear polysaccharide consisting of repeating glucosamine and uronic acid disaccharide units that are heterogeneously *N*- and *O*-sulfated (**Figure 1.4**).[22]

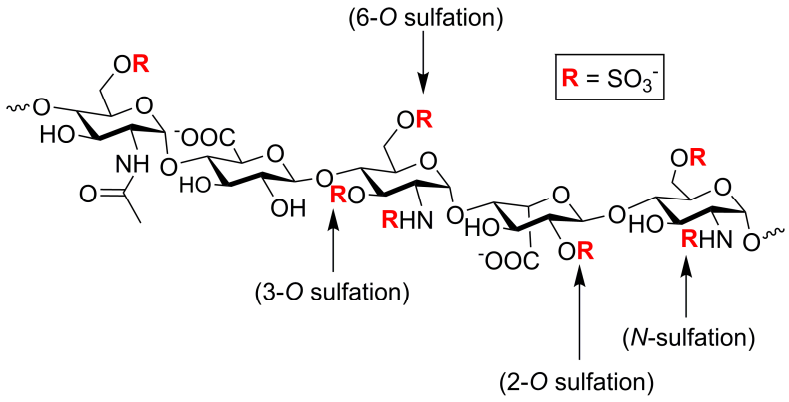

Figure 1.4: Heparan sulfate pentasaccharide subunit. Different sulfation sites are shown in red.

These complex cell surface carbohydrates are known to regulate important biological processes including cell proliferation, motility, development, and angiogenesis through their interaction with proteins and growth factors.[5,23,24] HS polysaccharide chains are assembled and attached to their core proteins in the Golgi apparatus by an array of specific enzymes. A trisaccharide residue, consisting of one xylose (Xyl) and two galactose (Gal) sugars, links the HS chain

to a serine residue on the core protein (**Figure 1.5**). Xylosyltransferases (XYLT1, XYLT2) initiate the attachment of Xyl to the core protein followed by the addition of two galactose sugars by galactosyltransferases 1 and 2 (GALT1, GALT2). Next, glucuronyltransferase 1 (GLCAT1) attaches a glucuronic acid (GlcA) residue to the galactose sugars, and exostosin-like glycosyltransferase 3 (EXTL3) inserts the first N-acetyl glucosamine (GlcNAc) sugar. The rest of the chain is elongated with GlcA and GlcNAc residues by exostosin glycosyltransferases (EXT1-2).[25,26] The synthesized HS polysaccharides are then processed further by sulfotransferases (*N*- or *O*- sulfation at specific sugar sites), N-deacetylases (NDST1-4), and a C5 epimerase (HSGLCE) which converts D-glucuronic to L-iduronic acid. Once assembled, these highly anionic HSPG's are expressed on the cell surface where they can interact with a plethora of proteins and are key contributors to cell-to-cell crosstalk.[22,26]

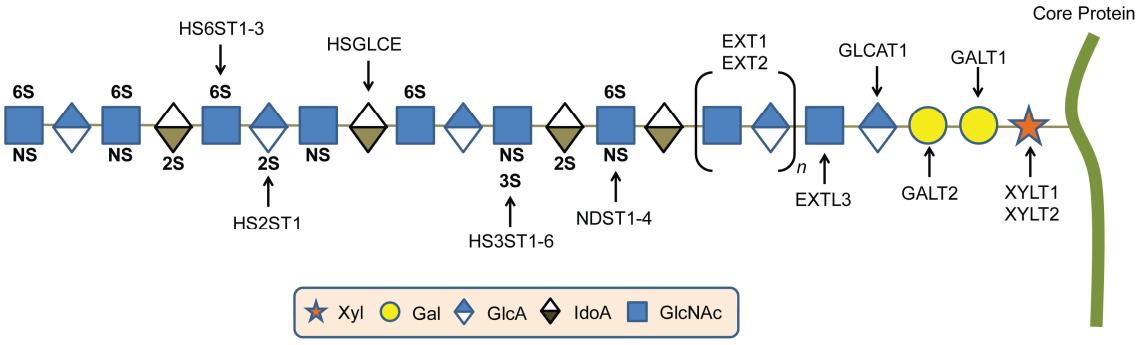

Figure 1.5: Heparan sulfate structure and biosynthesis. Respective *O*- and *N*-sulfotransferases (HS2ST, HS3ST, HS6ST, and NDST) sulfate specific sites along the HS chain (shown in bold).

1.3 Heparan Sulfate–Protein Interactions

The arrangement and orientation of the anionic sugar residues of HS specify the location of distinct ligand-binding sites on the cell surface. The HS-binding protein family includes growth factors, cytokines, chemokines, enzymes, enzyme inhibitors, and extracellular matrix proteins (e.g. fibronectin and collagen).[27] These HS-protein interactions are vital for the homeostasis of the cell and the functioning of many cellular processes. HS can bind certain chemokines (e.g. platelet factor-4 and interleukin-8) involved in cell migration and wound repair and promote their interactions with G-protein-coupled receptors at the cell surface.[28] Moreover, studies have shown that interactions with membrane-bound HS are essential for the activity of certain enzymes such as lipoprotein lipase (LPL). LPL attaches to the luminal surface of endothelial cells via HS where it hydrolyzes triglycerides into lipoproteins.[29] HS has also been found to act as a co-receptor for the binding of certain growth factors, such as fibroblast growth factor 2 (FGF2) and vascular endothelial growth factor (VEGF), to their native receptors.[30,31] In a well-studied example of HS as a co-receptor, FGF2, a potent mitogen and member of the heparin-binding growth factor family, has been shown to preferentially bind to the 2-O sulfated sites of cell surface and extracellular matrix HS.[32,33] The interaction of FGF2 and HS is reported to be necessary for the interaction of the growth factor with its tyrosine kinase receptor. A ternary complex is formed upon growth factor binding to HS with the FGF2 receptor (**Figure 1.6**). The FGF receptor is dimerized which, in turn, activates the

tyrosine kinase domain and initiates signal transduction. Additional 6-O sulfated sites of HS are essential for its interaction with FGF2 and the FGF receptor and to trigger a biological response in the cell. HSPG's help localize FGF2 at the cell surface and promote their cell signaling.[26,34,35] FGF signaling is an essential part of human biology and acts as a regulator of embryonic development, homeostasis, and multiple regenerative processes. However, FGF2's interaction with HS has also been implicated in certain pathophysiological conditions due to this growth factor's up-regulation in certain cancers such as prostate cancer and its action in angiogenesis during tumor growth.[36,37]

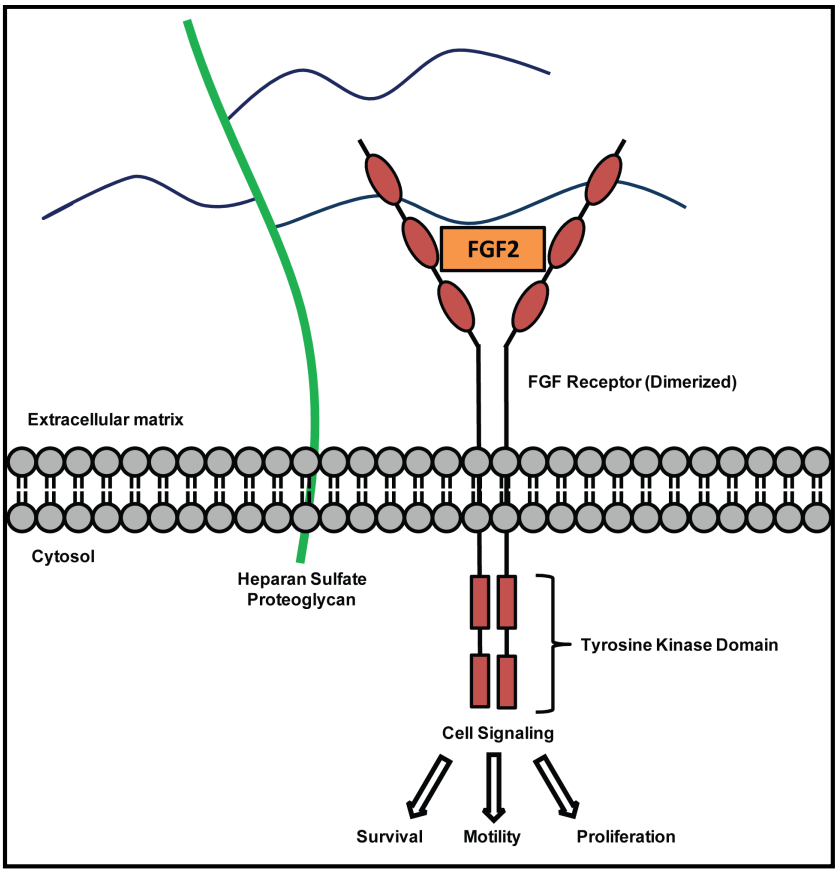

Figure 1.6: FGF2 binds to HS and forms a ternary complex with its receptor.

In another example of HS as a co-receptor, signaling for a transmembrane protein expressed at sites of vascular inflammation, the receptor for advanced glycation end products (RAGE), was recently shown to be dependent on the oligomerization of the protein through the formation of stable RAGE-HS complexes.[38] This protein has been implicated in many diseases including diabetes, cancer, and Alzheimer's disease.[39,40] In addition, HS proteoglycans can act in cell adhesion as a co-receptor with integrin, a transmembrane glycoprotein, to bind fibronectin and regulate cytoskeletal dynamics.[41,42] Overall, there are over one hundred HS-binding proteins, each with their own specificity, function, and preferred binding region. HS has been found to interact with growth factors, chemokines, cytokines, integral membrane receptors, signaling proteins, and extracellular matrix proteins. Their binding to HS can result in immobilization of proteins at their sites of production or in the extracellular matrix for future use. Moreover, HS-protein binding can effect enzyme activity and protect proteins from degradation.[26] There has been a considerable amount of research investigating the nature of HS-protein interactions.[43-56] While many of these interactions involve electrostatic complementarities of charge, some macromolecules were found to bind specific sequences of the GAG chains. These proteins, such as growth factors and their receptors, preferentially bind and recognize spatial arrangements of the sulfated sugar subunits of HS rather than specific sequences.[26]

As mentioned above, one of the first and most studied examples of GAG–protein binding is heparin's interaction with antithrombin III (AT). This highly

sulfated GAG binds to this serine protease inhibitor and facilitates a conformational change that accelerates AT's inhibition of specific coagulation factors. AT was found to bind a specific pentasaccharide sequence of heparin containing rare 3-*O* sulfated sugar residues.[57,58] This interaction is important due to heparin's extensive use as an anticoagulant agent in surgery, as an inner coating of tubes for renal dialysis, and treatment for certain thrombotic events such as pulmonary embolism, deep-vein thrombosis, and atrial fibrillation.[59]

1.4 Heparan Sulfate as a Drug Target

1.4.1 The Pathophysiology of Heparan Sulfate

Despite being an integral component of homeostasis and normal cell physiology, HSPGs have also been implicated in infection and disease. The proliferation mechanisms of certain diseases (e.g., cancer and Alzheimer's disease) involve certain cell-to-cell and cell-to-antigen interactions with HS.[60-64] Some of these HS–protein interactions can cause pathophysiological conditions including inflammation, tumor growth and metastasis, and facilitate viral infection.[65,66] HS is therefore a viable drug target.

HSPGs have been found to play a major role in the initial transformation from normal cells to tumor cells (also called tumorigenesis). Moreover, these anionic GAGs have been implicated in tumor progression and metastasis of cancer.[67] HS polysaccharide chains are found on the cell surface of tumor cells and can be released into the extracellular matrix where they are able to modulate tumor growth kinetics and metastatic potential through interactions with growth

factors (e.g. FGF2, VEGF) and certain cell adhesion proteins (e.g. integrins, P-selectin). Furthermore, HS-protein interactions are exploited by tumor cells to aid in coagulation, motility, angiogenesis, and proliferation.[68] Interestingly, cancer cells can dynamically regulate the structure and sequence of cell-surface or freely-soluble HS in order to differentially regulate key signaling processes in cancer.[69]

Many pathogens, including viruses and bacteria, are able to express HS-binding proteins that help facilitate their attachment to host cells, mediate cell entry, and increase infectivity. In most cases, HSPGs on the plasma membrane act as initial, low affinity co-receptors that concentrate the pathogen on the cell surface and promote binding to secondary receptors which promote internalization.[26,70] Many gram negative and gram positive bacteria are able to utilize HSPGs for host cell adhesion and internalization. *Neisseria gonorrhoeae*, a gram negative bacterium responsible for the sexually-transmitted disease Gonorrhea, was found to express a protein called Opa that can bind to HSPG receptors and promote uptake of the pathogen into cells.[71,72] Similarly, *Chlamydia pneumonia* was found to adhere to the cell surface and gain entry to host cells through a HS-dependent pathway.[73] Furthermore, multiple gram positive bacteria have been shown to enter host cells through adherence to cell-surface HSPGs. *Staphylococcus aureus* bacteria display proteins known as adhesins that mediate attachment to cell-surface HSPGs which, in turn, promotes infection.[74] Moreover, *Mycobacterium tuberculosis*, the gram-positive bacterium that causes tuberculosis, infects endothelial cells by expressing a

cationic protein called heparin-binding hemagglutinin adhesin that can interact with HSPGs on the cell surface.[75]

In another example of HS's role in pathogenesis, many viruses have been shown to attach and internalize into host cells through HS-dependent pathways. Herpes simplex virus (HSV) serotypes 1 and 2 display lysine-rich glycoproteins gB and gC that bind to HS on the cell surface which allows initial attachment to host endothelial cells. After this initial attachment, another glycoprotein known as gD interacts with other cell-surface receptors to mediate viral fusion.[76-78] Interestingly, rare 3-*O*-sulfated sites of specific HS subunits have also been proposed as receptors for gD-binding to mediate viral fusion and entry into target cells.[79] Furthermore, viral attachment of human immunodeficiency virus (HIV), the precursor to acquired immune deficiency syndrome (AIDS), is dependent on cell-surface HSPGs as co-receptors through their interaction with the viral envelope protein gp120.[80,81] HSPGs play an essential role, along with CD4 and chemokine receptors CXCR4 and CCR5, in HIV attachment and fusion. In order to further show the importance of HS in HIV infection, certain studies have shown that enzymatic cleavage of cell-surface HS, de-sulfation of GAGs on the cell surface, or the use of exogenous sulfated sugars such as dextran sulfate inhibit viral infection.[82] HIV's interaction with HSPGs is crucial for infection in many different cell types including T lymphocytes,[83] macrophages,[84] endothelial cells,[85] and dendritic cells.[86] Additionally, other viruses including dengue virus[87,88] and human papillomavirus (HPV)[89,90] utilize HSPGs as co-receptors in virion attachment and fusion at the cell surface.

While HSPGs have shown to play key roles in pathogen infection and the progression of devastating diseases such as cancer and HIV, these anionic macromolecules, which are ubiquitously expressed on all animal cells, have also been implicated in certain neurodegenerative disorders including prion disease (e.g. mad cow disease),[91-93] Parkinson's,[94,95] and Alzheimer's disease.[60] Here, we will focus on the latter. Alzheimer's disease (AD) is a chronic progressive neurological disease that causes cognitive and functional impairment through loss of neurons and synapses in the cerebral cortex of the brain. It is the most common form of dementia and affects over 5 million people in the US per year.[96,97] The disease is characterized by the formation of cerebral plaques consisting of aggregated β-amyloid (Aβ) peptides and neurofibrillary tangles (NFTs) containing tau proteins. Aβ peptides form from sequential proteolytic cleavage of the amyloid precursor protein (APP) by specific enzymes known as β- and γ-secretases.[98] HSPGs have been implicated in the pathogenesis of AD due to their high localization in the senile plaques and NFTs formed during the progression of the disease.[99,100] Although the relationship between amyloid deposition and cognitive deficit is still unclear, several studies have demonstrated that the interaction of Aβ and APP with HS is associated with the promotion and persistence of senile plaques.[101-103] It has been hypothesized that the binding of Aβ to HS could protect these peptides, promote aggregation, and prevent their degradation, hence leading to accumulation in the brain.[60,104] Other studies have shown that HS mediates Aβ internalization and cytotoxicity[105] and can induce the microtubule-association of the tau protein into NFTs in nerve cells.[106] Although

further research is necessary to elucidate the exact role of HS in the pathogenesis of AD, these anionic polysaccharides seem to be key contributors to the progression of this neurodegenerative disease.

1.4.2 Targeting Heparan Sulfate – A Therapeutic Approach

Due to the role of HS in the pathogenesis of certain diseases, multiple agents for antagonizing HS-protein interactions have been developed. Currently, the only GAG interaction exploited in routine clinical settings is the use of heparin as an anticoagulant in surgery and for treatment of certain clotting disorders.[59] Several different strategies have been explored to target HS-protein interactions including the inhibition of HS biosynthesis. Although inhibition of HS biosynthesis has the potential for many negative results considering the importance of HS in homeostasis, several groups have explored this field as a method to treat certain diseases. Classically, sodium chlorate (**1**) has been used as a modulator of HS biosynthesis through inhibition of PAPS (3'-phosphoadenosine-5'-phosphosulfate), the universal sulfonate donor and coenzyme to sulfotransferases. Sodium chlorate competitively binds to the active site of the corresponding PAPS synthase to prevent production of PAPS, which inhibits HS sulfation.[107-109] Studies have shown sodium chlorate to be effective in inhibiting certain bacterial[110,111] and viral[89,112] infections through the inhibition of GAG biosynthesis. However, due to its strong oxidative properties and ability to block other important processes in the cell, this treatment is too toxic for *in vivo* settings.[113] Another chemical approach for inhibiting HS biosynthesis utilizes the

fungal isoprenoid metabolite brefeldin A (BFA) (**2**). BFA affects HSPG synthesis through the inhibition of secretory vesicle transport by the Golgi apparatus.[114] Nevertheless, the promiscuous activity of BFA within the cell causes inhibition of other important glycoconjugates rendering it impractical for clinical application.[115]

The biosynthesis of GAG chains is initiated by xylosylation of a specific serine residue of the core protein (e.g. proteoglycan). Prior to attachment of repeating disaccharide units, one glucuronic acid and two galactose residues are assembled by specific enzymes to form a tetrasaccharide linker to the core protein.[116] A variety of β-D-xyloside analogs (**3**–**5**) have been synthesized as competitive inhibitors for the transfer of xylose to the core protein by xylotransferases (**Figure 1.7**).[117-121] However, as with sodium chlorate and other general GAG biosynthesis inhibitors, xyloside analogs are not practical for *in vivo* use due to toxicity concerns but are useful biological tools for studying GAG biosynthetic pathways.

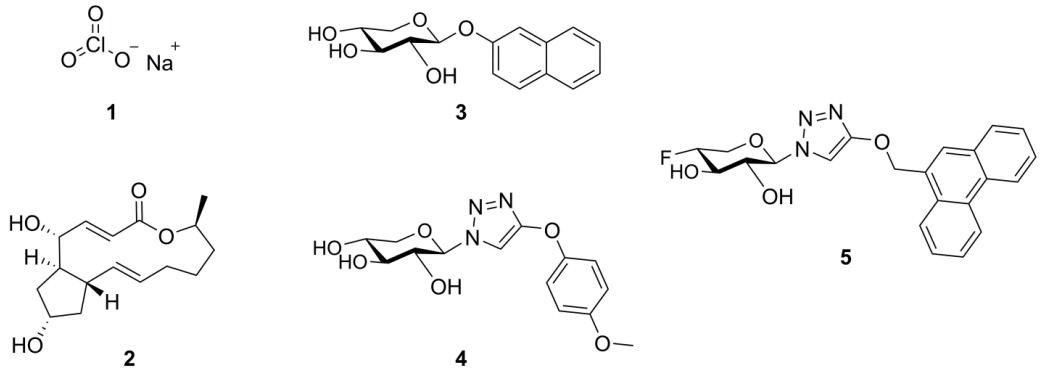

Figure 1.7: Examples of GAG biosynthesis inhibitors.

Enzymes such as bacterial heparinases and endosulfatases have also been explored as potential therapeutics for the treatment of disorders involving HS-protein interactions. Heparinases I (Hep I) and III (Hep III) from *Flavobacterium heparinum* specifically cleave the highly sulfated (Hep I) and undersulfated (Hep III) regions of the HS polysaccharide backbone (Hep II cleaves both regions),[122-124] while plasma membrane-bound endosulfatases remove sulfate residues from GAG chains (**Figure 1.8**).[10,125,126] These enzymes serve as important tools for biologists probing the role of HS in homeostasis and disease, but some groups have also looked at their effect on preventing infection and other processes dependent on interacting with cell-surface HS. Studies have shown that treatment of cells with heparinases inhibits the attachment or entry of several HS-binding pathogens including viruses,[86,89,127-130] bacteria,[131-133] and parasites.[134] Heparinase treatment has also been linked to the management of tumor growth/metastasis[69,135,136] and amyloid-related diseases.[137-139] Endosulfatases are important enzymes that edit the sulfated sites of HS by removing the 6-*O*-sulfate groups.[140] These biomolecules have been shown to limit *Chlamydia muridarum* bacterial infection.[141] Moreover, sulfatase 1 (Sulf1), a HS 6-*O*-endosulfatase, could possibly be used in cancer treatment as a regulator of the capacity of HSPGs to bind to certain proteins up regulated in tumors such as FGF2[142] and hepatocyte growth factor.[143] Additional research is necessary to fully probe the feasibility of utilizing HS-modifying enzymes as therapeutics for the treatment of diseases involving HSPGs.

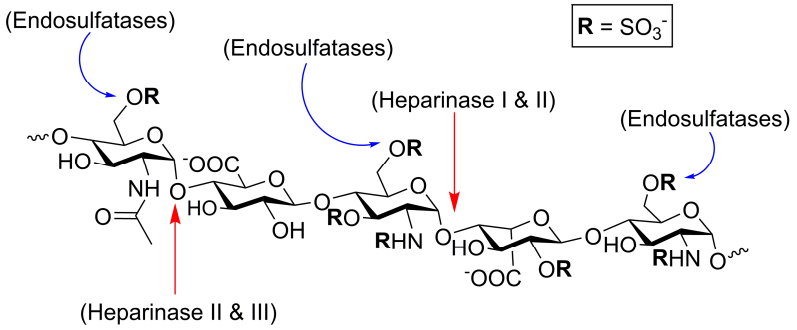

Figure 1.8: Heparinase (I-III) and endosulfatase (Sulf1, Sulf2) activity on a pentasaccharide region of heparin/HS.

Another method being explored for inhibiting HS-protein interactions is the use of exogenous heparin/HS or synthetic GAG mimetic compounds. Soluble heparin and HS have shown to inhibit infection of host cells by HS-binding pathogens including HSV,[144,145] HPV,[89] hepatitis B,[127,146] and different types of bacteria.[147-149] However, there are major drawbacks with using heparin in this way due to its potency as an anticoagulant and potential to cause certain blood disorders, such as thrombocytopenia.[150] The use of soluble HS to inhibit infection also has the potential for negative side effects due to its ability to bind to proteins and affect other off-target biosynthetic pathways. Therefore, many research groups have investigated the synthesis of GAG mimetic compounds to neutralize certain HS-pathogen interactions (**Figure 1.9**). These polyanionic molecules can be synthesized by digestion of heparin polysaccharides or through chemical and enzymatic modifications. In one example, a group engineered a nonsulfated K5 polysaccharide from *E. coli* for inhibition of viral infection by a set of sexually transmitted diseases.[151] Another study exploited the essential binding of HSV to 3-*O*-sulfated regions of HS by synthesizing a 3-*O*-sulfated octasaccharide that

inhibited viral infection in cells.[152] More recently, chemically modified heparin derivatives were shown to inhibit influenza H5N1 viral attachment. Selective desulfation of heparin minimized its anticoagulant effect while maintaining inhibitory activity.[153] Other groups have created depolymerized GAGs for the treatment of malaria[154] and utilized GAG mimetics 3-amino-1-propanesulfonic acid (**6**)[155] and eprodisate disodium (**7**)[156] as anti-amyloid agents for the treatment of Alzheimer's disease and amyloidosis. HS-imitative sulfated polysaccharides isolated from seaweed known as carrageenans (**8**) have also shown the ability to inhibit dengue virus[157] and HSV infection.[158] Furthermore, certain low molecular weight heparin mimetics, such as rhamnan sulfate[159] and PI-88 (**9**),[160,161] have also shown potent antiviral activity. Other GAG mimetics investigated as antagonists of HS-pathogen interactions include polysulfonated compounds such as suramin (**10**),[162] poly(sodium-4-styrene sulfonate) (**11**),[163,164] and sulfonate polymers.[165-167] Generally, GAG mimetic compounds have shown promise as therapeutics; yet, *in vitro* results have not always translated to *in vivo* success. Several of these compounds, such as PI-88, are currently under investigation in clinical trials but have shown toxic side effects related to dosing.[168]

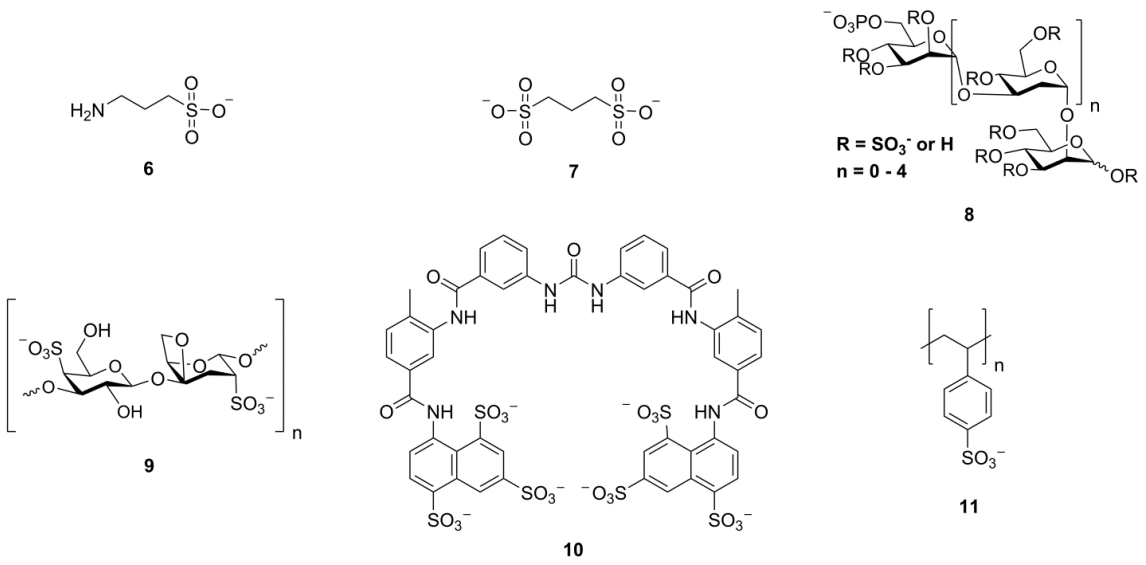

Figure 1.9: Examples of GAG mimetic compounds.

Other types of agents used as antagonists of HS-protein interactions are cationic proteins, foldamers, and small molecules. These molecules rely on electrostatic interactions between their positively-charged functional groups and the highly anionic sulfate and carboxylate moieties of heparin and HS. Lactoferrin, a heparin- and iron-binding protein found in the secretory granules of neutrophils, has been shown to neutralize heparin and antagonize certain HS-protein interactions through interactions with multiple cationic domains on its N-terminus.[169-171] This protein has proven to be an effective antimicrobial agent[172] and inhibitor of HSV,[173,174] hepatitis C (HCV),[175] HIV, and human cytomegalovirus (HCMV) infection.[176] However, clinical trials observing the treatment of HCV with a combination of lactoferrin and interferon[177] or interferon alpha-2b and ribavirin[178] showed no added benefits compared to treatments without lactoferrin. Other proteins have been developed as potent inhibitors of

heparin and its derivatives, including recombinant antithrombin (AT) variants designed to bind heparin and block its interaction with endogenous AT in the bloodstream.[179,180] These inactive chemically-modified proteins have shown promise *in vitro* and *in vivo* in mice, but they are too expensive to produce in large quantities for practical use in the clinic.

Multiple other cationic macromolecules have proven to be potent antagonists of GAG-protein interactions. Positively-charged arginine-rich proteins isolated from the sperm of salmon and other fish, known as protamine, have been used in the clinic to reverse the anticoagulant activity of heparin for years, despite undesired side effects and allergies observed in some patients.[181] Protamine binds irreversibly to heparin and blocks its interaction with antithrombin in the coagulation cascade. Protamine was also shown to inhibit hepatitis B viral infection through blocking viral interaction with cell-surface HSPGs.[146] Protamine, through its interaction with HS, also inhibits host cell infection of *Pseudomonas aeruginosa* by preventing bacterial-enhanced HSPG shedding.[182] Low molecular weight protamine (LMWP) has also been explored as a nontoxic alternative to protamine *in vitro*[183] and *in vivo* in dogs.[184,185] This arginine-rich protamine variant (VSRRRRRRGGRRRR), although effective, cannot be practically used on a large scale due to its overly complex production.

Protamine, despite undesirable side effects, is currently the only clinically used heparin reversal agent. Therefore, many other polycationic agents have been investigated as alternatives to protamine for heparin neutralization. In the early 1960's, hexadimethrine bromide (i.e. polybrene) (**12**) was one of the first

protamine alternatives investigated *in vivo*.[186,187] This fully synthetic cationic polymer showed promise early on, but was eventually abandoned due to toxicity and lower efficacy compared to protamine. Histones, polycationic proteins that normally function in DNA packing, and synthetic poly-DL-lysine (**13**) have also been explored as heparin neutralization agents. Nevertheless, they either proved to be inferior to protamine or exhibited high toxicity.[188] To improve on this model, a more recent study utilized poly-L-lysine dendrimers with glycine cores [Gly–$Lys_{63}(NH_2)_{64}$] as neutralization agents. When these dendrimers were pre-complexed with heparin, they disabled heparin's anticoagulant activity in rats.[189] Another recent study synthesized arginine-substituted poly(allylamine hydrochloride) derivatives (**14**) for potent reversal of heparin *in vitro* and *in vivo*.[190] Additionally, polycationic calix[8]arenes (**15**), flexible macrocylic compounds, have been shown to rapidly neutralize heparin in blood through tight electrostatic interactions.[191] A subsequent study showed these molecules, immobilized onto polymer matrix filters, were able to remove heparin from blood without being introduced systemically, therefore minimizing side effects associated with normal administration of heparin reversal agents.[192]

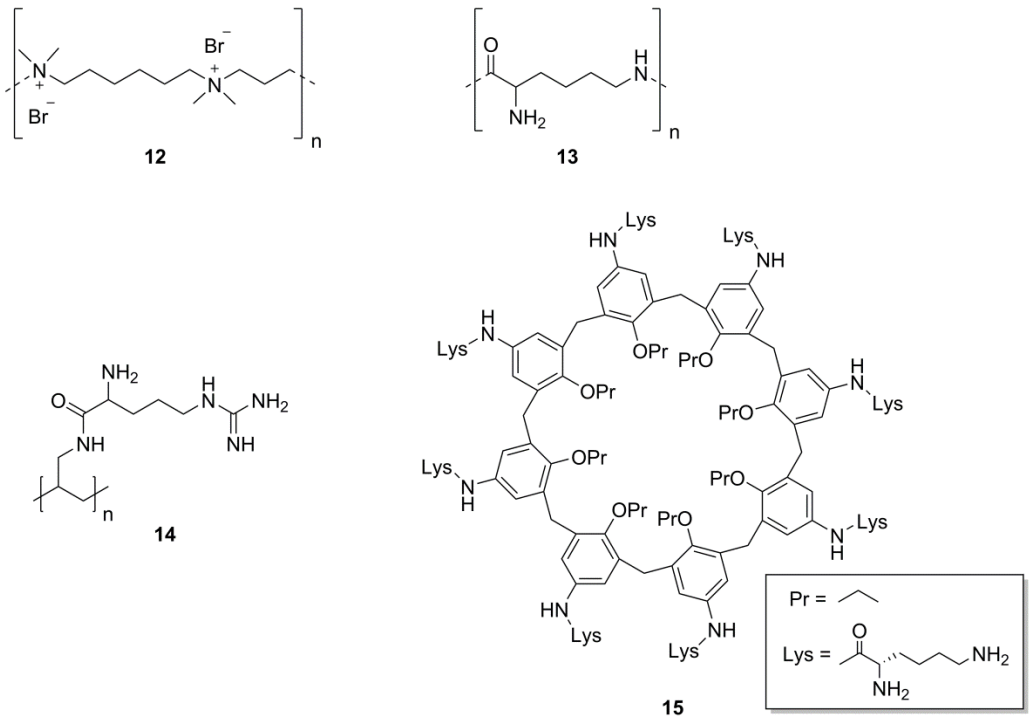

Figure 1.10: Examples of cationic antagonists of heparin and HS.

In searching even further for potent HS-antagonists, certain groups have looked at polyvalent peptide-derivatized dendrimers that display multiple cationic motifs for electrostatic interaction with heparin and HS. Arginine-rich polycationic virus-like particles were shown to neutralize heparin's interaction with antithrombin in human plasma,[193] branched dendrimer-based peptides inhibited HSV-1 and 2 infection,[194] and a large peptide isolated from human hemofiltrate blocked HCMV infection *in vitro* through a HS-dependent pathway.[195] Furthermore, synthetic self-assembling ligands (**16**) that form nanostructures have been explored as effective heparin binders. These compounds assemble into micelles in the presence of heparin and bind through electrostatic interactions of their protonated amine groups.[196] More recently, a group at the

University of British Columbia developed a universal synthetic heparin reversal agent (UHRA) based on branched dendritic polymers.[197] These UHRA molecules show great promise as safer alternatives to protamine for neutralization of heparin and its analogs; however, additional research is necessary to examine their application and safety in humans.

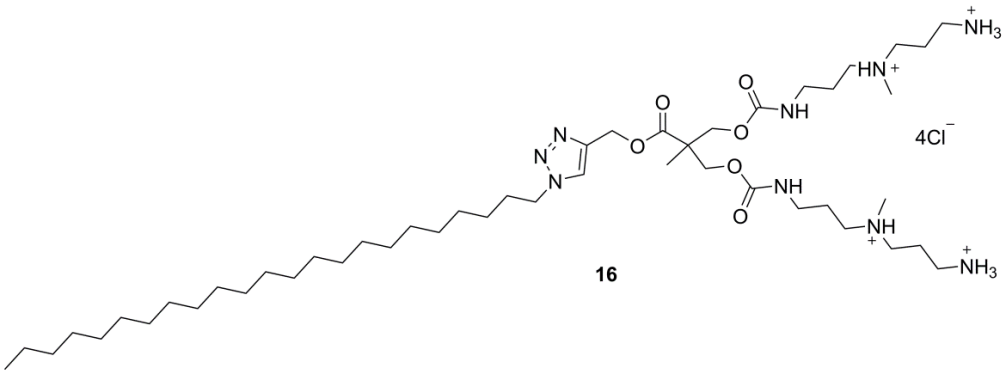

16

Figure 1.11: Self-assembling ligands for multivalent binding to heparin.

Similarly, small molecules (MW < 900 Da) have also been exploited as antagonists of HS and heparin. Small, chemically manufactured compounds make up 90% of approved drugs and are very important due to their versatility in targeting many different destinations in the body. They also provide manufacturing and delivery advantages over protein-based drugs due to their small size, biological stability, and simple synthetic nature. A dispirotripiperazine derivative, (DSTP 27) (**17**), was discovered to bind to HS on the cell surface and inhibit viral attachment, absorption, and replication of a wide range of virus families.[198] This compound proved to be a potent antiviral in a structure-activity relationship study with a novel class of antiviral compounds containing the *N*,*N*'-

bis-5-pyrimidyl moiety.[199] A subsequent study demonstrated the ability of DSTP 27 to block HS-dependent viral attachment of an HPV virus with long-term efficacy.[200] More recently, this molecule was shown to prevent HCMV infection through a combination of interactions with HSPGs and the virus itself.[201] In another study, a new family of planar aromatic cationic small molecule antagonists of HS were synthesized and probed as anti-inflammatory agents (e.g. **18-19**).[202] Specifically, they were investigated first as inhibitors of protein binding to HS in a 96-well ELISA-based assay, then the most potent compounds were evaluated for their ability to block acute inflammation in mice. Their mechanism of action was found to be due to direct binding to HS resulting in prevention of protein binding. Furthermore, a catechin extract from green tea, epigallocatechin gallate (EGCG) (**20**), was recently discovered to inhibit virion attachment of many unrelated viruses to HS and sialic acid, another type of polysaccharide found on the cell surface.[203] This broad-spectrum antiviral is one of the first small molecules effective against enveloped and nonenveloped viruses such as HSV-1, HCV, and influenza A virus (IAV). EGCG was able to block the HS-binding of HSV-1 and HCV, while also inhibiting attachment of IAV to sialic acid. These results suggest further development of small molecule-based broad-spectrum antiviral agents.

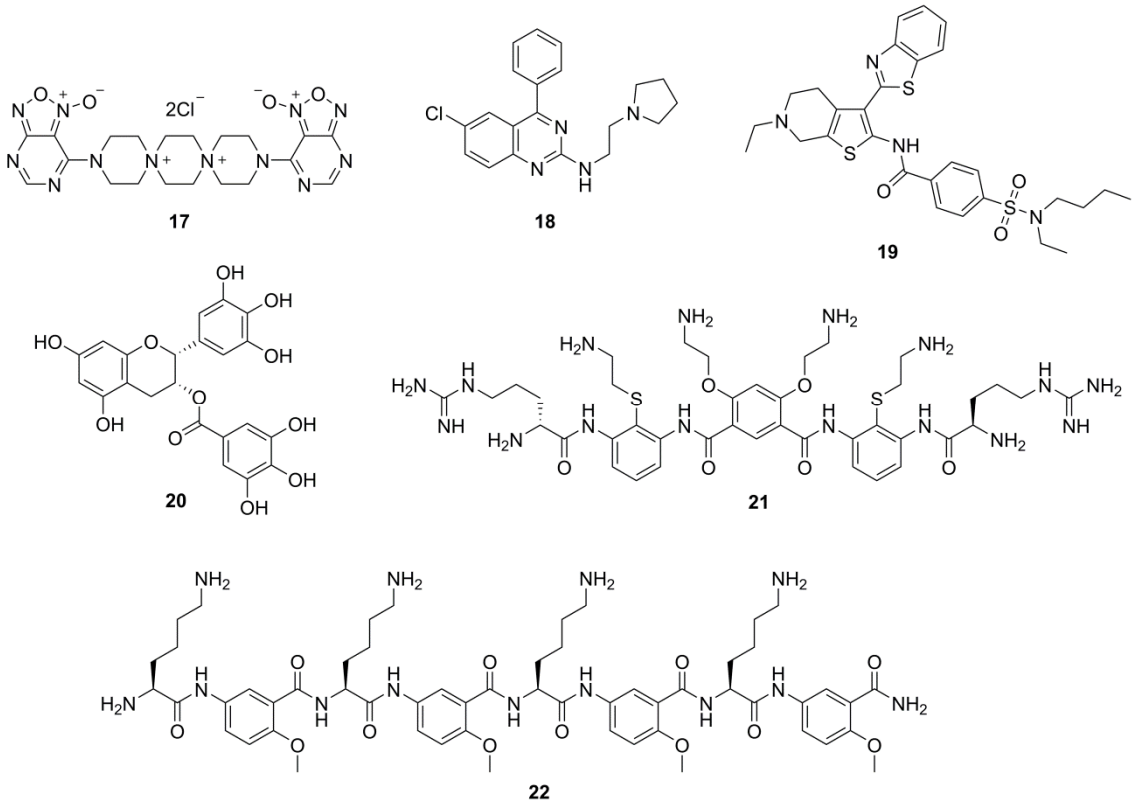

Figure 1.12: Small molecule antagonists of heparin and HS-protein interactions.

Synthetic small molecule peptide mimics known as foldamers (**21**), based on amine and guanidinium-substituted arylamides, have also been developed for *in vitro* neutralization of heparin's anticoagulant activity.[204,205] These molecules self-assemble to form β-like sheets with enhanced association to fondaparinux, a synthetic pentasaccharide analog of heparin. A novel salicylamide derivative, known as delparantag (**22**), was also developed as an alternative to protamine administration.[206] This compound, displaying multiple cationic lysines and aromatic amino acid units, neutralized heparin and enoxaparin, a low molecular weight heparin (LMWH), *in vivo* in rats and later showed promise in a small trial

in humans.[207] However, phase II clinical trials revealed unsafe toxicity profiles in patients, thus halting further development of this compound.

1.4.3 Surfen, a Small Molecule Antagonist of Glycosaminoglycans

In a high-throughput screen of the National Cancer Institute's (NCI) small molecule diversity set, our group identified *bis*-2-methyl-4-amino-quinolyl-6-carbamide (**23**), called surfen (NSC 12155), as a potent small molecule antagonist of HS.[208] In this study, surfen, a dimeric aminoquinoline, was shown to bind to multiple types of GAGs in solution, including heparin and HS. This small molecule was found to neutralize the ability of heparin to activate antithrombin in the coagulation cascade, block the sulfation and degradation of GAG chains by bacterial lyases *in vitro*, and inhibit angiogenesis initiated by the binding of HS-dependent growth factors. In addition, this study highlighted the use of this small molecule's heparin-neutralizing properties for potential therapeutic uses as an antiviral (inhibiting HS-mediated HSV-1 infection).

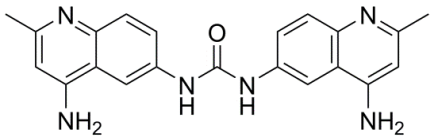

23

Figure 1.13: *Bis*-2-methyl-4-amino-quinolyl-6-carbamide (surfen).

Another group showed surfen was able to inhibit the enhancement of HIV-1 infection by amyloid fibrils found in semen (known as SEVI). Interestingly, it was discovered that surfen not only inhibited HS-mediated viral attachment but also directly bound to SEVI fibrils and disrupted their interaction with the HIV

virus.[209,210] Many other studies have utilized surfen's ability to antagonize HS as a tool to study HS interactions in biological systems. Surfen has been shown to regulate murine T-cell activation and proliferation[211], stimulate chondrogenesis *in vitro*,[212,213] and reduce lesion formation in demyelination of a multiple sclerosis mouse model.[214] Furthermore, a study in our group used surfen as an inhibitor of vascular endothermal growth factor (VEGF) phosphorylation and hyperpermeability in mice.[215]

Intriguingly, surfen has long history as a bioactive agent dating back to its original production at Hoechst. Surfen's discovery in 1938 as an excipient for the production of depot insulin propelled subsequent studies revealing its wide range of bioactivities.[216,217] Research showed surfen's activity as a trypanocidal agent[218] and as an inhibitor of the protease activity of anthrax lethal factor[219] and C5a receptor binding.[220] Moreover, recent NCI library screenings found surfen to be a potent inhibitor of polyphosphate, a polyanionic molecule implicated in inflammation and thrombosis[221], and an activator of G protein subunit (Gβγ) signaling in the chemotaxis of macrophages.[222] The overall evidence for surfen's biocompatibility and broad range of application to chemical biology supports the continuing investigation of the antagonist properties of this important small molecule. The extensive biological applications of surfen encouraged the design of more selective and potent analogs to target specific GAG–protein interactions and to gain insight into the interaction between surfen and GAGs.

1.5 Summary and Outlook

GAGs are vital components of the extracellular glycocalyx and are certainly involved in many important biological processes that are essential for maintaining homeostasis. HSPGs, in particular, perform vital roles in the normal function of all organ systems. HSPGs are involved in cell signaling, cell-to-cell interactions, and have been implicated in host-pathogen interactions. The heterogeneity and anionic nature of HS polysaccharides allow them to interact with a plethora of proteins through specific binding sites. However, due to their apparent pathophysiological roles in disease and infection, there has been an extensive amount of research dedicated to developing agents that can antagonize HS-protein and HS-pathogen interactions. As mentioned above, different methods for blocking these interactions have been explored including the inhibition of HS biosynthesis, enzymatic cleavage of HS at specific sites, GAG mimetic compounds as competitive protein binders, and various types of cationic molecules that bind competitively to HS and inhibit binding to protein ligands.

Overall, this is a relatively new field of research and there is still much to learn about HS-protein interactions. Additionally, new HS-binding ligands are regularly being discovered.[43] There are many challenges in developing novel therapeutics to combat diseases that involve these types of interactions (e.g. cancer, Alzheimer's disease). Most of the agents developed so far have failed to provide new approved treatments. Currently, the only clinically-approved drug

known to block GAG-protein interactions is the heparin-neutralizing agent protamine.[223] Heparin binds to the protease antithrombin, causing a conformational change, which leads to the inhibition of coagulation factors, such as thrombin and factor Xa. However, due to its heterogeneous nature and unpredictable dose requirement in individual patients, heparin overdose can occur resulting in excessive bleeding and thrombocytopenia.[224] Therefore, protamine is used to counteract heparin's anticoagulant activity in these situations. Unfortunately, protamine has exhibited adverse side effects when administered to patients as a heparin antidote.[225,226] More recently, newly developed heparin derivatives, such as the synthetic pentasaccharide fondaparinux,[227] are used frequently in hospitals yet protamine has proven to be ineffective against these anticoagulants.[228,229] There are currently no safe and effective agents approved to completely reverse these new low molecular weight heparins (LMWHs) despite the risk for adverse side effects. Thus, finding safer alternatives to protamine that can neutralize heparin and LMWHs is an important area of research.

Developing effective drugs that target GAG-protein interactions in disease is a challenge due to the apparent adverse effects caused by drug toxicity and lack of selectivity. Most GAG inhibitors rely on electrostatic interactions either with the anionic polysaccharides or proteins that interact with them. A major hurdle that exists in developing potent therapeutics is finding compounds that will function selectively in competitive conditions (e.g. blood, plasma). Moreover, a "potent" compound may not always be the best drug candidate and can cause

off-target toxicity, as has been observed in cancer drug research.[230] Therefore, drug discovery has proven to be an exciting yet complicated field.

The accessibility and versatility of small molecules make them particularly attractive as research tools and therapeutic agents. Surfen, a small molecule antagonist recently investigated in our lab, was revealed to be a promising new agent for blocking GAG-protein interactions.[208] Since its discovery, other groups have shown surfen's diverse properties in a wide range of applications.[209,211,214,221,222] The biocompatibility of surfen supports further research; however, due to this compound's relatively low efficacy (micromolar range), improvements must be made to encourage its clinical use. Hence, we synthesized a family of surfen analogs to search for more potent antagonists, to probe the interactions of surfen with HS, and to identify the key molecular determinants responsible for its activity. A structure-activity relationship was established in addition to expanding the biological applications for surfen-type compounds as small molecule GAG antagonists. Importantly, we found that a potent surfen analog was able to neutralize the synthetic pentasaccharide fondaparinux, for which no antidote exists, both *in vitro* and in mice.

Surfen was also previously shown to fluoresce upon binding to heparin and related GAGs in solution.[208] Due to the adverse side effects that can occur with heparin administration, monitoring the heparin plasma levels in patients is critical. Current methods for detecting heparin include activated clotting time (ACT), activated partial thromboplastin time (APTT), electrochemical assays, and anti-factor Xa activity. [231,232] However, these assays are expensive, time

consuming, or cannot be adapted to certain clinical settings. Therefore, there is a need for cheaper and more selective detection methods for monitoring the administration of heparin in patients. We investigated surfen as a “turn-on” fluorescent probe for simple and sensitive detection of heparin in human plasma. Additionally, we studied the unique photophysical properties of surfen to gain insight into its interaction with GAGs and to shed light on the mechanism of the turn-on fluorescence observed upon binding these anionic polysaccharides.

Acknowledgements

Chapter 1 is in full currently being prepared for submission: Weiss, R. J.; Esko, J. D.; Tor, Y. Targeting Glycosaminoglycans with Small Molecules. The dissertation author is the main author of this work.

1.6 References

(1) Weinbaum, S.; Tarbell, J. M.; Damiano, E. R. *Annual Review of Biomedical Engineering* **2007**, *9*, 121.

(2) Becker, B. F.; Chappell, D.; Bruegger, D.; Annecke, T.; Jacob, M. *Cardiovasc Res* **2010**, *87*, 300.

(3) Wheeler-Jones, C. P.; Farrar, C. E.; Pitsillides, A. A. *Curr Opin Investig Drugs* **2010**, *11*, 997.

(4) Salmon, A. H. J.; Satchell, S. C. *The Journal of Pathology* **2012**, *226*, 562.

(5) Bishop, J. R.; Schuksz, M.; Esko, J. D. *Nature* **2007**, *446*, 1030.

(6) Bernfield, M.; Kokenyesi, R.; Kato, M.; Hinkes, M. T.; Spring, J.; Gallo, R. L.; Lose, E. J. *Annual Review of Cell Biology* **1992**, *8*, 365.

(7) Filmus, J.; Selleck, S. B. *Journal of Clinical Investigation* **2001**, *108*, 497.

(8) Iozzo, R. V.; Cohen, I. R.; Grassel, S.; Murdoch, A. D. *Biochem J* **1994**, *302 (Pt 3)*, 625.

(9) Cole, G. J.; Halfter, W. *Perspect Dev Neurobiol* **1996**, *3*, 359.

(10) Dhoot, G. K.; Gustafsson, M. K.; Ai, X.; Sun, W.; Standiford, D. M.; Emerson Jr., C. P. *Science* **2001**, *293*, 1663.

(11) Fraser, J. R. E.; Laurent, T. C.; Laurent, U. B. G. *Journal of Internal Medicine* **1997**, *242*, 27.

(12) Silbert, J. E.; Sugumaran, G. *IUBMB Life* **2002**, *54*, 177.

(13) Hilton, B. J.; Lang, B. T.; Cregg, J. M. *The Journal of Neuroscience* **2012**, *32*, 4331.

(14) Mulloy, B.; Forster, M. J. *Glycobiology* **2000**, *10*, 1147.

(15) Wardrop, D.; Keeling, D. *British Journal of Haematology* **2008**, *141*, 757.

(16) McLean, J. *Circulation* **1959**, *19*, 75.

(17) Björk, I.; Lindahl, U. *Mol Cell Biochem* **1982**, *48*, 161.

(18) Evans, D. L.; Marshall, C. J.; Christey, P. B.; Carrell, R. W. *Biochemistry* **1992**, *31*, 12629.

(19) Ersdal-Badju, E.; Lu, A.; Zuo, Y.; Picard, V.; Bock, S. C. *Journal of Biological Chemistry* **1997**, *272*, 19393.

(20) Lever, R.; Page, C. R. *Nature Reviews Drug Discovery* **2002**, *1*, 140.

(21) Capila, I.; Linhardt, R. J. *Angewandte Chemie-International Edition* **2002**, *41*, 391.

(22) Sarrazin, S.; Lamanna, W. C.; Esko, J. D. *Csh Perspect Biol* **2011**, *3*.

(23) Hacker, U.; Nybakken, K.; Perrimon, N. *Nature Reviews Molecular Cell Biology* **2005**, *6*, 530.

(24) Bulow, H. E.; Hobert, O. *Annual Review of Cell and Developmental Biology* **2006**, *22*, 375.

(25) Gandhi, N. S.; Mancera, R. L. *Chemical Biology & Drug Design* **2008**, *72*, 455.

(26) Varki, A. *Essentials of glycobiology*; 2nd ed.; Cold Spring Harbor Laboratory Press: Cold Spring Harbor, N.Y., 2009.

(27) Sarrazin, S.; Lamanna, W. C.; Esko, J. D. *Cold Spring Harbor Perspectives in Biology* **2011**, *3*, a004952.

(28) Lortat-Jacob, H. *Current Opinion in Structural Biology* **2009**, *19*, 543.

(29) Saxena, U.; Klein, M. G.; Goldberg, I. J. *J Biol Chem* **1990**, *265*, 12880.

(30) Grünewald, F. S.; Prota, A. E.; Giese, A.; Ballmer-Hofer, K. *Biochimica et Biophysica Acta (BBA) - Proteins and Proteomics* **2010**, *1804*, 567.

(31) Yayon, A.; Klagsbrun, M.; Esko, J. D.; Leder, P.; Ornitz, D. M. *Cell* **1991**, *64*, 841.

(32) Turner, N.; Grose, R. *Nature Reviews Cancer* **2010**, *10*, 116.

(33) Maccarana, M.; Casu, B.; Lindahl, U. *J Biol Chem* **1993**, *268*, 23898.

(34) Yayon, A.; Klagsbrun, M. *Cancer and Metastasis Reviews* **1990**, *9*, 191.

(35) Mohammadi, M.; Olsen, S. K.; Ibrahimi, O. A. *Cytokine & Growth Factor Reviews* **2005**, *16*, 107.

(36) Polnaszek, N.; Kwabi-Addo, B.; Peterson, L. E.; Ozen, M.; Greenberg, N. M.; Ortega, S.; Basilico, C.; Ittmann, M. *Cancer Research* **2003**, *63*, 5754.

(37) Dow, J. K.; White, R. W. D. *Urology* **2000**, *55*, 800.

(38) Xu, D.; Young, J. H.; Krahn, J. M.; Song, D.; Corbett, K. D.; Chazin, W. J.; Pedersen, L. C.; Esko, J. D. *Acs Chemical Biology* **2013**, *8*, 1611.

(39) Sparvero, L.; Asafu-Adjei, D.; Kang, R.; Tang, D.; Amin, N.; Im, J.; Rutledge, R.; Lin, B.; Amoscato, A.; Zeh, H.; Lotze, M. *Journal of Translational Medicine* **2009**, *7*, 17.

(40) Donahue, J. E.; Flaherty, S. L.; Johanson, C. E.; Duncan, J. A., 3rd; Silverberg, G. D.; Miller, M. C.; Tavares, R.; Yang, W.; Wu, Q.; Sabo, E.; Hovanesian, V.; Stopa, E. G. *Acta neuropathologica* **2006**, *112*, 405.

(41) Morgan, M. R.; Humphries, M. J.; Bass, M. D. *Nat Rev Mol Cell Biol* **2007**, *8*, 957.

(42) Woods, A.; Longley, R. L.; Tumova, S.; Couchman, J. R. *Archives of Biochemistry and Biophysics* **2000**, *374*, 66.

(43) Xu, D.; Esko, J. D. *Annual Review of Biochemistry* **2014**, *83*, 129.

(44) Kreuger, J.; Spillmann, D.; Li, J.-p.; Lindahl, U. *The Journal of Cell Biology* **2006**, *174*, 323.

(45) Mahalingam, Y.; Gallagher, J. T.; Couchman, J. R. *Journal of Biological Chemistry* **2007**, *282*, 3221.

(46) Bernfield, M.; Götte, M.; Park, P. W.; Reizes, O.; Fitzgerald, M. L.; Lincecum, J.; Zako, M. *Annual Review of Biochemistry* **1999**, *68*, 729.

(47) Kjellen, L.; Lindahl, U. *Annual Review of Biochemistry* **1991**, *60*, 443.

(48) Kreuger, J.; Matsumoto, T.; Vanwildemeersch, M.; Sasaki, T.; Timpl, R.; Claesson-Welsh, L.; Spillmann, D.; Lindahl, U. *Role of heparan sulfate domain organization in endostatin inhibition of endothelial cell function*, 2002; Vol. 21.

(49) Lindahl, U.; Li, J. p. In *International Review of Cell and Molecular Biology*; Kwang, W. J., Ed.; Academic Press: 2009; Vol. Volume 276, p 105.

(50) Proudfoot, A. E. I. *Biochemical Society Transactions* **2006**, *34*, 422.

(51) Spillmann, D.; Witt, D.; Lindahl, U. *Journal of Biological Chemistry* **1998**, *273*, 15487.

(52) Vivès, R. R.; Sadir, R.; Imberty, A.; Rencurosi, A.; Lortat-Jacob, H. *Biochemistry* **2002**, *41*, 14779.

(53) Robinson, C. J.; Mulloy, B.; Gallagher, J. T.; Stringer, S. E. *Journal of Biological Chemistry* **2006**, *281*, 1731.

(54) Abramsson, A.; Kurup, S.; Busse, M.; Yamada, S.; Lindblom, P.; Schallmeiner, E.; Stenzel, D.; Sauvaget, D.; Ledin, J.; Ringvall, M.; Landegren,

U.; Kjellen, L.; Bondjers, G.; Li, J. P.; Lindahl, U.; Spillmann, D.; Betsholtz, C.; Gerhardt, H. *Genes Dev* **2007**, *21*, 316.

(55) Lortat-Jacob, H.; Turnbull, J. E.; Grimaud, J. A. *Biochemical Journal* **1995**, *310*, 497.

(56) Stringer, S. E.; Gallagher, J. T. *Journal of Biological Chemistry* **1997**, *272*, 20508.

(57) Jin, L.; Abrahams, J. P.; Skinner, R.; Petitou, M.; Pike, R. N.; Carrell, R. W. *Proceedings of the National Academy of Sciences* **1997**, *94*, 14683.

(58) Lindahl, U.; Backstrom, G.; Thunberg, L.; Leder, I. G. *P Natl Acad Sci-Biol* **1980**, *77*, 6551.

(59) Hirsh, J.; Anand, S. S.; Halperin, J. L.; Fuster, V. *Circulation* **2001**, *103*, 2994.

(60) van Horssen, J.; Wesseling, P.; van den Heuvel, L. P. W. J.; de Waal, R. M. W.; Verbeek, M. M. *The Lancet Neurology* **2003**, *2*, 482.

(61) Verbeek, M. M.; Otte-Holler, I.; van den Born, J.; van den Heuvel, L. P.; David, G.; Wesseling, P.; de Waal, R. M. *Am J Pathol* **1999**, *155*, 2115.

(62) Blackhall, F. H.; Merry, C. L. R.; Davies, E. J.; Jayson, G. C. *British Journal of Cancer* **2001**, *85*, 1094.

(63) Okolicsanyi, R. K.; van Wijnen, A. J.; Cool, S. M.; Stein, G. S.; Griffiths, L. R.; Haupt, L. M. *J Cell Biochem* **2014**, *115*, 967.

(64) Knelson, E. H.; Nee, J. C.; Blobe, G. C. *Trends Biochem Sci* **2014**, *39*, 277.

(65) Hallak, L. K.; Spillmann, D.; Collins, P. L.; Peeples, M. E. *Journal of Virology* **2000**, *74*, 10508.

(66) Alexopoulou, A. N.; Multhaupt, H. A. B.; Couchman, J. R. *International Journal of Biochemistry & Cell Biology* **2007**, *39*, 505.

(67) Sasisekharan, R.; Shriver, Z.; Venkataraman, G.; Narayanasami, U. *Nat Rev Cancer* **2002**, *2*, 521.

(68) Liu, D.; Shriver, Z.; Qi, Y.; Venkataraman, G.; Sasisekharan, R. *Semin Thromb Hemost* **2002**, *28*, 67.

(69) Liu, D.; Shriver, Z.; Venkataraman, G.; El Shabrawi, Y.; Sasisekharan, R. *Proceedings of the National Academy of Sciences* **2002**, *99*, 568.

(70) Bartlett, A. H.; Park, P. W. *Expert Reviews in Molecular Medicine* **2010**, *12*, 1.

(71) Freissler, E.; Meyer auf der Heyde, A.; David, G.; Meyer, T. F.; Dehio, C. *Cellular Microbiology* **2000**, *2*, 69.

(72) Van Putten, J. P. M.; Duensing, T. D.; Cole, R. L. *Molecular Microbiology* **1998**, *29*, 369.

(73) Wuppermann, F. N.; Hegemann, J. H.; Jantos, C. A. *Journal of Infectious Diseases* **2001**, *184*, 181.

(74) Liang, O. D.; Ascencio, F.; Fransson, L. A.; Wadström, T. *Infection and Immunity* **1992**, *60*, 899.

(75) Pethe, K.; Aumercier, M.; Fort, E.; Gatot, C.; Locht, C.; Menozzi, F. D. *J Biol Chem* **2000**, *275*, 14273.

(76) Shukla, D.; Spear, P. G. *The Journal of Clinical Investigation* **2001**, *108*, 503.

(77) Spear, P. G. *Seminars in Virology* **1993**, *4*, 167.

(78) Spear, P. G.; Shieh, M. T.; Herold, B. C.; WuDunn, D.; Koshy, T. I. *Adv Exp Med Biol* **1992**, *313*, 341.

(79) Shukla, D.; Liu, J.; Blaiklock, P.; Shworak, N. W.; Bai, X.; Esko, J. D.; Cohen, G. H.; Eisenberg, R. J.; Rosenberg, R. D.; Spear, P. G. *Cell* **1999**, *99*, 13.

(80) Patel, M.; Yanagishita, M.; Roderiquez, G.; Bou-Habib, D. C.; Oravecz, T.; Hascall, V. C.; Norcross, M. A. *AIDS Research and Human Retroviruses* **1993**, *9*, 167.

(81) Vivès, R. R.; Imberty, A.; Sattentau, Q. J.; Lortat-Jacob, H. *J Biol Chem* **2005**, *280*, 21353.

(82) Connell, B. J.; Lortat-Jacob, H. *Frontiers in Immunology* **2013**, *4*.

(83) Bobardt, M. D.; Saphire, A. C. S.; Hung, H.-C.; Yu, X.; Van der Schueren, B.; Zhang, Z.; David, G.; Gallay, P. A. *Immunity* **2003**, *18*, 27.

(84) Saphire, A. C. S.; Bobardt, M. D.; Zhang, Z.; David, G.; Gallay, P. A. *Journal of Virology* **2001**, *75*, 9187.

(85) Argyris, E. G.; Acheampong, E.; Nunnari, G.; Mukhtar, M.; Williams, K. J.; Pomerantz, R. J. *Journal of Virology* **2003**, *77*, 12140.

(86) de Witte, L.; Bobardt, M.; Chatterji, U.; Degeest, G.; David, G.; Geijtenbeek, T. B. H.; Gallay, P. *Proceedings of the National Academy of Sciences* **2007**, *104*, 19464.

(87) Hilgard, P.; Stockert, R. *Hepatology (Baltimore, Md.)* **2000**, *32*, 1069.

(88) Chen, Y.; Maguire, T.; Hileman, R. E.; Fromm, J. R.; Esko, J. D.; Linhardt, R. J.; Marks, R. M. *Nature medicine* **1997**, *3*, 866.

(89) Giroglou, T.; Florin, L.; Schäfer, F.; Streeck, R. E.; Sapp, M. *Journal of Virology* **2001**, *75*, 1565.

(90) Joyce, J. G.; Tung, J.-S.; Przysiecki, C. T.; Cook, J. C.; Lehman, E. D.; Sands, J. A.; Jansen, K. U.; Keller, P. M. *J Biol Chem* **1999**, *274*, 5810.

(91) Ben-Zaken, O.; Tzaban, S.; Tal, Y.; Horonchik, L.; Esko, J. D.; Vlodavsky, I.; Taraboulos, A. *Journal of Biological Chemistry* **2003**, *278*, 40041.

(92) Warner, R. G.; Hundt, C.; Weiss, S.; Turnbull, J. E. *Journal of Biological Chemistry* **2002**, *277*, 18421.

(93) Horonchik, L.; Tzaban, S.; Ben-Zaken, O.; Yedidia, Y.; Rouvinski, A.; Papy-Garcia, D.; Barritault, D.; Vlodavsky, I.; Taraboulos, A. *Journal of Biological Chemistry* **2005**, *280*, 17062.

(94) Cohlberg, J. A.; Li, J.; Uversky, V. N.; Fink, A. L. *Biochemistry* **2002**, *41*, 1502.

(95) Holmes, B. B.; DeVos, S. L.; Kfoury, N.; Li, M.; Jacks, R.; Yanamandra, K.; Ouidja, M. O.; Brodsky, F. M.; Marasa, J.; Bagchi, D. P.; Kotzbauer, P. T.; Miller, T. M.; Papy-Garcia, D.; Diamond, M. I. *Proceedings of the National Academy of Sciences* **2013**, *110*, E3138.

(96) Querfurth, H. W.; LaFerla, F. M. *New England Journal of Medicine* **2010**, *362*, 329.

(97) Ballard, C.; Gauthier, S.; Corbett, A.; Brayne, C.; Aarsland, D.; Jones, E. *The Lancet*, *377*, 1019.

(98) Selkoe, D. J. *Alzheimer's Disease: Genes, Proteins, and Therapy*, 2001; Vol. 81.

(99) Small, D. H.; Williamson, T.; Reed, G.; Clarris, H.; Beyreuther, K.; Masters, C. L.; Nurcombe, V. *Annals of the New York Academy of Sciences* **1996**, *777*, 316.

(100) Zhang, G.-l.; Zhang, X.; Wang, X.-m.; Li, J.-P. *BioMed Research International* **2014**, *2014*, 9.

(101) Bame, K. J.; Danda, J.; Hassall, A.; Tumova, S. *J Biol Chem* **1997**, *272*, 17005.

(102) Narindrasorasak, S.; Lowery, D.; Gonzalez-DeWhitt, P.; Poorman, R. A.; Greenberg, B.; Kisilevsky, R. *J Biol Chem* **1991**, *266*, 12878.

(103) Buée, L.; Ding, W.; Anderson, J. P.; Narindrasorasak, S.; Kisilevsky, R.; Boyle, N. J.; Robakis, N. K.; Delacourte, A.; Greenberg, B.; Fillit, H. M. *Brain Research* **1993**, *627*, 199.

(104) Gupta-Bansal, R.; Frederickson, R. C.; Brunden, K. R. *J Biol Chem* **1995**, *270*, 18666.

(105) Sandwall, E.; O'Callaghan, P.; Zhang, X.; Lindahl, U.; Lannfelt, L.; Li, J.-P. *Glycobiology* **2010**, *20*, 533.

(106) Goedert, M.; Jakes, R.; Spillantini, M. G.; Hasegawa, M.; Smith, M. J.; Crowther, R. A. *Nature* **1996**, *383*, 550.

(107) Safaiyan, F.; Kolset, S. O.; Prydz, K.; Gottfridsson, E.; Lindahl, U.; Salmivirta, M. *J Biol Chem* **1999**, *274*, 36267.

(108) Greve, H.; Cully, Z.; Blumberg, P.; Kresse, H. *J Biol Chem* **1988**, *263*, 12886.

(109) Venkatachalam, K. V. *IUBMB Life* **2003**, *55*, 1.

(110) Fadel, S.; Eley, A. *Journal of Medical Microbiology* **2004**, *53*, 93.

(111) Baron, M. J.; Bolduc, G. R.; Goldberg, M. B.; Aupérin, T. C.; Madoff, L. C. *J Biol Chem* **2004**, *279*, 24714.

(112) Barth, H.; Schäfer, C.; Adah, M. I.; Zhang, F.; Linhardt, R. J.; Toyoda, H.; Kinoshita-Toyoda, A.; Toida, T.; van Kuppevelt, T. H.; Depla, E.; von Weizsäcker, F.; Blum, H. E.; Baumert, T. F. *J Biol Chem* **2003**, *278*, 41003.

(113) Steffen, C.; Wetzel, E. *Toxicology* **1993**, *84*, 217.

(114) Uhlin-Hansen, L.; Yanagishita, M. *J Biol Chem* **1993**, *268*, 17370.

(115) Sherwood, A. L.; Holmes, E. H. *J Biol Chem* **1992**, *267*, 25328.

(116) Esko, J. D.; Selleck, S. B. *Annual Review of Biochemistry* **2002**, *71*, 435.

(117) Fritz, T. A.; Lugemwa, F. N.; Sarkar, A. K.; Esko, J. D. *J Biol Chem* **1994**, *269*, 300.

(118) Garud, D. R.; Tran, V. M.; Victor, X. V.; Koketsu, M.; Kuberan, B. *J Biol Chem* **2008**, *283*, 28881.

(119) OKAYAMA, M.; KIMATA, K.; SUZUKI, S. *Journal of Biochemistry* **1973**, *74*, 1069.

(120) Kuberan, B.; Ethirajan, M.; Victor, X. V.; Tran, V.; Nguyen, K.; Do, A. *ChemBioChem* **2008**, *9*, 198.

(121) Siegbahn, A.; Manner, S.; Persson, A.; Tykesson, E.; Holmqvist, K.; Ochocinska, A.; Ronnols, J.; Sundin, A.; Mani, K.; Westergren-Thorsson, G.; Widmalm, G.; Ellervik, U. *Chemical Science* **2014**, *5*, 3501.

(122) Ernst, S.; Langer, R.; Cooney, C. L.; Sasisekharan, R. *Critical reviews in biochemistry and molecular biology* **1995**, *30*, 387.

(123) Pojasek, K.; Shriver, Z.; Hu, Y.; Sasisekharan, R. *Biochemistry* **2000**, *39*, 4012.

(124) Ernst, S.; Venkataraman, G.; Winkler, S.; Godavarti, R.; Langer, R.; Cooney, C. L.; Sasisekharan, R. *Biochemical Journal* **1996**, *315*, 589.

(125) Morimoto-Tomita, M.; Uchimura, K.; Werb, Z.; Hemmerich, S.; Rosen, S. D. *J Biol Chem* **2002**, *277*, 49175.

(126) Freeman, S. D.; Keino-Masu, K.; Masu, M.; Ladher, R. K. *Developmental dynamics : an official publication of the American Association of Anatomists* **2015**, *244*, 168.

(127) Leistner, C. M.; Gruen-Bernhard, S.; Glebe, D. *Cell Microbiol* **2008**, *10*, 122.

(128) Tiwari, V.; Clement, C.; Xu, D.; Valyi-Nagy, T.; Yue, B. Y.; Liu, J.; Shukla, D. *J Virol* **2006**, *80*, 8970.

(129) Broutian, T. R.; Brendle, S. A.; Christensen, N. D. *The Journal of General Virology* **2010**, *91*, 531.

(130) Nasimuzzaman, M.; Persons, D. A. *Mol Ther* **2012**, *20*, 1158.

(131) Alvarez-Dominguez, C.; Vazquez-Boland, J. A.; Carrasco-Marin, E.; Lopez-Mato, P.; Leyva-Cobian, F. *Infect Immun* **1997**, *65*, 78.

(132) de Vries, F. P.; Cole, R.; Dankert, J.; Frosch, M.; van Putten, J. P. *Mol Microbiol* **1998**, *27*, 1203.

(133) Moelleken, K.; Hegemann, J. H. *Mol Microbiol* **2008**, *67*, 403.

(134) Vogt, A. M.; Barragan, A.; Chen, Q.; Kironde, F.; Spillmann, D.; Wahlgren, M. *Heparan sulfate on endothelial cells mediates the binding ofPlasmodium falciparum–infected erythrocytes via the DBL1α domain of PfEMP1*, 2003; Vol. 101.

(135) Sasisekharan, R.; Moses, M. A.; Nugent, M. A.; Cooney, C. L.; Langer, R. *P Natl Acad Sci USA* **1994**, *91*, 1524.

(136) Liu, D.; Pojasek, K.; Shriver, Z.; Holley, K.; El-Shabrawi, Y.; Venkataraman, G.; Sasisekharan, R.; Google Patents: 2011.

(137) Bateman, D.; McLaurin, J.; Chakrabartty, A. *BMC Neuroscience* **2007**, *8*, 29.

(138) Li, J.-P.; Galvis, M. L. E.; Gong, F.; Zhang, X.; Zcharia, E.; Metzger, S.; Vlodavsky, I.; Kisilevsky, R.; Lindahl, U. *P Natl Acad Sci USA* **2005**, *102*, 6473.

(139) Kanekiyo, T.; Zhang, J.; Liu, Q.; Liu, C. C.; Zhang, L.; Bu, G. *The Journal of neuroscience : the official journal of the Society for Neuroscience* **2011**, *31*, 1644.

(140) Ai, X.; Do, A. T.; Kusche-Gullberg, M.; Lindahl, U.; Lu, K.; Emerson, C. P., Jr. *J Biol Chem* **2006**, *281*, 4969.

(141) Kim, J. H.; Chan, C.; Elwell, C.; Singer, M. S.; Dierks, T.; Lemjabbar-Alaoui, H.; Rosen, S. D.; Engel, J. N. *Cell Microbiol* **2013**, *15*, 1560.

(142) Wang, S.; Ai, X.; Freeman, S. D.; Pownall, M. E.; Lu, Q.; Kessler, D. S.; Emerson, C. P. *P Natl Acad Sci USA* **2004**, *101*, 4833.

(143) Lai, J.; Chien, J.; Staub, J.; Avula, R.; Greene, E. L.; Matthews, T. A.; Smith, D. I.; Kaufmann, S. H.; Roberts, L. R.; Shridhar, V. *J Biol Chem* **2003**, *278*, 23107.

(144) Feyzi, E.; Trybala, E.; Bergström, T.; Lindahl, U.; Spillmann, D. *J Biol Chem* **1997**, *272*, 24850.

(145) Laquerre, S.; Argnani, R.; Anderson, D. B.; Zucchini, S.; Manservigi, R.; Glorioso, J. C. *J Virol* **1998**, *72*, 6119.

(146) Schulze, A.; Gripon, P.; Urban, S. *Hepatology (Baltimore, Md.)* **2007**, *46*, 1759.

(147) Henry-Stanley, M.; Hess, D. J.; Erickson, E.; Garni, R. M.; Wells, C. *Medical microbiology and immunology* **2003**, *192*, 107.

(148) Henry-Stanley, M. J.; Hess, D. J.; Erlandsen, S. L.; Wells, C. L. *Shock (Augusta, Ga.)* **2005**, *24*, 571.

(149) Yan, Y.; Silvennoinen-Kassinen, S.; Leinonen, M.; Saikku, P. *Microbes and infection / Institut Pasteur* **2006**, *8*, 866.

(150) Ahmed, I.; Majeed, A.; Powell, R. *Postgraduate Medical Journal* **2007**, *83*, 575.

(151) Rusnati, M.; Vicenzi, E.; Donalisio, M.; Oreste, P.; Landolfo, S.; Lembo, D. *Pharmacology & Therapeutics* **2009**, *123*, 310.

(152) Copeland, R.; Balasubramaniam, A.; Tiwari, V.; Zhang, F.; Bridges, A.; Linhardt, R. J.; Shukla, D.; Liu, J. *Biochemistry* **2008**, *47*, 5774.

(153) Skidmore, M. A.; Kajaste-Rudnitski, A.; Wells, N. M.; Guimond, S. E.; Rudd, T. R.; Yates, E. A.; Vicenzi, E. *MedChemComm* **2015**.

(154) Vogt, A. M.; Pettersson, F.; Moll, K.; Jonsson, C.; Normark, J.; Ribacke, U.; Egwang, T. G.; Ekre, H.-P.; Spillmann, D.; Chen, Q.; Wahlgren, M. *PLoS Pathog* **2006**, *2*, e100.

(155) Tremblay, P.; Aisen, P.; Garceau, D. *Alzheimer's & Dementia* **2005**, *1*, S2.

(156) Rumjon, A.; Coats, T.; Javaid, M. M. *International Journal of Nephrology and Renovascular Disease* **2012**, *5*, 37.

(157) Talarico, L. B.; Damonte, E. B. *Virology* **2007**, *363*, 473.

(158) Carlucci, M. J.; Scolaro, L. A.; Damonte, E. B. *Chemotherapy* **1999**, *45*, 429.

(159) Lee, J.-B.; Hayashi, K.; Hayashi, T.; Sankawa, U.; Maeda, M. *Planta Med* **1999**, *65*, 439.

(160) Nyberg, K.; Ekblad, M.; Bergström, T.; Freeman, C.; Parish, C. R.; Ferro, V.; Trybala, E. *Antiviral Research* **2004**, *63*, 15.

(161) Lee, E.; Pavy, M.; Young, N.; Freeman, C.; Lobigs, M. *Antiviral Research* **2006**, *69*, 31.

(162) Garson, J. A.; Lubach, D.; Passas, J.; Whitby, K.; Grant, P. R. *Journal of Medical Virology* **1999**, *57*, 238.

(163) Herold, B. C.; Bourne, N.; Marcellino, D.; Kirkpatrick, R.; Strauss, D. M.; Zaneveld, L. J.; Waller, D. P.; Anderson, R. A.; Chany, C. J.; Barham, B. J.; Stanberry, L. R.; Cooper, M. D. *The Journal of infectious diseases* **2000**, *181*, 770.

(164) Kisilevsky, R.; Lemieux, L. J.; Fraser, P. E.; Kong, X.; Hultin, P. G.; Szarek, W. A. *Nature medicine* **1995**, *1*, 143.

(165) Cheshenko, N.; Keller, M. J.; MasCasullo, V.; Jarvis, G. A.; Cheng, H.; John, M.; Li, J. H.; Hogarty, K.; Anderson, R. A.; Waller, D. P.; Zaneveld, L. J.; Profy, A. T.; Klotman, M. E.; Herold, B. C. *Antimicrobial agents and chemotherapy* **2004**, *48*, 2025.

(166) Keller, M. J.; Zerhouni-Layachi, B.; Cheshenko, N.; John, M.; Hogarty, K.; Kasowitz, A.; Goldberg, C. L.; Wallenstein, S.; Profy, A. T.; Klotman, M. E.; Herold, B. C. *The Journal of infectious diseases* **2006**, *193*, 27.

(167) Taylor, D. L.; Brennan, T. M.; Bridges, C. G.; Mullins, M. J.; Tyms, A. S.; Jackson, R.; Cardin, A. D. *Antiviral Res* **1995**, *28*, 159.

(168) Basche, M.; Gustafson, D. L.; Holden, S. N.; O'Bryant, C. L.; Gore, L.; Witta, S.; Schultz, M. K.; Morrow, M.; Levin, A.; Creese, B. R.; Kangas, M.; Roberts, K.; Nguyen, T.; Davis, K.; Addison, R. S.; Moore, J. C.; Eckhardt, S. G. *Clinical cancer research : an official journal of the American Association for Cancer Research* **2006**, *12*, 5471.

(169) Metz-Boutigue, M. H.; Jolles, J.; Mazurier, J.; Schoentgen, F.; Legrand, D.; Spik, G.; Montreuil, J.; Jolles, P. *European journal of biochemistry / FEBS* **1984**, *145*, 659.

(170) Wu, H.; Lundblad, R.; Church, F. *Neutralization of heparin activity by neutrophil lactoferrin*, 1995; Vol. 85.

(171) Sánchez, L.; Calvo, M.; Brock, J. H. *Archives of Disease in Childhood* **1992**, *67*, 657.

(172) Farnaud, S.; Evans, R. W. *Molecular Immunology* **2003**, *40*, 395.

(173) Fujihara, T.; Hayashi, K. *Archives of Virology* **1995**, *140*, 1469.

(174) Andersen, J. H.; Jenssen, H.; Sandvik, K.; Gutteberg, T. J. *J Med Virol* **2004**, *74*, 262.

(175) EL-Fakharany, E.; Sanchez, L.; Al-Mehdar, H.; Redwan, E. *Virology Journal* **2013**, *10*, 199.

(176) Harmsen, M. C.; Swart, P. J.; Béthune, M.-P. d.; Pauwels, R.; Clercq, E. D.; The, T. B.; Meijer, D. K. F. *Journal of Infectious Diseases* **1995**, *172*, 380.

(177) Hirashima, N.; Orito, E.; Ohba, K.; Kondo, H.; Sakamoto, T.; Matsunaga, S.; Kato, A.; Nukaya, H.; Sakakibara, K.; Ohno, T.; Kato, H.; Sugauchi, F.; Kato, T.; Tanaka, Y.; Ueda, R.; Mizokami, M. *Hepatology Research* **2004**, *29*, 9.

(178) Ishibashi, Y.; Takeda, K.; Tsukidate, N.; Miyazaki, H.; Ohira, K.; Dosaka-Akita, H.; Nishimura, M. *Hepatology Research* **2005**, *32*, 218.

(179) Bianchini, E. P.; Fazavana, J.; Picard, V.; Borgel, D. *Development of a recombinant antithrombin variant as a potent antidote to fondaparinux and other heparin derivatives*, 2011; Vol. 117.

(180) Fazavana, J.; Bianchini, E. P.; Saller, F.; Smadja, C.; Picard, V.; Taverna, M.; Borgel, D. *Journal of Thrombosis and Haemostasis* **2013**, *11*, 1128.

(181) Dehmer, G. J.; Fisher, M.; Tate, D. A.; Teo, S.; Bonnem, E. M. *Circulation* **1995**, *91*, 2188.

(182) Park, P. W.; Pier, G. B.; Hinkes, M. T.; Bernfield, M. *Nature* **2001**, *411*, 98.

(183) Chang, L. C.; Liang, J. F.; Lee, H. F.; Lee, L. M.; Yang, V. C. *AAPS pharmSci* **2001**, *3*, E18.

(184) Chang, L.-C.; Wrobleski, S.; Wakefield, T. W.; Lee, L. M.; Yang, V. C. *AAPS pharmSci* **2001**, *3*, 24.

(185) Byun, Y.; Singh, V. K.; Yang, V. C. *Thrombosis Research* **1999**, *94*, 53.

(186) Weiss, W. A.; Gilman, J. S.; Catenacci, A. J.; Osterberg, A. E. *Journal of the American Medical Association* **1958**, *166*, 603.

(187) Lillehei, C. W.; Sterns, L. P.; Long, D. M.; Lepley, D. *Annals of Surgery* **1960**, *151*, 11.

(188) Fabian, I.; Aronson, M. *Thrombosis Research*, *17*, 239.

(189) Al-Jamal, K. T.; Al-Jamal, W. T.; Kostarelos, K.; Turton, J. A.; Florence, A. T. *Results in Pharma Sciences* **2012**, *2*, 9.

(190) Kaminski, K.; Kalaska, B.; Koczurkiewicz, P.; Michalik, M.; Szczubialka, K.; Mogielnicki, A.; Buczko, W.; Nowakowska, M. *MedChemComm* **2014**, *5*, 489.

(191) Mecca, T.; Consoli, G. M. L.; Geraci, C.; La Spina, R.; Cunsolo, F. *Organic & Biomolecular Chemistry* **2006**, *4*, 3763.

(192) Mecca, T.; Cunsolo, F. *Polymers for Advanced Technologies* **2010**, *21*, 752.

(193) Udit, A. K.; Everett, C.; Gale, A. J.; Kyle, J. R.; Ozkan, M.; Finn, M. G. *Chembiochem* **2009**, *10*, 503.

(194) Luganini, A.; Nicoletto, S. F.; Pizzuto, L.; Pirri, G.; Giuliani, A.; Landolfo, S.; Gribaudo, G. *Antimicrobial agents and chemotherapy* **2011**, *55*, 3231.

(195) Borst, E. M.; Ständker, L.; Wagner, K.; Schulz, T. F.; Forssmann, W.-G.; Messerle, M. *Antimicrobial agents and chemotherapy* **2013**, *57*, 4751.

(196) Rodrigo, A. C.; Barnard, A.; Cooper, J.; Smith, D. K. *Angewandte Chemie International Edition* **2011**, *50*, 4675.

(197) Shenoi, R. A.; Kalathottukaren, M. T.; Travers, R. J.; Lai, B. F. L.; Creagh, A. L.; Lange, D.; Yu, K.; Weinhart, M.; Chew, B. H.; Du, C.; Brooks, D. E.; Carter, C. J.; Morrissey, J. H.; Haynes, C. A.; Kizhakkedathu, J. N. *Science Translational Medicine* **2014**, *6*, 260ra150.

(198) Schmidtke, M.; Karger, A.; Meerbach, A.; Egerer, R.; Stelzner, A.; Makarov, V. *Virology* **2003**, *311*, 134.

(199) Schmidtke, M.; Riabova, O.; Dahse, H. M.; Stelzner, A.; Makarov, V. *Antiviral Res* **2002**, *55*, 117.

(200) Selinka, H.-C.; Florin, L.; Patel, H. D.; Freitag, K.; Schmidtke, M.; Makarov, V. A.; Sapp, M. *Journal of Virology* **2007**, *81*, 10970.

(201) Paeschke, R.; Woskobojnik, I.; Makarov, V.; Schmidtke, M.; Bogner, E. *Antimicrobial agents and chemotherapy* **2014**, *58*, 1963.

(202) Harris, N.; Kogan, F. Y.; Il'kova, G.; Juhas, S.; Lahmy, O.; Gregor, Y. I.; Koppel, J.; Zhuk, R.; Gregor, P. *Biochimica Et Biophysica Acta-General Subjects* **2014**, *1840*, 245.

(203) Colpitts, C. C.; Schang, L. M. *Journal of Virology* **2014**, *88*, 7806.

(204) Montalvo, G. L.; Zhang, Y.; Young, T. M.; Costanzo, M. J.; Freeman, K. B.; Wang, J.; Clements, D. J.; Magavern, E.; Kavash, R. W.; Scott, R. W.; Liu, D.; DeGrado, W. F. *Acs Chemical Biology* **2014**, *9*, 967.

(205) Choi, S.; Clements, D. J.; Pophristic, V.; Ivanov, I.; Vemparala, S.; Bennett, J. S.; Klein, M. L.; Winkler, J. D.; DeGrado, W. E. *Angewandte Chemie-International Edition* **2005**, *44*, 6685.

(206) Kuziej, J.; Litinas, E.; Hoppensteadt, D. A.; Dahui Liu; Walenga, J. M.; Fareed, J.; Jeske, W. *Clinical and Applied Thrombosis/Hemostasis* **2010**, *16*, 377.

(207) McAllister, R. E. *Thrombosis Research*, *125*, S162.

(208) Schuksz, M.; Fuster, M. M.; Brown, J. R.; Crawford, B. E.; Ditto, D. P.; Lawrence, R.; Glass, C. A.; Wang, L.; Tor, Y.; Esko, J. D. *Proceedings of the National Academy of Sciences* **2008**, *105*, 13075.

(209) Roan, N. R.; Sowinski, S.; Muench, J.; Kirchhoff, F.; Greene, W. C. *Journal of Biological Chemistry* **2010**, *285*, 1861.

(210) Castellano, L. M.; Shorter, J. *Biology* **2012**, *1*, 58.

(211) Warford, J.; Doucette, C. D.; Hoskin, D. W.; Easton, A. S. *Biochemical and Biophysical Research Communications* **2014**, *443*, 524.

(212) Huegel, J.; Mundy, C.; Sgariglia, F.; Nygren, P.; Billings, P. C.; Yamaguchi, Y.; Koyama, E.; Pacifici, M. *Developmental biology* **2013**, *377*, 100.

(213) Huegel, J.; Sgariglia, F.; Enomoto-Iwamoto, M.; Koyama, E.; Dormans, J. P.; Pacifici, M. *Developmental dynamics : an official publication of the American Association of Anatomists* **2013**, *242*, 1021.

(214) Warford, J.; Madera, L.; Hoskin, D.; Easton, A. *Journal of Neuroimmunology* **2014**, *275*, 73.

(215) Xu, D.; Fuster, M. M.; Lawrence, R.; Esko, J. D. *Journal of Biological Chemistry* **2011**, *286*, 737.

(216) Umber, F.; Störring, F. K.; Föllmer, W. *Klin Wochenschr* **1938**, *17*, 443.

(217) Lautenschlaeger, K. L.; Doerzbach, E.; Schaumann, O.; Google Patents: 1942.

(218) Goble, F. C. *Journal of Pharmacology and Experimental Therapeutics* **1950**, *98*, 49.

(219) Panchal, R. G.; Hermone, A. R.; Nguyen, T. L.; Wong, T. Y.; Schwarzenbacher, R.; Schmidt, J.; Lane, D.; McGrath, C.; Turk, B. E.; Burnett, J.; Aman, M. J.; Little, S.; Sausville, E. A.; Zaharevitz, D. W.; Cantley, L. C.; Liddington, R. C.; Gussio, R.; Bavari, S. *Nature Structural & Molecular Biology* **2004**, *11*, 67.

(220) Lanza, T. J.; Durette, P. L.; Rollins, T.; Siciliano, S.; Cianciarulo, D. N.; Kobayashi, S. V.; Caldwell, C. G.; Springer, M. S.; Hagmann, W. K. *Journal of Medicinal Chemistry* **1992**, *35*, 252.

(221) Smith, S. A.; Choi, S. H.; Collins, J. N. R.; Travers, R. J.; Cooley, B. C.; Morrissey, J. H. *Blood* **2012**, *120*, 5103.

(222) Surve, C. R.; Lehmann, D.; Smrcka, A. V. *J Biol Chem* **2014**, *289*, 17791.

(223) Pai, M.; Crowther, M. In *Heparin - A Century of Progress*; Lever, R., Mulloy, B., Page, C. P., Eds.; Springer Berlin Heidelberg: 2012; Vol. 207, p 265.

(224) Alban, S. In *Heparin - A Century of Progress*; Lever, R., Mulloy, B., Page, C. P., Eds.; Springer Berlin Heidelberg: 2012; Vol. 207, p 211.

(225) Portmann, A. F.; Holden, W. D. *Journal of Clinical Investigation* **1949**, *28*, 1451.

(226) Weiler, J. M.; Freiman, P.; Sharath, M. D.; Metzger, W. J.; Smith, J. M.; Richerson, H. B.; Ballas, Z. K.; Halverson, P. C.; Shulan, D. J.; Matsuo, S.; Wilson, R.L. *J Allergy Clin Immunol* **1985**, *75*, 297.

(227) Nagler, M.; Haslauer, M.; Wuillemin, W. A. *Thrombosis Research* **2012**, *129*, 407.

(228) van Veen, J. J.; Maclean, R. M.; Hampton, K. K.; Laidlaw, S.; Kitchen, S.; Toth, P.; Makris, M. *Blood Coagul Fibrinolysis* **2011**, *22*, 565.

(229) Schroeder, M.; Hogwood, J.; Gray, E.; Mulloy, B.; Hackett, A. M.; Johansen, K. B. *Anal Bioanal Chem* **2011**, *399*, 763.

(230) López-Lázaro, M. *Oncoscience* **2015**, *2*, 91.

(231) Vandiver, J. W.; Vondracek, T. G. *Pharmacotherapy: The Journal of Human Pharmacology and Drug Therapy* **2012**, *32*, 546.

(232) Raymond, P. D.; Ray, M. J.; Callen, S. N.; Marsh, N. A. *Perfusion* **2003**, *18*, 269.

Chapter 2:

Small Molecule Antagonists of Cell-Surface Heparan Sulfate and Heparin–Protein Interactions

2.1 Introduction

Heparan sulfate proteoglycans (HSPGs) are expressed on virtually all animal cells and in the extracellular matrix. Each HSPG consists of a core protein with one or more covalently attached linear glycosaminoglycan chains composed of alternating glucosamine and uronic acids that are heterogeneously *N*- and *O*-sulfated (**Figure 2.1**). These complex cell surface carbohydrates regulate important biological processes including cell proliferation and motility, development, and organ physiology through their interaction with a large number of matrix proteins and growth factors.[1-3] Sometimes these processes go awry, for example in cancer, inflammation, and neurodegenerative disorders.[4,5] Thus, much interest exists in agents controlling HS–protein interactions as both therapeutics and glycobiology tools.

The biological function of HSPGs is largely determined through interactions of the HS chains with protein ligands. Multiple agents for antagonizing HS-protein interactions have been developed including heparin mimetic compounds[6,7] and metabolic inhibitors that alter its biosynthesis.[8,9] Other approaches use proteins[10], polypeptides[11,12], foldamers[13,14], or small molecule antagonists[15-18] containing positively charged residues that bind to the negatively

charged carboxylate or sulfate groups on HS. The accessibility and versatility of small molecules that antagonize HS–protein interactions make them particularly attractive as potential research tools and therapeutic agents.

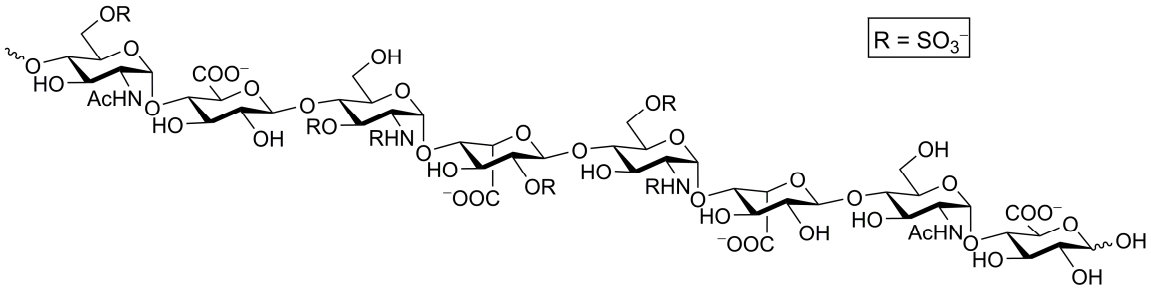

Figure 2.1: Heparan sulfate (HS). An arbitrary octasaccharide is shown.

We previously identified surfen (**1**) in the National Cancer Institute small molecule Diversity Set as an antagonist of heparan sulfate (HS) and heparin (**Figure 2.2**).[19] Binding of surfen to heparin blocks its degradation by bacterial lyases and prevents its ability to activate antithrombin. In cell culture, surfen inhibits angiogenesis by preventing the interaction of HS with fibroblast growth factor 2 (FGF2) and inhibits Type I Herpes simplex virus-infection. Surfen also blocks the enhancement of HIV-1 infection by amyloid fibrils found in semen,[20,21] alters murine T-cell activation and proliferation,[22] and blocks C5a receptor binding,[23] suggesting that some of these processes might also depend on HS–protein interactions. Surfen also acts independently of HS, as a trypanocidal agent[24] and as an inhibitor of the protease activity of anthrax lethal factor.[25] These diverse properties of surfen suggest the possibility of designing more selective and potent analogs to target HS–protein interactions.

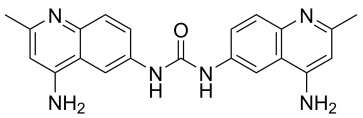

1

Figure 2.2: *Bis*-2-methyl-4-amino-quinolyl-6-carbamide (Surfen).

To probe the interactions of surfen with HS, identify the key molecular determinants responsible for its activity, and potentially discover more potent antagonists, a small set of analogs was synthesized and studied. A structure-activity relationship was established through quantifying their ability to inhibit cell surface HS–FGF2 binding *in vitro*. Certain analogs proved to be more potent antagonists of HS and were shown to inhibit other types of GAG–protein interactions, including cell surface binding of soluble RAGE and neutralization of the anticoagulant activity of unfractionated heparin and LMWHs. Importantly, we found that surfen analogs were able to neutralize the synthetic pentasaccharide fondaparinux, for which no antidote exists, both *in vitro* and *in vivo*.[26] These observations imply that small molecule antagonists of heparan sulfate can potentially be of therapeutic value and can serve as tools for chemical biologists interested in probing HS-dependent cellular processes.

2.2 Results

Derivative design

Surfen is a symmetric small molecule (MW 372) consisting of two quinoline moieties linked together through a urea. The quinoline rings are functionalized with a methyl group at the 2-position and an exocyclic amine at the 4-position. It has been previously proposed that the exocyclic amines and urea

linker region of surfen could electrostatically interact with the anionic carboxylate and sulfate moieties of HS through hydrogen bonding.[19] It is also possible that the distance between the aminoquinoline moieties and their orientation are essential for its biological activity. To examine these possibilities, we synthesized a series of surfen analogs (**Figure 2.3**).

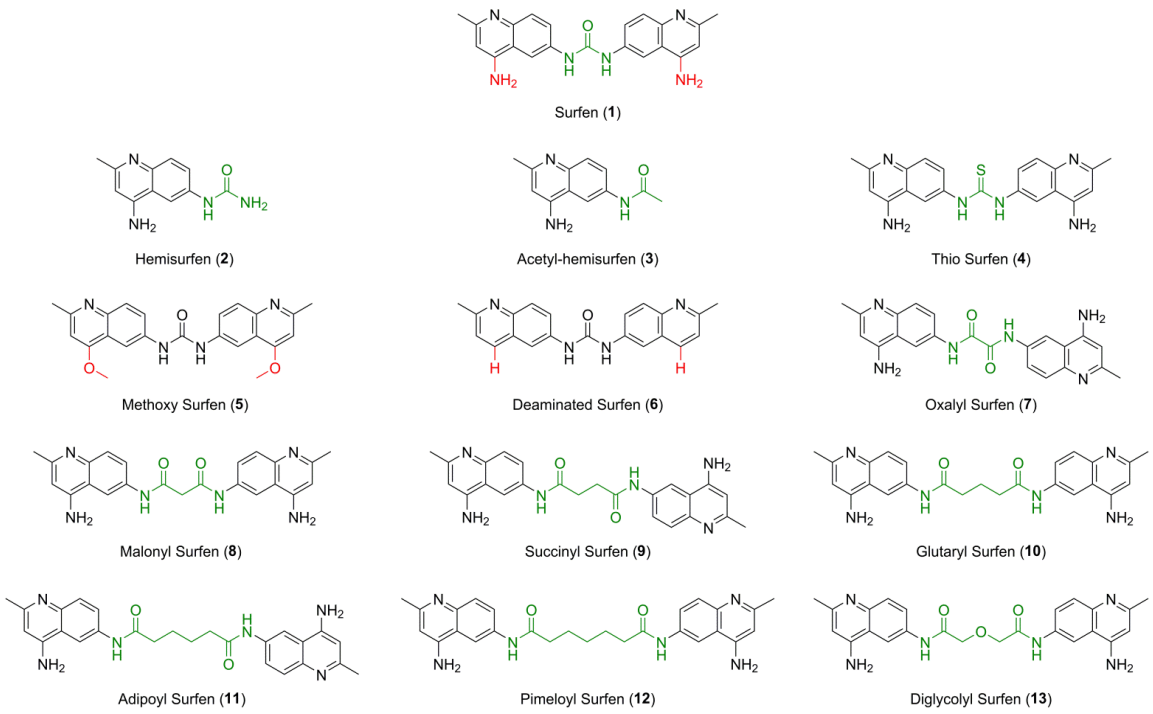

Figure 2.3: Structures of surfen (**1**) and its analogs. Modifications highlighted in red and green.

"Monomeric" versions of surfen, containing a single quinoline moiety (**2**, **3**), were synthesized to probe the importance of the dimeric structure of surfen for its biological activity. Here we refer to these compounds as hemisurfen (**2**) and acetyl-hemisurfen (**3**). A thiocarbonyl analog of surfen (**4**), referred to as "thio surfen" in this study, was made with a thiourea core, a modification that replaces oxygen with larger, less electronegative sulfur. This substitution should primarily

affect the hydrogen bonding capability of the linker region. Furthermore, to investigate the importance of the 4-aminopyridine fragment within the aminoquinoline moieties in binding HS, the exocyclic amines were replaced by methoxy groups (**5**) or removed altogether (**6**). For simplicity, these compounds are referred to here as “methoxy surfen” and “deaminated surfen”, respectively. To assess the significance of the distance between the aminoquinoline moieties, compounds **7**–**12** were prepared. The linker between the two heterocycles was extended which also increased the hydrophobicity of this region. Additionally, the urea group was substituted with two amide bonds. A compound with a glycol-like linker region (**13**), trivially named here “diglycolyl surfen”, was synthesized to probe whether increasing the hydrophilicity of the extended linker would impact its interaction with HS.

Synthesis

The core heterocycle in surfen, 4,6-diamino-2-methylquinoline (**14**), was synthesized as previously reported and was used in the synthesis of surfen analogs **2**–**4** and **7**–**13** (Scheme 2.1, 2.2).[27,28] 4-aminoacetanilide (**15**) was condensed with ethyl acetoacetate to give ethyl-β-(*p*-acetamidophenylamino) crotonate (**16**). This ethyl ester intermediate then underwent thermal cyclization in Dowtherm A to yield 6-acetamide-4-hydroxy-2-methylquinoline (**17**). The hydroxyquinoline intermediate was then methylated with dimethyl sulfate to yield the methoxy derivative (**18**). This compound then underwent a two-step reaction to yield 4,6-diamino-2-methylquinoline (**14**) through a 6-acetamido-4-

aminoquinaldine intermediate (**19**). This building block was used in the synthesis of specific surfen analogs (**4–13**) (Scheme 2.2, 2.3).

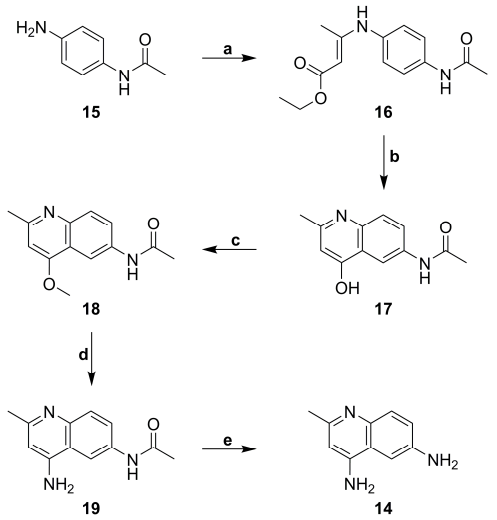

Scheme 2.1: Synthesis of 4,6-diamino-2-methylquinoline building block (**14**). *Reagents and Conditions:* (a) ethyl acetoacetate, MeOH, reflux, (b) Dowtherm A, 265°C, (c) dimethyl sulfate, toluene, 120°C, (d) ammonium acetate, 135°C, (e) 37% HCl, 90°C.

1,3-bis(2-methylquinolin-6-yl)urea (deaminated surfen) (**6**) was synthesized by reacting triphosgene with the commercially available 6-amino-2-methylquinoline in acetic acid. Furthermore, compounds **7–13** were synthesized using their respective diacid chlorides in acetic acid at room temperature. These compounds (**7–13**) were named according to the diacid chloride used in their synthesis. This procedure was adapted from a previous report.[23] 4-Amino-2-methyl-6-quinolyl-urea (hemisurfen) (**2**) was prepared using potassium cyanate, 10% acetic acid, and water followed by recrystallization from water. Finally, 6-acetamido-4-aminoquinaldine (acetyl-hemisurfen) (**3**) was synthesized by reacting 4,6-diaminoquinaldine with acetic chloride in acetic acid, and *N*,*N*'-bis-(4-amino-2-methyl-6-quinolyl)-thiourea (thio surfen) (**4**) was synthesized using

thiophosgene in DMF. Hemisurfen and acetyl-hemisurfen were recrystallized from water, while all other final products were recrystallized from hot DMF by the addition of diethyl ether. To synthesize the methoxy analog 1,3-bis(4-methoxy-2-methyl-quinolin-6-yl)urea (methoxy surfen) (**5**), 6-acetamido-4-methoxyquinaldine (**18**) was deprotected with 37% HCl in H_2O to form 6-amino-4-methoxyquinaldine (**20**). This compound was then reacted with triphosgene to yield **5** (Scheme 2.3).

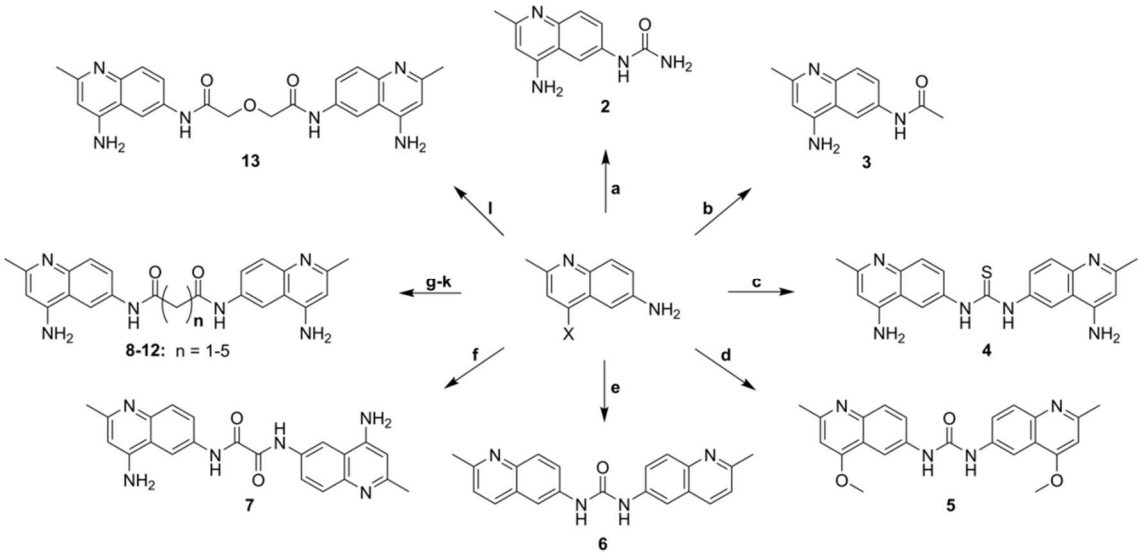

Scheme 2.2: Synthesis of surfen derivatives. *Reagents and Conditions:* (a) (X = NH_2) potassium cyanate, 10% acetic acid, H_2O, rt, (b) (X = NH_2) acetyl chloride, acetic acid, rt, (c) (X = NH_2) thiophosgene, DMF, rt, (d) (X = OCH_3) triphosgene, 1,4-dioxane, acetic acid, rt, (e) (X = H) triphosgene, 1,4-dioxane, acetic acid, rt, (f) (X = NH_2) oxalyl chloride, acetic acid, rt, (g) (X = NH_2) malonyl chloride, acetic acid, rt, (h) (X = NH_2) succinyl chloride, acetic acid, rt, (i) (X = NH_2) glutaryl chloride, acetic acid, rt, (j) (X = NH_2) adipoyl chloride, acetic acid, rt, (k) (X = NH_2) pimeloyl chloride, acetic acid, rt, (l) (X = NH_2) diglycolyl chloride, acetic acid, rt.

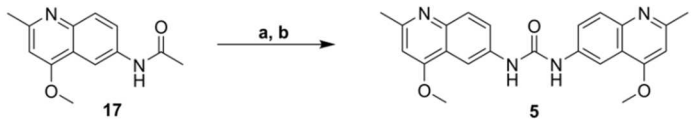

Scheme 2.3: Synthesis of methoxy surfen (**5**). *Reagents and Conditions:* (a) 37% HCl, 90°C, (b) triphosgene, 1,4-dioxane, acetic acid, rt.

Surfen (*bis*-2-methyl-4-amino-quinolyl-6-carbamide) was previously obtained from the National Cancer Institute as a hydrochloride salt (NCI 12155). All compounds were therefore converted to their hydrochloride salts to be used in biological assays. The hydrochloride products were precipitated from an appropriate solvent using 4M HCl in 1,4-dioxane (Scheme 2.4). The products were analyzed using ^{1}H NMR, ^{13}C NMR, and ESI-MS. An X-ray crystal structure of one of the analogs (**13**) confirmed that these molecules are doubly protonated on their aminoquinoline ring systems (**Figure 2.4**). Furthermore, the X-ray structures of 1 and 13 displayed *syn* orientations in regards to their quinoline ring systems (**Figure 2.4a, d**), while the crystal structures of oxalyl and adipoyl surfen displayed *anti* orientations (**Figure 2.4b–c**). These structures suggest that surfen analogs within this collection could present diverse molecular configurations that could affect their interactions with the anionic subunits of HS.

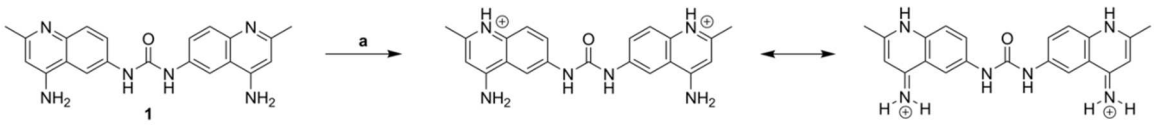

Scheme 2.4: Example of synthesis of the HCl salt form. *Reagents and Conditions:* (a) 4M HCl in 1,4-dioxane, MeOH, rt.

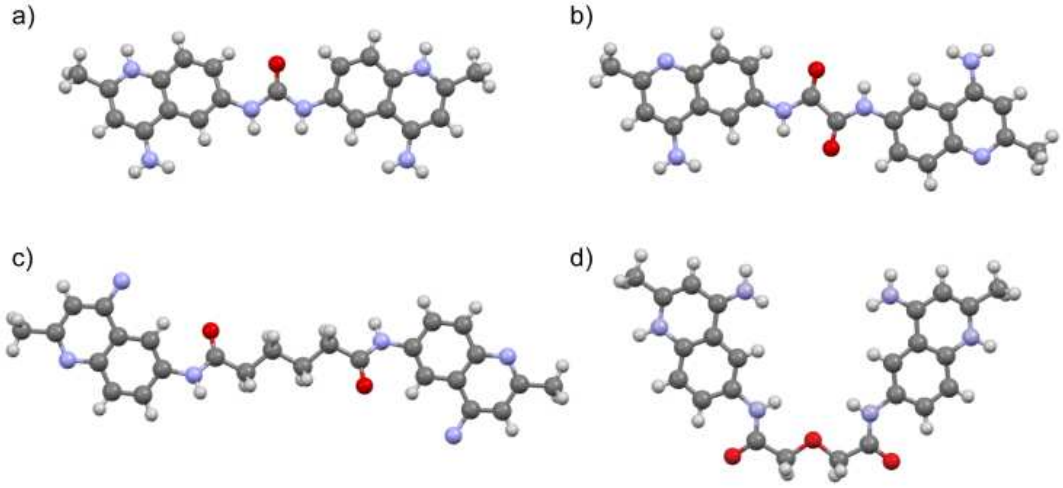

Figure. 2.4: X-ray crystal structures of a) surfen•2CF_3COOH (**1**), b) oxalyl surfen (**7**), c) adipoyl surfen (**11**), and d) diglycolyl surfen•2HCl (**13**). Counterions and solvent molecules omitted for clarity.

Inhibition of HS Binding

To determine the potency of surfen and its analogs as HS antagonists, their ability to inhibit the binding of FGF2 was quantified *in vitro*, as previously reported.[19] CHO cells express very low levels of FGF receptors, thus binding occurs through cell surface HSPGs. Each surfen analog was pre-incubated with CHO cells. Biotinylated FGF2 was then added, followed by the addition of fluorescently-tagged streptavidin thus forming a conjugate with cell-bound biotin-FGF2. Flow cytometry was utilized to monitor the fluorescence of bound ligand. FGF inhibition curves were generated by plotting the percentage of maximum FGF binding obtained in the absence of any antagonist versus the concentration of the molecule of interest (see **Figure 2.5** for a representative example). IC_{50} values were obtained by fitting the dose-response curves to a classic sigmoidal response (**Table 2.1**).

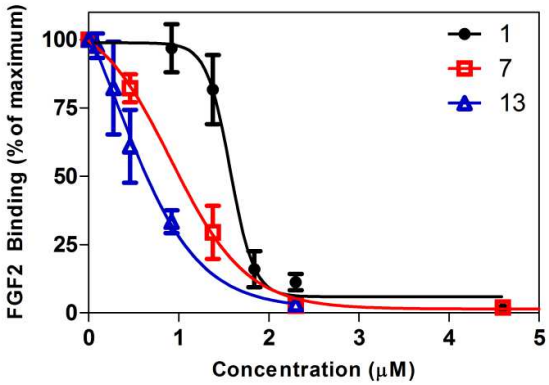

Figure 2.5: Representative inhibition curves. Surfen (**1**), oxalyl surfen (**7**), and diglycolyl surfen (**13**) were tested as inhibitors of FGF2 binding.

As shown in **Table 2.1**, analogs with oxalyl, malonyl, succinyl and diglycolyl amide linkers (**7–9**, **13**) showed enhanced inhibition of FGF2 binding to HS compared to surfen (**1**), the parent compound. Interestingly, the glutaryl (**10**) and adipoyl (**11**) analogs showed slightly decreased activity compared to native surfen, while pimeloyl surfen (**12**) showed minimal inhibitory activity up to 100 μM. The thiocarbonyl analog (**4**) showed lower activity compared to surfen, while the diglycolyl derivative (**13**) showed the highest activity. Molecules with modification of the exocyclic amine (**5**, **6**) or that altered the dimeric structure of surfen (**2**, **3**) were ineffective up to 100 μM.

Table 2.1: Inhibitory concentrations of surfen and analogs against FGF2 binding. [a] Values represent the mean ± SD of n = 3-4 experiments.

Compound	**IC_{50} (μM)[a]**
Surfen (**1**)	1.6 ± 0.04
Hemisurfen **(2**)	>100
Acetyl-hemisurfen (**3**)	>100
Thio Surfen (**4**)	8.0 ± 0.20
Methoxy Surfen (**5**)	>100
Deaminated Surfen (**6**)	>100
Oxalyl Surfen (**7**)	0.9 ± 0.08
Malonyl Surfen (**8**)	1.2 ± 0.03
Succinyl Surfen (**9**)	1.2 ± 0.11
Glutaryl Surfen (**10**)	61.5 ± 0.70
Adipoyl Surfen (**11**)	8.4 ± 1.2
Pimeloyl Surfen (**12**)	>100
Diglycolyl Surfen (**13**)	0.7 ± 0.12

We investigated the ability of surfen-type molecules to antagonize binding of the soluble ectodomain of RAGE (Receptor for Advanced Glycation Endproducts) to HS, which results in RAGE oligomerization.[29] Succinyl surfen (**9**) showed dose-dependent inhibition of binding (IC_{50} = 1.4 ± 0.2 μM) (**Figure 2.6**). Acetyl-hemisurfen (**3**) showed no inhibitory activity and was used as a negative control (IC_{50} > 100 μM).

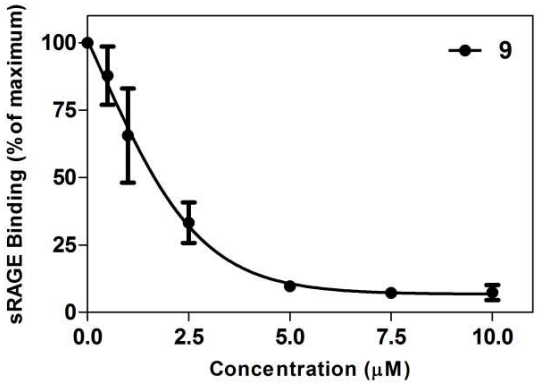

Figure 2.6: Succinyl surfen (**9**) inhibits sRAGE binding to HS.

Surfen Analogs Neutralize the Anticoagulant Activity of Heparin and Low Molecular Weight Heparins

Based on their capacity to inhibit HS–protein interactions *in vitro*, surfen (**1**) and the most active analogs (**7**, **9**, and **13**) were tested for their ability to neutralize the capacity of unfractionated heparin (UFH) to bind and activate antithrombin III (AT), a protease inhibitor that blocks the blood coagulation protease Factor Xa. In this assay, heparin binds to AT, induces a conformation change, and triggers the inhibition of Factor Xa. Thus, molecules that prevent heparin from interacting with AT prevent loss of Factor Xa activity, which is readily assessed using a chromogenic substrate (S-2765). IC_{50} values were determined by varying the concentration of surfen and its analogs. Surfen yielded an IC_{50} value of 2 ± 0.06 μM, whereas oxalyl surfen (**7**), succinyl surfen (**9**) and diglycolyl surfen (**13**) gave IC_{50} values of 1.2 ± 0.04, 4.6 ± 0.07, and 2 ± 0.03 μM, respectively (**Figure 2.7a**).

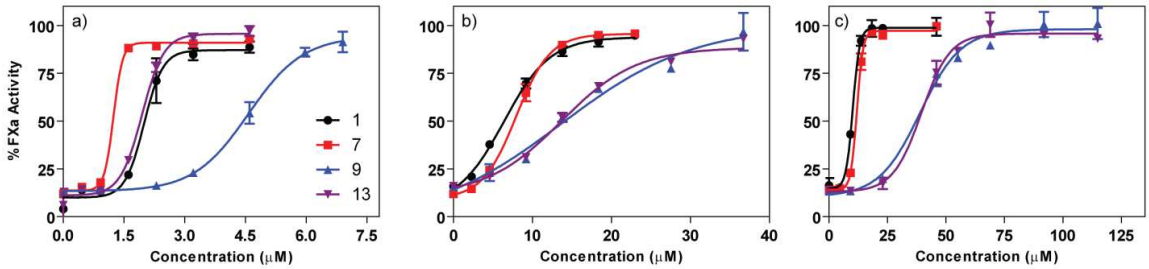

Figure 2.7: Dose-dependent neutralization of a) unfractionated heparin (UFH), b) enoxaparin (LMWH), c) fondaparinux (pentasaccharide). Curves were fit using a classic sigmoidal-dose response.

Selected surfen molecules were also tested as neutralizing agents of enoxaparin, a low molecular weight heparin (**Figure 2.7b**). Using the Factor Xa assay, we found that surfen, oxalyl surfen, succinyl surfen, and diglycolyl surfen neutralized enoxaparin in the low micromolar range (EC_{50} = 6.4 ± 0.4, 8 ± 0.2, 13.7 ± 2.7, 13.6 ± 0.6 μM, respectively). These compounds also neutralized fondaparinux, a synthetic pentasaccharide, albeit with slightly lower potency (IC_{50} = 10.2 ± 0.2, 11.9 ± 0.2, 38.9 ± 2.1, 39.5± 1.6 μM, respectively) (**Figure 2.7c**).

Oxalyl Surfen Neutralizes Heparin and Fondaparinux in Mice

To test if the surfen analogs remained potent and had acceptable pharmacokinetic properties *in vivo*, the most potent analog (**7**) was evaluated as a reversal agent for heparin anticoagulant activity in mice treated with a high anticoagulant dose of either UFH or fondaparinux (**Figure 2.8**). UFH at 1200 IU/kg (> 5-fold the therapeutic dose) was injected subcutaneously and, after 1 hour, oxalyl surfen (6 mg/kg) or vehicle control were injected intravenously. Protamine (16 mg/kg) was used for comparison. After 5 minutes, blood was collected, centrifuged, and the plasma was isolated and analyzed for FXa

activity. A calibration curve was established to determine the amount of active UFH or fondaparinux that remained. The concentration of UFH in the plasma was found to be significantly reduced in the oxalyl surfen-treated (0.08 ± 0.001 IU/mL) and protamine-treated (0.09 ± 0.01 IU/mL) groups compared to the control mice (1.46 ± 0.9 IU/mL) (**Figure 2.8a**). In a similar experiment, 0.5 mg/kg fondaparinux (~5-fold the therapeutic dose) was injected subcutaneously, and after 10 minutes, protamine (16 mg/kg), oxalyl surfen (16 mg/kg) or vehicle control were injected intravenously. Fondaparinux in plasma was significantly reduced in oxalyl surfen-treated mice compared to the control-treated group (0.14 ± 0.06 mg/L vs. 2.1 ± 0.33 mg/L, respectively) and was equivalent to a 93 ± 2.8 % decrease in anti-FXa activity (**Figure 2.8b**). As previously reported,[26] we found protamine ineffective in neutralizing fondaparinux *in vivo*. The results demonstrate that oxalyl surfen can reverse the anticoagulant activity of fondaparinux *in vitro* and *in vivo* and thus has the potential to be developed as an antidote in humans.

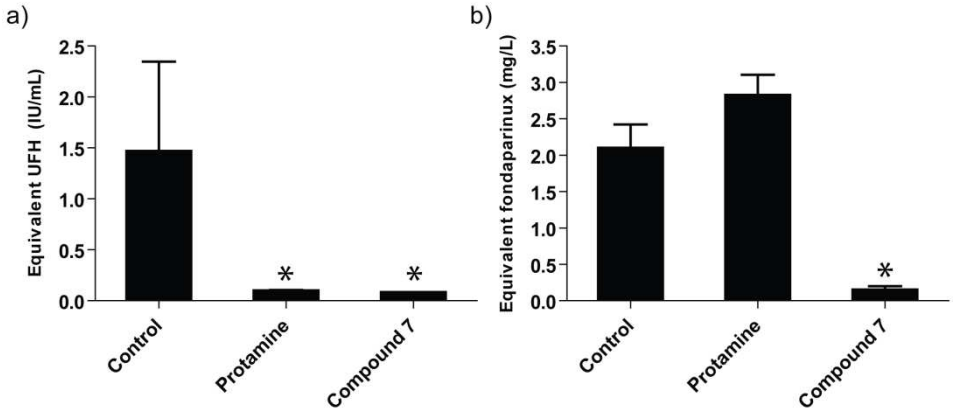

Figure 2.8: *In vivo* neutralization of a) UFH and b) fondaparinux in mice (n = 3 for each group). The values represent the means ± SD. **P* < 0.05 compared with the control group.

2.3 Discussion

Surfen, a dimeric quinoline-containing molecule found in the NCI compound database, was recently described as a small molecule antagonist of certain HS–protein interactions.[19] The nature of the interaction between surfen and HS is not, however, fully understood. To shed light on its interactions with HS and to identify more potent antagonists, several strategically modified surfen analogs were synthesized. Their ability to inhibit the binding of FGF2 to cell-surface HS on wild-type CHO cells was quantified to generate structure-activity relationships. FGF2, a potent mitogen and member of the heparin-binding growth factor family, has been shown to preferentially bind to the 2-*O* sulfated sites of cell surface and extracellular matrix HS (**Figure 2.1**).[30,31] FGF signaling is an essential part of human biology and acts as a regulator of embryonic development, homeostasis, and multiple regenerative processes. However, FGF2's interaction with HS has also been implicated in certain pathophysiological conditions due to this growth factor's up-regulation in certain cancers such as prostate cancer and its action in angiogenesis during tumor growth.[32,33] Therefore, antagonizing FGF2 binding to HS with pharmacological agents has been explored as a feasible approach to regulating tumor growth.[34-36] Similarly, signaling for a transmembrane protein expressed at sites of vascular inflammation, the receptor for advanced glycation end products (RAGE), was recently shown to be dependent on the oligomerization of the protein through the formation of stable RAGE-HS complexes.[29] This protein has been implicated in

many diseases including diabetes, cancer, and Alzheimer's disease. Recent research has explored inhibition of RAGE signaling using different pharmacological agents, including small molecules.[37-39]

In general, surfen analogs with the dimeric aminoquinoline moiety intact showed a dose-dependent inhibition of FGF2 binding similar to that of surfen (**Table 2.1**). Analogs lacking the exocyclic amines on the quinoline ring systems (e.g., **5**, **6**) showed low inhibitory activity (IC_{50} > 100 μM). The lack of improvement in binding seen in these derivatives with modifications at the 4-position is not surprising. The protonated form of 4-aminoquinoline was previously shown to display lower acidity (pK_a ~ 8.5) compared with aminoquinoline derivatives substituted at other positions.[40] Similarly, the basic 4-aminoquinoline moieties of surfen, upon protonation, can electrostatically interact with the negatively charged sulfate and carboxyl groups of HS via hydrogen bonding (Scheme 2.4).

Hemisurfen (**2**) and acetyl-hemisurfen (**3**) did not inhibit FGF2 binding. These derivatives only contain one aminoquinoline moiety, while maintaining a urea or an amide unit mimicking the linker region. The lack of activity of these "monomeric" forms of surfen suggests a critical role for the dimeric structure of the parent molecule. A similar effect was observed recently with a small molecule involved in enhancing cell adhesion through interactions with HS.[41] It is possible that the three dimensional arrangement, length, or valency of surfen-type antagonists could affect their activity and interaction with HS. Investigation of multivalent analogs of HS-binding molecules reported cooperative and enhanced

binding to HS upon increasing the number of cationic HS-binding moieties.[42,43] These findings suggest that surfen analogs that display multiple aminoquinoline moieties might exhibit enhanced binding to HS as well.

Certain analogs with extended linkers (e.g., **7**–**9**, **13**), where the central urea moiety was replaced with a diamide linker, showed enhanced ability to inhibit FGF2 binding to HS compared to surfen. Similarly, **9** also blocked binding of sRAGE to HS. Enhancing the H-bonding ability and spreading the aminoquinoline recognition domains may account for enhanced potency, as engagement with additional sites along the long and heterogeneous HS chains might occur. The enhanced inhibitory activity of the oxalyl (**7**), malonyl (**8**), and succinyl (**9**) analogs compared to surfen (**1**) supports this idea. Interestingly, extending the linker region further (e.g., **10–12**) hinders the interaction with HS and lowers the inhibitory activity, possibly due to their more hydrophobic nature. A similar loss of activity of derivatives with longer linker regions has been previously observed in a study of surfen-type compounds as inhibitors of anaphylatoxic C5a receptor.[23] Due to the decreased activity of derivatives with more hydrophobic linkers, an analog with a more hydrophilic linker region, diglycolyl surfen (**13**), was synthesized. Diglycolyl surfen proved to be the most potent in regards to inhibition of FGF2 binding to HS, suggesting that adding additional H-bonding sites to the linker region enhances the interaction with HS.

The observations discussed above correlating activity and linker lengths are not necessarily universal since the adipoyl surfen analog (**11**) showed better inhibitory activity compared to the glutaryl and pimeloyl analogs (**10** and **12**,

respectively). Other reports have shown that the conformation of the binding domains of certain proteins is critical for their interaction with the anionic sugar residues of glycosaminoglycans, such as HS.[44,45] In a similar way, it is possible that even-numbered linkers, due to preferred hydrocarbon conformation and its impact on the projection of the heterocycles, display a more favorable molecular configuration for binding to HS compared to odd numbered linkers.

To assess the significance of the urea core, it was modified to a thiourea, while the rest of the structure was kept intact. Although a minor modification in regards to the entire molecular structure, the thio surfen analog (**4**) displayed lower FGF inhibitory potency compared to surfen, due to altered hydrogen bonding.[46,47] Consequently, thio surfen is a less active HS antagonist compared to surfen, although it remains a micromolar inhibitor under the conditions of our assays.

Heparin, a highly sulfated form of HS, binds to antithrombin III (AT), a serine protease inhibitor found in the coagulation cascade, and facilitates a conformational change that accelerates the inhibition of coagulation factors such as factor Xa and thrombin.[48] Heparin has been used as an anticoagulant agent in surgery and treatment for certain thrombotic diseases for many years. However, adverse side effects can occur in some patients including excessive bleeding and thrombocytopenia.[49] Numerous agents have been developed over the years to neutralize heparin.[13,14,50-55] Currently, protamine, a mixture of arginine-rich proteins (MW ~5,000) is approved therapeutically for reversing the action of heparin in patients. However, protamine has displayed adverse side effects in

some patients and demonstrates low efficacy towards reversing more recently developed low molecular weight heparins (LMWH), such as enoxaparin, and it is ineffective in neutralizing fondaparinux, a synthetic pentasaccharide analog of heparin.[56-61]

Interestingly, selected surfen analogs showed complete neutralization of unfractionated heparin (UFH), LMWH (enoxaparin) and the synthetic pentasaccharide(fondaparinux) both *in vitro* (**Figure 2.7**) and *in vivo* (**Figure 2.8**). Surfen (**1**) and oxalyl surfen (**7**) displayed the highest potency against each heparinoid (micromolar range), while succinyl surfen (**9**) had the lowest activity. Diglycolyl surfen (**13**) showed high activity against UFH compared to native surfen, while displaying inferior activity against LMWH. It appears that analogs with longer linker regions (**9**, **13**) display lower activity against LMWH compared to surfen and oxalyl surfen (**1**, **7**). All four surfen analogs tested show a potency trend of UFH > enoxaparin > fondaparinux, suggesting that neutralization may depend on the number of potential binding sites in the substrate. Although not studied here, we suspect that surfen molecules could align along each negatively-charged sugar chain in a cooperative manner and block the necessary AT binding sites. Regardless of their mechanism, these findings suggest that surfen analogs, such as oxalyl surfen, could be alternatives for protamine and can be further developed as therapeutic agents.

2.4 Conclusions

In this study, a collection of surfen analogs was synthesized to illuminate their interaction with HS and to look for more potent HS antagonists. A cell culture-based structure-activity relationship, generated by monitoring the inhibition of FGF2 binding, suggests that the dimeric structure, exocyclic amines, and urea linker region play essential roles in the interaction of surfen with HS. Conserving the dimeric aminoquinoline moieties preserved the biological activity of the molecule, while certain modifications to the linker region either lowered or enhanced their antagonistic properties suggesting the hydrogen bonding capability of the linker as well as the separation and orientation of the heterocycles can impact the interaction with HS. Some extended analogs of surfen proved to be more potent antagonists of FGF2 binding to HS. Furthermore, these molecules were shown to dose-dependently antagonize the HS-binding of soluble RAGE protein and neutralize UFH and LMWH in a factor Xa chromogenic assay. Finally, a potent surfen analog was shown to neutralize heparin and fondaparinux *in vivo* in mice. Taken together, these findings illustrate the potential of small molecules as antagonists of heparan sulfate and raise the possibility of using surfen-type compounds to serve as biochemical tools and as potential effectors in disorders that involve glycosaminoglycan–protein interactions.

2.5 Experimental

Mice

Eight-week old C57BL/6 mice were purchased from Charles Rivers Laboratories. All animals were housed in barrier conditions in the vivaria of the School of Medicine of the University of California San Diego that were approved by the Association for Assessment and Accreditation of Laboratory Animal Care. All procedures were approved by the local Animal Care Program. Mice were maintained on a 12-hour light–dark cycle, and were fed ad libitum water and PicoLab 5053 rodent chow.

Materials

Unless otherwise specified, materials purchased from commercial suppliers were used without further purification. Surfen (bis-2-methyl-4-amino-quinolyl-6-carbamide) was obtained from the Open Chemical Repository in the Developmental Therapeutic Program of the National Cancer Institute (NSC12155). All other anhydrous solvents and reagents were purchased from Sigma-Aldrich, with the exception of 4M HCl in 1,4-dioxane (Alfa-Aesar) and 6-amino-2-methylquinoline (Acros Organics). NMR solvents were purchased from Cambridge Isotope Laboratories (Andover, MA). Basic FGF2 (E. Coli recombinant) was purchased from Peprotech, and the sulfo-NHS-LC-Biotin linker was purchased from Thermo Scientific. PBS (Dulbecco's phosphate buffered saline), F12 Media, Cell Dissociation Buffer (PBS-based, Enzyme Free), and streptavidin-Cy5 were purchased from Life Technologies (Carlsbad, CA). FACS

buffer (Isotonic solution 0.85% w/v, phosphate buffered pH 7.1–7.3) and streptavidin-PE-Cy5 were purchased from BD Biosciences. Trypsin/EDTA was purchased from VWR (Mediatech). Tissue culture plates (20 mm) were from BD Falcon (BD Biosciences). Heparin (Scientific Protein Laboratories, 188.9 IU/mg), enoxaparin sodium (Lovenox®, 100 mg/mL) and fondaparinux sodium (Arixtra®, 5 mg/mL) were obtained from their manufacturers. Salmon protamine (Grade IV) was purchased from Sigma-Aldrich.

Instrumentation

NMR spectra were recorded on Varian Mercury 300 and 400 MHz, and Varian VX 500 MHz spectrometers. Mass spectra were recorded at the UCSD Chemistry and Biochemistry Mass Spectrometry Facility, utilizing an Agilent 6230 HR-ESI-TOF mass spectrometer. Flow cytometry studies were performed on a BD FACSCalibur. Absorbance measurements for the factor Xa assay were performed on a VersaMax microplate reader (Molecular Devices) using Softmax Pro software.

Synthesis of Quinoline Building Blocks

The synthesis for ethyl-β-(*p*-acetamidophenylamino) crotonate (**16**), 6-acetamido-4-hydroxyquinaldine (**17**), 6-Acetamido-4-methoxyquinaldine (**18**), 4,6-diaminoquinaldine (**19**), and 6-amino-4-methoxyquinaldine (**20**) were previously reported.[23,62,63]

Synthesis of Surfen Analogs

The synthesis for certain analogs (**3, 7**–**12**) was adapted from previously published procedures.[23,62]

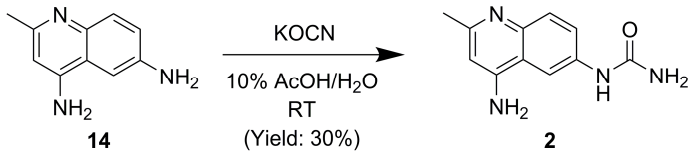

Scheme 2.5: Synthesis of hemisurfen (**2**).

(4-amino-2-methyl-6-quinolyl)-urea (hemisurfen) (2). 4,6-diamino-2-methylquinoline (**14**) (40 mg, 0.23 mmol) was suspended in water (1 ml). Potassium cyanate (22.5 mg, 0.28 mmol), dissolved in 0.8 ml of 10% acetic acid, was added dropwise to the suspension at room temperature and allowed to react overnight. Once the reaction was complete, 37% NaOH was added dropwise to the reaction mixture until basic. A precipitate formed overnight. The crude solid was filtered, washed with water, and dried overnight. The solid was recrystallized from water. Product: tan solid (15 mg, 0.069 mmol, 30%). ^{1}H NMR (400 MHz, DMSO-d_6): δ 8.48 (s, 1H), 7.83 (d, J = 2 Hz, 1H), 7.61 (d, J = 2.4 Hz, 1H), 7.55 (d, J = 9.2 Hz, 1H), 6.38 (s, 1H), 6.31 (brd, 2H), 5.91 (brd, 2H), 2.36 (s, 3H). ^{13}C NMR (125 MHz, DMSO-d_6): δ 156.13, 155.97, 150.67, 144.48, 135.53, 128.35, 122.85, 117.48, 108.81, 102.29, 24.60. HR-ESI-MS calculated for $C_{11}H_{13}N_4O$ $[M+H]^+$ 217.1084, found 217.1083.

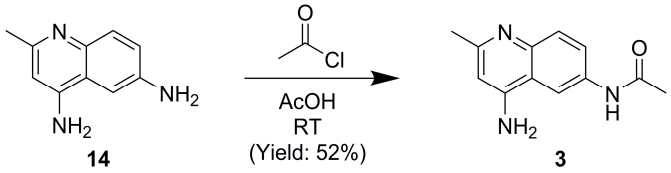

Scheme 2.6: Synthesis of acetyl-hemisurfen (**3**).

6-Acetamido-4-aminoquinaldine (acetyl-hemisurfen) (3). 4,6-diamino-2-methyl-quinoline (**14**) (40 mg, 0.23 mmol) was dissolved in glacial acetic acid (0.5 ml) under argon. Acetyl chloride (16.4 µl, 0.23 mmol) was slowly added. The mixture was stirred for 3 hours at room temperature and a heavy precipitate formed. Diethyl ether (3 ml) was added to the reaction mixture, and the solid was filtered and washed with diethyl ether. The hydrochloride salt was dissolved in 4 ml of warm water, cooled to room temperature, and made basic with 37% NaOH. The precipitated solid was filtered, washed with water, and dried under high vacuum overnight. The crude product was then recrystallized from water. Product: tan solid (25 mg, 0.12 mmol, 52%). ^{1}H NMR (400 MHz, DMSO-d_6): δ 10.00 (s, 1H), 8.16 (s, 1H), 7.65-7.47 (m, 2H), 6.41 (s, 1H), 6.35 (brd, 2H), 2.37 (s, 3H), 2.07 (s, 3H). ^{13}C NMR (125 MHz, DMSO-d_6): δ 168.19, 156.95, 151.07, 145.50, 134.03, 128.59, 123.46, 117.29, 111.25, 102.50, 24.77, 23.89. HR-ESI-MS calculated for $C_{12}H_{14}N_3O$ $[M+H]^+$ 216.1131, found 216.1132.

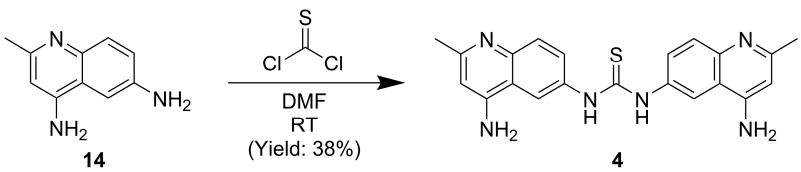

Scheme 2.7: Synthesis of thio surfen (**4**).

***N,N*'-bis-(4-amino-2-methyl-6-quinolyl)-thiourea (thio surfen) (4).** 4,6-diamino-2-methyl-quinoline (**14**) (100 mg, 0.58 mmol) was dissolved in dry DMF (0.6 ml) under argon. The solution was placed on ice and thiophosgene (TOXIC! 22.1 µl, 0.29 mmol) was slowly added. The mixture was stirred overnight and allowed to return to room temperature. A precipitate formed overnight with stirring. Methanol (2 ml) was added to quench any remaining thiophosgene. The reaction mixture was evaporated to dryness and dried under high vacuum overnight. The crude product was dissolved in 7.5 ml of warm water. The solution was cooled to room temperature and made basic with 37% NaOH. The precipitated solid was filtered, washed with water, and dried overnight under high vacuum. Recrystallization was accomplished by dissolving the solid in a minimum amount of hot DMF, filtering, and adding diethyl ether until the solution became turbid. The crystals were collected by filtration, washed with ether, and dried under high vacuum. Product: dark yellow solid (43 mg, 0.11 mmol, 38%). IR spectrum: 1631 cm^{-1} (C=S). ^{1}H NMR (400 MHz, DMSO-d_6): δ 9.79 (s, 2H), 7.93 (s, 2H), 7.68–7.53 (m, 4H), 6.57 (brd, 4H), 6.41 (s, 2H), 2.39 (s, 6H). ^{13}C NMR (125 MHz, DMSO-d_6): δ 180.74, 157.57, 151.24, 146.30, 134.07, 128.31, 127.85, 117.72, 116.92, 102.02, 24.55. HR-ESI-MS calculated for $C_{21}H_{21}N_6S$ $[M+H]^+$ 389.1543, found 389.1542.

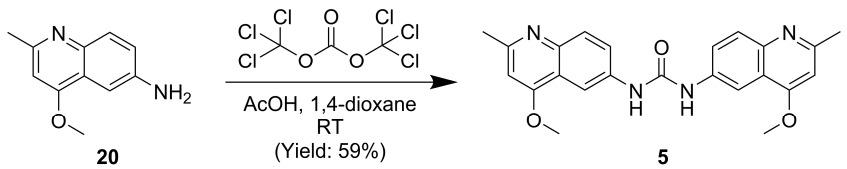

Scheme 2.8: Synthesis of methoxy surfen (**5**).

1,3-bis(4-methoxy-2-methyl-6-quinolyl)-urea (methoxy surfen) (5). 6-amino-4-methoxyquinaldine (**20**) (105 mg, 0.56 mmol) was dissolved in glacial acetic acid (3 mL) under argon. Triphosgene (TOXIC! 28 mg, 0.093 mmol) was dissolved in dioxane (150 µL) and slowly added to the reaction mixture. A heavy precipitate formed, and the reaction was stirred at room temperature for 2 hrs. Methanol (8 mL) was added to the solution to quench any unreacted triphosgene. The solution was then evaporated and the residue co-evaporated with toluene to azeotropically remove remaining acetic acid. The product was then dried under high vacuum. The hydrochloride salt was dissolved in warm water (2 ml). The solution was cooled to room temperature and was made basic with 37% NaOH. The precipitated solid was filtered, washed with water, and dried on high vacuum overnight. Recrystallization was accomplished by dissolving the solid in a minimum amount of hot DMF, filtering, and adding diethyl ether until the solution became turbid. The crystals were collected by filtration, washed with ether, and dried under high vacuum. Product: tan solid (22 mg, 0.055 mmol, 59%). ^{1}H NMR (400 MHz, DMSO-d_6): δ 9.03 (s, 2H), 8.41 (d, J = 2.3 Hz, 2H), 7.78 (d, J = 9.0 Hz, 2H), 7.58 (dd, J = 9.0, 2.4 Hz, 2H), 6.89 (s, 2H), 4.04 (s, 6H), 2.58 (s, 6H). ^{13}C NMR (125 MHz, DMSO-d_6): δ 160.95, 157.61, 152.56, 144.32, 136.28, 128.41, 122.70, 119.55, 107.37. 101.36, 55.80, 25.09. HR-ESI-MS calculated for $C_{23}H_{23}N_4O_3$ $[M+H]^+$ 403.1765, found 403.1766.

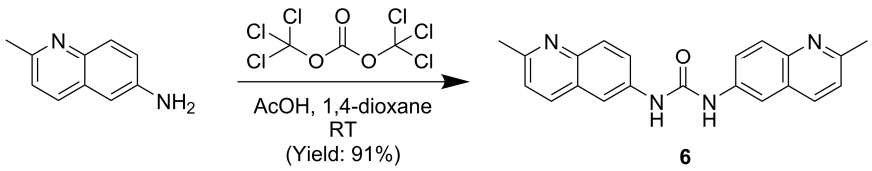

Scheme 2.9: Synthesis of deaminated surfen (**6**).

1,3-bis(2-methyl-6-quinolyl)-urea (deaminated surfen) (6). 6-Amino-2-methylquinoline (106 mg, 0.67 mmol) was dissolved in glacial acetic acid (2 mL) under argon. Triphosgene (TOXIC! 33 mg, 0.11 mmol) was dissolved in 150 µL of dioxane and slowly added dropwise to the reaction mixture. A heavy precipitate formed, and the reaction was stirred at room temperature for 2 hours. Next, 8 mL of methanol was added to the solution to quench any unreacted triphosgene. Solution was then rotoevaporated completely. Toluene was added to the reaction flask and rotoevaporated to aziotrope remaining acetic acid. The crude product was dried on high vacuum overnight. The hydrochloride salt was dissolved in 2 ml of warm water, the solution was cooled to room temperature, and it was made basic with 37% NaOH. The precipitated solid was filtered, washed with water, and dried on high vacuum overnight. Recrystallization was accomplished by dissolving the solid in a minimum amount of hot DMF, filtering, and adding diethyl ether until the solution became turbid. The crystals were collected by filtration, washed with diethyl ether, and dried under high vacuum. Product: tan solid (35 mg, 0.10 mmol, 91%). ^{1}H NMR (400 MHz, DMSO-d_6): δ 9.09 (s, 2H), 8.17 (d, J = 4.9 Hz, 2H), 8.14 (s, 2H), 7.85 (d, J = 8.9 Hz, 2H), 7.67 (d, J = 8.9 Hz, 2H), 7.36 (d, J = 8.4 Hz, 2H), 2.62 (s, 6H). ^{13}C NMR (125 MHz, DMSO-d_6): δ 156.62, 152.78, 143.82, 136.93, 135.46, 128.86, 126.82, 122.90,

122.50, 113.39, 24.71. HR-ESI-MS calculated for $C_{21}H_{19}N_4O$ $[M+H]^+$ 343.1553, found 343.1551.

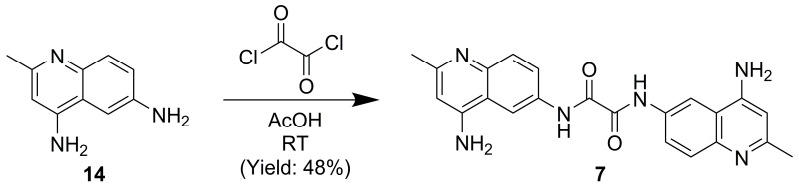

Scheme 2.10: Synthesis of oxalyl surfen (**7**).

Bis(4-amino-2-methyl-6-quinolyl)-oxalamide (oxalyl surfen) (7). 4-6-diamino-2-methyl-quinoline (**14**) (100 mg, 0.58 mmol) was dissolved in glacial acetic acid (0.6 ml) under argon. Oxalyl chloride (25 µl, 0.29 mmol) was slowly added to the solution. A heavy precipitate formed, and the mixture was stirred for 1 hour at room temperature. After addition of diethyl ether (2.5 ml), the solid was filtered, washed with diethyl ether and dried under vacuum overnight. The hydrochloride salt was dissolved in warm water (8 ml), the solution was cooled to room temperature, and it was made basic with 37% NaOH. The precipitated solid was filtered, washed with water, and dried on high vacuum. Recrystallization was accomplished by dissolving the solid in a minimum amount of hot DMF, filtering, and adding diethyl ether until the solution became turbid. The crystals were collected by filtration, washed with ether, and dried under high vacuum. Product: tan solid (54 mg, 0.14 mmol, 48%). ^{1}H NMR (400 MHz, DMSO-d_6): δ 10.85 (s, 2H), 8.36 (d, J = 1.6 Hz, 2H), 7.91 (d, J = 9.0 Hz, 2H), 7.69 (d, J = 9.0 Hz, 2H), 6.49 (brd, 4H), 6.46 (s, 2H), 2.41 (s, 6H). ^{13}C NMR (125 MHz, DMSO-d_6): δ

158.49, 157.68, 151.11, 146.07, 132.06, 128.52, 123.93, 116.99, 113.50, 102.43, 24.65. HR-ESI-MS calculated for $C_{22}H_{21}N_6O_2$ $[M+H]^+$ 401.1721, found 401.1722.

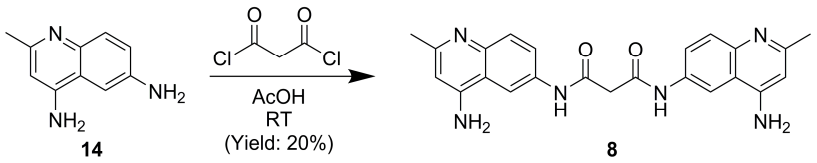

14 **8**

Scheme 2.11: Synthesis of malonyl surfen (**8**).

N,N'-bis(4-amino-2-methylquinolin-6-yl)malonamide (malonyl surfen) (8). 4-6-diamino-2-methyl-quinoline (**14**) (60 mg, 0.35 mmol) was dissolved in glacial acetic acid (0.3 ml) under argon. Malonyl chloride (16.8 µl, 0.17 mmol) was slowly added to the solution. A heavy precipitate formed, and the mixture was stirred for 1 hour at room temperature. After addition of diethyl ether (2 mL), the solid was filtered, washed with diethyl ether, and dried under vacuum overnight. The hydrochloride salt was dissolved in 4 ml of warm water, the solution was cooled to room temperature, and it was made basic with 37% NaOH. The precipitated solid was filtered, washed with water, and dried on high vacuum overnight. Recrystallization was accomplished by dissolving the solid in a minimum amount of hot DMF, filtering, and adding diethyl ether until the solution became turbid. The crystals were collected by filtration, washed with ether, and dried under high vacuum. Product: tan solid (14.1 mg, 0.034 mmol, 20%). ^{1}H NMR (400 MHz, DMSO-d_6): δ 10.35 (s, 2H), 8.26 (s, 2H), 7.69-7.63 (m, 4H), 6.59 (brd, 4H), 6.43 (s, 2H), 3.58 (s, 2H), 2.39 (s, 6H). ^{13}C NMR (125 MHz, DMSO-d_6): δ 165.41, 156.66, 151.53, 146.83, 133.86, 128.04, 123.45, 117.09, 111.22,

102.45, 45.47, 24.31. HR-ESI-MS calculated for $C_{23}H_{22}N_6O_2$ $[M+H]^+$ 415.1877, found 415.1874.

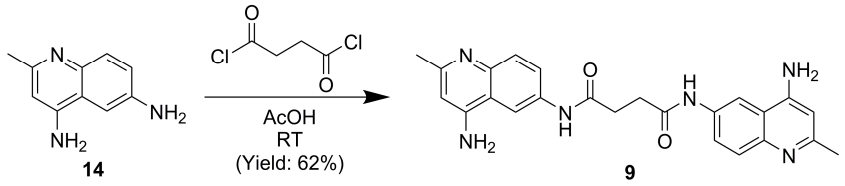

Scheme 2.12: Synthesis of succinyl surfen (**9**).

N,N'-bis(4-azanyl-2-methyl-6-quinolyl)-butanediamide (succinyl surfen) (9). 4-6-diamino-2-methyl-quinoline (**14**) (100 mg, 0.58 mmol) was dissolved in glacial acetic acid (0.6 ml) under argon. Succinyl chloride (32 µl, 0.29 mmol) was slowly added to this solution. A heavy precipitate formed, and the mixture was stirred for 2 hours at room temperature. After addition of diethyl ether (5 ml), the solid was filtered, washed with diethyl ether and dried under high vacuum. The hydrochloride salt was dissolved in warm water (7.5 ml). The solution was cooled to room temperature and was made basic with 37% NaOH. The precipitated solid was filtered, washed with water, and dried on high vacuum. Recrystallization was accomplished by dissolving the solid in a minimum amount of hot DMF, filtering, and adding diethyl ether until the solution became turbid. The crystals were collected by filtration, washed with diethyl ether, and dried under high vacuum. Product: tan solid (75 mg, 0.18 mmol, 62%). ^{1}H NMR (400 MHz, DMSO-d_6): δ 10.12 (s, 2H), 8.24 (s, 2H), 7.64–7.57 (m, 4H), 6.41 (brd, 6H), 2.74 (s, 4H), 2.38 (s, 6H). ^{13}C NMR (125 MHz, DMSO-d_6): δ 170.53, 157.08, 151.28, 145.21,

134.31, 128.45, 123.33, 117.30, 110.70, 102.64, 31.14, 24.60. HR-ESI-MS calculated for $C_{24}H_{24}N_6O_2$ $[M+H]^+$ 429.2034, found 429.2031.

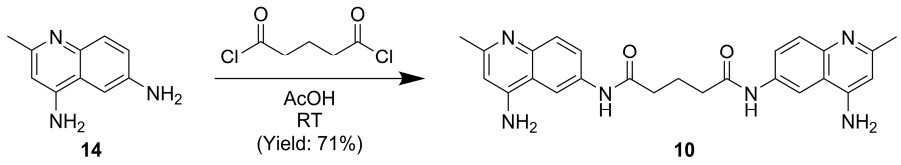

14 10

Scheme 2.13: Synthesis of glutaryl surfen (**10**).

N,N'-bis(4-amino-2-methylquinolin-6-yl)glutaramide (glutaryl surfen) (10). 4-6-diamino-2-methyl-quinoline (**14**) (20 mg, 0.12 mmol) was dissolved in glacial acetic acid (0.3 ml) under argon. Glutaryl chloride (7.4 µl, 0.058 mmol) was slowly added to the solution. A heavy precipitate formed, and the mixture was stirred for 1 hour at room temperature. After addition of diethyl ether, the solid was filtered, washed with diethyl ether and dried under vacuum. The hydrochloride salt was dissolved in warm water, and the solution was cooled to room temperature and made basic with 37% NaOH. The precipitated solid was filtered, washed with water, and dried on high vacuum. Product: tan solid (18 mg, 0.041 mmol, 71%). ^{1}H NMR (500 MHz, DMSO-d_6): δ 10.07 (s, 2H), 8.27 (s, 2H), 7.64–7.56 (m, 4H), 6.56 (s, 2H), 6.42 (brd, 4H), 2.45 (t, J = 7.2 Hz, 4H), 2.39 (s, 6H), 2.03-1.92 (m, 2H). ^{13}C NMR (125 MHz, DMSO-d_6): δ 170.78, 156.47, 151.56, 148.31, 134.27, 127.88, 123.74, 117.13, 111.17, 102.43, 35.46, 24.34, 21.04. HR-ESI-MS calculated for $C_{25}H_{26}N_6O_2$ $[M+H]^+$ 443.2190, found 443.2191.

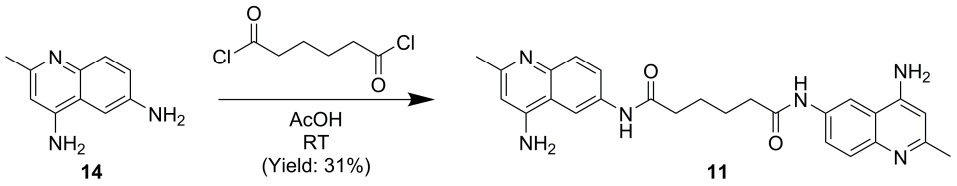

Scheme 2.14: Synthesis of adipoyl surfen (**11**).

N,N'-bis(4-amino-2-methylquinolin-6-yl)adipamide (adipoyl surfen) (11). 4-6-diamino-2-methyl-quinoline (**14**) (50 mg, 0.29 mmol) was dissolved in glacial acetic acid (0.3 ml) under argon. Adipoyl chloride (21 µl, 0.14 mmol) was slowly added to this solution. A heavy precipitate formed, and the mixture was stirred for 1 hour at room temperature. After addition of diethyl ether (2.5 ml), the solid was filtered, washed with diethyl ether and dried under vacuum. The hydrochloride salt was dissolved in warm water (4 ml) and the solution was made basic with 37% NaOH. A solid precipitate formed, and the heterogeneous solution was allowed to cool to room temperature. The precipitated solid was filtered, washed with water, and dried on high vacuum overnight. Recrystallization was accomplished by dissolving the solid in a minimum amount of hot DMF, filtering, and adding diethyl ether until the solution became turbid. The crystals were collected by filtration, washed with ether, and dried under high vacuum. Product: white solid (19.5 mg, 0.043 mmol, 31%). ^{1}H NMR (400 MHz, DMSO-d_6): δ 10.01 (s, 2H), 8.22 (s, 2H), 7.64–7.55 (m, 4H), 6.41 (brd, 6H), 2.43–2.39 (m, 4H), 2.37 (s, 6H), 1.77–1.64 (m, 4H).^{13}C NMR (125 MHz, DMSO-d_6): δ 168.22, 156.92, 151.13, 145.39, 134.06, 128.50, 123.50, 117.27, 111.23, 102.49, ~38.90 (hidden by DMSO solvent peak), 24.72, 23.89. HR-ESI-MS calculated for $C_{26}H_{28}N_6O_2$ $[M+H]^+$ 457.2347, found 457.2346.

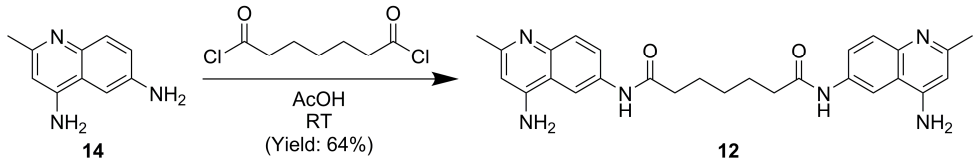

14 12

Scheme 2.15: Synthesis of pimeloyl surfen (**12**).

N,N'-bis(4-amino-2-methylquinolin-6-yl)heptanediamide (pimeloyl surfen) (12). 4-6-diamino-2-methyl-quinoline (**14**) (32 mg, 0.19 mmol) was dissolved in glacial acetic acid (0.3 ml) under argon. Pimeloyl chloride (15 µl, 0.092 mmol) was slowly added to this solution. A heavy precipitate formed, and the mixture was stirred for 1 hour at room temperature. After addition of diethyl ether (2.5 ml), the solid was filtered, washed with diethyl ether and dried under vacuum. The hydrochloride salt was dissolved in warm water (3 ml). The solution was cooled to room temperature and made basic with 37% NaOH. The precipitated solid was filtered, washed with water, and dried on high vacuum. Product: maroon solid (28 mg, 0.059 mmol, 64%). ^{1}H NMR (400 MHz, DMSO-d_6): δ 9.98 (s, 2H), 8.23 (s, 2H), 7.59 (brd, 4H), 6.46 (brd, 4H), 6.42 (s, 2H), 2.38 (brd, 10H), 1.77–1.57 (m, 4H), 1.49–1.30 (m, 2H). ^{13}C NMR (125 MHz, DMSO-d_6): δ 171.21, 156.68, 151.46, 144.90, 134.27, 128.13, 123.68, 117.22, 111.15, 102.50, 36.18, 28.50, 25.11, 24.48. HR-ESI-MS calculated for $C_{27}H_{30}N_6O_2$ $[M+H]^+$ 471.2503, found 471.2504.

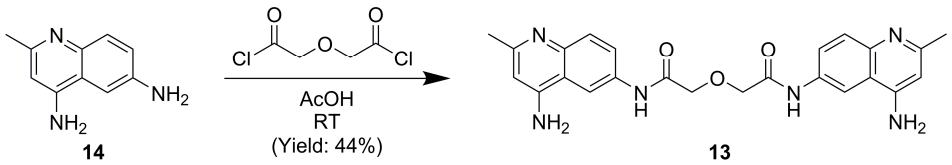

14 13

Scheme 2.16: Synthesis of diglycolyl surfen (**13**).

2,2'-oxybis(N-(4-amino-2-methylquinolin-6-yl)acetamide) (diglycolyl surfen) (13). 4-6-diamino-2-methyl-quinoline (**14**) (40 mg, 0.23 mmol) was dissolved in glacial acetic acid (0.3 ml) under argon. Diglycolyl chloride (13.7 µl, 0.12 mmol) was slowly added to this solution. A heavy precipitate formed, and the mixture was stirred for 1 hour at room temperature. After addition of diethyl ether (2.5 ml), the solid was filtered, washed with diethyl ether and dried under vacuum. The hydrochloride salt was dissolved in warm water (4 ml) and the solution was made basic with 37% NaOH. The solution was allowed to cool to room temperature, and the precipitated solid was filtered, washed with water, and dried under high vacuum. Product: tan solid (23.5 mg, 0.053 mmol, 44%). ^{1}H NMR (400 MHz, DMSO-d_6): δ 10.13 (s, 2H), 8.22 (s, 2H), 7.72 (d, J = 9.2 Hz, 2H), 7.65 (d, J = 9.2 Hz, 2H), 6.45 (s, 4H), 6.43 (s, 2H), 4.33 (s, 4H), 2.39 (s, 6H). ^{13}C NMR (125 MHz, DMSO-d_6): δ 167.87, 157.41, 151.19, 145.89, 132.85, 128.66, 124.25, 117.22, 112.88, 102.49, 70.76, 24.79. HR-ESI-MS calculated for $C_{24}H_{24}N_6O_3$ $[M+H]^+$ 445.1983, found 445.1981.

Spectrum 2.1: Hemisurfen (**2**).

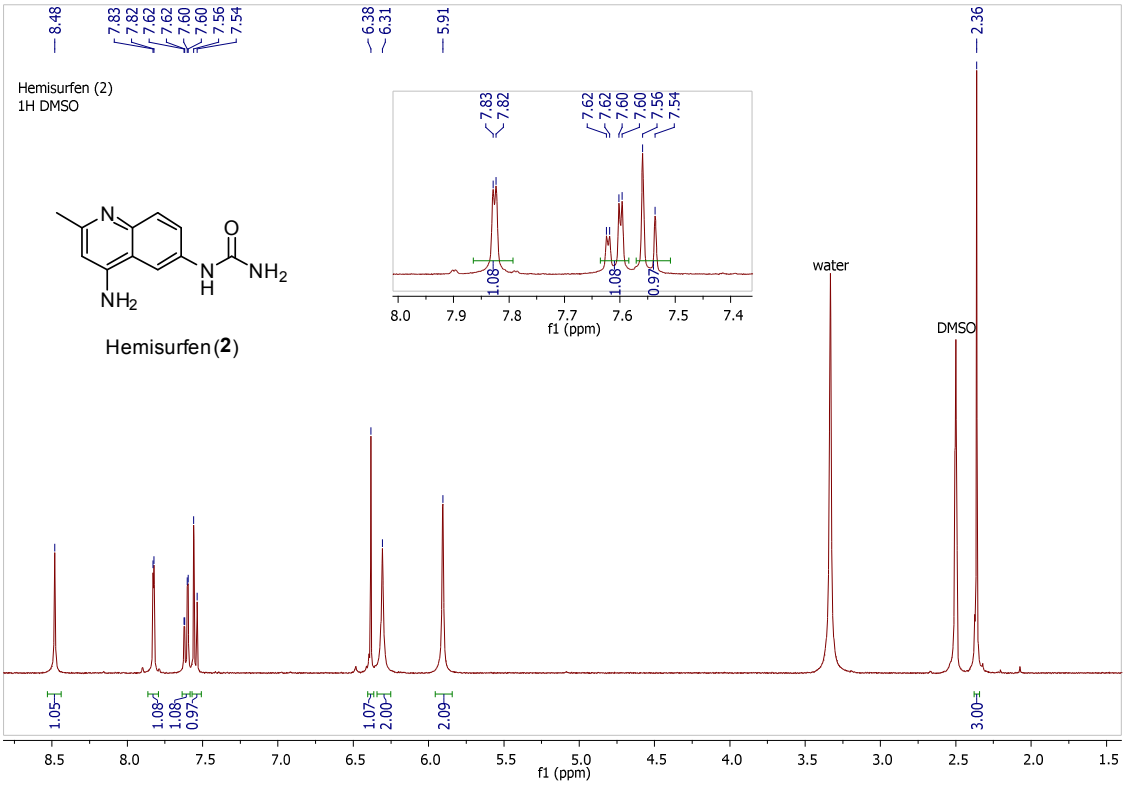

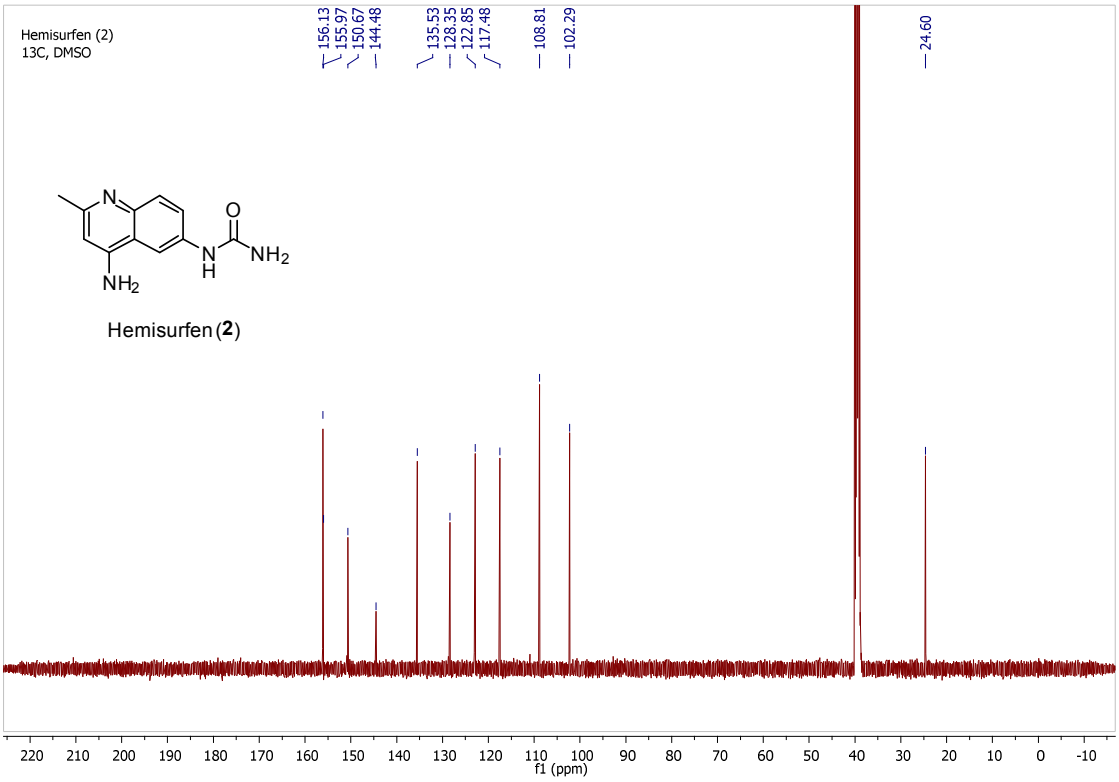

Spectrum 2.2: Acetyl-hemisurfen (**3**).

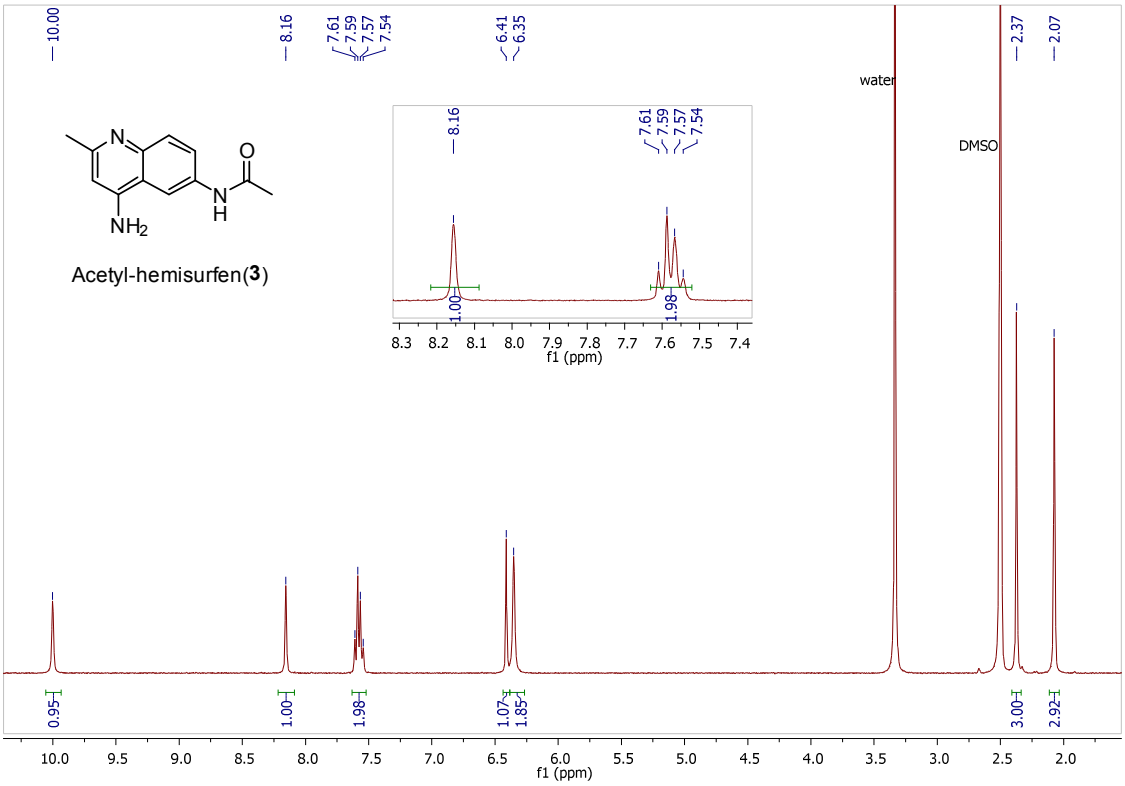

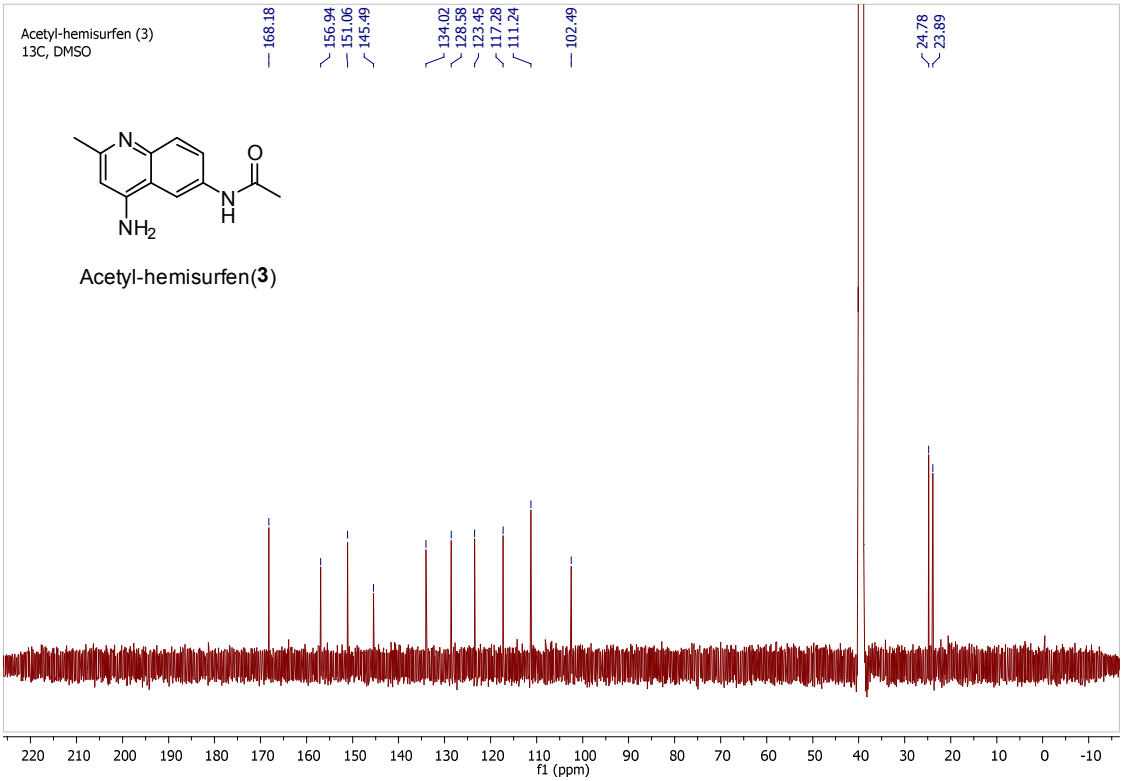

Spectrum 2.3: Thio Surfen (**4**).

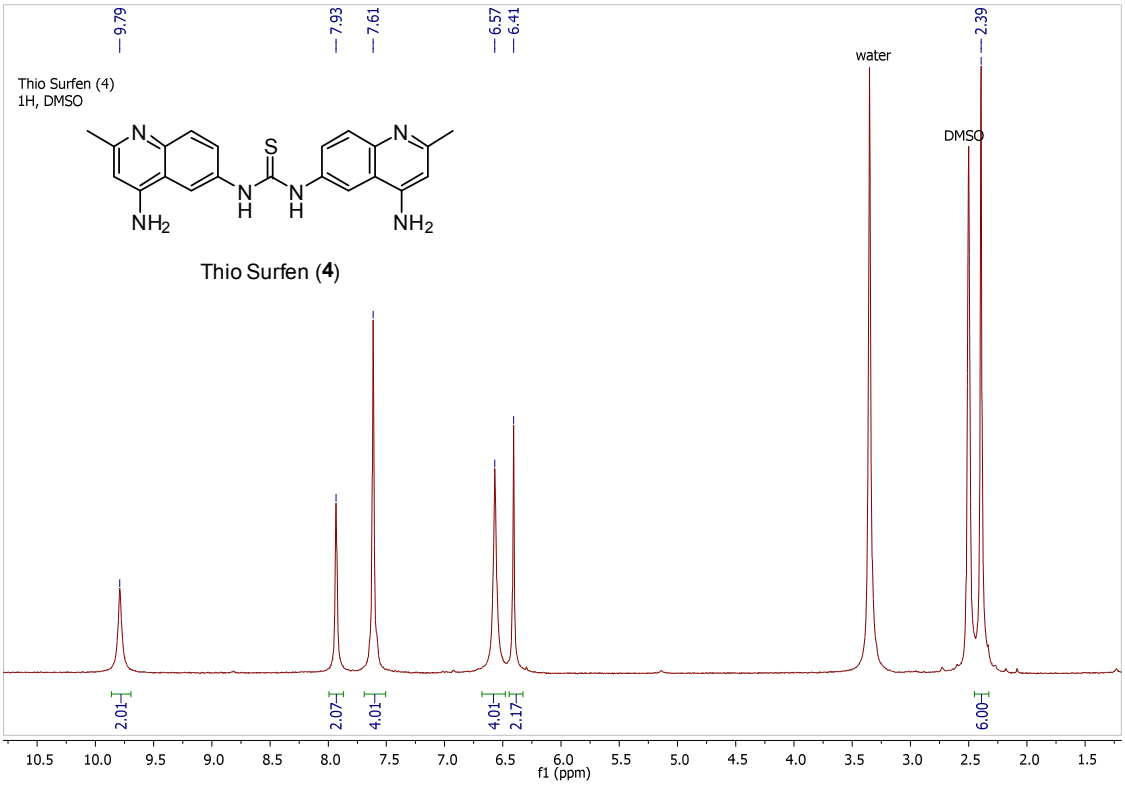

Thio Surfen (**4**)

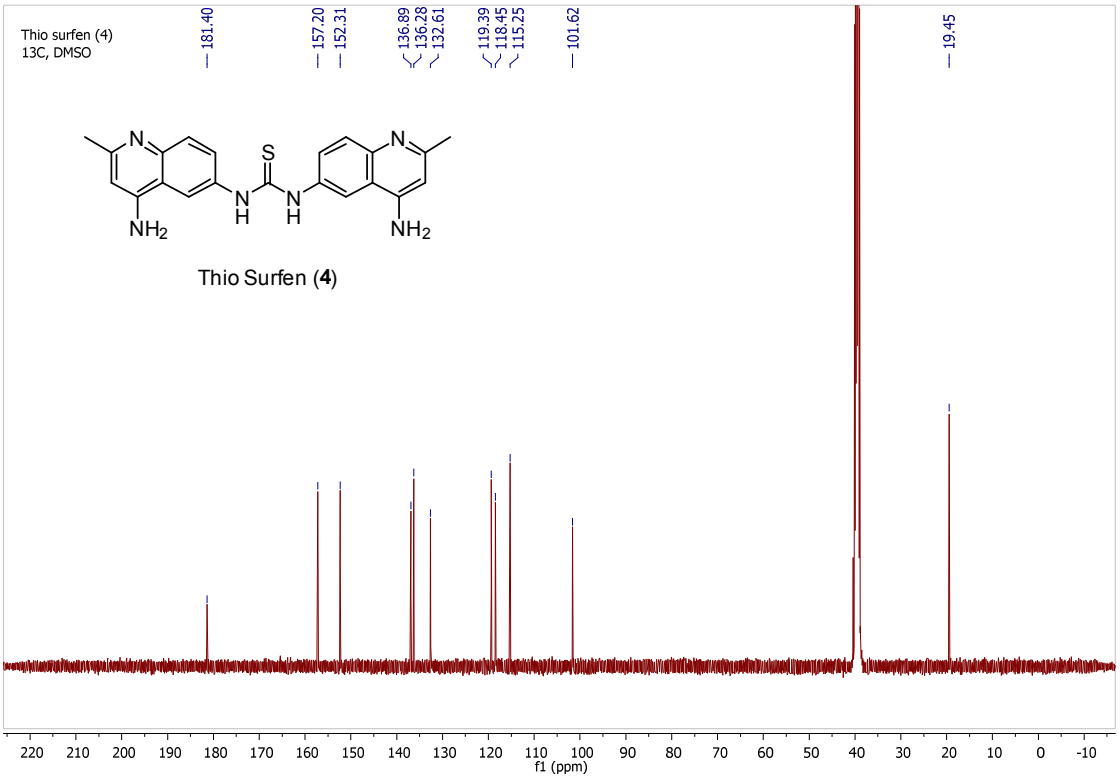

Thio Surfen (**4**)

Spectrum 2.4: Methoxy Surfen (**5**).

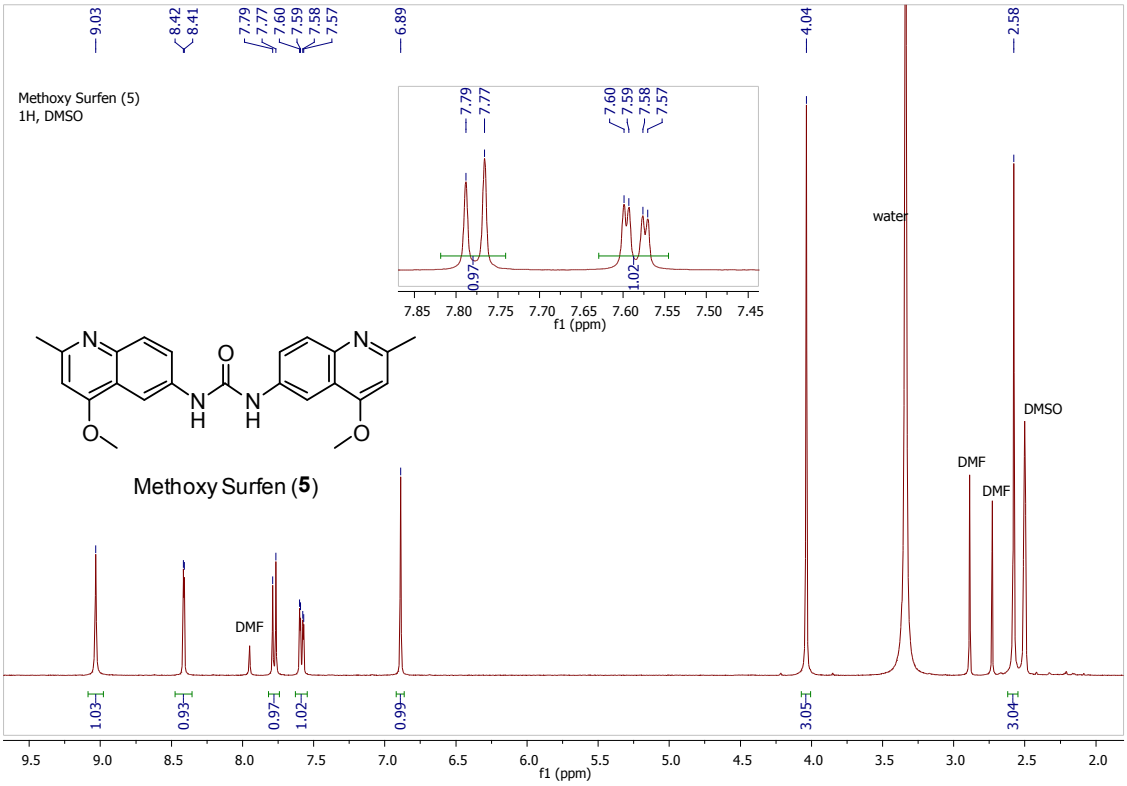

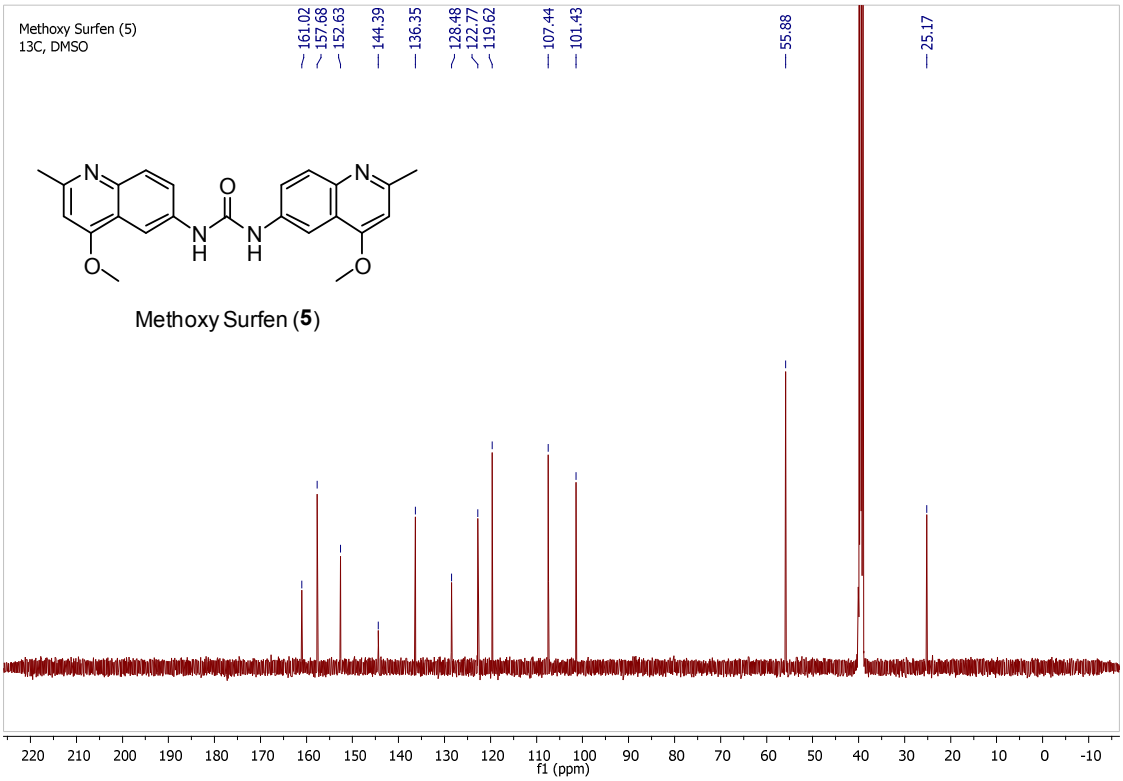

Spectrum 2.5: Deaminated Surfen (**6**).

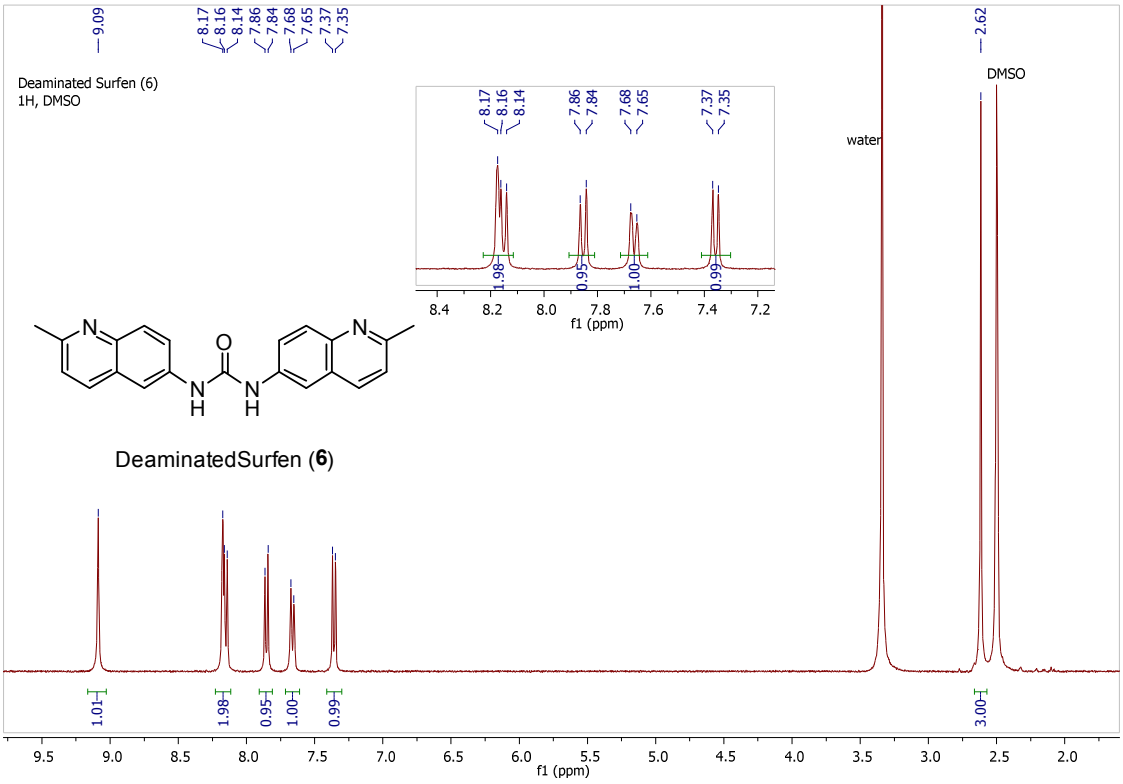

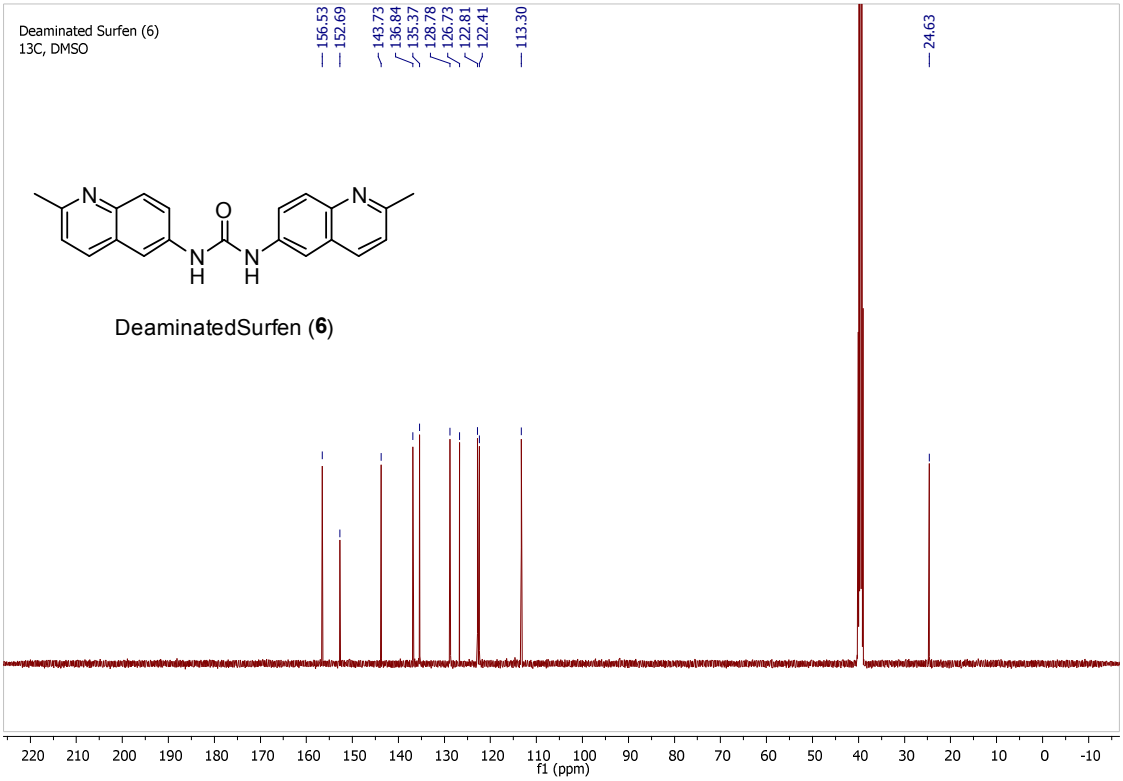

Spectrum 2.6: Oxalyl Surfen (**7**).

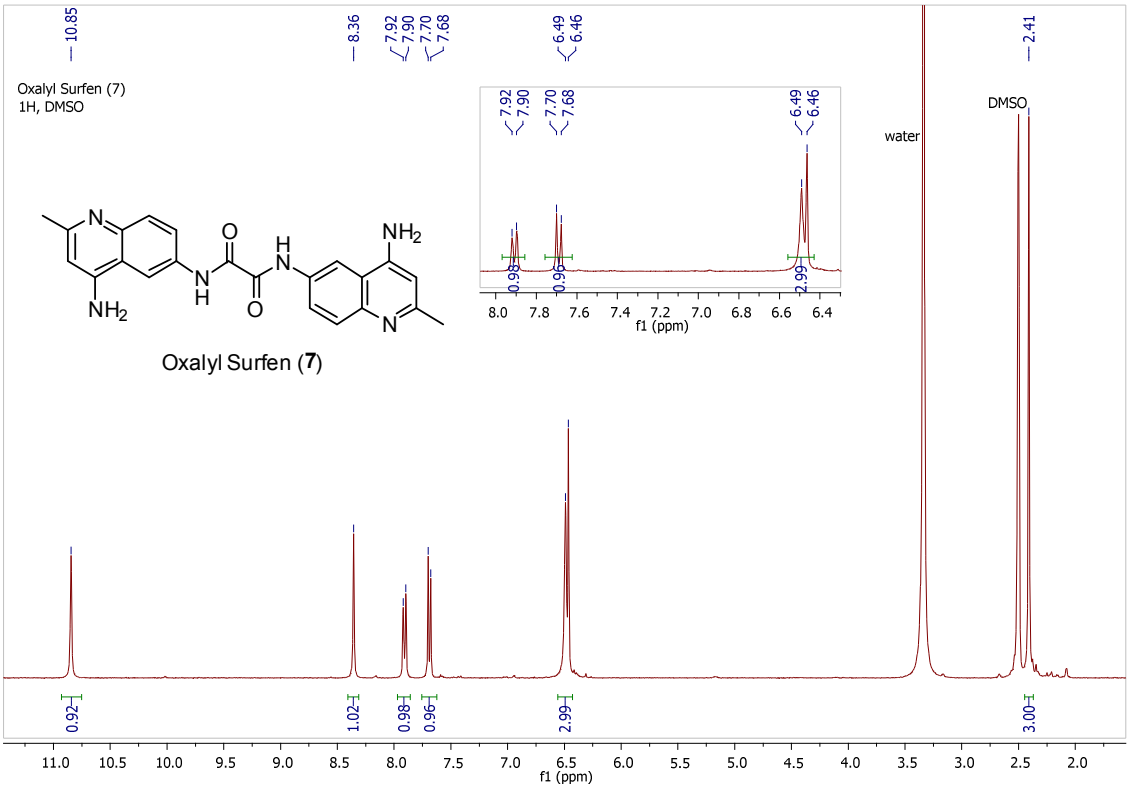

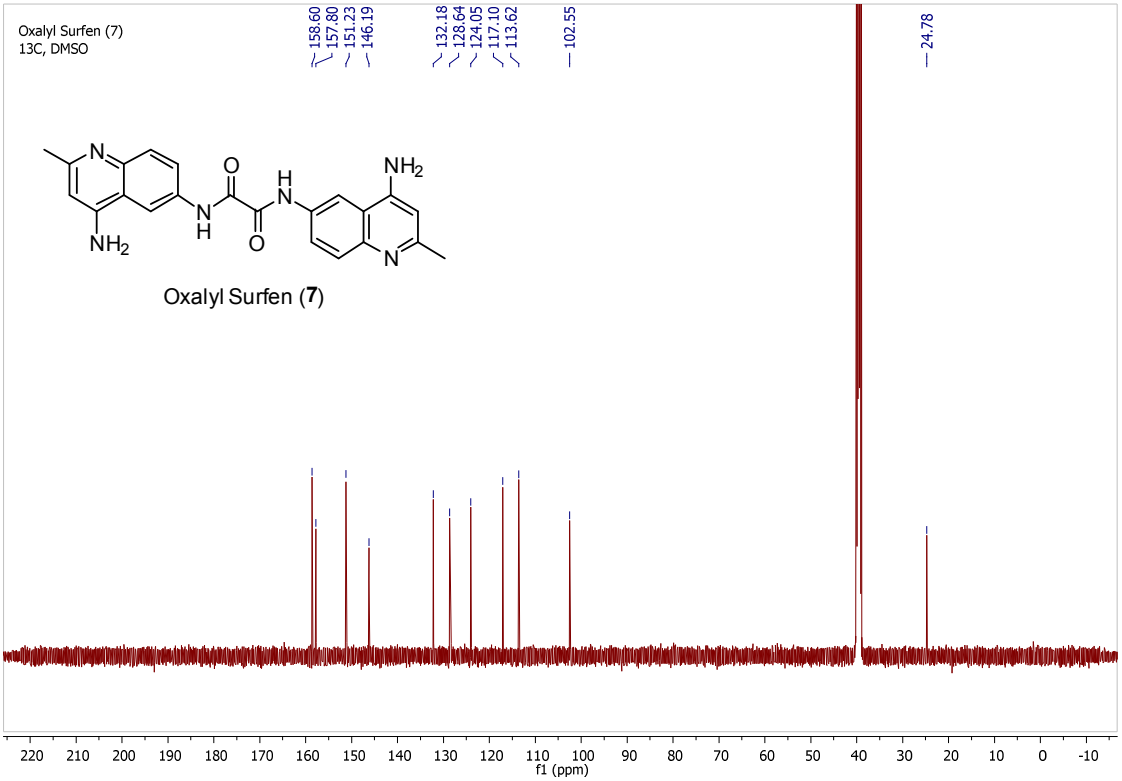

Spectrum 2.7: Malonyl Surfen (**8**).

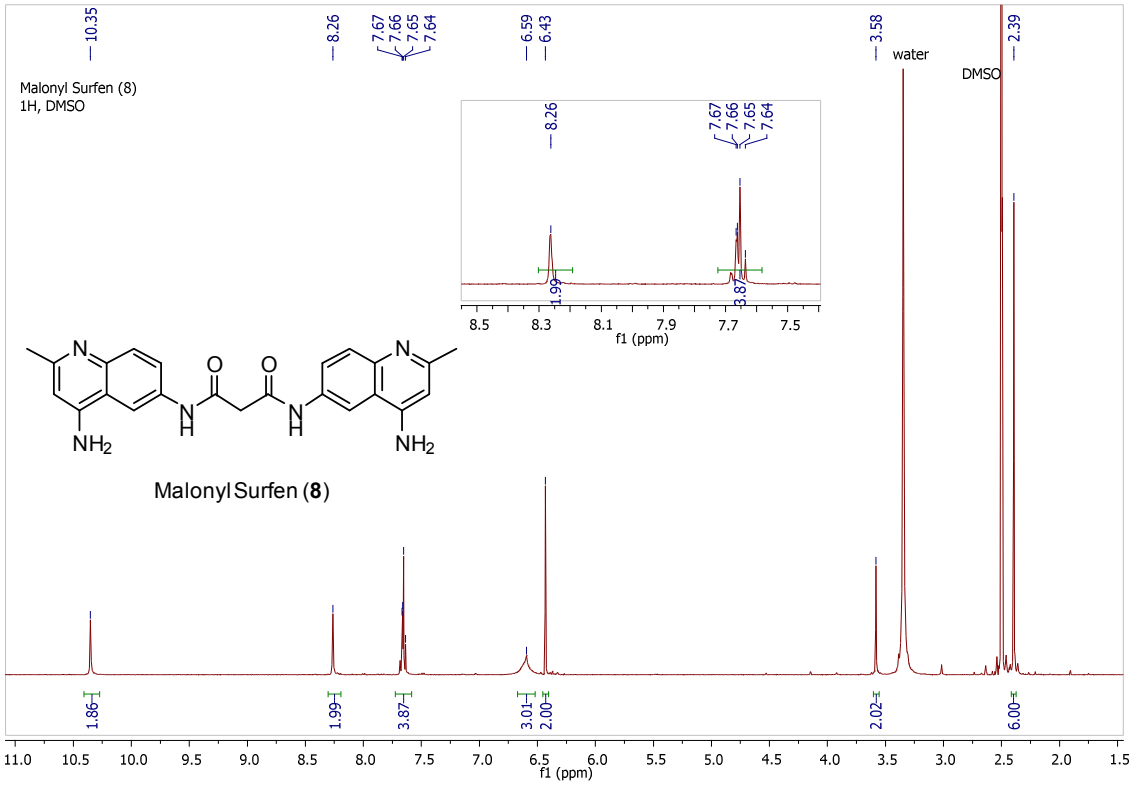

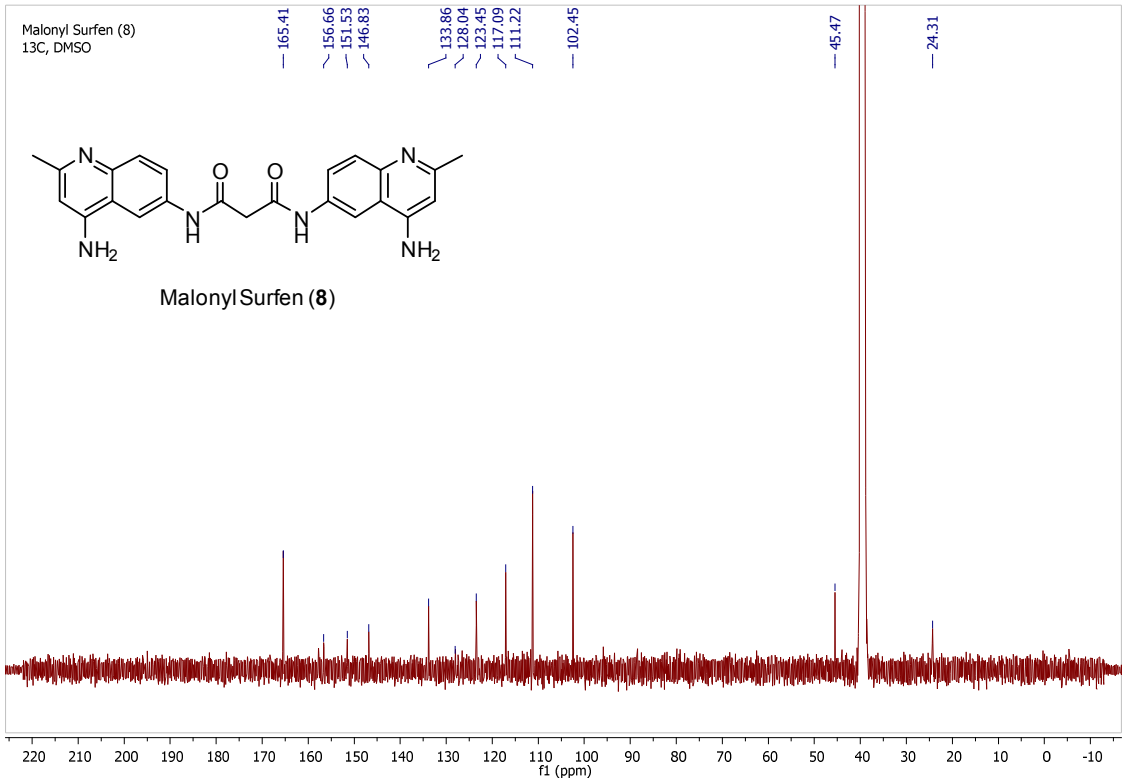

Spectrum 2.8: Succinyl Surfen (**9**).

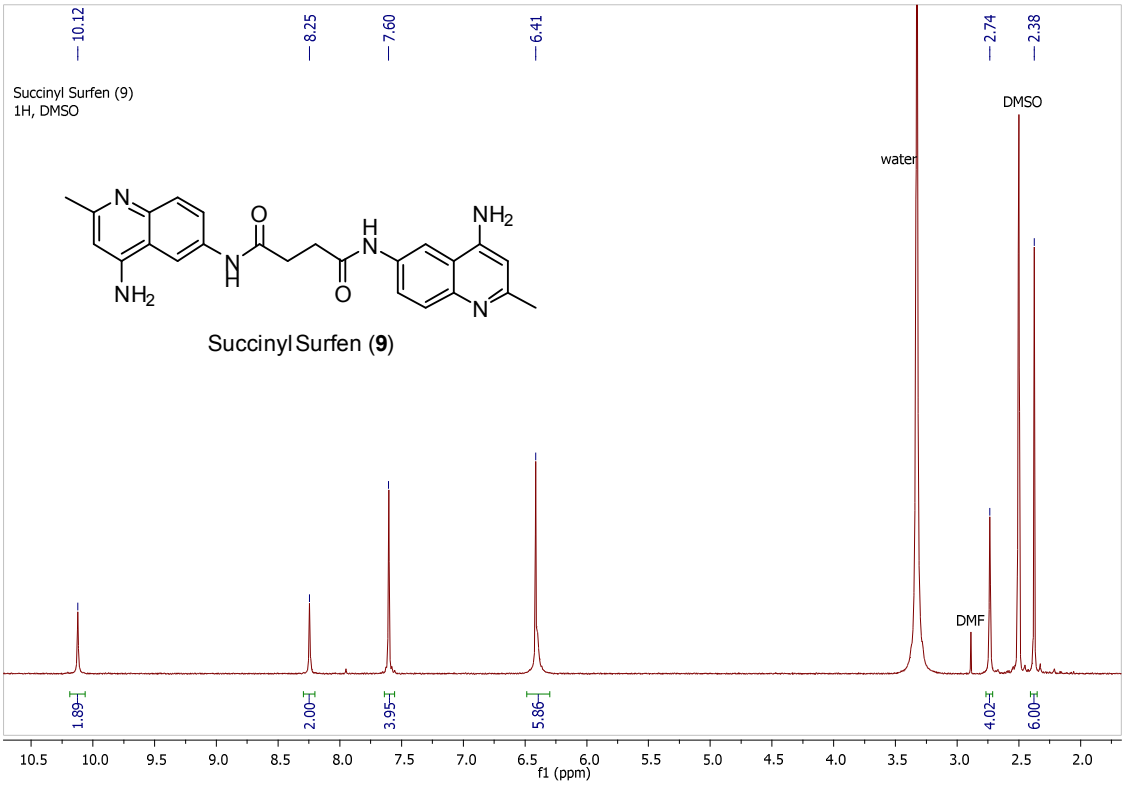

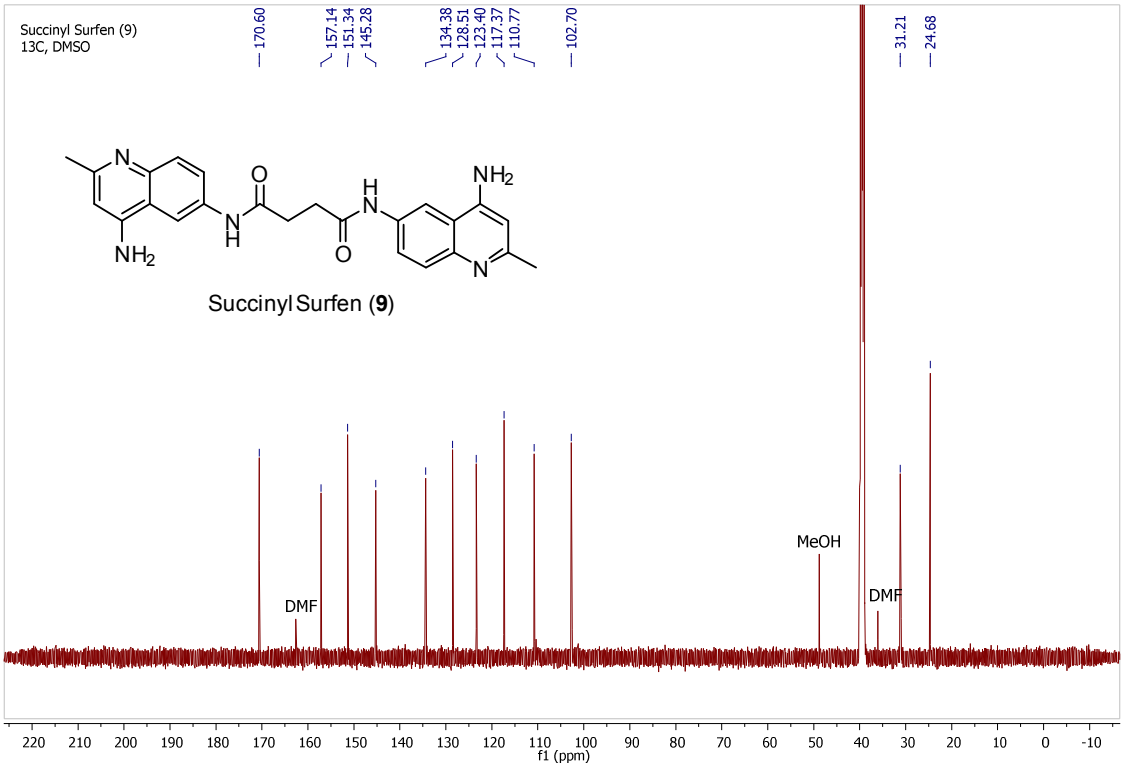

Spectrum 2.9: Glutaryl Surfen (**10**).

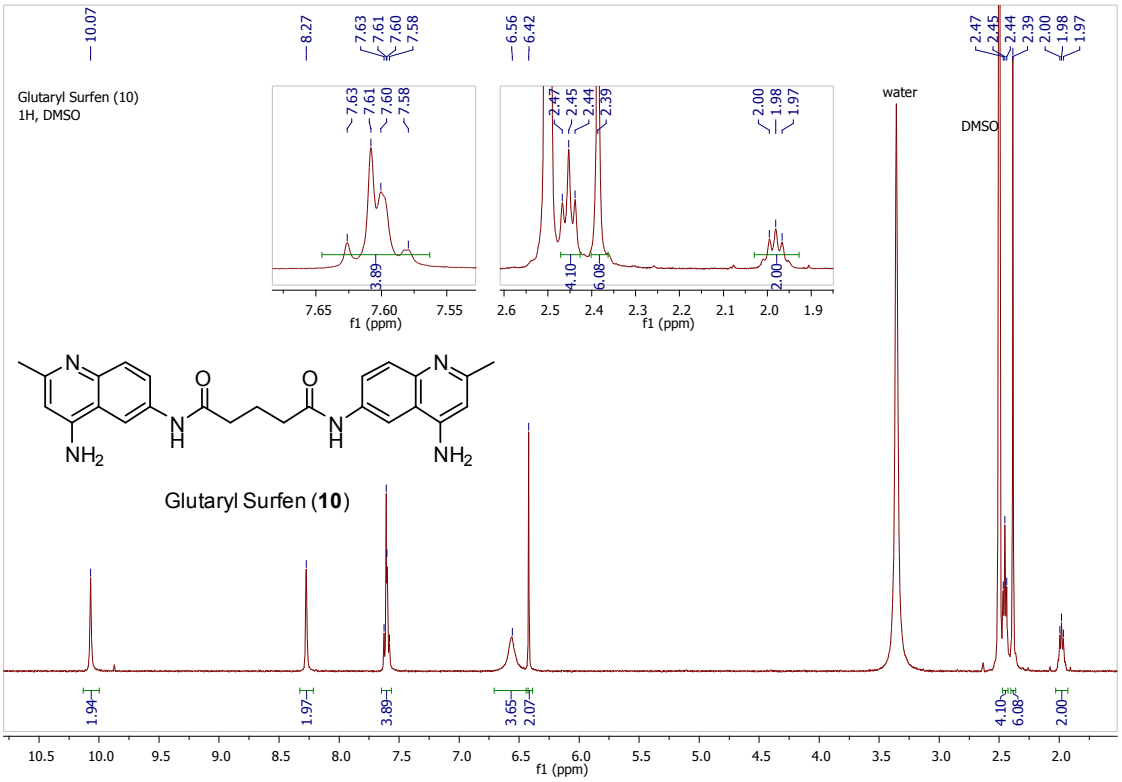

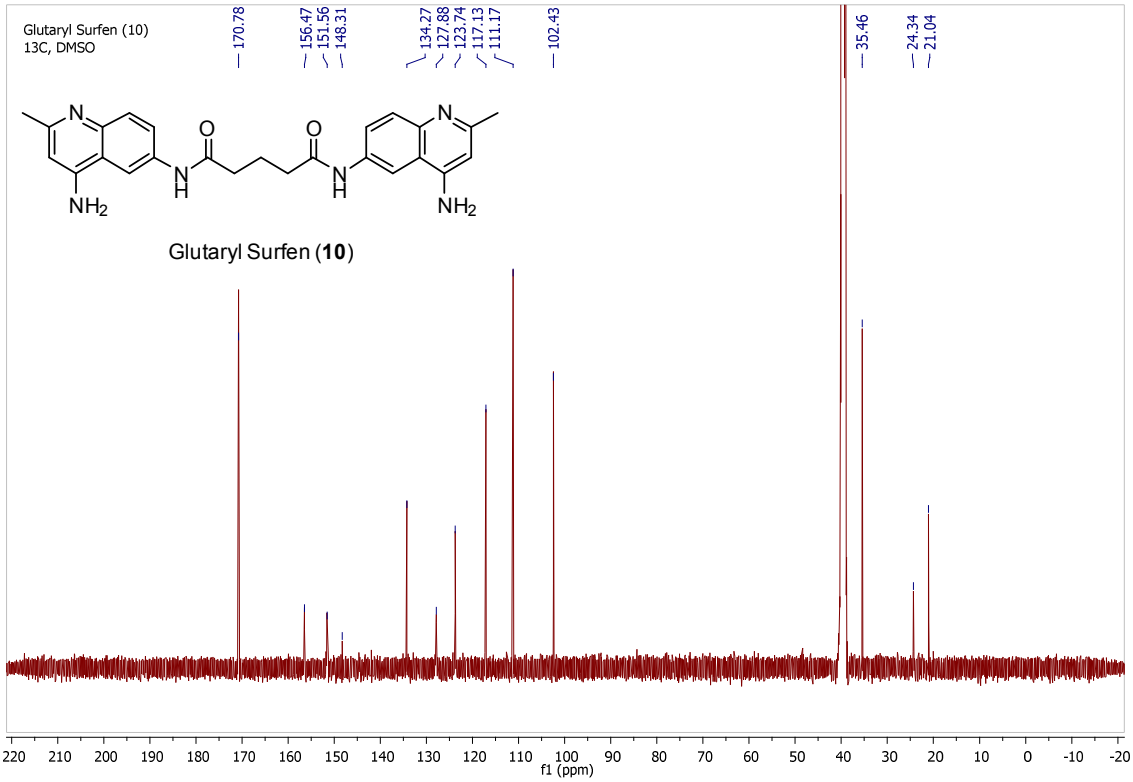

Spectrum 2.10: Adipoyl Surfen (**11**).

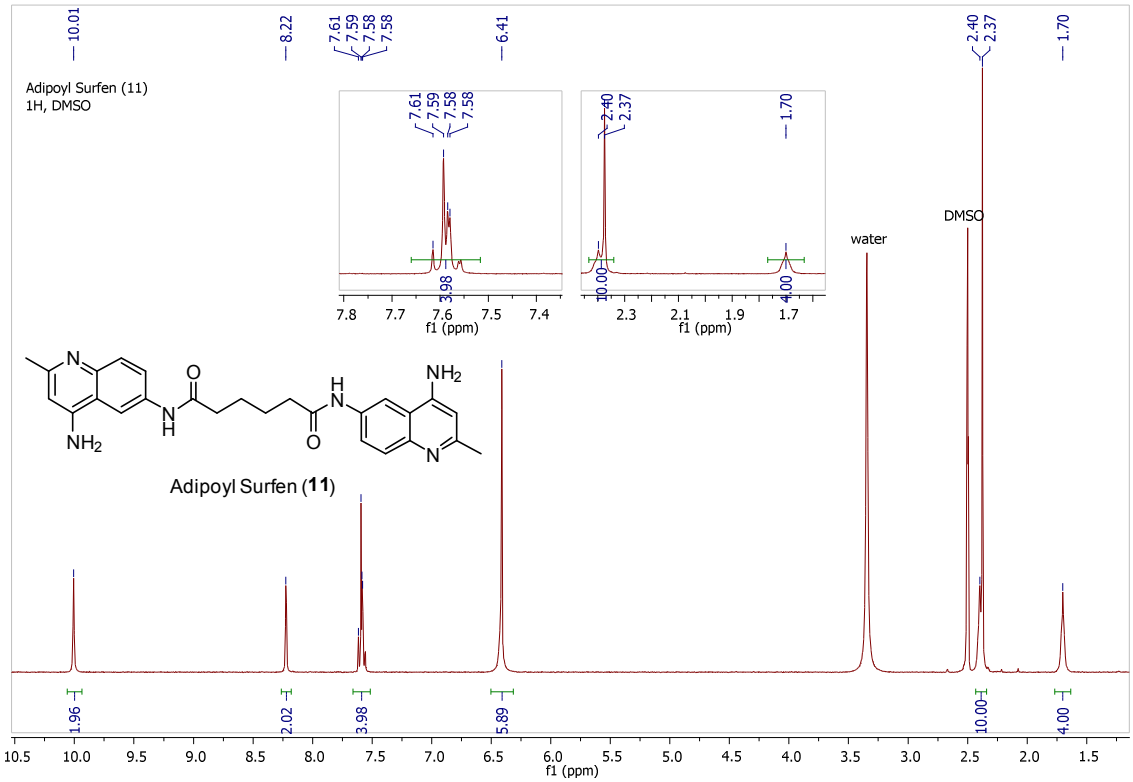

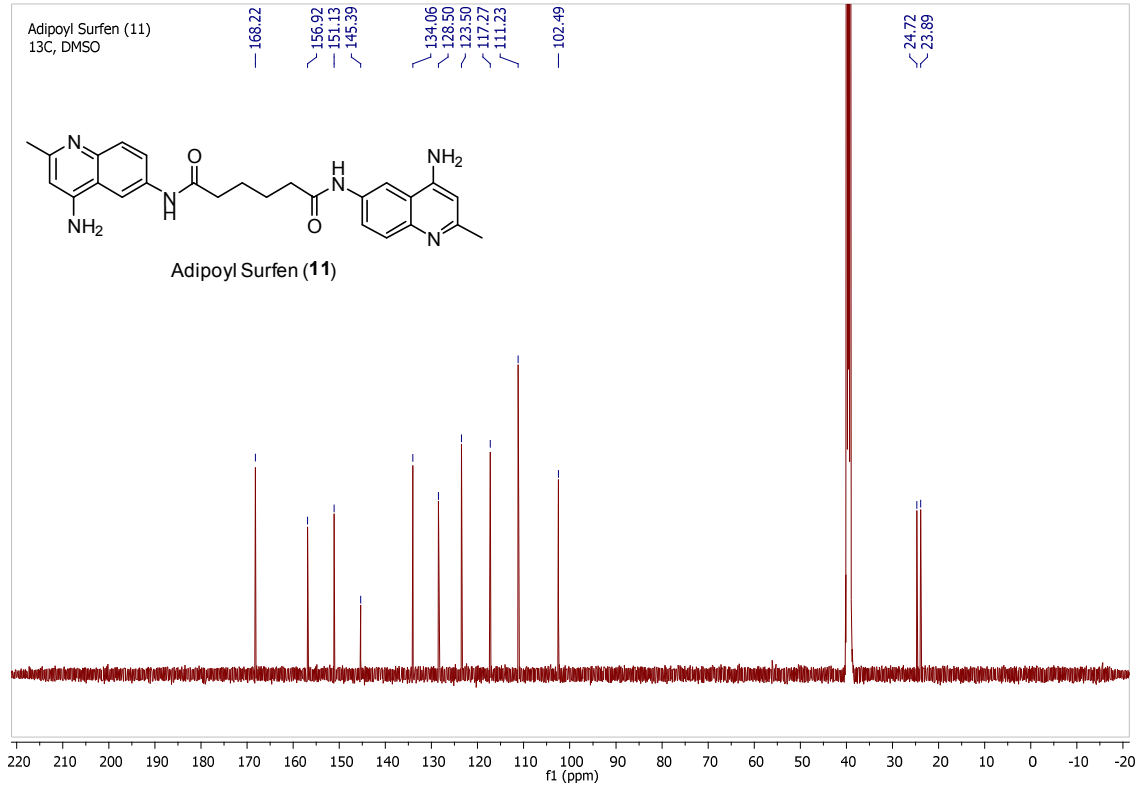

Spectrum 2.11: Pimeloyl Surfen (**12**).

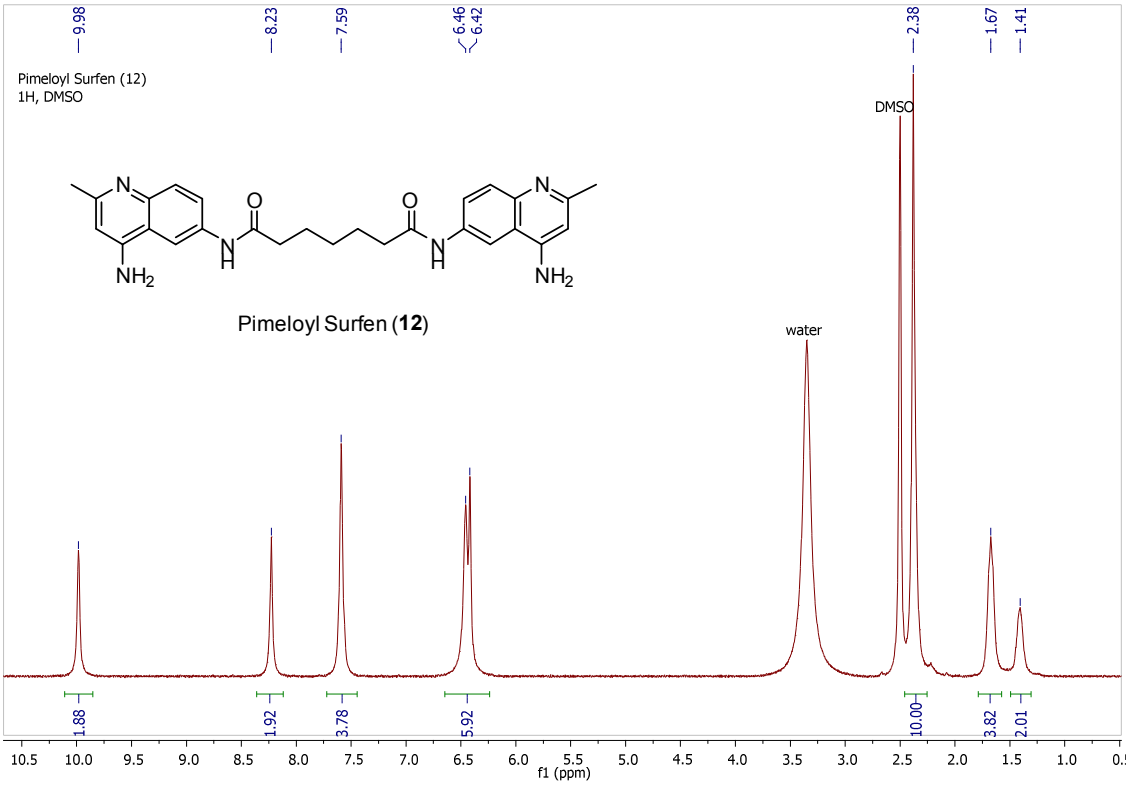

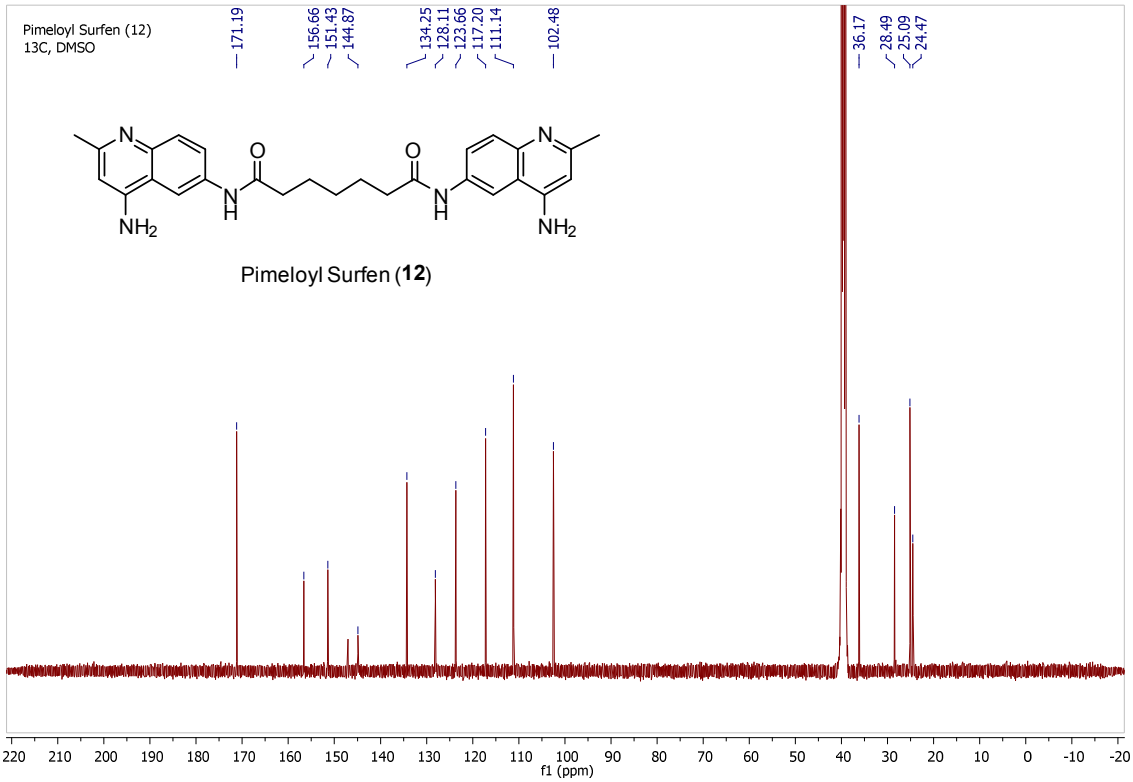

Spectrum 2.12: Diglycolyl Surfen (**13**).

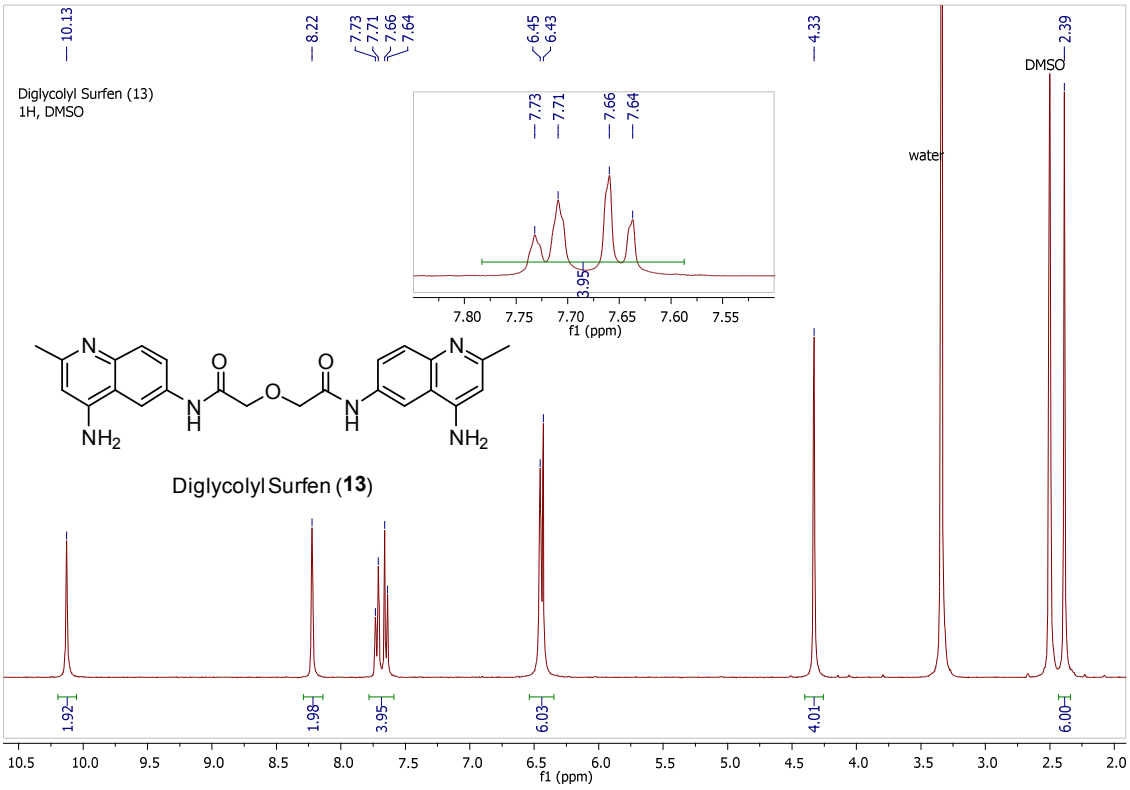

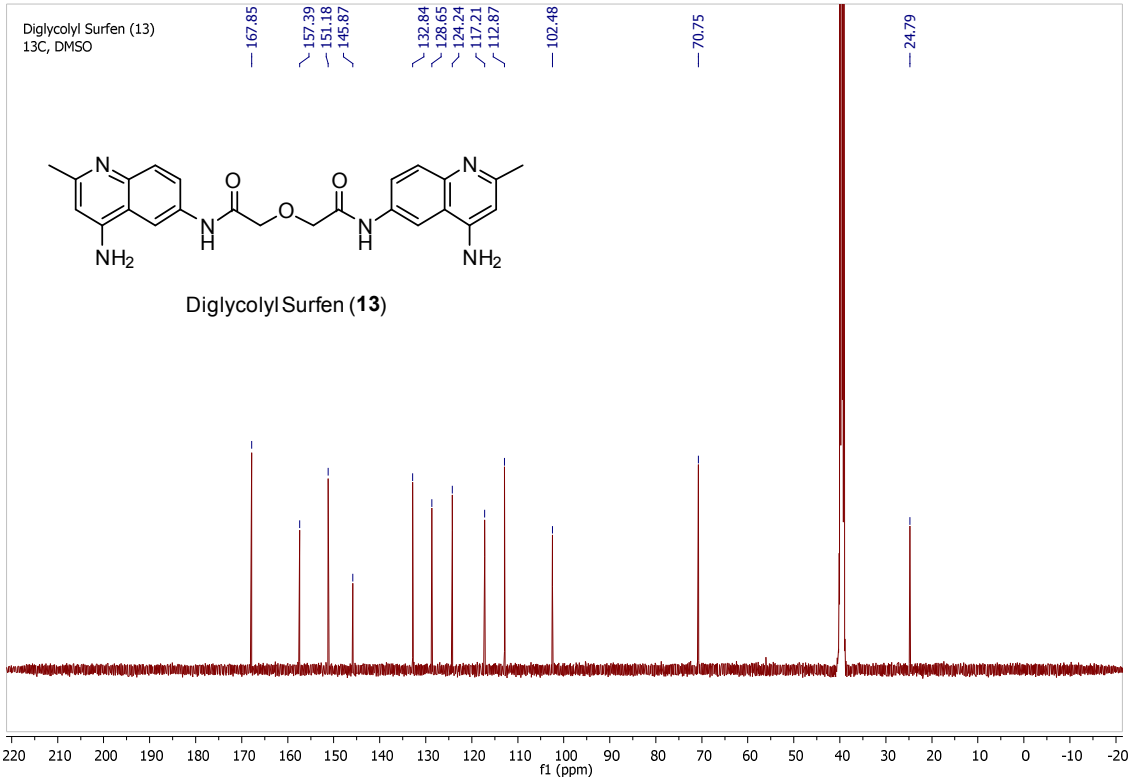

Precipitation of HCl salts

Surfen analog (1 eq.) was dissolved in a minimum amount of methanol. In some cases, the solid did not initially dissolve. HCl in dioxane (4M solution, 1 eq.) was added generating a homogeneous solution. The solution was stirred until the HCl salt precipitated out. Diethyl ether was added to the reaction mixture to further assist in precipitation. The product was filtered, washed with diethyl ether, and dried on high vacuum overnight.

Hemisurfen HCl (2a). Product: tan solid (4.8 mg, .019 mmol, 95%). ^{1}H NMR (400 MHz, DMSO-*d*$_6$): δ 9.04 (s, 1H), 8.53 (s, 2H), 8.21 (s, 1H), 7.89 (dd, *J* = 9.1, 1.9 Hz, 1H), 7.76 (d, *J* = 9.1 Hz, 1H), 6.53 (s, 1H), 6.15 (s, 2H), 2.55 (s, 3H). HR-ESI-MS calculated for $C_{11}H_{13}N_4O$ $[M+H]^+$ 217.1085, found 217.1084.

Acetyl-hemisurfen HCl (3a). Product: tan solid (11.8 mg, 0.047 mmol, 97%). ^{1}H NMR (400 MHz, DMSO-*d*$_6$): δ 10.48 (s, 1H), 8.71 (brd, 2H), 8.56 (s, 1H), 7.86 (d, *J* = 2.2 Hz, 2H), 6.57 (s, 1H), 2.57 (s, 3H), 2.12 (s, 3H). HR-ESI-MS calculated for $C_{11}H_{13}N_4O$ $[M+H]^+$ 217.1085, found 217.1084.

Thio Surfen HCl (4a). Product: yellow solid (15 mg, 0.035 mmol, 46%). ^{1}H NMR (400 MHz, DMSO-*d*$_6$): δ 10.10 (s, 2H), 8.23 (s, 2H), 7.59 (d, *J* = 2.4 Hz, 4H), 6.41 (s, 2H), 6.34 (s, 4H), 2.37 (s, 6H). HR-ESI-MS calculated for $C_{21}H_{21}N_6S$ $[M+H]^+$ 389.1543, found 389.1545.

Methoxy Surfen HCl (5a). Product: tan solid (4.9 mg, 0.01 mmol, 86%). ^{1}H NMR (500 MHz, DMSO-*d*$_6$): δ 10.28 (s, 2H), 8.61 (d, *J* = 2.3 Hz, 2H), 8.10 (d, *J* = 9.2

Hz, 2H), 7.96 (dd, *J* = 9.2, 2.0 Hz, 2H), 7.48 (s, 2H), 4.28 (s, 6H), 2.84 (s, 6H). HR-ESI-MS calculated for $C_{23}H_{23}N_4O_3$ $[M+H]^+$ 403.1766, found 403.1765.

Deaminated Surfen HCl (6a). Product: yellow solid (11 mg, 0.026 mmol, 76%). ^{1}HNMR (400 MHz, DMSO-d_6): δ 10.26 (s, 2H), 8.88 (d, *J* = 7.5 Hz, 2H), 8.49 (s, 2H), 8.22 (d, *J* = 9.1 Hz, 2H), 8.03 (d, *J* = 9.1 Hz, 2H), 7.83 (d, *J* = 8.2 Hz, 2H), 2.88 (s, 6H). HR-ESI-MS calculated for $C_{21}H_{19}N_4O$ $[M+H]^+$ 343.1553, found 343.1556.

Oxalyl Surfen HCl (7a). Product: tan solid (16 mg, 0.04 mmol, 56%). ^{1}H NMR (400 MHz, DMSO-d_6) δ 11.22 (s, 2H), 8.64 (brd, 6H), 8.17 (d, *J* = 9.3 Hz, 2H), 7.94 (d, *J* = 9.3 Hz, 2H), 6.63 (s, 2H), 2.60 (s, 6H). HR-ESI-MS calculated for $C_{22}H_{21}N_6O_2$ $[M+H]^+$ 401.1721, found 401.1718.

Malonyl Surfen HCl (8a). Product: white solid (4.1 mg, 0.008 mmol, 87%). ^{1}H NMR (400 MHz, DMSO-d_6): δ 10.72 (s, 2H), 8.59 (brd, 6H), 7.91 (d, *J* = 9.6 Hz, 2H), 7.83 (d, *J* = 9.3 Hz, 2H), 6.56 (s, 2H), 3.66 (s, 2H), 2.56 (s, 6H). HR-ESI-MS calculated for $C_{23}H_{23}N_6O_2$ $[M+H]^+$ 415.1877, found 415.1879.

Succinyl Surfen HCl (9a). Product: tan solid (4 mg, 0.01 mmol, 84%). ^{1}H NMR (400 MHz, DMSO-d_6): δ 10.54 (s, 2H), 8.61 (s, 6H), 7.95–7.73 (m, 2H), 6.56 (s, 2H), 2.79 (s, 4H), 2.56 (s, 6H). HR-ESI-MS calculated for $C_{24}H_{24}N_6O_2$ $[M+H]^+$ 429.2034, found 429.2036.

Glutaryl Surfen HCl (10a). Product: tan solid (2.6 mg, 0.005 mmol, 80%). ^{1}H NMR (400 MHz, DMSO-d_6) δ 10.49 (s, 2H), 8.63 (brd, 6H), 7.85 (s, 4H), 6.56 (s,

2H), 2.57 (s, 6H), 2.53–2.51 (m, 4H), 2.04–1.94 (m, 2H). HR-ESI-MS calculated for $C_{25}H_{27}N_6O_2$ $[M+H]^+$ 443.2190, found 443.2192.

Adipoyl Surfen HCl (11a). Product: white solid (14.6 mg, 0.0276 mmol, 98%). ^{1}H NMR (400 MHz, DMSO-*d*$_6$): δ 10.40 (s, 1H), 8.57 (s, 1H), 8.36 (s, 1H), 7.88–7.73 (m, *J* = 0.5 Hz, 1H), 6.54 (s, 1H), 2.54 (s, 2H), 2.48–2.40 (m, 1H), 1.75–1.66 (m, 1H). HR-ESI-MS calculated for $C_{26}H_{29}N_6O_2$ $[M+H]^+$ 457.2347, found 457.2346.

Pimeloyl Surfen HCl (12a). Product: white solid (7.2 mg, 0.014 mmol, 100%). ^{1}H NMR (400 MHz, DMSO-*d*$_6$): δ 10.44 (s, 2H), 8.60 (s, 6H), 7.91–7.77 (m, 4H), 6.56 (s, 2H), 2.57 (s, 6H), 2.42 (t, *J* = 7.3 Hz, 4H), 1.74–1.61 (m, 4H), 1.47–1.34 (m, 2H). HR-ESI-MS calculated for $C_{27}H_{31}N_6O_2$ $[M+H]^+$ 471.2503, found 471.2501.

Diglycolyl Surfen HCl (13a). Product: white solid (13.2 mg, 0.0255 mmol, 97%). ^{1}H NMR (400 MHz, DMSO-*d*$_6$): δ 10.52 (s, 2H), 8.62 (brd, 6H), 8.03 (dd, *J* = 9.1, 2.0 Hz, 2H), 7.88 (d, *J* = 9.1 Hz, 2H), 6.59 (s, 2H), 4.39 (s, 4H), 2.58 (s, 6H). HR-ESI-MS calculated for $C_{24}H_{25}N_6O_3$ $[M+H]^+$ 445.1983, found 445.1984. 0

X-ray crystal structures

The single crystal X-ray diffraction studies were carried out on a Bruker Kappa APEX-II CCD diffractometer equipped with Mo K$_\alpha$ radiation (λ = 0.71073 Å) at the UCSD Chemistry and Biochemistry Small Molecule X-ray Facility. Crystals were mounted on a Cryoloop with Paratone oil. Data were collected in a

nitrogen gas stream at 100(2) K using ϕ and ϖ scans. The data were integrated using the Bruker SAINT software program and scaled using the SADABS software program. Solution by direct methods (SHELXT) produced a complete phasing model consistent with the proposed structure. All nonhydrogen atoms were refined anisotropically by full-matrix least-squares (SHELXL-2014). All hydrogen atoms were placed using a riding model. Their positions were constrained relative to their parent atom using the appropriate HFIX command in SHELXL-2014. Crystallographic data are summarized in **Table 2.2–2.5**.

Crystal structures were deposited in the Cambridge Crystallographic Data Centre.

The data have been assigned the following deposition numbers:

Summary of Data CCDC 1057474

Compound Name: **adipoyl surfen (11)**

Formula: C26 H28 N6 O2,2(H2 O1)

Unit Cell Parameters: a 8.5132(5) b 21.0477(13) c 7.2003(4) P21/c

Crystallization procedure: slow evaporation from methanol

Summary of Data CCDC 1057475

Compound Name: **oxalyl surfen (7)**

Formula: C22 H20 N6 O2,4(C1 H4 O1)

Unit Cell Parameters: a 6.2877(7) b 8.8655(9) c 12.0399(13) P-1

Crystallization procedure: recrystallization from hot methanol with slow cooling

Summary of Data CCDC 1057476

Compound Name: **diglycolyl surfen•2HCl (13)**

Formula: C24 H25 N6 O3 1+,H2 Cl1 O1,H2 O1,Cl1 1-

Unit Cell Parameters: a 5.0339(9) b 37.994(7) c 7.1360(11) P21/m

Crystallization procedure: slow evaporation from methanol

Summary of Data CCDC 1057477

Compound Name: **surfen•2CF$_3$COOH (1)**

Formula: 2(C21 H22 N6 O1 1+),(C3 H8 F6 Na1 O7)n,2(C3 F6 O3)n,2(C2 F3 O2 1-),x(F1),x(C1 F1),F1,4(C1 O2)

Unit Cell Parameters: a 14.0292(11) b 22.3313(16) c 9.5059(10) C2/m

Crystallization procedure: dissolved in 0.1% TFA-water, lyophilized, then vapor diffusion of DCM into DMSO solution

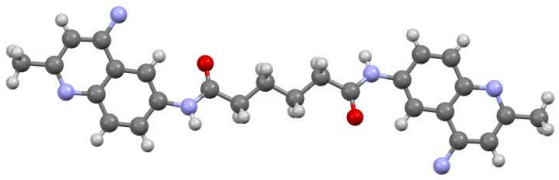

Figure 2.9: X-ray crystal structure of adipoyl surfen (**11**).

Table 2.2: Crystal data and structure refinement for Tor86 (**adipoyl surfen**).

Identification code	Tor86	
Empirical formula	C26 H28 N6 O4 (with 2 H_2O)	
Formula weight	488.54	
Temperature	100(2) K	
Wavelength	0.71073 Å	
Crystal system	Monoclinic	
Space group	P 21/c	
Unit cell dimensions	a = 8.5132(5) Å	α= 90°.
	b = 21.0477(13) Å	β= 113.595(2)°.
	c = 7.2003(4) Å	γ = 90°.
Volume	1182.31(12) $Å^3$	
Z, Z'	2, 0.5	
Density (calculated)	1.372 Mg/m^3	
Absorption coefficient	0.095 mm^{-1}	
F(000)	516	
Crystal size	0.300 x 0.100 x 0.070 mm^3	
Theta range for data collection	2.611 to 26.402°.	
Index ranges	-10<=h<=10, -26<=k<=26, -9<=l<=9	
Reflections collected	20966	
Independent reflections	2413 [R(int) = 0.0491]	
Completeness to theta = 25.000°	99.8 %	
Absorption correction	Multi-scan	
Refinement method	Full-matrix least-squares on F^2	
Data / restraints / parameters	2413 / 0 / 172	
Goodness-of-fit on F^2	1.064	
Final R indices [I>2sigma(I)]	R1 = 0.0463, wR2 = 0.1290	
R indices (all data)	R1 = 0.0502, wR2 = 0.1325	
Extinction coefficient	n/a	
Largest diff. peak and hole	0.812 and -0.199 $e.Å^{-3}$	

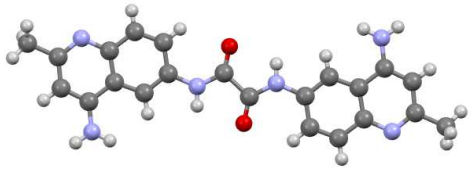

Figure 2.10: X-ray crystal structure of oxalyl surfen (**7**).

Table 2.3: Crystal data and structure refinement for Tor88 (**oxalyl surfen**).

Identification code	Tor88	
Empirical formula	C13 H18 N3 O3	
Formula weight	264.30	
Temperature	100.0 K	
Wavelength	1.54178 Å	
Crystal system	Triclinic	
Space group	P -1	
Unit cell dimensions	a = 6.2877(7) Å	α= 102.993(5)°.
	b = 8.8655(9) Å	β= 91.548(6)°.
	c = 12.0399(13) Å	γ = 92.630(6)°.
Volume	652.79(12) $Å^3$	
Z	2	
Density (calculated)	1.345 Mg/m^3	
Absorption coefficient	0.800 mm^{-1}	
F(000)	282	
Crystal size	0.317 x 0.031 x 0.015 mm^3	
Crystal color, habit	Light Yellow Needle	
Theta range for data collection	3.770 to 69.433°.	
Index ranges	-7<=h<=7, -10<=k<=10, -12<=l<=14	
Reflections collected	20226	
Independent reflections	2357 [R(int) = 0.0331]	
Completeness to theta = 68.000°	98.3 %	
Absorption correction	Semi-empirical from equivalents	
Max. and min. transmission	0.7532 and 0.6330	
Refinement method	Full-matrix least-squares on F^2	
Data / restraints / parameters	2357 / 5 / 195	
Goodness-of-fit on F^2	1.059	
Final R indices [I>2sigma(I)]	R1 = 0.0427, wR2 = 0.1156	
R indices (all data)	R1 = 0.0490, wR2 = 0.1203	
Extinction coefficient	n/a	
Largest diff. peak and hole	0.283 and -0.214 $e.Å^{-3}$	

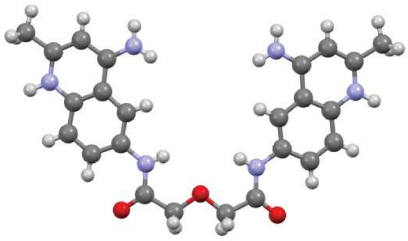

Figure 2.11: X-ray crystal structure of diglycolyl surfen•2HCl (**13**). Counterions omitted for clarity.

Table 2.4: Crystal data and structure refinement for Tor90 (**diglycolyl surfen•2HCl**).

Identification code	Tor90	
Empirical formula	C24 H29 Cl2 N6 O5	
Formula weight	552.43	
Temperature	100.0 K	
Wavelength	0.71073 Å	
Crystal system	Monoclinic	
Space group	P 1 21/m 1	
Unit cell dimensions	a = 5.0339(9) Å	α= 90°.
	b = 37.994(7) Å	β= 110.533(11)°.
	c = 7.1360(11) Å	γ = 90°.
Volume	1278.1(4) $Å^3$	
Z	2	
Density (calculated)	1.435 Mg/m^3	
Absorption coefficient	0.302 mm^{-1}	
F(000)	578	
Crystal size	0.24 x 0.2 x 0.08 mm^3	
Crystal color, habit	Colorless Plate	
Theta range for data collection	2.144 to 26.490°.	
Index ranges	-6<=h<=6, -47<=k<=45, -8<=l<=8	
Reflections collected	7858	
Independent reflections	2635 [R(int) = 0.0438]	
Completeness to theta = 25.000°	99.3 %	
Absorption correction	Semi-empirical from equivalents	
Max. and min. transmission	0.0932 and 0.0478	
Refinement method	Full-matrix least-squares on F^2	
Data / restraints / parameters	2635 / 3 / 189	
Goodness-of-fit on F^2	1.188	
Final R indices [I>2sigma(I)]	R1 = 0.0751, wR2 = 0.1702	
R indices (all data)	R1 = 0.0944, wR2 = 0.1780	
Extinction coefficient	n/a	
Largest diff. peak and hole	0.380 and -0.316 e.$Å^{-3}$	

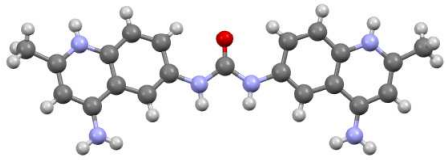

Figure 2.12: X-ray crystal structure of surfen•2CF_3COOH (**1**). Counterions omitted for clarity.

Table 2.5: Crystal data and structure refinement for Tor99 (**surfen•2CF_3COOH**).

Identification code	Tor99	
Empirical formula	C26 H26 F7.50 N6 Na0.50 O9	
Formula weight	720.52	
Temperature	100.0 K	
Wavelength	0.71073 Å	
Crystal system	Monoclinic	
Space group	C 1 2/m 1	
Unit cell dimensions	a = 14.0292(11) Å	α= 90°.
	b = 22.3313(16) Å	β= 92.950(2)°.
	c = 9.5059(10) Å	γ = 90°.
Volume	2974.2(4) $Å^3$	
Z	4	
Density (calculated)	1.609 Mg/m^3	
Absorption coefficient	0.157 mm^{-1}	
F(000)	1476	
Crystal size	0.053 x 0.021 x 0.016 mm^3	
Crystal color, habit	Colorless Block	
Theta range for data collection	1.716 to 25.356°.	
Index ranges	-16<=h<=16, -26<=k<=26, -11<=l<=11	
Reflections collected	20193	
Independent reflections	2807 [R(int) = 0.0924]	
Completeness to theta = 25.000°	100.0 %	
Absorption correction	Semi-empirical from equivalents	
Max. and min. transmission	0.0917 and 0.0617	
Refinement method	Full-matrix least-squares on F^2	
Data / restraints / parameters	2807 / 99 / 298	
Goodness-of-fit on F^2	1.041	
Final R indices [I>2sigma(I)]	R1 = 0.1119, wR2 = 0.2863	
R indices (all data)	R1 = 0.1943, wR2 = 0.3458	
Extinction coefficient	n/a	
Largest diff. peak and hole	0.891 and -0.599 e.$Å^{-3}$	

FGF2 and sRAGE binding inhibition

Wild-type CHO cells (ATCC CCL-61) were grown in F12 growth medium supplemented with 10% (v/v) fetal bovine serum, 100 µg/ml of streptomycin sulfate, and 100 units/ml of penicillin G. Cells were grown to confluence, lifted with Cell Dissociation Buffer, washed with PBS buffer, and pre-incubated with specific concentrations of surfen or surfen analog in PBS/0.1% BSA on ice for 10 min. Next, biotinylated FGF2 (2.5 nM, 1:1000) or biotin-sRAGE (2 µg/ml, 1:100) were added and incubated for 30 min or 1 hour on ice, respectively. Cells were washed, and bound biotinylated protein was detected by using streptavidin-PE-Cy5 or streptavidin-Cy5 (1:1000, PharMingen) and flow cytometry (FACSCalibur, BD Biosciences). Certain compounds (**1**, **4**, **5**, **7**) required use of streptavidin-Cy5 due to interference. Crude data was interpreted using FlowJo Analytical Software (Tree Star Inc.). Protein binding was quantified by the geometric mean fluorescence intensity. Results are represented as the extent of binding compared with a sample incubated in the absence of surfen (**Figure 2.10**). These values were plotted and further analyzed using GraphPad Prism v5.0.

Stock solutions were made for each compound in DMSO (30 mM). Stock solutions for analogs **7** and **11** were made in 1:1 DMSO-H_2O mixture due to solubility. For each experiment, the stock solutions were diluted first to 10 mM in DMSO, then the appropriate serial dilutions were made in PBS buffer (with 0.1% BSA). DMSO solutions were made and stored in glass containers because

surfen has been previously found to stick to plastic. Compounds and DMSO stock solutions were stored under argon at -20°C.

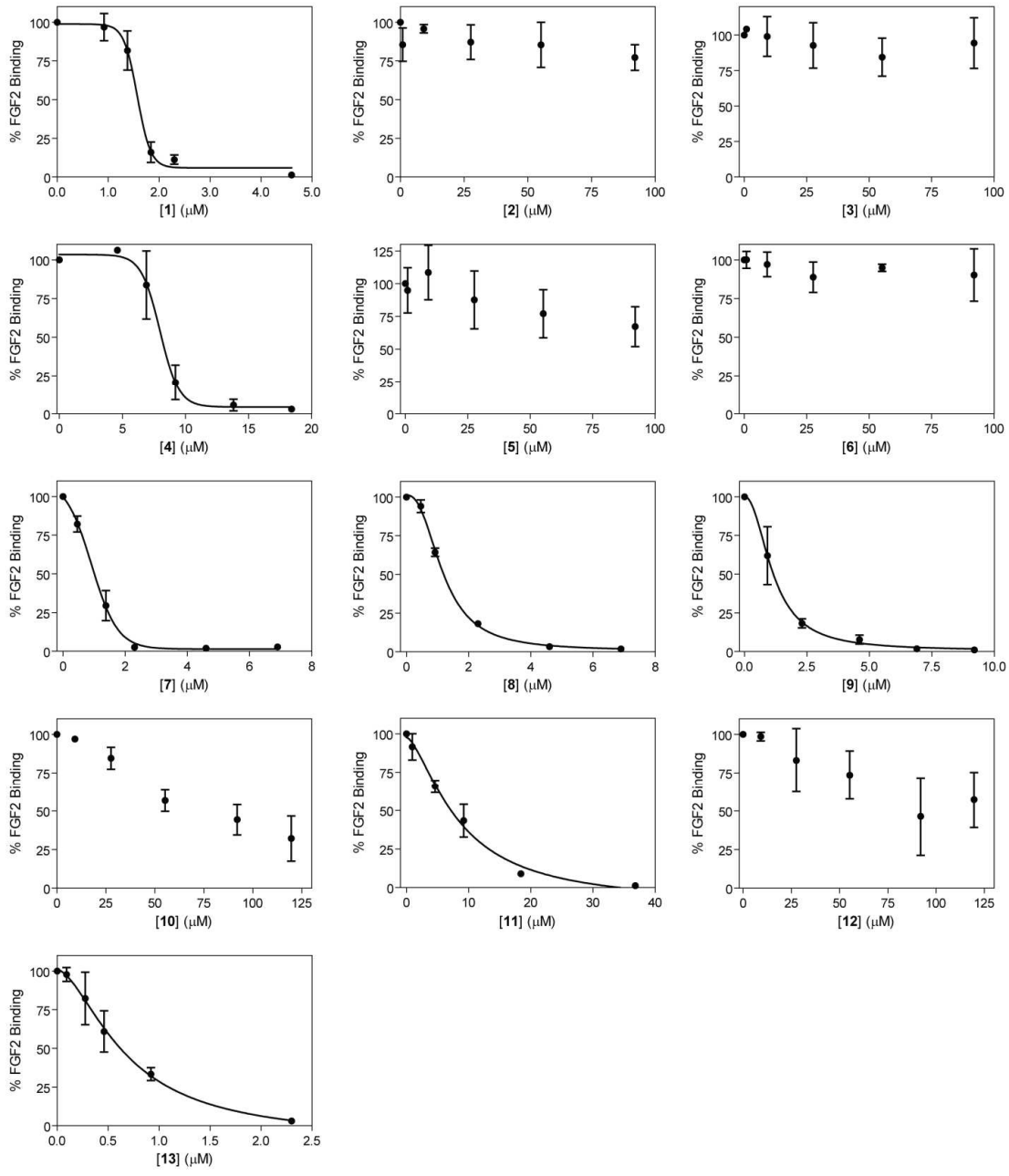

Figure 2.13: FGF2 binding inhibition curves for surfen (**1**), hemisurfen (**2**), acetyl-hemisurfen (**3**), thio surfen (**4**), methoxy surfen (**5**), deaminated surfen (**6**), oxalyl surfen (**7**), malonyl surfen (**8**), succinyl surfen (**9**), glutaryl surfen (**10**), adipoyl surfen (**11**), pimeloyl surfen (**12**), and diglycolyl surfen (**13**).

Biotinylation of FGF2

150 µg of bFGF (35 µl in H_2O, E. coli recombinant, Peprotech) was mixed at room temperature for 2 hours with 10 µl of heparin (20 mg/ml), 50 ul of HEPES buffer (200 mM, pH 8.4), and 5 µl of Sulfo-NHS-LC-Biotin (4 mg/ml in H_2O, Thermo Scientific). Next, 20 µl of glycine (10 mg/ml) was added to stop the reaction. A 500 µl heparin-Sepharose HP column was equilibrated with wash buffer (0.5 M NaCl, 0.2% BSA, 20 mM HEPES, pH 7.4). The reaction mixture was diluted in 10 ml of wash buffer, loaded onto the column, and subsequently eluted with 2 ml of elution buffer (3 M NaCl, 0.2% BSA, 20 mM HEPES, pH 7.4). Biotinylated FGF2 was stored at 4°C for further use.

Biotinylation of sRAGE

Recombinant soluble RAGE protein, generated in *Escherichia coli*,[64] was diluted in 3 ml of PBS and was loaded onto a 200-µl heparin-Sepharose column. Sulfo-NHS-LC-biotin in PBS (500 µl of a 1 mM solution, pH 8) was then applied to the column, and biotinylation was allowed to proceed for 30 min at room temperature. The reaction was stopped by applying 600 µl of PBS containing 100 mM glycine, pH 7. After washing the column with 1 ml of 20 mM HEPES buffer (pH 7.1) containing 150 mM NaCl, the column was eluted sequentially with 600 mM NaCl and 1 M NaCl in 20 mM HEPES buffer (800 µl). Protein eluted by 1 mM NaCl was used for all binding experiments.

Example of flow cytometry (FACS) histograms for inhibition experiments

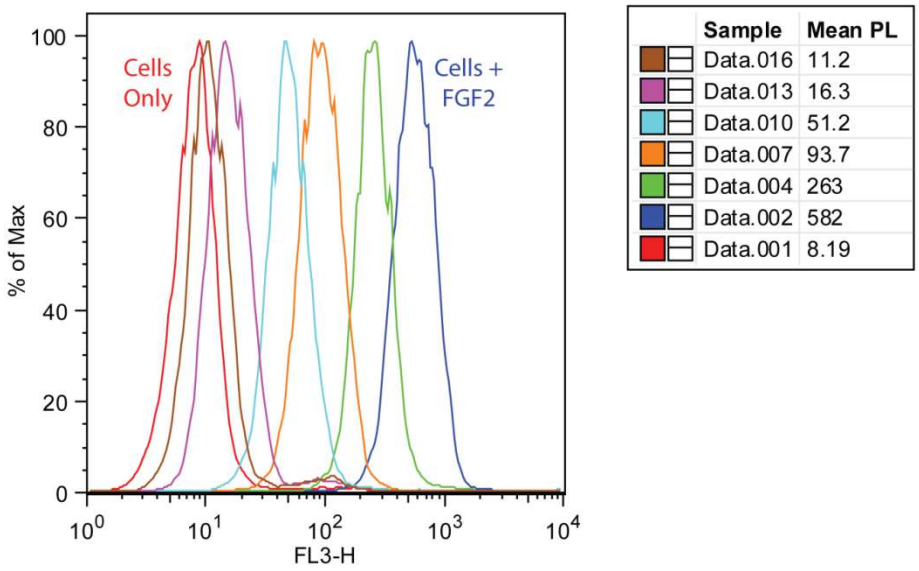

Figure 2.14: Example of a histogram from FGF2 binding experiments with succinyl surfen (**9**) and biotinylated-FGF2. Data sets 001 and 002 refer to cells only and cells + biotin-FGF2 conjugated to streptavidin PE-Cy5 (absence of surfen analog), respectively. Data sets 004–016 refer to histograms obtained in the presence of **9** at 1 μM, 2.5 μM, 5 μM, 7.5 μM, 10 μM, respectively.

Factor Xa inhibition assay

Human antithrombin III (66 μg/mL; Enzyme Research Laboratories), heparin or heparinoid (0.2 IU/mL), and various concentrations of surfen or surfen analog were prepared in a solution containing 25 mM HEPES (N-[2-hydroxyethyl] piperazine-N'- [2-ethanesulfonic acid]), 150 mM NaCl and 0.1% bovine serum albumin (pH 7.5) in a 96-well microtiter plate. Human factor Xa (0.4 μg/mL, 50 uL; Enzyme Research Laboratories) was added to each well and the solutions were incubated for 10 min. at room temperature with frequent mixing. Chromogenic substrate specific for factor Xa (0.5 mg/mL, 50 μl; S-2765 Diapharma) was added, incubated for 5 min at room temperature, and absorbance was measured at 405 nm. Background absorption at 405 nm was

subtracted prior to analysis of the results. A heparin/heparinoid concentration with approximately ~85% factor Xa inhibition was selected for measurement of neutralization (0.2 IU/well). Results are represented as the extent of factor Xa activity compared with a sample incubated with heparin/heparinoid in the absence of surfen. Surfen and analogs had no direct effect on factor Xa activity measured in the absence of heparin (**Figure 2.11**).

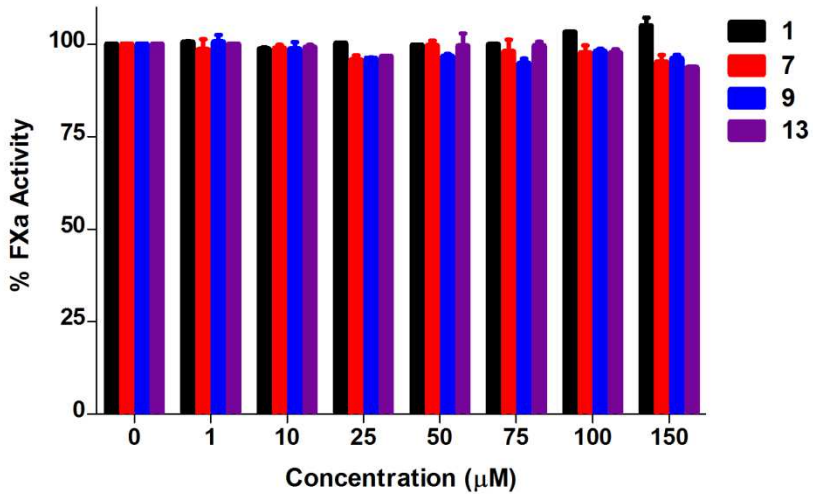

Figure 2.15: Surfen and selected analogs do not affect FXa activity *in vitro*.

In vivo heparin neutralization

Wild-type mice (8 weeks old, weight ~20-30 g) were divided into a control group (n=3), an oxalyl surfen-treated group (n=3), and a protamine-treated group (n=3). Thirty min before heparin administration, blood was collected by tail bleeding in 3.2% sodium citrate tubes (9:1 blood to citrate ratio). Each mouse received a subcutaneous injection of UFH (1200 IU/kg, PBS) or fondaparinux (0.5 mg/kg, PBS). Next, mice received an intravenous injection (via tail vein) of

DMSO-H2O solution (control), protamine (16 mg/kg, PBS), or oxalyl surfen (6 or 16 mg/kg, DMSO-water) 60 min after UFH and 10 min after fondaparinux administration. Five min after administration of the reversal agent, blood was collected via submandibular bleeds into 3.2% sodium citrate tubes. Plasma was collected immediately (2200 *g* for 15 min) and stored at -80°C. A heparin anti-FXa colorimetric assay was used to analyze the neutralization effect of protamine and oxalyl surfen (**7**). Their activity was compared to a heparin control without reversal agent as described above. The change in the absorption at 405 nm for each sample was compared with a standard calibration curve to determine the amount of heparin present. The basis of this assay is to analyze the amount of UFH or fondaparinux remaining in plasma by indirectly measuring the residual activity of FXa. Heparinized plasma (3 µL) was mixed with antithrombin, forming an AT-heparin complex. The amount of UFH or fondaparinux remaining in plasma was plotted against the reversal agent dosage.

Acknowledgements

Chapter 2 is a full reprint from: Weiss, R. J.; Gordts, P. L.; Le, D.; Esko, J. D.; Tor, Y. Small Molecule Antagonists of Cell-Surface Heparan Sulfate and Heparin–Protein Interactions. *Chemical Science*, in revision. The dissertation author is the main author and researcher of this work.

2.6 References

(1) Hacker, U.; Nybakken, K.; Perrimon, N. *Nature Reviews Molecular Cell Biology* **2005**, *6*, 530.

(2) Bishop, J. R.; Schuksz, M.; Esko, J. D. *Nature* **2007**, *446*, 1030.

(3) Bulow, H. E.; Hobert, O. *Annual Review of Cell and Developmental Biology* **2006**, *22*, 375.

(4) Hallak, L. K.; Spillmann, D.; Collins, P. L.; Peeples, M. E. *Journal of Virology* **2000**, *74*, 10508.

(5) Alexopoulou, A. N.; Multhaupt, H. A. B.; Couchman, J. R. *International Journal of Biochemistry & Cell Biology* **2007**, *39*, 505.

(6) Manetti, F.; Corelli, F.; Botta, M. *Current Pharmaceutical Design* **2000**, *6*, 1897.

(7) Zhu, X. T.; Hsu, B. T.; Rees, D. C. *Structure* **1993**, *1*, 27.

(8) Baeuerle, P. A.; Huttner, W. B. *Biochemical and Biophysical Research Communications* **1986**, *141*, 870.

(9) Fritz, T. A.; Lugemwa, F. N.; Sarkar, A. K.; Esko, J. D. *Journal of Biological Chemistry* **1994**, *269*, 300.

(10) Hekman, A. *Biochimica Et Biophysica Acta* **1971**, *251*, 380.

(11) Fuchs, S. M.; Raines, R. T. *Biochemistry* **2004**, *43*, 2438.

(12) Udit, A. K.; Everett, C.; Gale, A. J.; Kyle, J. R.; Ozkan, M.; Finn, M. G. *Chembiochem* **2009**, *10*, 503.

(13) Montalvo, G. L.; Zhang, Y.; Young, T. M.; Costanzo, M. J.; Freeman, K. B.; Wang, J.; Clements, D. J.; Magavern, E.; Kavash, R. W.; Scott, R. W.; Liu, D.; DeGrado, W. F. *Acs Chemical Biology* **2014**, *9*, 967.

(14) Choi, S.; Clements, D. J.; Pophristic, V.; Ivanov, I.; Vemparala, S.; Bennett, J. S.; Klein, M. L.; Winkler, J. D.; DeGrado, W. E. *Angewandte Chemie-International Edition* **2005**, *44*, 6685.

(15) D'Ilario, L.; Francolini, I.; Martinelli, A.; Piozzi, A. *Dyes and Pigments* **2009**, *80*, 343.

(16) Schmidtke, M.; Karger, A.; Meerbach, A.; Egerer, R.; Stelzner, A.; Makarov, V. *Virology* **2003**, *311*, 134.

(17) Selinka, H.-C.; Florin, L.; Patel, H. D.; Freitag, K.; Schmidtke, M.; Makarov, V. A.; Sapp, M. *Journal of Virology* **2007**, *81*, 10970.

(18) Harris, N.; Kogan, F. Y.; Il'kova, G.; Juhas, S.; Lahmy, O.; Gregor, Y. I.; Koppel, J.; Zhuk, R.; Gregor, P. *Biochimica Et Biophysica Acta-General Subjects* **2014**, *1840*, 245.

(19) Schuksz, M.; Fuster, M. M.; Brown, J. R.; Crawford, B. E.; Ditto, D. P.; Lawrence, R.; Glass, C. A.; Wang, L.; Tor, Y.; Esko, J. D. *Proceedings of the National Academy of Sciences of the United States of America* **2008**, *105*, 13075.

(20) Roan, N. R.; Sowinski, S.; Muench, J.; Kirchhoff, F.; Greene, W. C. *Journal of Biological Chemistry* **2010**, *285*, 1861.

(21) Castellano, L. M.; Shorter, J. *Biology* **2012**, *1*, 58.

(22) Warford, J.; Doucette, C. D.; Hoskin, D. W.; Easton, A. S. *Biochemical and Biophysical Research Communications* **2014**, *443*, 524.

(23) Lanza, T. J.; Durette, P. L.; Rollins, T.; Siciliano, S.; Cianciarulo, D. N.; Kobayashi, S. V.; Caldwell, C. G.; Springer, M. S.; Hagmann, W. K. *Journal of Medicinal Chemistry* **1992**, *35*, 252.

(24) Goble, F. C. *Journal of Pharmacology and Experimental Therapeutics* **1950**, *98*, 49.

(25) Panchal, R. G.; Hermone, A. R.; Nguyen, T. L.; Wong, T. Y.; Schwarzenbacher, R.; Schmidt, J.; Lane, D.; McGrath, C.; Turk, B. E.; Burnett, J.; Aman, M. J.; Little, S.; Sausville, E. A.; Zaharevitz, D. W.; Cantley, L. C.; Liddington, R. C.; Gussio, R.; Bavari, S. *Nature Structural & Molecular Biology* **2004**, *11*, 67.

(26) Warkentin, T. E.; Crowther, M. A. *Canadian journal of anaesthesia = Journal canadien d'anesthesie* **2002**, *49*, S11.

(27) Jensch, H. *Angewandte Chemie* **1948**, *60*, 248.

(28) Peng, C. T.; Daniels, T. C. *Journal of the American Chemical Society* **1956**, *78*, 3703.

(29) Xu, D.; Young, J. H.; Krahn, J. M.; Song, D.; Corbett, K. D.; Chazin, W. J.; Pedersen, L. C.; Esko, J. D. *Acs Chemical Biology* **2013**, *8*, 1611.

(30) Turner, N.; Grose, R. *Nature Reviews Cancer* **2010**, *10*, 116.

(31) Maccarana, M.; Casu, B.; Lindahl, U. *Journal of Biological Chemistry* **1993**, *268*, 23898.

(32) Polnaszek, N.; Kwabi-Addo, B.; Peterson, L. E.; Ozen, M.; Greenberg, N. M.; Ortega, S.; Basilico, C.; Ittmann, M. *Cancer Research* **2003**, *63*, 5754.

(33) Dow, J. K.; White, R. W. D. *Urology* **2000**, *55*, 800.

(34) Aviezer, D.; Cotton, S.; David, M.; Segev, A.; Khaselev, N.; Galili, N.; Gross, Z.; Yayon, A. *Cancer Research* **2000**, *60*, 2973.

(35) Aviezer, D.; Seddon, A. P.; Wildey, M. J.; Bohlen, P.; Yayon, A. *Journal of biomolecular screening* **2001**, *6*, 171.

(36) Taraboletti, G.; Rusnati, M.; Ragona, L.; Colombo, G. *Oncotarget* **2010**, *1*, 662.

(37) Lanati, N.; Emanuele, E.; Brondino, N.; Geroldi, D. *Current Vascular Pharmacology* **2010**, *8*, 86.

(38) Sessa, L.; Gatti, E.; Zeni, F.; Antonelli, A.; Catucci, A.; Koch, M.; Pompilio, G.; Fritz, G.; Raucci, A.; Bianchi, M. E. *Plos One* **2014**, *9*.

(39) Sabbagh, M. N.; Agro, A.; Bell, J.; Aisen, P. S.; Schweizer, E.; Galasko, D. *Alzheimer Disease and Associated Disorders* **2011**, *25*, 206.

(40) Albert, A.; Goldacre, R. *Nature* **1944**, *153*, 467.

(41) Takemoto, N.; Suehara, T.; Frisco, H. L.; Sato, S.; Sezaki, T.; Kusamori, K.; Kawazoe, Y.; Park, S. M.; Yamazoe, S.; Mizuhata, Y.; Inoue, R.; Miller, G. J.; Hansen, S. U.; Jayson, G. C.; Gardiner, J. M.; Kanaya, T.; Tokitoh, N.; Ueda, K.; Takakura, Y.; Kioka, N.; Nishikawa, M.; Uesugi, M. *Journal of the American Chemical Society* **2013**, *135*, 11032.

(42) Dix, A. V.; Fischer, L.; Sarrazin, S.; Redgate, C. P. H.; Esko, J. D.; Tor, Y. *Chembiochem* **2010**, *11*, 2302.

(43) Kawamura, K. S.; Sung, M.; Bolewska-Pedyczak, E.; Gariépy, J. *Biochemistry* **2006**, *45*, 1116.

(44) Gandrille, S.; Aiach, M.; Lane, D. A.; Vidaud, D.; Molho-Sabatier, P.; Caso, R.; de Moerloose, P.; Fiessinger, J. N.; Clauser, E. *The Journal of biological chemistry* **1990**, *265*, 18997.

(45) Margalit, H.; Fischer, N.; Ben-Sasson, S. A. *The Journal of biological chemistry* **1993**, *268*, 19228.

(46) Testa, S. M.; Disney, M. D.; Turner, D. H.; Kierzek, R. *Biochemistry* **1999**, *38*, 16655.

(47) Nishiguc.T; Iwakura, Y. *Journal of Organic Chemistry* **1970**, *35*, 1591.

(48) Jin, L.; Abrahams, J. P.; Skinner, R.; Petitou, M.; Pike, R. N.; Carrell, R. W. *Proceedings of the National Academy of Sciences of the United States of America* **1997**, *94*, 14683.

(49) Warkentin, T. E.; Levine, M. N.; Hirsh, J.; Horsewood, P.; Roberts, R. S.; Gent, M.; Kelton, J. G. *New England Journal of Medicine* **1995**, *332*, 1330.

(50) Chang, L. C.; Liang, J. F.; Lee, H. F.; Lee, L. M.; Yang, V. C. *Aaps Pharmsci* **2001**, *3*, art. no.

(51) Lee, L. M.; Chang, L. C.; Wrobleski, S.; Wakefield, T. W.; Yang, V. C. *Aaps Pharmsci* **2001**, *3*, art. no.

(52) Wakefield, T. W.; Andrews, P. C.; Wrobleski, S. K.; Kadell, A. M.; Tejwani, S.; Hulin, M. S.; Stanley, J. C. *Journal of Surgical Research* **1996**, *63*, 280.

(53) Onoue, S.; Nemoto, Y.; Harada, S.; Yajima, T.; Kashimoto, K. *Life Sciences* **2003**, *73*, 2793.

(54) Fromm, J. R.; Hileman, R. E.; Caldwell, E. E. O.; Weiler, J. M.; Linhardt, R. J. *Archives of Biochemistry and Biophysics* **1997**, *343*, 92.

(55) Mecca, T.; Consoli, G. M. L.; Geraci, C.; La Spina, R.; Cunsolo, F. *Organic & Biomolecular Chemistry* **2006**, *4*, 3763.

(56) Weiss, W. A.; Gilman, J. S.; Catenacci, A. J.; Osterberg, A. E. *Jama-Journal of the American Medical Association* **1958**, *166*, 603.

(57) Choay, J.; Petitou, M.; Lormeau, J. C.; Sinay, P.; Casu, B.; Gatti, G. *Biochemical and Biophysical Research Communications* **1983**, *116*, 492.

(58) Chawla, L. S.; Moore, G.; Seneff, M. G. *Obesity Surgery* **2004**, *14*, 695.

(59) van Veen, J. J.; Maclean, R. M.; Hampton, K. K.; Laidlaw, S.; Kitchen, S.; Toth, P.; Makris, M. *Blood Coagulation & Fibrinolysis* **2011**, *22*, 565.

(60) Suryanarayan, D.; Schulman, S. *Thrombosis Research* **2014**, *133*, S158.

(61) Weitz, J. I.; Hirsh, J.; Samama, M. M. *Chest* **2008**, *133*, 234S.

(62) Pratt, M. G.; Archer, S. *Journal of the American Chemical Society* **1948**, *70*, 4065.

(63) Iensch, H. *Angewandte Chemie* **1937**, *50*, 0891.

(64) Xu, D.; Young, J.; Song, D. Y.; Esko, J. D. *Journal of Biological Chemistry* **2011**, *286*, 41736.

Chapter 3:

Surfen as a Turn-on Fluorescence Probe for Detecting Heparin in Plasma

3.1 Introduction

Sulfated glycosaminoglycans (GAGs) are a family of highly charged polysaccharides, consisting of variably sulfated alternating *N*-acetylhexosamine and uronic acid residues. Among them, heparin is the most highly sulfated with the highest negative charge density of any known biomolecule. Its structure consists predominantly of repeating trisulfated disaccharides, with chains of ~15 kDa (**Figure 3.1**).[1] Heparin is administered to more than 12 million patients per year as an anticoagulant agent in surgery and for treating certain thrombotic diseases such as venous thromboembolism.[2,3] Adverse side effects can occur with heparin administration, including bleeding and thrombocytopenia.[4,5] Numerous assays have therefore been developed over the years to monitor heparin plasma levels in patients. Traditional detection methods include activated clotting time (ACT), activated partial thromboplastin time (APTT), and measurement of antithrombin dependent anti-Factor Xa activity.[6-9] Most techniques are, however, indirect, expensive, and cannot be applied to all clinical settings.[10,11]

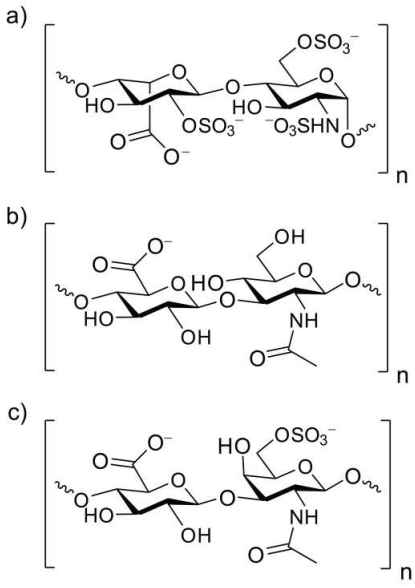

Figure 3.1: Primary repeating disaccharide units of a) heparin, b) hyaluronic acid, and c) chondroitin sulfate.

Fluorescence spectroscopy is a sensitive technique that can be used to monitor molecular-scale events in real time.[12] Fluorescence refers to the emission of a photon of light from the excited singlet state of a chromophore. Excited states are typically populated through absorption of energy in the UV-visible range of the electromagnetic spectrum. Upon energy absorption, fluorescent molecules, also called fluorophores, enter the excited state where they then can radiatively decay back to the ground state through emission of a photon. This process is represented in what is known as the Jablonski diagram (**Figure 3.2**).[13]

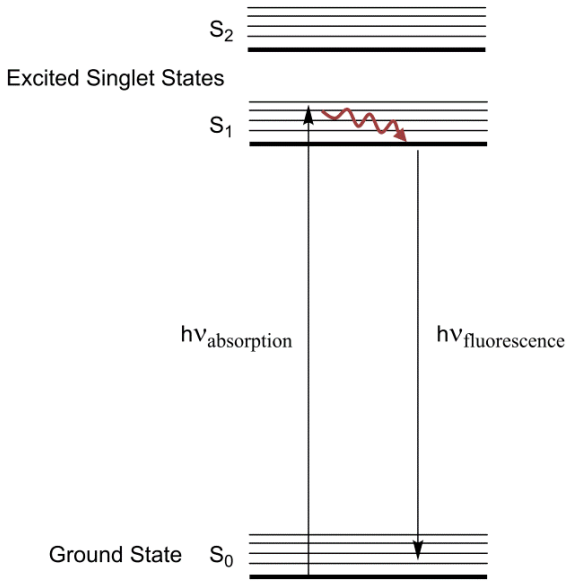

Figure 3.2: Simplified Jablonski diagram.

Multiple colorimetric and fluorometric methods have also been developed as potentially less expensive and more sensitive techniques for detecting heparin. Cationic dyes such as the phenothiazine derivatives methylene blue[14] and azure A[15] exhibit a UV response when bound to heparin, but only function in noncompetitive media (e.g. water and certain aqueous buffers) lacking high levels of electrolytes. More recently, tripodal boronic acid sensors,[16,17] benzimidazolium dyes[18] and a UV-responsive dye called Mallard Blue[19] showed sensitivity and selectivity for binding heparin in competitive media (e.g. serum and plasma). Other heparin sensors have utilized aggregation-induced emission (AIE) fluorogens that display “turn-on” features when bound to heparin.[20-23] While sensors have indeed been explored, many have limitations including “turn off” spectroscopic responses and poor sensitivity. Thus, there is still a need to develop simple, selective and sensitive sensors for detecting heparin in

biologically relevant media within the appropriate clinical therapeutic range (0.2–1.2 IU ml^{-1} therapeutic, 2–8 IU ml^{-1} cardiac surgery).[24,25]

Bis-2-methyl-4-amino-quinolyl-6-carbamide, known as surfen (**Figure 3.3a**), is a small molecule that has been studied extensively since its discovery in 1938 as an excipient for the production of depot insulin.[26-32] A recent study in our group identified surfen in the National Cancer Institute small molecule Diversity Set (NSC12155) as an antagonist of heparin and heparan sulfate (HS).[33] We showed surfen was able to neutralize heparin's ability to activate antithrombin in the inflammatory process, inhibit fibroblast growth factor binding and signaling *in vitro*, and block HS-mediated cell attachment and viral infection. This investigation also showed surfen's ability to bind to multiple types of GAGs in solution through changes in its photophysical features. Here, we demonstrate the ability of surfen to detect unfractionated heparin (UFH) via enhanced visible emission in clinically-relevant plasma samples using a simple 96-well plate format. We analyze its selectivity towards heparin compared to other GAG's such as chondroitin sulfate and hyaluronic acid, as well as towards other charged biomolecules and various analytes. Further photophysical studies were performed to investigate possible mechanisms of the fluorescent enhancement upon binding heparin in solution.

3.2 Results and Discussion

3.2.1 Surfen Detects Heparin in Plasma

Surfen displays weak fluorescence in neutral aqueous solutions with an

emission maximum at 480 nm upon excitation at 340 nm, which is significantly enhanced upon addition of heparin. The color change could be seen with the naked eye under UV illumination (**Figure 3.3b)**. In PBS (pH = 7.4), surfen (8 μM) displayed a stepwise increase in emission intensity at 480 nm upon titration of heparin (0–43 μM) with eventual saturation (**Figure 3.3c**). The quantum yield (Φ) of surfen was 0.02 and 0.003 with and without heparin, respectively. A 1:1 binding curve fit of a plot of the emission intensity at 480 nm with the amount of heparin added gave a K_d of 0.97 ± 0.08 μM (**Figure 3.3d**). Surfen displayed a detection range of 0.03 to 43 μM heparin (0.004–5.3 IU ml^{-1}) under these conditions.

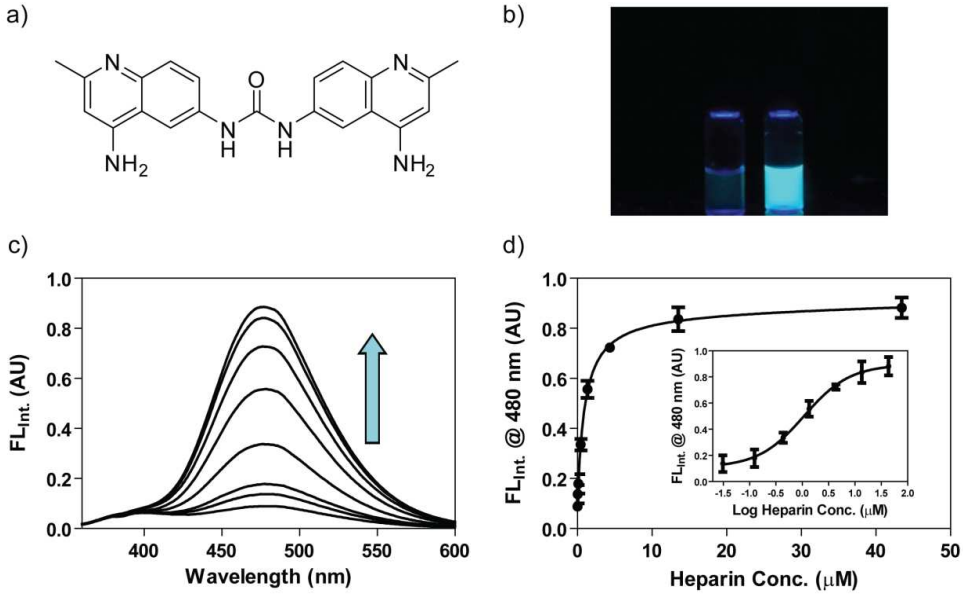

Figure 3.3: a) *Bis*-2-methyl-4-amino-quinolyl-6-carbamide (surfen); b) surfen solution without (left) and with (right) heparin; c) fluorescence emission spectra (excitation: 340 nm, cutoff: 360 nm) of surfen with 0–43 μM UFH in PBS buffer (pH = 7.4); d) fluorescent emission intensity at 480 nm upon addition of UFH at indicated concentrations in PBS buffer (pH = 7.4) [inset: fluorescent emission intensity at 480 nm plotted against log heparin concentration]. All experiments were performed in triplicate. Due to the heterogeneity of UFH, we used the repeating disaccharide as the unit of molecular weight for heparin (644.2 g/mol).[16]

Next, we tested surfen's selectivity for heparin compared to other glycosaminoglycans and various biologically-relevant analytes (**Figure 3.4**). Surfen was first titrated with increasing amounts of chondroitin sulfate (CS) or hyaluronic acid (HA) (repeating disaccharide structures shown in **Figure 3.1**). Chondroitin sulfate, a less sulfated GAG (~0.95 sulfated groups per disaccharide vs. ~2.4 for heparin) found in connective tissues[34] and at low concentrations (~4 μg ml^{-1}) in plasma,[35] gave a ~40% fluorescence response compared to heparin in this screen, whereas hyaluronic acid, an anionic nonsulfated GAG and vital component of the extracellular matrix,[36] gave minimal response. These results indicate that surfen binds selectively to sulfated GAGs, and that the level of GAG sulfation dictates the degree of binding and fluorescence response (heparin > CS >> HA). Additionally, surfen was incubated with human plasma (20% in PBS) and various analytes typically found in plasma such as sodium chloride (NaCl), sodium phosphate (NaH_2PO_4), sodium sulfate (Na_2SO_4), glucose, and trisodium citrate ($Na_3C_6H_5O_7$). Surfen exhibited the highest fluorescence response for heparin and a minimal response to the other analytes tested (**Figure 3.4b**). These results suggest that surfen could be used to selectively bind and detect heparin in highly competitive media, such as human plasma. Furthermore, to illustrate that the fluorescence enhancement is not a simple outcome of binding to negatively charged polymers, titration with single-stranded DNA (27-mer) gave minimal fluorescence response (**Figure 3.4b**). This confirms surfen's selectivity for binding to heparin in solution.

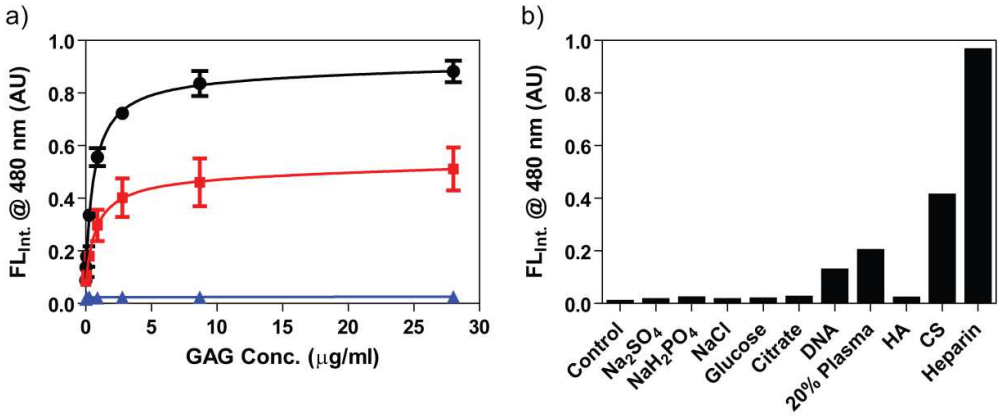

Figure 3.4: a) Titration of glycosaminoglycans with surfen (8 μM) in PBS buffer (pH = 7.4): ● heparin, ■ chondroitin sulfate, ▲ hyaluronic acid (performed in triplicate); b) surfen fluorescence emission intensity upon addition of analytes [all analytes were at 43 μM in PBS buffer (pH = 7.4); control is PBS buffer].

Finally, we investigated the detection of heparin in clinically-relevant human plasma in a 96-well plate using a fluorescence plate reader. Due to background fluorescence from the components of plasma and to increase the signal-to-noise ratio, we used a higher concentration of surfen (20 μM) for these experiments. Human plasma (20% in PBS) was spiked with varying concentrations of heparin (0–15 μM) before surfen was added to each well. These heparin concentrations were chosen based on the amount of heparin administered therapeutically to patients, which is in the range of 0.2–1.2 IU ml^{-1} (1.7–10 μM).[24] Surfen gave minimal fluorescence increase in 20% plasma alone. However, in the presence of increasing amounts of heparin, a stepwise increase in emission intensity at 480 nm upon excitation at 340 nm was observed (**Figure 3.5a**). A semilog plot of heparin concentration against the observed fluorescence intensity gave a linear correlation (**Figure 3.5b**). The convenience of sample preparation and the sensitive detection of heparin suggest that this assay could

easily be translated into a practical method for detecting heparin in human plasma samples.

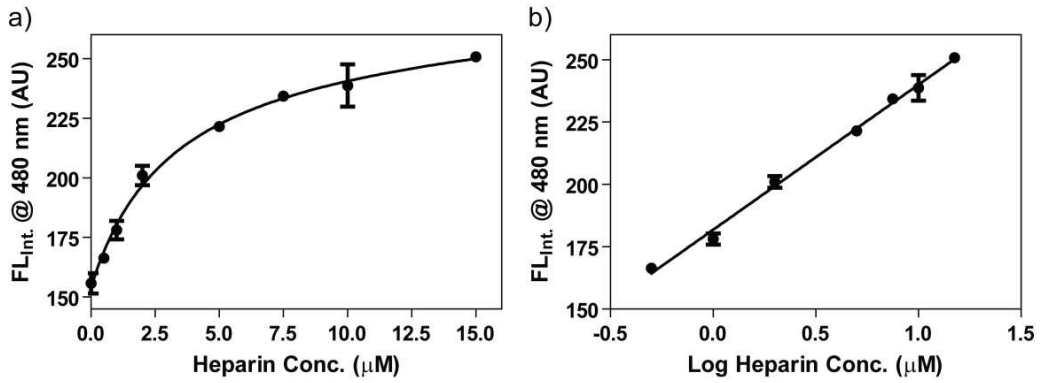

Figure 3.5: a) Fluorescence emission intensity at 480 nm of Surfen (20 μM) with 0-15 μM UFH in 20% pooled human plasma (in PBS buffer); b) linear fit of the logarithmic scale of graph (a).

To the best of our knowledge, the fundamental mechanism underlying this rather dramatic fluorescence enhancement has not been investigated. It is likely that at physiological pH the anionic sulfate and carboxylate groups of heparin could electrostatically interact with the urea and exocyclic amines of surfen through hydrogen bonding. It is possible that the protonated aminoquinolines (pk_a ≈ 9)[37] could be rigidified by aligning along the anionic polysaccharide chain, which will likely suppress certain non-radiative deactivation pathways leading to enhanced fluorescence. In the next section, we sought to shed light on surfen's fundamental photophysical features in order to further understand its interaction with heparin in solution.

3.2.2 Mechanism and Photophysical Study

To probe the mechanism of surfen's interaction with heparin and the nature of this enhanced emission upon binding, we set out to systematically

investigate the photophysical properties of this intriguing small molecule. Surfen's dimeric structure presents multiple potential hydrogen bonding sites, including the exocyclic amines, quinoline nitrogens, and urea linker region. Electrostatic interactions with the negatively-charged sulfate and carboxylate groups of heparin most likely induce the spectroscopic changes we observe. Here, we have considered a number of possible mechanisms for the unique turn-on fluorescence of surfen including aggregation-induced emission (AIE),[38] twisted intermolecular charge transfer (TICT),[39,40] and conformational planarization.[41] Fluorescence and absorption spectroscopy, circular dichroism, and X-ray crystallography were utilized to shed light on surfen's distinct binding mechanism and unique photophysical properties.

Aggregation and Supramolecular Assembly with Heparin

Surfen displays weak fluorescence at 480 nm upon excitation at 340 nm in aqueous solutions. Upon addition of heparin, we observed a large increase in fluorescence intensity at 480 nm with eventual saturation (**Figure 3.1**). Surfen displays characteristic absorption maxima at 266 nm, 300 nm, and 340 nm in its UV spectrum. Upon titration of heparin to a surfen solution in pure water, we observed a stepwise decrease and red-shift of the absorption at 340 nm and appearance of a new peak at 375 nm with an isosbestic point at 363 nm (**Figure 3.6**). This distinct red shift of absorption with trailing in the visible region is characteristic of light scattering due to the formation of aggregate structures in the ground state.[42,43] Similar bathochromic shifts in the absorption have been

observed in other small molecules upon formation of supramolecular assemblies with large biomolecules, such as heparin.[44-46] Heparin-binding dyes, such as methylene blue and acridine orange, have also displayed unique photophysical characteristics, including the formation of aggregates, in the presence of anionic GAG chains.[47-49] Therefore, we hypothesized that aggregation could be responsible for the enhanced fluorescence upon binding heparin. This phenomenon is known as aggregation-induced emission (AIE).[50]

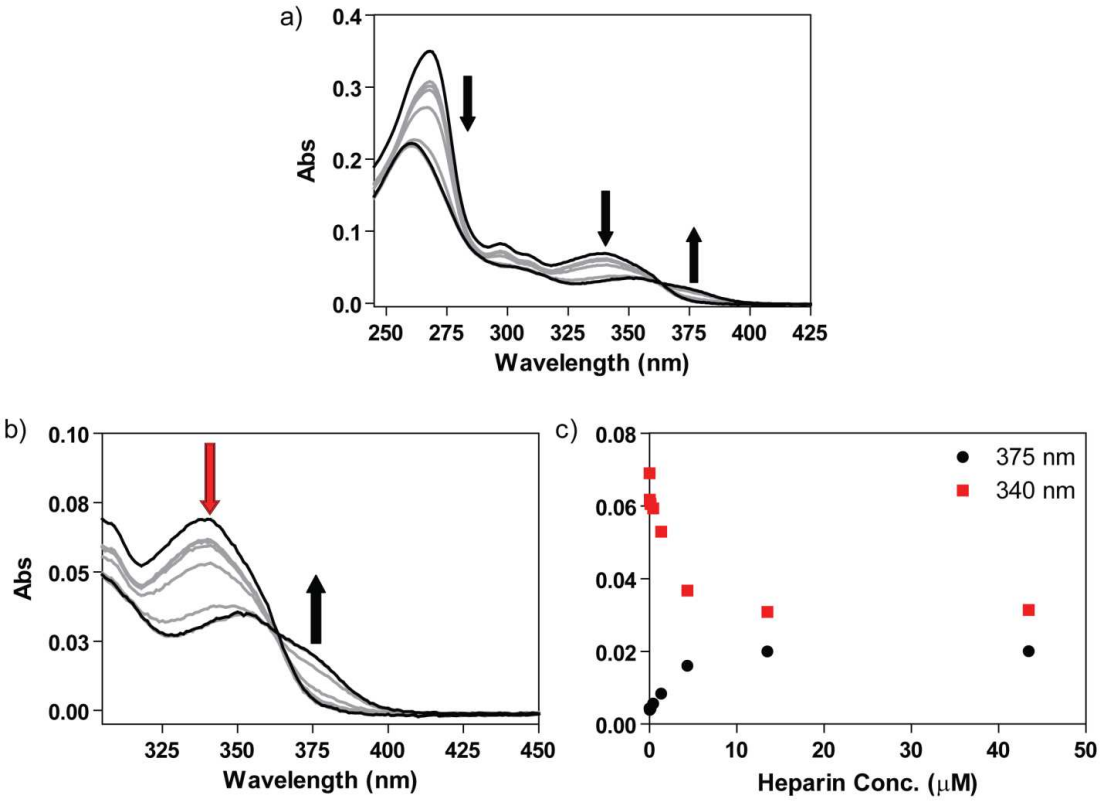

Figure 3.6: a) Absorption spectra of surfen upon addition of heparin in pure water at 20°C; b) visible region of absorption spectra; c) absorption changes upon addition of heparin (0-43 μM).

To determine whether this fluorescence enhancement is unique to the dimeric nature of surfen, we monitored the fluorescence properties of a "monomeric" analog of surfen, named trivially hemisurfen (**2**), upon addition of

heparin in solution. We previously showed that hemisurfen was unable to antagonize HS-protein interactions *in vitro*, thus suggesting it does not bind to GAGs (see Chapter 2). Hemisurfen displays a single emission peak at 400 nm upon excitation at 340 nm in aqueous buffer (PBS). The UV spectrum gave distinct absorption maxima at 252, 296, 308, and 340 nm. As anticipated, the emission and absorption were minimally altered upon addition of heparin (**Figure 3.7**). This further supports the notion that the dimeric structure of surfen is essential for its interaction with heparin and that its turn-on fluorescence is a result of binding to heparin in solution.

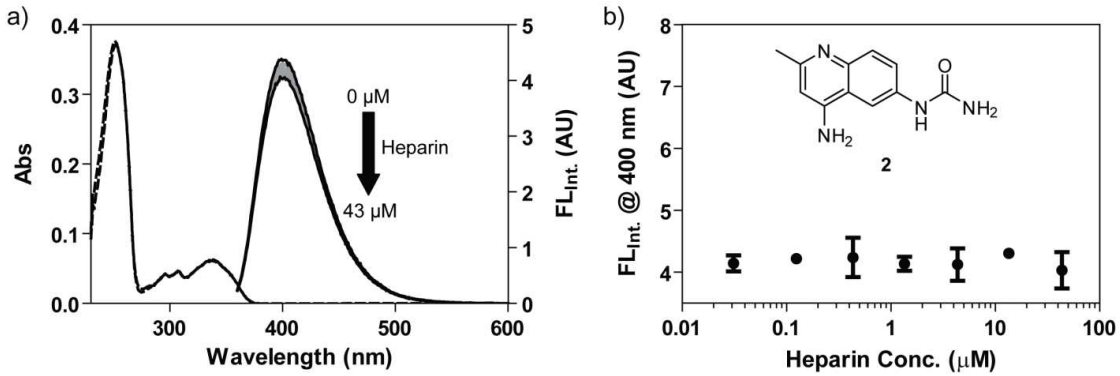

Figure 3.7: a) Hemisurfen (**2**) absorption (dashed lines) and emission (solid lines) spectra upon heparin addition (0-43 μM); b) fluorescence intensity at 400 nm upon addition of heparin (log scale) [inset: hemisurfen structure]; emission were recorded after excitation at 340 nm at 20°C.

Next, we investigated the interaction between surfen and heparin using circular dichroism (CD) spectroscopy. CD spectroscopy is a powerful technique that can give insight into the binding mode of a chromophore to a larger chiral biomolecule by utilizing the difference in absorption of circularly polarized light (e.g., left- and right-handed light). Depending on the conformation in solution, a chiral molecule or complex will absorb left- and right-handed polarized light

differently, which can present a positive or negative CD signal. Previous studies have utilized CD spectroscopy to monitor the chiral conformational change of heparin-binding molecules as they bind and aggregate along the helical, negatively-charged heparin chains.[48,51,52] Heparin's long asymmetric sugar residues provide chiral templates for the binding of cationic small molecules, which can induce a distinct CD signal that gives key information about the binding mode and nature of the heparin-chromophore complex.

Surfen is an achiral molecule that is not CD-active. However, upon addition of heparin to a surfen solution, we observed an induced CD effect with a positive signal at 272 nm and a negative CD signal at 252 nm. An isoelliptical point was observed at 263 nm, which correlates closely with the far UV (π-π*) absorption maximum of surfen (**Figure 3.8**). These results provide evidence that surfen molecules bind to heparin and organize along the sugar backbone to form a supramolecular complex with a distinct conformation. The positive cotton effect indicates a right-handed helical arrangement of the surfen–heparin complex. It is possible that upon binding, surfen molecules aggregate at distinct sites and create intermolecular interactions as they align along the polysaccharide chains.

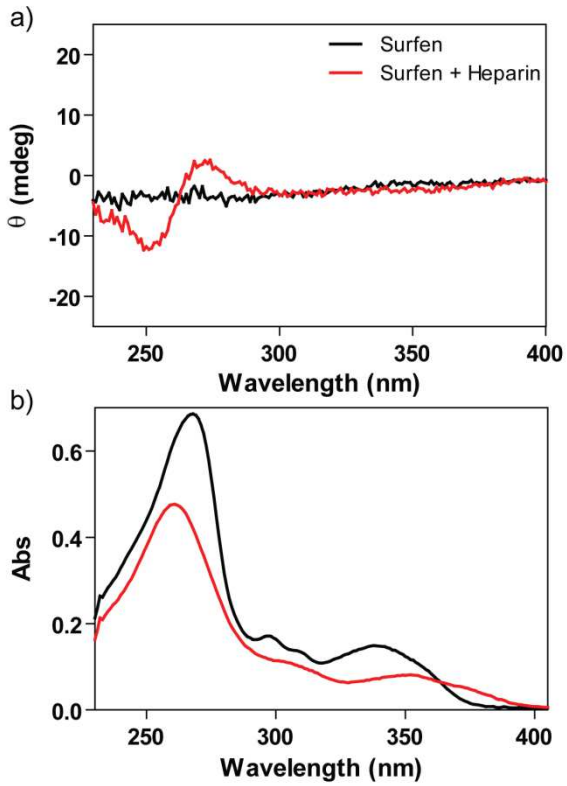

Figure 3.8: a) CD and b) absorption spectra of surfen with and without heparin (6.7 μM) in pure water at 25°C.

To examine the potential aggregation of surfen, we took a detailed look at the molecular geometry and packing arrangements of surfen in the solid state (**Figure 3.9**). In solid powder form, we noticed that surfen exhibited green fluorescence when illuminated with UV light (**Figure 3.9b**). In the single crystal structure of the TFA salt form of surfen (CCDC 1057477), we noticed the molecule's lack of planarity due to rotation around the C–N bond between the urea linker region and each aminoquinoline ring (torsion angles = ±12.07°). Also, the three-dimensional crystal packing revealed parallel offset intermolecular stacking in a ladder-type arrangement with a distance of 3.281 angstroms (Å) between the quinoline ring systems (**Figure 3.9c**). This intermolecular distance

and molecular arrangement are characteristic of π-π interactions.[53] The network of protonated surfen molecules is organized through hydrogen bonding with TFA counterions. Similar fluorescence-enhanced π-π stacking has been observed in other types of quinoline-containing molecules upon binding to analytes.[54-59] In a similar way, it's possible that electrostatic interaction with the anionic sulfate and carboxylate groups of heparin cause surfen molecules to align along the polysaccharide backbone and create aggregate structures. The intermolecular interactions induced through aggregation could be responsible for the surfen's enhanced fluorescence observed upon binding heparin.

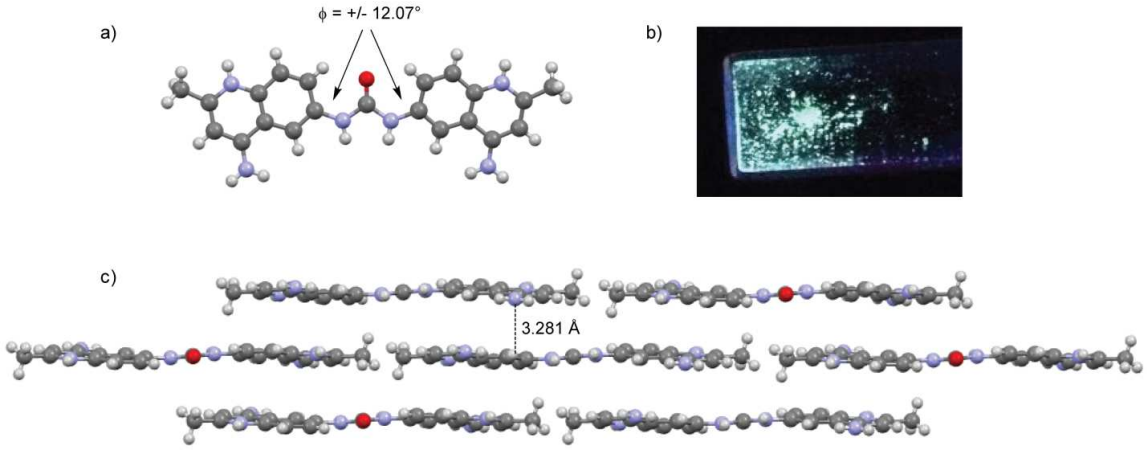

Figure 3.9: a) X-ray crystal structure of **surfen•2CF$_3$COOH**; b) surfen solid state fluorescence under UV light illumination; c) x-ray crystal packing of surfen. Distances and torsion angles were measured using Mercury v3.3. Counterions and water molecules omitted for clarity.

Due to the involvement of counterions in the molecular organization of surfen in the solid state, we explored whether we could observe any enhancement of emission upon binding anions in solution. Interestingly, titration of increasing amounts of sodium chloride (NaCl) into a surfen solution in pure water gave an increase of fluorescence intensity at 480 nm (**Figure 3.10**). We

also observed a red-shift in the absorption spectra with slight trailing in the visible region upon addition of NaCl (experimental section). However, upon addition of perchlorate anion, a weakly-coordinating anion,[60] there was no appearance of this new emission peak. It was necessary to introduce large (millimolar) amounts of NaCl in order to see any fluorescence response, while micromolar amounts of heparin gave a much higher signal. This is most likely due to heparin's ability to offer multiple anionic binding sites compared to individual chloride ions of NaCl. These results suggest that anion binding is involved in the emission enhancement of surfen in solution.

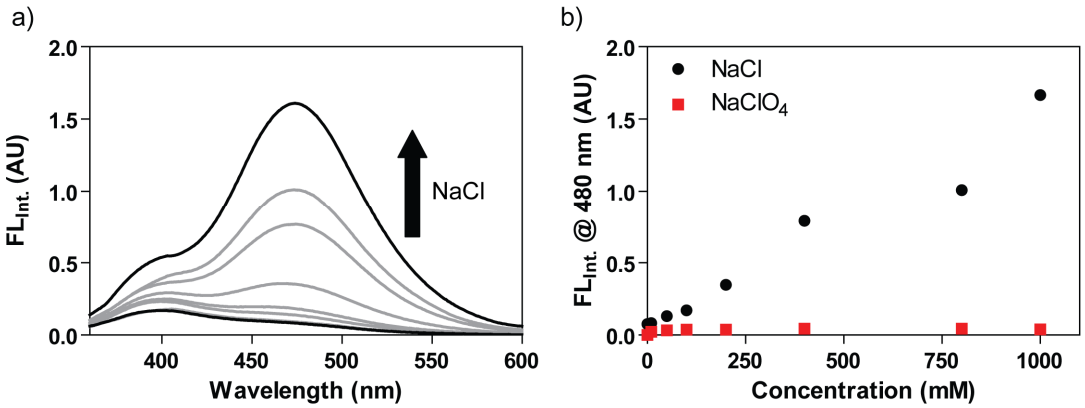

Figure 3.10: a) Emission spectra of surfen upon addition of NaCl (excitation at 340 nm at 20°C); b) comparison of fluorescence intensity at 480 nm vs. NaCl or $NaClO_4$ concentration (mM).

Many urea-based receptors have shown similar turn-on spectroscopic responses when bound to anions in solution.[61-65] Coordination of the sulfate and carboxylate groups to the urea moiety of surfen could aid in the formation of a supramolecular complex with heparin. To probe the interaction of surfen with anions, we performed ^1H NMR titrations in DMSO- d_6 with titration of increasing amounts of NaCl. Upon addition of NaCl, we observed a downfield shift of the N–

H urea protons (**Figure 3.11**). Titration of sodium perchlorate ($NaClO_4$) yielded minimal changes in chemical shift of the N-H signal. This supports our hypothesis that surfen can coordinate to chloride ions through the urea. In a similar way, surfen could bind to the sulfate and carboxylate groups of heparin to form a supramolecular complex.

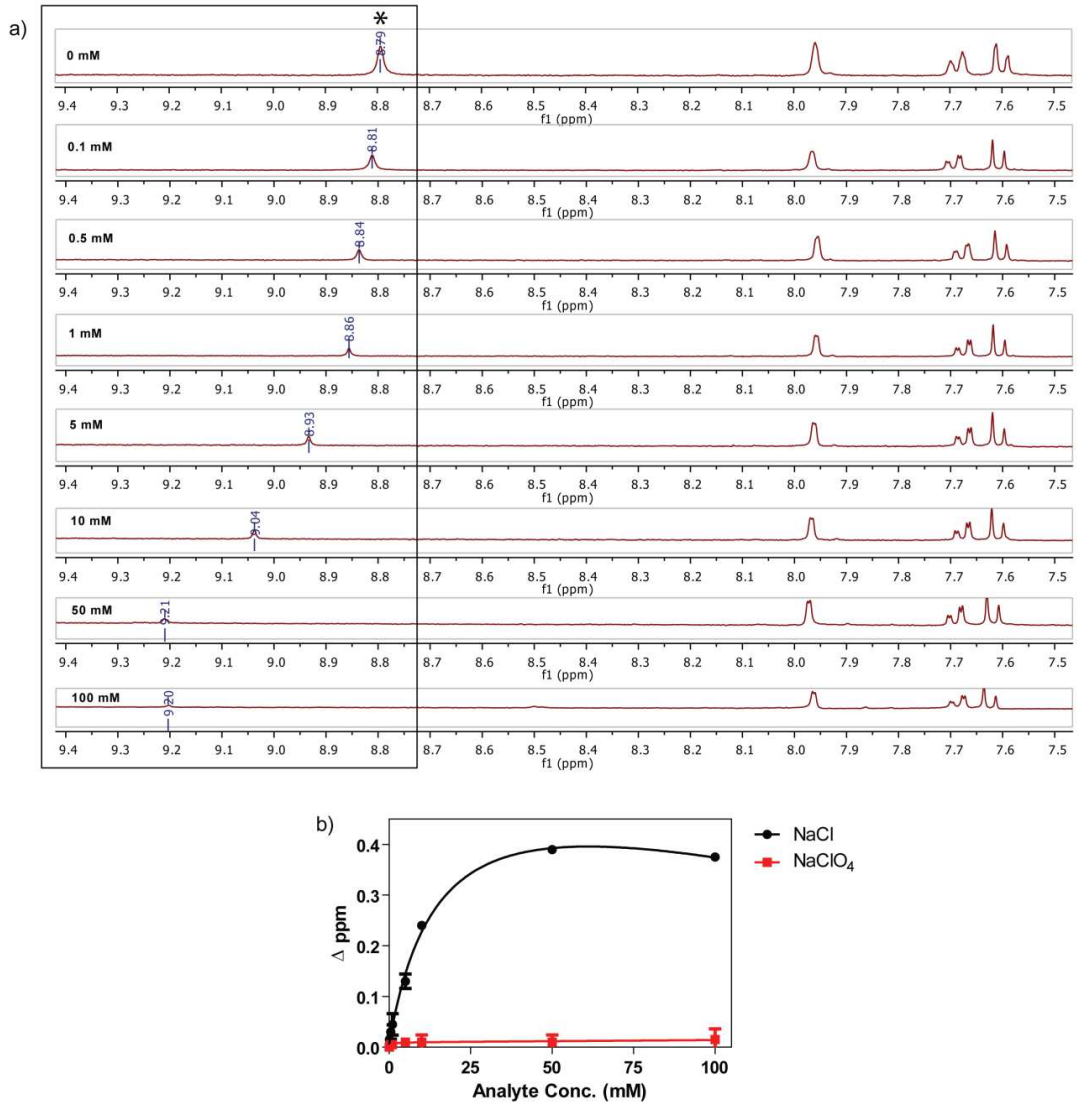

Figure 3.11: a) ^{1}H NMR (400 MHz, DMSO–d_6) titrations showing the downfield shift of the urea N-H signal of surfen (1 mM) in the presence of increasing amounts of NaCl at 25°C. Equivalents added of NaCl are 0, 0.1, 0.5, 1, 5, 10, 50, 100 mM in D_2O. b) Analyte concentration plotted against the change in chemical shift of the N-H signal.

Restricting Intramolecular Rotation: Surfen as a Molecular Rotor

Aggregation formation imposes physical rotational restraints. Due to the nonplanar structure of surfen and ability for the quinoline moieties to rotate about the C–N bond, it is possible that molecular planarization or restriction of intramolecular rotation prompted by binding to heparin could be responsible for surfen's fluorescent enhancement. Fluorophores sensitive to viscosity changes, frequently referred to as molecular rotors, are characterized by their ability to form twisted excited states upon photoexcitation due to rotational motion. They typically contain donor-acceptor moieties that can interact through charge transfer, a process known as twisted intramolecular charge transfer (TICT). The extent of charge transfer is dependent on the donor-acceptor energy gap and their molecular orientation in the excited state. The rotational motion of these moieties in low viscosity media can lead to non-radiative decay processes in the excited state resulting in minimized fluorescence. However, increasing the viscosity can restrict intramolecular rotation leading to radiative deexcitation and enhanced emission (**Figure 3.12**).[41,66] Molecular rotors possessing aggregation-induced emission properties have been previously reported to showcase this phenomenon.[38,50]

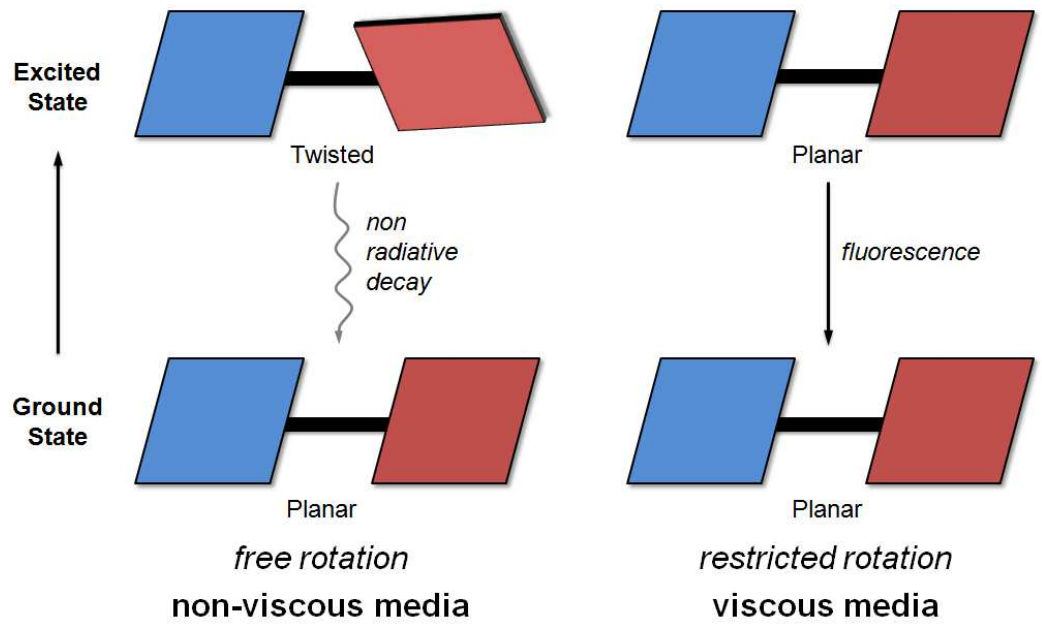

Figure 3.12: Mechanism of enhanced emission for molecular rotors in viscous media.

Glycerol is a highly viscous liquid that is fully miscible with many polar solvents. Mixtures of glycerol with methanol, whose viscosity is around 1720-fold lower than glycerol at room temperature, can create solvent mixtures with very diverse viscosities and minimal polarity differences.[66,67] Here, we evaluated the viscosity effect on the emissive behavior of surfen in glycerol-methanol mixtures with different fractions (volume %) of glycerol. Surfen showed a steady increase in fluorescence intensity at 395 nm with increasing fractions of glycerol (**Figure 3.13**). A log-log plot of fluorescence intensity and calculated viscosities gave a linear correlation, and there were no major changes in the ground state absorption spectra (experimental section).

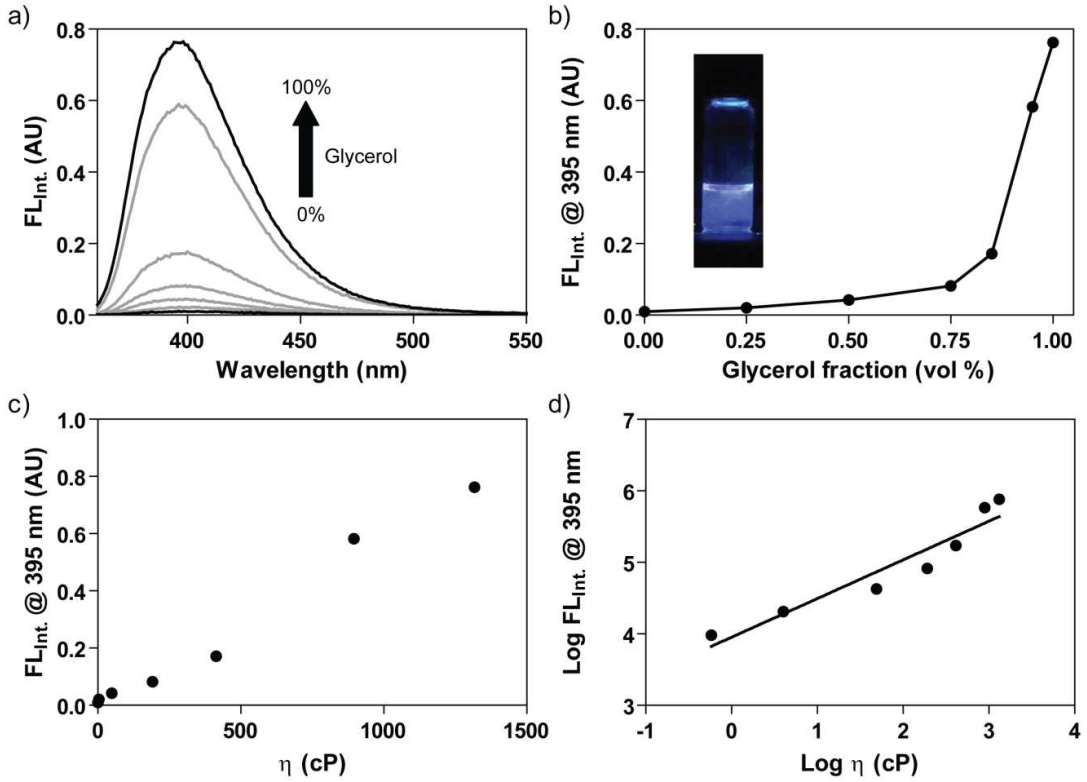

Figure 3.13: a) Surfen sensitivity to viscosity in glycerol-methanol solutions (0, 25, 50, 75, 85, 95, 100% glycerol); b) fluorescence intensity at 395 nm vs. glycerol fraction (% vol) [inset: surfen fluorescence in 100% glycerol solution upon UV illumination]; c) fluorescence intensity vs. viscosity (cP); d) log-log plot of fluorescence intensity vs. viscosity; emission were recorded after excitation at 340 nm at 20°C.

To confirm that the fluorescent enhancement at 395 nm was due to increasing the viscosity, we investigated surfen's response to temperature induced viscosity changes (**Figure 3.14**). Literature viscosity values for glycerol at different temperatures were used to graph the fluorescence intensity versus the change in viscosity.[66] Surfen displays a step-wise decrease in fluorescence intensity at 395 nm with increasing temperatures in a solution of 100% glycerol. The fluorescence enhancement given when intramolecular rotation is restricted seems to be unrelated to the red-shifted emission observed upon binding to heparin. These results suggest that surfen indeed shows sensitivity to viscosity

changes. The emission at 395 nm is attributed to the quinoline-centered emission that is restored upon impeding its intramolecular rotation between the aminoquinoline ring systems and the urea group. Therefore, it is suggested that intermolecular interactions upon aggregation could be responsible for the red-shifted emission observed in the presence of heparin.

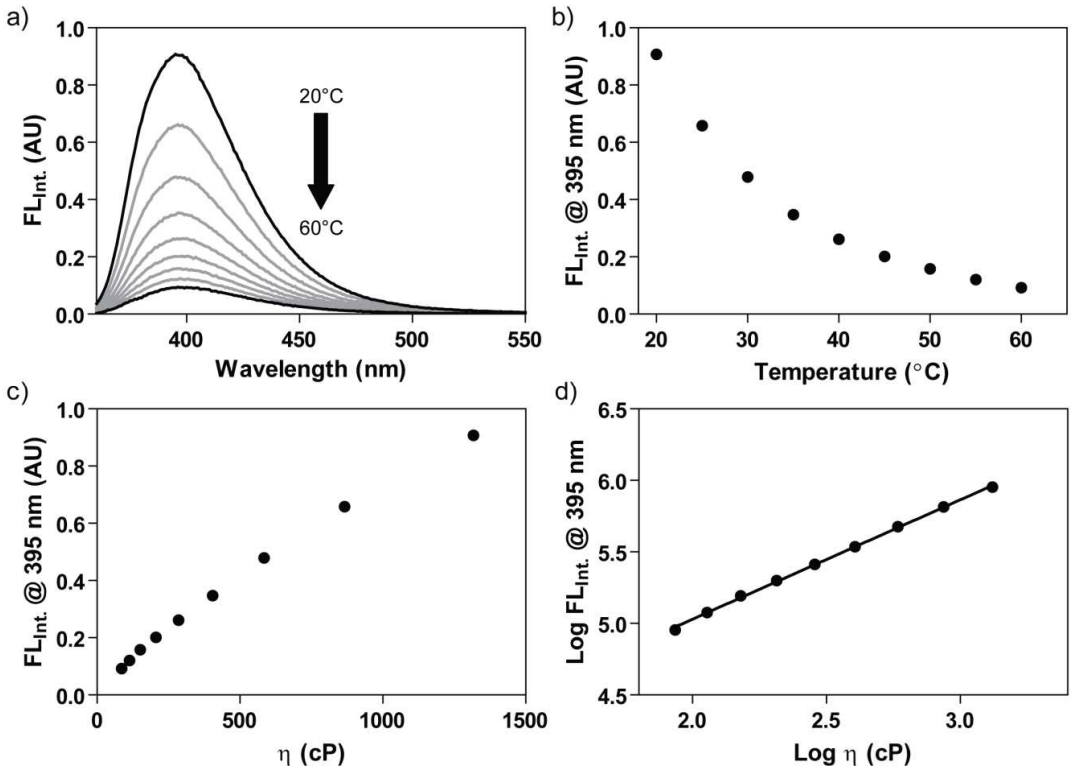

Figure 3.14: a) Surfen sensitivity to temperature-induced viscosity changes in 100% glycerol; b) fluorescence intensity at 395 nm vs. temperature (°C) and c) viscosity (cP); d) log-log plot of fluorescence intensity vs. viscosity; emission were recorded after excitation at 340 nm.

Solvent polarity can also play a major role in the stabilization of the twisted excited state of flexible donor-acceptor molecules. Polar solvents have been shown to stabilize the TICT state to yield red-shifted fluorescence albeit with lower intensity due to non-radiative decay through rotational motion.[40,68] To investigate solvent effects, we explored surfen's spectroscopic properties in

various solvents to study the effect of polarity. Surfen displayed diverse emission spectra depending on the solvent environment (**Figure 3.15a**). Surfen's emission was mostly quenched in polar protic solvents (e.g. water and methanol); however, the fluorescence (~400 nm) was enhanced in certain aprotic solvents (e.g. acetonitrile, dioxane), which could be attributed to the quinoline emission, a known fluorophore.[56,69] Sensitivity toward polarity can typically be reflected by the changes in Stokes shift (ν_{abs}–ν_{em}). Stokes shifts can be plotted against solvent $E_T(30)$ values, a microenvironmental polarity parameter, to give a correlation with changes in the Stokes shift.[70] Stokes shift values for surfen in different solvents were plotted against literature $E_T(30)$ values[71] to yield a linear response to polarity for most of the solvents used (**Figure 3.15c**). Interestingly, a distinct red-shifted emissive peak was observed in dichloromethane (DCM) and dioxane solutions. Stokes shift values for these low polarity solvents did not follow the linear trend when plotted with values obtained from other solvents. Also, the absorption spectra for these two solvents revealed a distinctive red-shift and trailing in the long wavelength region (**Figure 3.15b**). Therefore, this secondary red-shifted peak, similar to the one observed upon heparin addition, could be attributed to aggregation due to surfen's low solubility in these solvents. This type of unique fluorescence has been observed in bis-4-aminobenzamidines that are able to fluoresce upon binding to DNA, another highly anionic biomolecule.[72,73] Surfen appears to display TICT properties in the excited state in certain solvents. However, the red-shifted emission observed in low polarity solvents (e.g. DCM and dioxane) does not correlate to typical TICT states. Moreover, a broader

absorption band with trailing in the visible region suggests changes in the ground state could be related to this new emission.

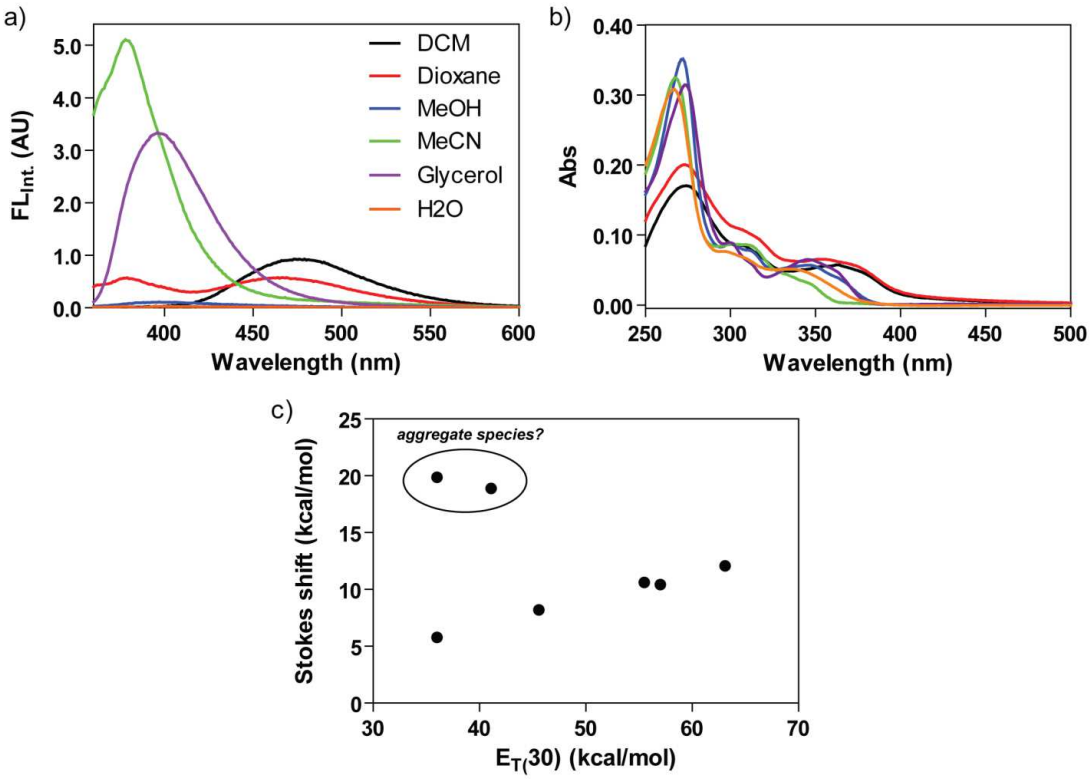

Figure 3.15: a) Emission and b) absorption spectra of surfen (6 μM) in various solvents; c) surfen sensitivity to polarity in various solvents; emission were recorded after excitation at 340 nm and corrected for changes in absorption.

To investigate this red-shifted emission in DCM and the possibility of aggregation in the ground state, we performed measurements of solvent mixtures of methanol and DCM to monitor whether this new red-shifted emission peak would appear upon increasing the amount of DCM, the poorer solvent, in the solution. Surfen exhibits weak emission in methanol, and the signal remains low when up to 97% DCM is present in the solution. When the amount of DCM was increased further, the fluorescence intensity at 480 nm rose swiftly (**Figure 3.16a-b**). Moreover, the absorption spectrum exhibited a step-wise increase of

intensity at 360 nm along with light scattering in the visible region upon addition of higher amounts of DCM (**Figure 3.16c-d**). These spectroscopic changes suggest aggregation is involved in the enhanced emission at 480 nm as surfen's solubility decreases in larger amounts of DCM.[74]

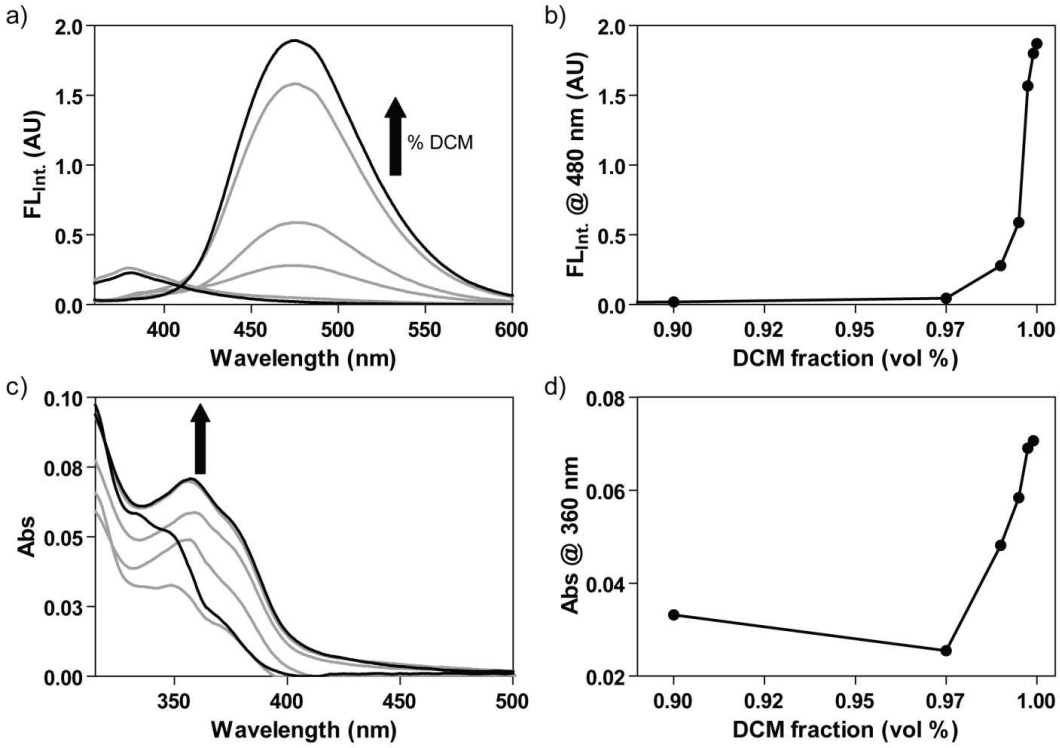

Figure 3.16: a) Emission and c) absorption spectra of surfen in methanol-DCM mixtures; b) fluorescence intensity at 480 nm and d) absorbance values at 360 nm in methanol-DCM mixtures; emission were recorded after excitation at 340 nm at 20°C.

3.3 Conclusions

In summary, we have utilized surfen, an easily accessible small molecule antagonist of heparin and heparan sulfate, as a selective and sensitive fluorescent probe for heparin in solution and in clinically-relevant plasma samples. Surfen was able to selectively distinguish heparin from other structurally-related GAGs and functioned in the presence of certain analytes and

in competitive media. Its high sensitivity and ease-of-use encourage further development of this important small molecule for point-of-care detection of heparin.

A detailed photophysical analysis revealed this small molecule's remarkable properties as a fluorescent probe for heparin. Surfen appears to aggregate upon binding to heparin to form a supramolecular complex in solution. Intermolecular interactions formed through binding-induced aggregation could be responsible for the turn-on emission observed in the presence of heparin. Surfen also acts as a fluorescent molecular rotor with sensitivity to viscosity and solvent polarity. This was found to be separate from the emission gained upon binding to heparin. In highly viscous media, a blue-shifted emissive peak appears and is attributed to restriction of intramolecular rotation resulting in enhanced radiative deexcitation. These studies show that surfen is a highly complex fluorescent probe with distinct photophysical behaviors based on its microenvironment. Computational studies and time-resolved spectroscopy could shed additional light on the nature of its unique fluorescence properties. Further studies could also uncover more applications for this unique small molecule as a fluorescent sensor, and analogs with more favorable fluorescent properties could also be explored to enhance selectivity and act as sensors in more complex biological systems.

3.4 Experimental

Materials

Unless otherwise specified, materials purchased from commercial suppliers were used without further purification. Surfen (bis-2-methyl-4-amino-quinolyl-6-carbamide) was obtained from the Open Chemical Repository in the Developmental Therapeutic Program of the National Cancer Institute (NSC12155). Hemisurfen was synthesized according to procedures outlined in Chapter 2 of this thesis. All solvents used were spectroscopic grade and were obtained from Alfa Aesar. Spectroscopic grade glycerol was from Acros, and DCM and acetonitrile were obtained from Sigma Aldrich. Sodium chloride and sodium perchlorate were obtained from Fisher Scientific. NMR solvents were purchased from Cambridge Isotope Laboratories (Andover, MA). PBS (Dulbecco's phosphate buffered saline, pH=7.4) was purchased from Life Technologies (Carlsbad, CA). Heparin (sodium salt, activity ≈188.9 IU/mg) was obtained from Scientific Protein Laboratories. Chondroitin sulfate (sodium salt from shark cartilage) and hyaluronic acid (sodium salt from *Streptococcus equi*) were purchased from Sigma Aldrich. Pooled citrated human plasma was obtained from George King Bio-medical Inc. Unmodified DNA oligonucleotide (27-mer, single-stranded; sequence shown below) was obtained from Integrated DNA Technologies, Inc.

5′-T 3′-d-ATT ATG CTG AGT GAT ATC GCG GCA CGT-5′

Figure 3.17: Single-stranded DNA template (27-mer).

Aqueous samples were prepared with milli-Q water. For all spectroscopic measurements, a 1 cm four-sided Helma quartz cuvette was used. All surfen samples were prepared from concentrated DMSO stock solutions, hence, all samples contain 0.3 v% DMSO. DMSO solutions were made and stored in glass containers because surfen has been previously found to stick to plastic. These solutions were stored under argon at -20°C.

Instrumentation

Absorption spectra were measured on a Shimadzu UV-2450 UV-Vis spectrophotometer with 1 nm resolution and corrected for the blank. The sample temperature was kept constant at 20°C using a thermostat controlled ethylene glycol-water bath fitted to a specially designed cell holder. Steady state emission spectra were taken on a PTI luminescence spectrometer with a 1 nm resolution. The sample temperature was controlled with a Quantum Northwest TLC50 fluorescence cuvette holder in conjunction with a software controllable TC 125 temperature controller. All CD spectra were recorded on an Aviv 215 Circular Dichroism Spectrometer in a 1.5 mL quartz cell with a path length of 1 cm at 25°C. NMR spectra were recorded on Varian Mercury 400 MHz spectrometer at ambient temperature. Fluorescence measurements for the 96-well plate assay were performed on a SpectraMax M3 plate reader (Molecular Devices) using Softmax Pro software. All data was plotted and analyzed using GraphPad Prism v5.0.

Heparin, CS, and HA titrations

Heparin, chondroitin sulfate (CS), and hyaluronic acid (HA) stock solutions were made in pure water. GAG solutions were titrated stepwise into a surfen or hemisurfen solution (8 μM in PBS) to give 0, 0.02, 0.08, 0.28, 0.89, 2.8, 8.7, and 28 μg/ml GAG concentrations. Fluorescence spectra were measured (λ_{ex} = 340 nm, slit widths 1.2 mm) and the intensity at 480 nm was plotted against GAG concentration (μg/mL). Titrations were performed in triplicate.

For hemisurfen titrations, heparin solutions were titrated stepwise into a hemisurfen solution (8 μM in PBS) to give 0, 0.03, 0.12, 0.43 1.35, 4.35, 13.5, and 43 μM heparin concentrations. Fluorescence spectra were measured (λ_{ex} = 340 nm, slit widths 1.2 mm) and the intensity at 400 nm was plotted against heparin concentration (μM). Titrations were performed in duplicate.

For absorption titrations, heparin stock solutions were made in pure water and were titrated stepwise into a surfen solution (8 μM in pure water). Absorption spectra were measured after each addition and the values at 340 and 375 nm were plotted against heparin concentration (μM). Titrations were performed in duplicate.

Surfen in the presence of various analytes

Surfen solutions (8 μM) were made in solutions containing various analytes (43 μM final concentration in PBS). The fluorescence emission was measured upon excitation at 340 nm (slit widths 1.2 mm). Background

fluorescence without surfen was subtracted for each sample. Results are presented as emission intensity at 480 nm.

Heparin detection in 20% human plasma (96-well plate assay)

20% human plasma solutions (in PBS) were placed in a black polystyrene 96-well plate (Corning®) and spiked with known concentrations of heparin (0–15 μM; 0–1.82 IU/mL). Next, a surfen stock solution (PBS, 0.7 v% DMSO) was added to each well to yield a final concentration of 20 μM. The fluorescence was measured immediately on a fluorescent plate reader (340/480 nm; cutoff 475 nm). Measurements were run in triplicate. Standard curves were plotted as the emission intensity at 480 nm against the concentration of heparin (μM). The curves were fitted with linear regression (R^2 = 0.9826).

Quantum yield

Quantum yields were determined using Coumarin-1 in ethanol (Φ = 0.73) as a standard for surfen using dilute sample solutions with an optical density (O.D.) < 0.1 at the λ_{ex}, using the equation 1:

(1)

$$\Phi_s = \frac{I_s}{I_{ref}} \cdot \frac{O.D._{ref}}{O.D._s} \cdot \left(\frac{n_s}{n_{ref}}\right)^2 \cdot \Phi_{ref}$$

Here Φ, I, O.D., and n stand for quantum yield, integrated emission intensity, optical density at λ_{ex} and refractive index (n_{water} = 1.333, $n_{ethanol}$ = 1.361), respectively. Sample and reference are denoted by *s* and *ref*, respectively. The λ_{ex} is in very close proximity for the sample and reference

solutions to circumvent correction of the difference in excitation energy at different wavelengths.

Viscosity studies

Samples of different viscosity were prepared by mixing the appropriate amounts (volume %) of methanol with glycerol in different ratios along with a calculated amount of the DMSO sample stock solution (0.3 v% DMSO) to give a final surfen concentration of 6 μM. All samples were heated and mixed thoroughly before pouring into the cuvette. The solutions were allowed to equilibrate back to room temperature prior to emission (λ_{exc} = 340 nm, slit widths 0.8 mm) and absorption scanning. The sample viscosity was calculated based on the literature viscosity for the pure glycerol and methanol and their mixing ratio using equation 2.[41]

(2)

$$\ln \eta_{mix} = \sum_{i=1}^{2} \omega_i \cdot \ln \eta_i$$

In equation 2, η_{mix} and η_i stand for the viscosity of the mixture and the viscosity of component i respectively. Factor ω_i stands for the weight fraction of component i. In all cases, we observed minimal changes in the absorption spectra at different glycerol-methanol mixtures (**Figure 3.18**). All emission spectra were corrected for small changes in O.D. at the λ_{ex} using equation 3.

(3)

$$FL_{corr\ int.} = \frac{0.1}{Abs_{\lambda_{ex}}} \times FL_{int.}$$

In this equation, $FL_{corr.int.}$ stands for the corrected fluorescence intensity at λ_{em}. $Abs_{\lambda ex}$ and $FL_{int.}$ are the observed absorption at λ_{ex} and fluorescence intensity, respectively.

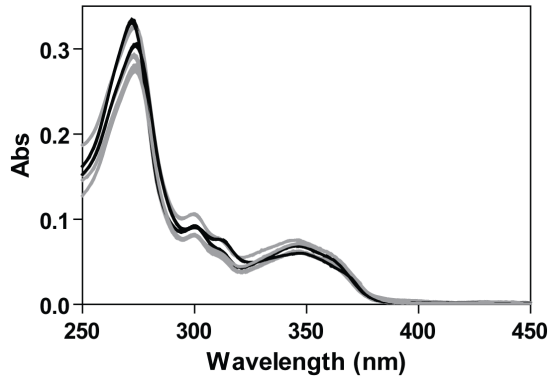

Figure 3.18: Absorption spectra of surfen (6 μM) in glycerol-methanol mixtures. 100% glycerol and methanol solutions shown in black, while all other mixtures shown in gray.

For temperature studies in 100% glycerol, surfen solutions (6μM) were made in 100% glycerol and run in duplicate (excitation at 340 nm) at 20-60°C in 5°C increments. Literature viscosity values[66] at each temperature (**Table 3.1**) were plotted against fluorescence intensity at 395 nm (λ_{exc} = 340 nm, slit widths 0.8 mm).

Table 3.1: Literature viscosity values for glycerol at different temperatures.

Temperature (°C)	Viscosity (cP)[66]
20	1317
25	866.3
30	584.8
35	404.3
40	285.8
45	206.1
50	151.5
55	113.4
60	86.19

NaCl and $NaClO_4$ titrations

NaCl and $NaClO_4$ stock solutions were made in pure water. Salt solutions were titrated stepwise into a surfen solution (8 μM in PBS) to give 0, 10, 50, 100, 200, 400, 800, and 1000 mM salt concentrations. Absorption (**Figure 3.19**) and fluorescence (λ_{ex} = 340 nm, slit widths 1.2 mm) spectra were measured. The mean fluorescence intensity at 480 nm was plotted against salt concentration (mM). Titrations were performed in duplicate. All emission spectra were corrected for changes in O.D. at the λ_{ex} using equation 3.

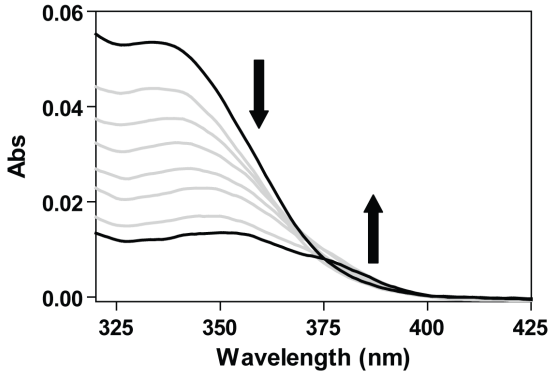

Figure 3.19: Absorption spectra of surfen (8 μM) upon addition of NaCl (0-1000 mM).

^{1}H NMR titrations

For ^{1}H NMR titration experiments, a 1 mM solution of surfen (in DMSO-d_6) was loaded into an NMR tube. A standard scan with no added anion was taken as a control. Stock solutions of either NaCl or $NaClO_4$ were prepared in D_2O and added. Measurements were taken after one addition and then again after each subsequent addition. NMR experiments measured response when equivalents of 0, 0.1, 0.5, 1, 5, 10, 50, and 100 (mM) of salts were added. NMR titration results (in duplicate) were plotted as salt concentration versus the change in chemical shift (Δ ppm) and fitted using 1:1 total binding with Prism v5.0. Minimal chemical shifts observed upon titration of D_2O alone were subtracted as background prior to analysis of results.

Solvent polarity study

Surfen solutions (6μM) were made in various spectroscopic grade solvents from DMSO stock solutions (0.3 v% DMSO). All emission spectra are corrected for small changes in O.D. at λ_{ex} (equation 3). Normalized emission spectra are shown below (**Figure 3.20**). Emission and absorption maxima,

Stokes shifts, and literature $E_T(30)$ values (at room temperature)[71] are shown in **Table 3.2**.

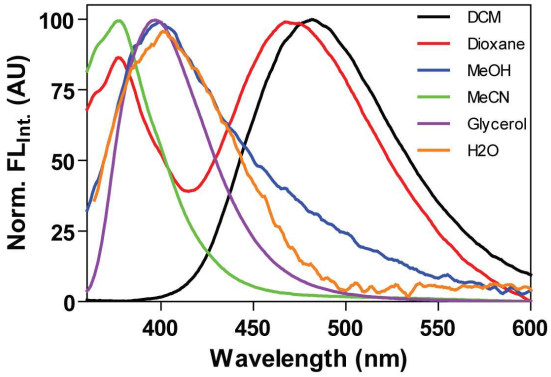

Figure 3.20: Normalized emission of surfen (6 μM) in various solvents (excitation at 340 nm, slit widths 1.2 mm).

Table 3.2: Photophysical properties of surfen in various solvents

Solvent	**λ_{abs} Max (nm)**	**λ_{em} Max (nm)**	**Stokes shift (cm^{-1})**	**Stokes shift (kcal/mol)**	**$E_T(30)$ (kcal/mol)**
DCM	361	480	6867	19.6	40.7
Dioxane	352	379/469	2024/7087	5.79/20.3	36.0
MeOH	346	397	3713	10.6	55.4
MeCN	341	378	2871	8.21	45.6
Glycerol	346	395	3649	10.4	57.0
H_2O	340	397	4223	12.1	63.1

Dichloromethane-methanol mixtures

Samples were prepared by mixing the appropriate amounts (volume %) of dichloromethane (DCM) with methanol in different ratios along with a calculated amount of a DMSO sample stock solution (0.3 v% DMSO) to give a final surfen concentration of 6 μM. The emission and absorption of 0.1, 0.25, 0.5, 1, 2.5, and 10% methanol-DCM mixtures were measured (excitation at 340 nm, slit widths 1.5 mm). Emission (at 480 nm) and absorption (at 360 nm) intensities were plotted against the amount of DCM (volume %).

Acknowledgments

Chapter 3 is in full currently in preparation for submission: Weiss, R. J.; White, C. M.; Esko, J. D.; Tor, Y. Surfen as a Turn-on Fluorescent Probe for Detecting Heparin in Plasma. The dissertation author is the main author and researcher of this work.

3.5 References

(1) Hirsh, J.; Raschke, R. *Chest* **2004**, *126*, 188S.

(2) Capila, I.; Linhardt, R. J. *Angewandte Chemie International Edition* **2002**, *41*, 390.

(3) Jang, I.-K.; Hursting, M. J. *Circulation* **2005**, *111*, 2671.

(4) Warkentin, T. E.; Levine, M. N.; Hirsh, J.; Horsewood, P.; Roberts, R. S.; Gent, M.; Kelton, J. G. *New England Journal of Medicine* **1995**, *332*, 1330.

(5) Francis, J. L.; Groce, J. B.; Heparin Consensus, G. *Pharmacotherapy: The Journal of Human Pharmacology and Drug Therapy* **2004**, *24*, 108S.

(6) Simko, R. J.; Tsung, F. F.; Stanek, E. J. *The Annals of pharmacotherapy* **1995**, *29*, 1015.

(7) Gravlee, G. P.; Case, L. D.; Angert, K. C.; Rogers, A. T.; Miller, G. S. *Anesthesia and Analgesia* **1988**, *67*, 469.

(8) Bowers, J.; Ferguson, J. J. *Texas Heart Institute Journal* **1993**, *20*, 258.

(9) Bates, S. M.; Weitz, J. I. *Circulation* **2005**, *112*, e53.

(10) Walenga, J. M.; Hoppensteadt, D. A. *Semin Thromb Hemost* **2004**, *30*, 683.

(11) Levine, M. N.; Hirsh, J.; Gent, M.; Turpie, A. G.; Cruickshank, M.; Weitz, J.; Anderson, D.; Johnson, M. *Archives of internal medicine* **1994**, *154*, 49.

(12) Sinkeldam, R. W.; Greco, N. J.; Tor, Y. *Chemical Reviews* **2010**, *110*, 2579.

(13) Albani, J. R. *Principles and Applications of Fluorescence Spectroscopy*, 2007.

(14) Jiao, Q. C.; Liu, Q.; Sun, C.; He, H. *Talanta* **1999**, *48*, 1095.

(15) Klein, M. D.; Drongowski, R. A.; Linhardt, R. J.; Langer, R. S. *Analytical biochemistry* **1982**, *124*, 59.

(16) Wright, A. T.; Zhong, Z.; Anslyn, E. V. *Angewandte Chemie International Edition* **2005**, *44*, 5679.

(17) Zhong, Z.; Anslyn, E. V. *Journal of the American Chemical Society* **2002**, *124*, 9014.

(18) Wang, S.; Chang, Y.-T. *Chemical Communications* **2008**, 1173.

(19) Bromfield, S. M.; Wilde, E.; Smith, D. K. *Chemical Society Reviews* **2013**, *42*, 9184.

(20) Liu, H.; Song, P.; Wei, R.; Li, K.; Tong, A. *Talanta* **2014**, *118*, 348.

(21) Kwok, R. T. K.; Geng, J.; Lam, J. W. Y.; Zhao, E.; Wang, G.; Zhan, R.; Liu, B.; Tang, B. Z. *Journal of Materials Chemistry B* **2014**, *2*, 4134.

(22) Xu, B. W.; Wu, X. F.; Li, H. B.; Tong, H.; Wang, L. X. *Polymer* **2012**, *53*, 490.

(23) Wang, M.; Zhang, D.; Zhang, G.; Zhu, D. *Chemical Communications* **2008**, 4469.

(24) Hirsh, J.; Anand, S. S.; Halperin, J. L.; Fuster, V. *Circulation* **2001**, *103*, 2994.

(25) Sauceda, J. C.; Duke, R. M.; Nitz, M. *ChemBioChem* **2007**, *8*, 391.

(26) Iensch, H. *Angewandte Chemie* **1937**, *50*, 891.

(27) Goble, F. C. *The Journal of pharmacology and experimental therapeutics* **1950**, *98*, 49.

(28) Warford, J.; Doucette, C. D.; Hoskin, D. W.; Easton, A. S. *Biochemical and biophysical research communications* **2014**, *443*, 524.

(29) Lanza, T. J.; Durette, P. L.; Rollins, T.; Siciliano, S.; Cianciarulo, D. N.; Kobayashi, S. V.; Caldwell, C. G.; Springer, M. S.; Hagmann, W. K. *Journal of medicinal chemistry* **1992**, *35*, 252.

(30) Panchal, R. G.; Hermone, A. R.; Nguyen, T. L.; Wong, T. Y.; Schwarzenbacher, R.; Schmidt, J.; Lane, D.; McGrath, C.; Turk, B. E.; Burnett, J.; Aman, M. J.; Little, S.; Sausville, E. A.; Zaharevitz, D. W.; Cantley, L. C.; Liddington, R. C.; Gussio, R.; Bavari, S. *Nature structural & molecular biology* **2004**, *11*, 67.

(31) Roan, N. R.; Sowinski, S.; Munch, J.; Kirchhoff, F.; Greene, W. C. *The Journal of biological chemistry* **2010**, *285*, 1861.

(32) Smith, S. A.; Choi, S. H.; Collins, J. N. R.; Travers, R. J.; Cooley, B. C.; Morrissey, J. H. *Blood* **2012**, *120*, 5103.

(33) Schuksz, M.; Fuster, M. M.; Brown, J. R.; Crawford, B. E.; Ditto, D. P.; Lawrence, R.; Glass, C. A.; Wang, L.; Tor, Y.; Esko, J. D. *Proceedings of the National Academy of Sciences* **2008**, *105*, 13075.

(34) Volpi, N. *Chondroitin Sulfate: Structure, role and pharmacological activity*; Elsevier Science, 2006.

(35) Volpi, N.; Maccari, F. *Clinica Chimica Acta* **2005**, *356*, 125.

(36) Laurent, T. C.; Fraser, J. R. *The FASEB Journal* **1992**, *6*, 2397.

(37) Albert, A.; Goldacre, R. *Nature* **1944**, *153*, 467.

(38) Hong, Y.; Lam, J. W. Y.; Tang, B. Z. *Chemical Society Reviews* **2011**, *40*, 5361.

(39) Grabowski, Z. R.; Rotkiewicz, K.; Rettig, W. *Chemical Reviews* **2003**, *103*, 3899.

(40) Hu, R.; Lager, E.; Aguilar-Aguilar, A.; Liu, J.; Lam, J. W. Y.; Sung, H. H. Y.; Williams, I. D.; Zhong, Y.; Wong, K. S.; Peña-Cabrera, E.; Tang, B. Z. *The Journal of Physical Chemistry C* **2009**, *113*, 15845.

(41) Haidekker, M. A.; Theodorakis, E. A. *Organic & Biomolecular Chemistry* **2007**, *5*, 1669.

(42) Hao, E.; Sibrian-Vazquez, M.; Serem, W.; Garno, J. C.; Fronczek, F. R.; Vicente, M. G. H. *Chemistry – A European Journal* **2007**, *13*, 9035.

(43) Fan, X.; Zheng, W.; Singh, D. J. *Light Sci Appl* **2014**, *3*, e179.

(44) Zsila, F.; Gedeon, G. *Biochemical and Biophysical Research Communications* **2006**, *346*, 1267.

(45) Nalage, S. V.; Bhosale, S. V.; Bhargava, S. K.; Bhosale, S. V. *Tetrahedron Letters* **2012**, *53*, 2864.

(46) Toby, T. K.; Sommers, C. D.; Keire, D. A. *Analytical Methods* **2012**, *4*, 1488.

(47) Patil, K.; Pawar, R.; Talap, P. *Physical Chemistry Chemical Physics* **2000**, *2*, 4313.

(48) Zhang, S.; Zhao, F.; Li, N.; Li, K.; Tong, S. *Spectrochim Acta A Mol Biomol Spectrosc* **2002**, *58*, 2613.

(49) Stone, A. L.; Bradley, D. F. *Biochimica et Biophysica Acta (BBA) - General Subjects* **1967**, *148*, 172.

(50) Hong, Y.; Lam, J. W. Y.; Tang, B. Z. *Chemical Communications* **2009**, 4332.

(51) Salter, M. K.; Rippon, W. B.; Abrahamson, E. W. *Biopolymers* **1976**, *15*, 1213.

(52) Stanley, F. E.; Warner, A. M.; Gutierrez, S. M.; Stalcup, A. M. *Biochemical and Biophysical Research Communications* **2009**, *388*, 28.

(53) Hunter, C. A.; Sanders, J. K. M. *Journal of the American Chemical Society* **1990**, *112*, 5525.

(54) Ghosh, K.; Adhikari, S. *Tetrahedron Letters* **2006**, *47*, 3577.

(55) Pramanik, A.; Das, G. *Tetrahedron* **2009**, *65*, 2196.

(56) Ghosh, K.; Adhikari, S.; Chattopadhyay, A. P.; Chowdhury, P. R. *Beilstein Journal of Organic Chemistry* **2008**, *4*, 52.

(57) Ghosh, K.; Adhikari, S. *Tetrahedron Letters* **2008**, *49*, 658.

(58) Yoshioka, H.; Nakatsu, K. *Chemical Physics Letters* **1971**, *11*, 255.

(59) Kalita, D.; Deka, H.; Samanta, S. S.; Guchait, S.; Baruah, J. B. *Journal of Molecular Structure* **2011**, *990*, 183.

(60) Krossing, I.; Raabe, I. *Angewandte Chemie International Edition* **2004**, *43*, 2066.

(61) Russ, T. H.; Pramanik, A.; Khansari, M. E.; Wong, B. M.; Hossain, M. A. *Natural Product Communications* **2012**, *7*, 301.

(62) Amendola, V.; Fabbrizzi, L.; Mosca, L. *Chemical Society Reviews* **2010**, *39*, 3889.

(63) Smith, P. J.; Reddington, M. V.; Wilcox, C. S. *Tetrahedron Letters* **1992**, *33*, 6085.

(64) Bergamaschi, G.; Boiocchi, M.; Monzani, E.; Amendola, V. *Organic & Biomolecular Chemistry* **2011**, *9*, 8276.

(65) Kassl, C. J.; Christopher Pigge, F. *Tetrahedron Letters* **2014**, *55*, 4810.

(66) Sinkeldam, R. W.; Wheat, A. J.; Boyaci, H.; Tor, Y. *ChemPhysChem* **2011**, *12*, 567.

(67) Reichardt, C. *Chemical Society Reviews* **1992**, *21*, 147.

(68) Hu, R.; Gomez-Duran, C. F. A.; Lam, J. W. Y.; Belmonte-Vazquez, J. L.; Deng, C.; Chen, S.; Ye, R.; Pena-Cabrera, E.; Zhong, Y.; Wong, K. S.; Tang, B. Z. *Chemical Communications* **2012**, *48*, 10099.

(69) Li, G.; Zhu, D.; Xue, L.; Jiang, H. *Organic Letters* **2013**, *15*, 5020.

(70) Sinkeldam, R. W.; Tor, Y. *Organic & Biomolecular Chemistry* **2007**, *5*, 2523.

(71) Reichardt, C. *Chemical Reviews* **1994**, *94*, 2319.

(72) Dähne, S.; Freyer, W.; Teuchner, K.; Dobkowski, J.; Grabowski, Z. R. *Journal of Luminescence* **1980**, *22*, 37.

(73) Vazquez, O.; Sanchez, M. I.; Martinez-Costas, J.; Vazquez, M. E.; Mascarenas, J. L. *Org Lett* **2010**, *12*, 216.

(74) Cho, D. W.; Cho, D. W. *New Journal of Chemistry* **2014**, *38*, 2233.

Chapter 4:

Additional Experiments and Future Directions

4.1 Surfen Analogs Antagonize β-Amyloid Protein (Aβ40) Binding to Cell-Surface Heparan Sulfate

Alzheimer's disease (AD) is a progressive and irreversible neurodegenerative disease that affects over 35 million people worldwide. This chronic disease is characterized by the formation of pathological lesions in the brain consisting of aggregated β–amyloid (Aβ) plaques and neurofibrillary tangles that cause memory loss and cognitive decline in patients.[1] It was discovered that senile plaques found in the brain parenchyma and cerebral blood vessels of Alzheimer's patients consisted of the aggregate form of Aβ peptides that originate from the proteolysis of the amyloid precursor protein (APP) by specific enzymes including beta-site amyloid precursor protein–cleaving enzyme 1 (BACE-1), γ-secretase, and β-secretase.[2] Although the mechanism and cause of neuronal degeneration and resulting cognitive decline are still unknown and highly debated,[3-7] a large amount of evidence points to the formation of amyloid deposits containing insoluble Aβ fibrils being a major cause of neurotoxicity and memory loss. [8-11] Many studies have explored developing agents to target Aβ peptides for the treatment of AD. One strategy is to use small molecules to block the production of Aβ through inhibiting specific enzymes, including β- and γ-secretase.[12-14] An alternative strategy involves inhibiting the aggregation of Aβ to

prevent senile plaque formation.[15-17] However, unfortunately most of the anti-Alzheimer's drugs developed so far have failed in clinical trials or have been minimally effective in treating the disease.[18]

HSPGs have been shown to play a key role in the pathogenesis of AD through binding to Aβ proteins and enhancing their uptake into neurons.[19,20] Research has shown that these proteins present specific HS binding sites and that their attachment to HS induces their aggregation.[21-23] It's also been hypothesized that binding to HS could protect Aβ peptides from degradation[24] or removal by microglial cells.[25] One group also showed that Aβ competes for a common HS-binding site with FGF2, a neuroprotective protein, consisting of 2-*O* and 6-*O* sulfated hexasaccharide regions.[26] Therefore, finding agents that could block the interaction between Aβ and HS could be a potential effective therapeutic route for treating AD. HS and heparin mimetic compounds have shown promise as anti-Alzheimer's drugs through interfering with the deposition and aggregation of Aβ.[27-33] Furthermore, small molecules that bind to HS have been probed as potential Alzheimer's treatments.[34,35] Due to the ability of surfen and its analogs to antagonize diverse HS-protein interactions (e.g. FGF2 and sRAGE), we investigated the ability of these molecules to antagonize the binding of Aβ peptides to HS.

We utilized a cell binding inhibition assay similar to the one described for FGF2 in Chapter 2, except FGF2 was replaced with biotinylated Aβ (1-40 amino acid region). We investigated whether one of the more potent surfen analogs, succinyl surfen (**1**), could antagonize binding of Aβ to HS on the cell surface of

wild-type CHO cells. Acetyl-hemisurfen (**2**) was used as a negative control. Each surfen analog was pre-incubated with CHO cells at increasing micromolar concentrations. Biotinylated Aβ(1-40) was added, followed by the addition of fluorescently-tagged streptavidin thus forming a conjugate with cell-bound biotin-Aβ(1-40). Flow cytometry was utilized to monitor the fluorescence of bound ligand. Aβ(1-40) inhibition curves were generated by plotting the percentage of maximum Aβ binding obtained in the absence of any antagonist versus the concentration of the molecule of interest. Succinyl surfen dose-dependently inhibited Aβ binding to CHO cells ($IC_{50} \approx 8$ μM) while acetyl-hemisurfen showed no activity up to 20 μM (**Figure 4.1**). Under these conditions, succinyl surfen did not fully inhibit Aβ binding to 100%, but further studies could probe for more potent surfen analogs and investigate their antagonistic properties with different forms of Aβ (e.g. aggregated, fibrillar). Recently, surfen was shown to bind to amyloid fibrils (SEVI) and prevent their interaction with viruses and HS.[36] Therefore, surfen could also possibly bind to Aβ to prevent its interaction with HS. Overall, these preliminary results suggest that surfen-type compounds could be developed as inhibitors of Aβ-HS binding as a new therapeutic approach to preventing the progression of AD.

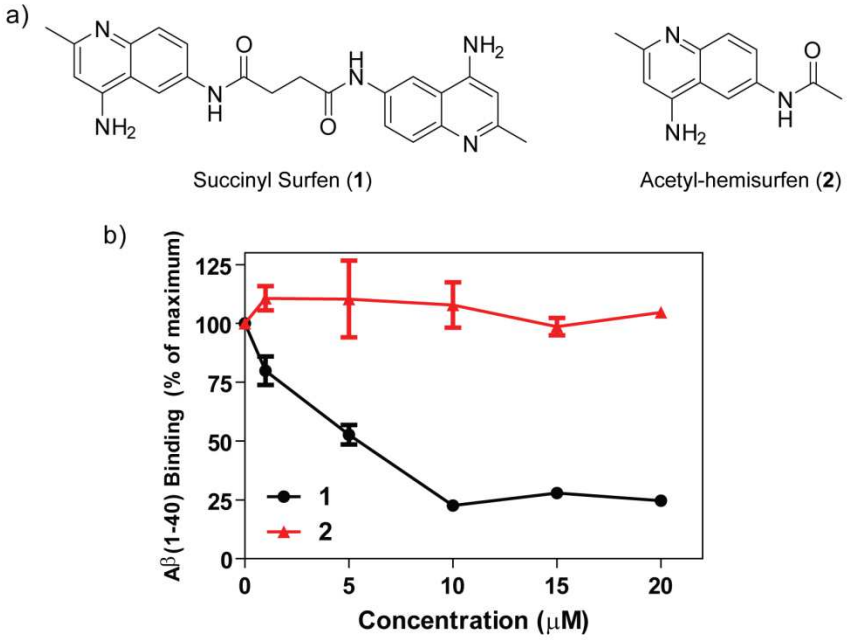

Figure 4.1: a) Surfen analog structures; b) succinyl surfen (**1**) inhibits binding of Aβ(1-40) to CHO cells. Experiments were run in triplicate.

4.2 Surfen Inhibits HIV Infection *in vitro*

According to the UNAIDS 2014 report, nearly 34 million people worldwide are currently living with HIV/AIDS. In 2013, 2.1 million people were newly infected with the HIV virus, and there were ~1.5 million AIDS-related deaths reported.[37] While this epidemic has basically been controlled in most of the western world, there are still particular regions such as sub-Saharan Africa and Eastern Europe that are severely affected by this devastating disease. Although many HIV antiviral drug therapies have successfully been developed over the years,[38] there are still problems with HIV drug resistance,[39,40] adverse drug reactions,[41,42] and the possibility of HIV "superinfections."[43] Furthermore, many of the newly developed drugs are often expensive or do not have the desired

effectiveness. Therefore, there is still a need to develop novel effective HIV therapeutics.

Cell-surface HSPGs were discovered to be essential co-receptors for HIV attachment due to their interaction with V3 loop of the viral envelope protein gp120.[44,45] HSPGs, along with CD4 and chemokine receptors CXCR4 and CCR5, play an essential role in HIV attachment and cell entry.[46] Early studies utilizing exogenous heparin and other anionic sugars (e.g. dextran sulfate) as inhibitors of HIV viral attachment suggested that blocking HIV's interaction with cell-surface HS could be a viable therapeutic target.[47-49] Likewise, we hypothesized that surfen (**3**), a small molecule antagonist of HS[50] and inhibitor of the enhancement of HIV infection by SEVI amyloid fibrils,[51] and its analogs could potentially be exploited as inhibitors of HIV attachment and cell entry.

In this preliminary study, we tested surfen (**3**) as an inhibitor of HIV infection through research services provided by the UCSD Center for AIDS Research (CFAR). Drug susceptibility assays with two different cell lines were used to assess surfen's ability to block HIV infection *in vitro*. In the first experiment, engineered HeLa cells called P4R5 indicator cells were used as targets for HIV infection. These cells express HS, CD4, CCR5, CXCR4, and a β-galactosidase enzyme under the control of the HIV-1 long terminal repeat. Thus, β-galactosidase will only be active in cells infected with HIV.[52] First, cells were infected with HIV for two hours. Next, they were incubated with varying concentrations (0-100 μM) of surfen to determine the compound's ability to inhibit the propagation of HIV infection. Two days later, the cells were fixed then treated

with the chromogenic substrate X-gal (**4**), a lactose analog that stains infected cells blue upon cleavage by active β-galactosidase and subsequent dimerization.[53] Surfen dose-dependently reduced HIV infection in P4R5 cells (IC_{50} ≈ 18 μM) with maximum activity of ~60% at 100 μM (**Figure 4.2**).

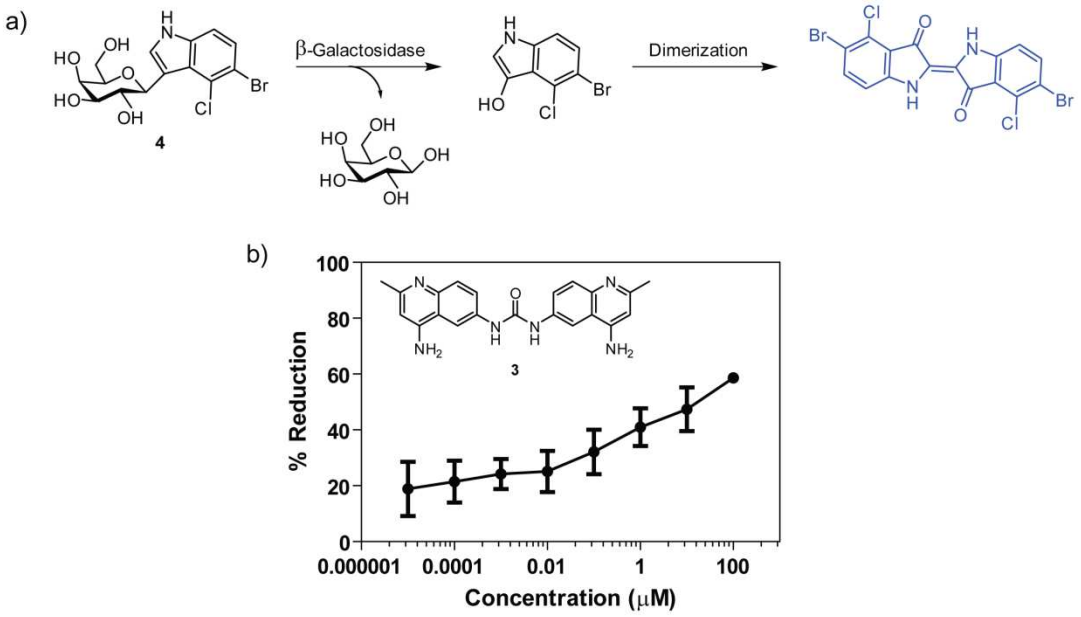

Figure 4.2: a) X-gal staining mechanism; b) surfen (**3**) inhibits HIV infection in P4R5 cells. Experiments performed in duplicate.

Next, surfen was tested as an inhibitor of HIV infection in human donor peripheral blood mononuclear (PMBC) cells. Three hours after infection with the HIV virus, the cells were isolated by centrifugation and passaged into new plates containing varying concentrations of surfen (0-100 μM). The reverse-transcriptase antiretroviral drugs AZT[54] and NVP[55] were included as positive controls. After seven days, the supernatant was harvested from each well and HIV infection was quantified using a standard p24 ELISA-based assay.[56] Surfen dose-dependent reduced HIV infection (IC_{50} ≈ 20 μM) albeit with lower efficacy

compared to the other antiretroviral drugs tested in this assay (**Figure 4.3**). Overall, these results suggest that surfen and related compounds could be explored further as inhibitors of HIV infection. Furthermore, these experiments demonstrate surfen's potency and lack of toxicity in cell-based experiments over extended periods of time. Development of more potent analogs with improved activity could prove useful in the search for effective anti-HIV drugs.

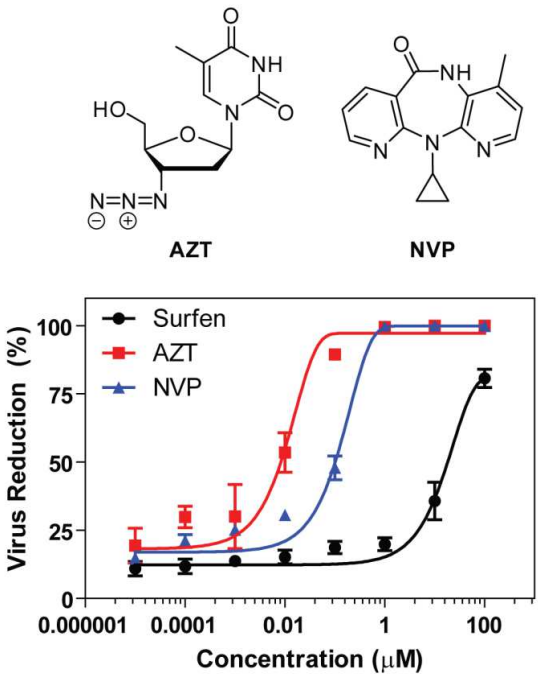

Figure 4.3: HIV propagation inhibition in PMBC cells by surfen, AZT, and NVP. Experiments performed in triplicate.

4.3 Formulation Development of Oxalyl Surfen for Neutralization of Fondaparinux in Mice

While the *in vivo* fondaparinux neutralization studies with oxalyl surfen (**5**) described in Chapter 2 gave very promising results, the intravenous delivery vehicle (DMSO/H_2O) needed to be improved for further development of this small

molecule as a heparinoid reversal agent *in vivo*. DMSO (**6**) has been shown to cause varying degrees of toxicity *in vitro* and *in vivo*; hence, it is not the most ideal vehicle for intravenous delivery.[57] Due to oxalyl surfen's poor water solubility, we needed to explore alternative nontoxic solubilizing agents to replace DMSO. Many drugs on the market today also exhibit poor water solubility, such as the cancer drug paclitaxel.[58] Consequently, an entire field of research has been developed for the discovery of nontoxic solubilizing reagents for drug formulation, including cyclodextrins (**7**) and surface-active excipients such as Solutol HS 15 (**8**) and Cremaphor EL.[59] Cyclodextrins can form a supramolecular complexes with hydrophobic drug molecules to increase water solubility,[60] while non-ionic surfactants such as Solutol HS 15 encapsulate insoluble compounds into micelles.[61] Here, we selected excipients that could potentially dissolve oxalyl surfen without interfering with its *in vivo* activity.

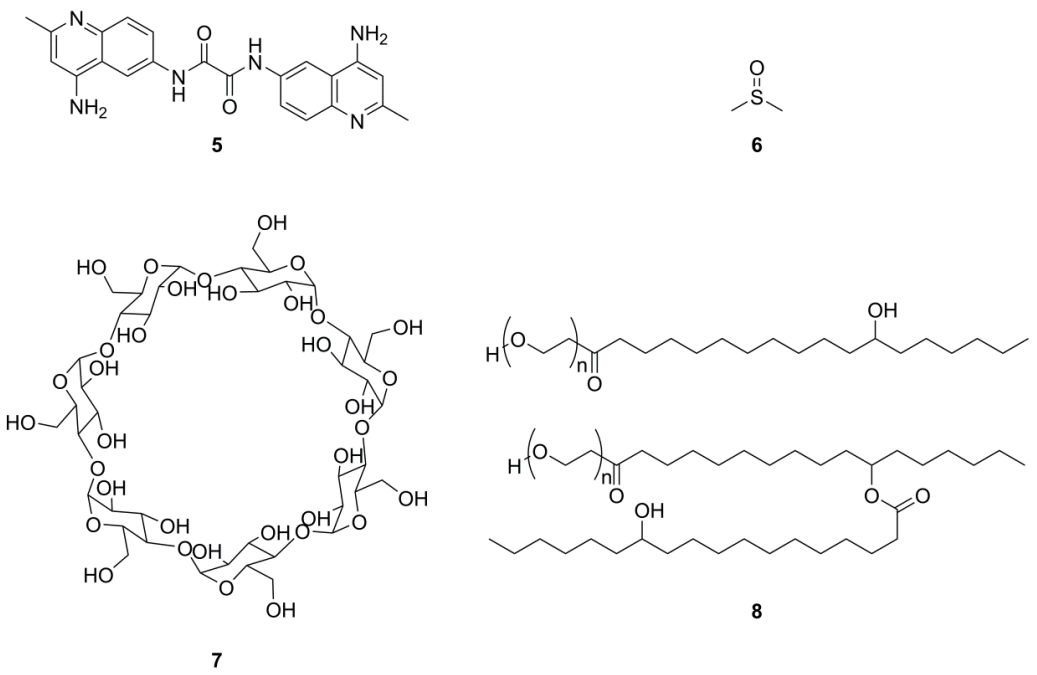

Figure 4.4: Structures of oxalyl surfen (**5**), DMSO (**6**), cyclodextrin (**7**), and Solutol HS 15 (**8**).

We first attempted to dissolve oxalyl surfen in a range of formulations shown to be nontoxic in mice. The compound was discovered to be partially soluble in aqueous solutions of 40% hydroxy-β-cyclodextrin and 20% Cremaphor EL and fully soluble in an aqueous solution of 30% Solutol HS 15.

Subsequently, we chose to use 30% Solutol HS 15 as the excipient for fondaparinux reversal studies in mice due to its ability to fully dissolve oxalyl surfen at the concentrations needed for *in vivo* use. We investigated whether oxalyl surfen would dose-dependently neutralize fondaparinux in wild-type mice (0-16 mg/kg). We used the same *in vivo* protocol as described in Chapter 2; however, the DMSO-H_2O vehicle was replaced with an aqueous solution of 30% Solutol HS 15. Each mice group (n = 3) was injected subcutaneously with 0.5 mg/kg fondaparinux, and after 10 minutes, oxalyl surfen (1.6, 4, 8, or 16 mg/kg)

or vehicle control (30% Solutol HS 15 solution in H_2O) were injected intravenously. After 5 minutes, blood was collected, centrifuged, and the plasma was isolated and analyzed for anti-FXa activity. Fondaparinux in plasma was dose-dependently reduced in the oxalyl surfen-treated mice compared to the control-treated group (**Figure 4.5**). Based on these results, it appears that Solutol HS 15 works well as a safer alternative excipient to DMSO for *in vivo* delivery of oxalyl surfen in mice. Moreover, according to the dose-response, the ED_{50} lies between 8 and 16 mg/kg. Further studies are needed to deduce the exact ED_{50} in mice and to probe oxalyl surfen's ability to neutralize fondaparinux in other animal models.

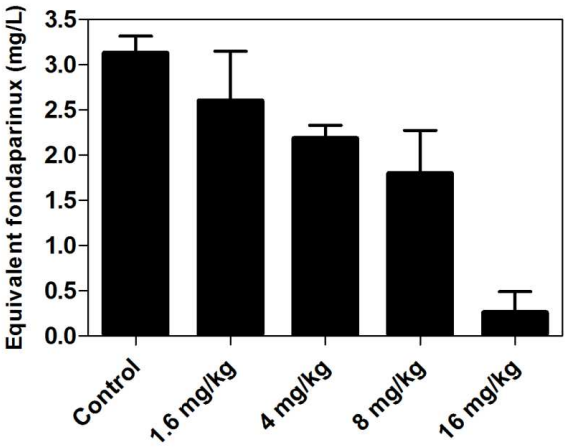

Figure 4.5: Oxalyl surfen (in 30% Solutol HS15) dose-dependently neutralizes fondaparinux in mice (n = 3).

4.4 Surfen Exhibits Turn-on Fluorescence in CHO Cells

While the fluorescence detection of heparin and other analytes in solution are interesting and useful, monitoring analyte levels in living cells could be an interesting application for surfen due to its unique turn-on fluorescence

properties. Nuclear stains, such as DAPI (4,6-diamidino-2-phenylindol), fluoresce when excited with UV light upon binding to the minor groove of DNA in the cell nucleus.[62] Similarly, we hypothesized that surfen could light up inside cells upon binding intracellular analytes. This small molecule could be able to penetrate the cell membrane or be taken up by certain endocytotic pathways upon binding HS or proteins on the cell surface. Previous studies showed surfen's ability to alter processes within the cell, such as GAG biosynthesis, thus suggesting that surfen could be internalized.[63] Upon internalization, surfen could potentially exhibit turn-on fluorescence upon interaction with intracellular analytes.

To explore the potential of utilizing this small molecule for cell imaging, we incubated surfen with CHO cells using a standard cell-staining protocol. To determine whether presentation of GAGs on the cell surface would be a factor in its internalization, surfen was added to either CHO-K1 (wild-type) or GAG-deficient pgsA-745 CHO cells.[64] When bound to heparin and other analytes in solution, surfen exhibits a red-shifted absorption maximum at 360 nm and an emission maximum at 480 nm. Therefore, we could monitor its fluorescence using standard DAPI filter sets. After incubating the cells in serum-free media in the presence of surfen for 15 minutes, we washed and fixed the cells before obtaining bright fluorescence images of the stained cells (**Figure 4.6**). Cells incubated in the absence of surfen showed no staining, while both the wild-type and mutant cell lines exhibited bright blue fluorescence after incubation with surfen. Closer examination of the cell images reveals that surfen molecules predominantly visualize in the cytoplasmic regions. Weaker fluorescence signals

are seen in the nucleus regions, potentially due binding to anionic DNA.[65] Subsequent experiments also showed the capability to monitor the kinetics of surfen internalization in live cells in real-time (experimental section).

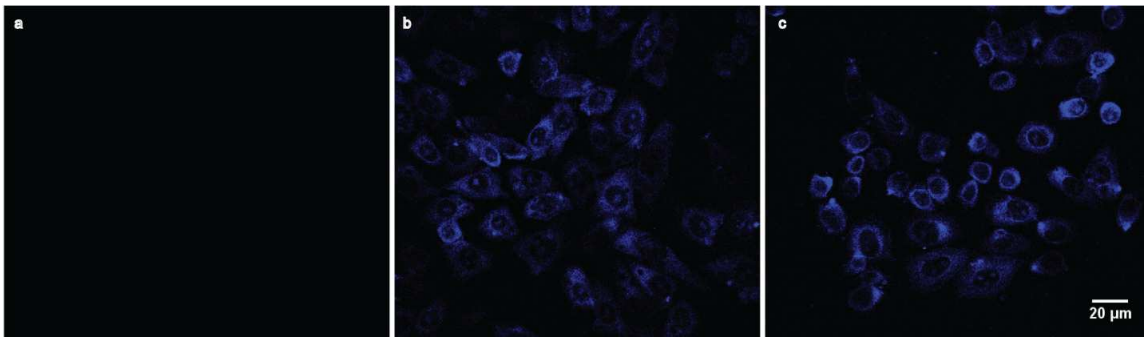

Figure 4.6: Intracellular localization of surfen (blue). a) CHO-K1 cells without surfen (DMSO control), b) CHO-K1 cells with surfen (10 μM), c) CHO pgsA-745 cells with surfen (10 μM).

While the uptake mechanism is not clear at this time, the cell-imaging results demonstrate that surfen can easily penetrate the cell membrane and readily stain live cells under standard cell incubation conditions. All of the cells stained by surfen look healthy, indicative of good biocompatibility at these concentrations. Taking into consideration the relatively high levels of negatively charged entities in the cell, this “turn-on” bioprobe could find application to an array of biological applications as a simple visualization tool for mapping negatively-charged biomolecules in the cell (e.g. DNA, HS, etc.). Further studies could probe organelle localization and possible internalization mechanisms. Moreover, surfen could be explored as a cell membrane probe by performing the experiments at 4°C, which could prevent uptake. Due to surfen’s ability to enter both cell lines, it seems that surfen can enter the cell through a HS-independent uptake mechanism. Novel derivatives varying surfen’s structure could also be

explored to improve selectivity and potentially red-shift the fluorescence for compatibility with other lasers and filters (e.g. FITC, far-red).

4.5 Synthesis and Biological Activity of Additional Surfen Analogs

Prior investigation of multivalent analogs of HS-binding molecules reported cooperative and enhanced binding to HS upon increasing the number of cationic HS-binding moieties. These multivalent analogs were superior to their "monomeric" counterparts in regards to HS-binding.[66,67] Therefore, we hypothesized that surfen-type compounds displaying multiple aminoquinoline motifs may show enhanced binding to HS compared to dimeric surfen (**3**). Here, we investigated whether increasing the valency of surfen would affect its interaction with HS. "Multivalent" surfen derivatives were synthesized from previously reported building blocks.[68-70] In these preliminary studies, we investigated the HS-antagonistic properties of trimeric surfen analogs with the 4,6-diamino-2-methylquinoline moiety conserved. We synthesized two different multivalent surfen analogs containing three aminoquinoline moieties in order to examine the importance of linker flexibility, length, and valency for biological activity. These compounds were tested as inhibitors of FGF2 binding to cell-surface HS.

First, a trimeric analog of surfen, trivially named trimesoyl surfen (**9**), was explored. We chose this scaffold based on the availability of the starting materials and ease of synthesis. This compound was synthesized by reacting

4,6-diamino-2-methylquinoline (**10**) with commercially available trimesoyl chloride (**11**) in DMF with triethylamine at 0°C. When the reaction mixture was allowed to gradually warm to room temperature overnight, a solid precipitate formed. The crude product was dissolved in water (0.1% TFA) and purified using HPLC.

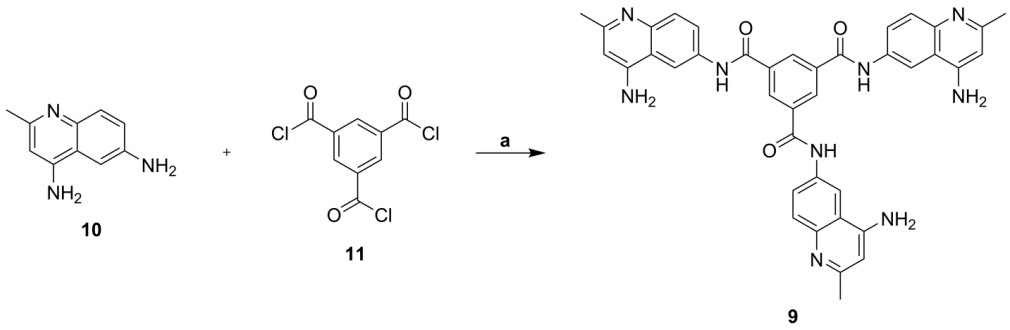

Scheme 4.1: Synthesis of **9**. *Reagents and conditions:* (a) triethylamine, DMF, 0°C-rt.

Moreover, an alternative trimeric form of surfen (**12**) was synthesized to investigate whether a flexible glycol-containing motif would aid in antagonizing HS-protein interactions (Scheme 4.2). The synthesis of the flexible core was adapted from the previous synthesis of modified polyols.[68-70] First, 2-(hydroxymethyl)-2-ethylpropane-1,3-diol (**13**) was reacted with acrylonitrile under basic conditions at room temperature to yield **14**, which was then hydrolyzed to the tri-acid (**15**) with 32% HCl. Without further purification, the tri-acid product was converted to the tri-acid chloride (**16**) which was then reacted with 4,6-diamino-2-methylquinoline (**10**) to yield **12**. The crude product was desalted then purified using HPLC.

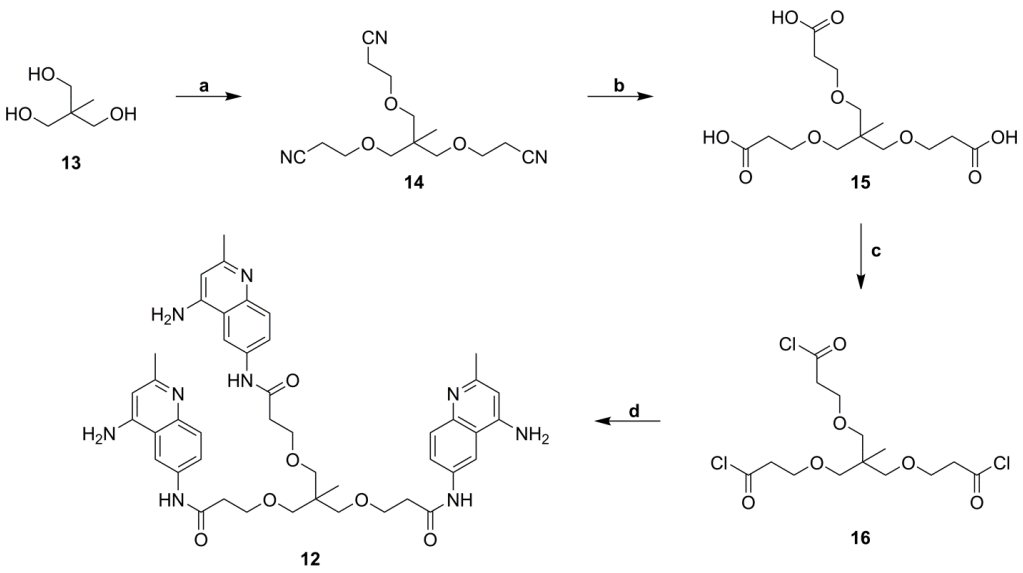

Scheme 4.2: Synthesis of **12**. *Reagents and conditions:* (a) acrylonitrile, 40% NaOH, 0°C-rt, (b) 32% HCl, 95°C, (c) oxalyl surfen, DMF (11 mol%), DCM, reflux, (d) **10**, K_2CO_3, DMF, rt.

With these compounds in hand, we tested their ability to antagonize FGF2-HS binding by utilizing the *in vitro* assay previously introduced. Each multivalent analog was pre-incubated with CHO cells at increasing micromolar concentrations. Biotinylated FGF2 was then added, followed by the addition of streptavidin-Cy5 thus forming a conjugate with cell-bound biotin-FGF2. Flow cytometry was utilized to monitor the fluorescence of bound ligand. FGF2 inhibition curves were generated by plotting the percentage of maximum FGF2 binding obtained in the absence of any antagonist versus the concentration of the molecule of interest (**Figure 4.7**). Interestingly, in these preliminary experiments, neither of the trimeric compounds showed better FGF2 binding inhibition compared to native surfen (**1**). The trimesoyl derivative (**9**) showed minimal inhibitory activity (>100 μM) while **12** exhibited lower activity (IC_{50} ≈ 10 μM) compared to surfen. It seems that the three dimensional arrangement and length

of multivalent surfen-type antagonists affects their activity and interaction with HS. Further studies are needed to probe the importance of the core linker region and valency for these molecules' interaction with cell-surface HS. However, these preliminary experiments suggest that merely increasing the valency is not enough to enhance their antagonistic properties.

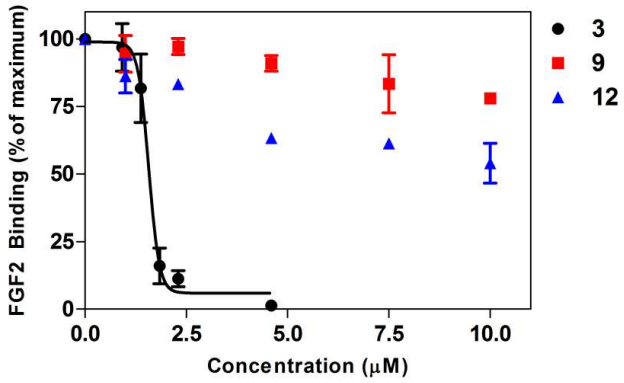

Figure 4.7: FGF2 binding inhibitory activity of surfen (**3**), trimesoyl surfen (**9**), and triQ surfen (**12**).

Due to the availability of the building block **10**, we also explored other first generation analogs of surfen in the pursuit of more potent analogs and to gain further insight into their interaction with cell-surface HS. A structure-activity relationship discussed earlier (Chapter 2) showed the enhanced activity of diglycolyl surfen (**17**) compared to surfen in regards to FGF2 binding inhibition. Therefore, we synthesized novel analogs to examine the importance of the oxygen in the linker region for its improved biological activity by replacing it with a less electronegative sulfur atom (**18**) and extending the linker region with a longer glycol-containing chain (**19**).

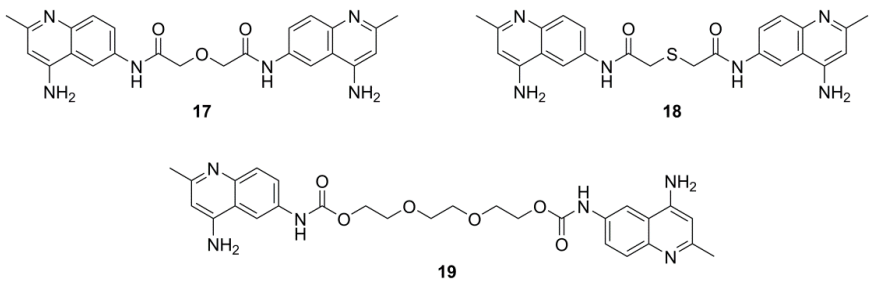

Figure 4.8: Structure of surfen analogs exploring glycol-containing linkers.

For synthesis of **18**, commercially available 2,2′-thiodiacetic acid (**20**) was first converted to the corresponding diacyl chloride **21**, which was reacted with building block **10** to yield thio-diglycolyl surfen (**18**). This compound was purified via recrystallization in hot DMF followed by addition of diethyl ether. Pure crystalline product formed after placing the flask in the refrigerator at 4°C overnight.

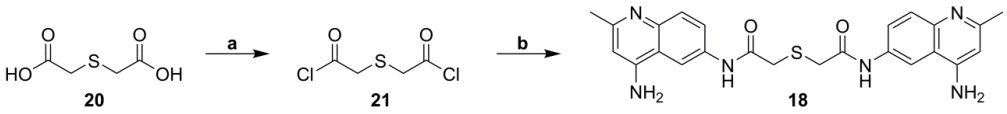

Scheme 4.3: Synthesis of **18**. *Reagents and conditions:* (a) oxalyl chloride, pyridine, benzene, rt, (b) **10**, acetic acid, rt.

Compound **19** was synthesized by reacting commercially available tri(ethylene glycol) bis(chloroformate) (**22**) with building block **10** in acetic acid at room temperature. The crude precipitate was recrystallized in hot DMF with addition of diethyl ether**.**

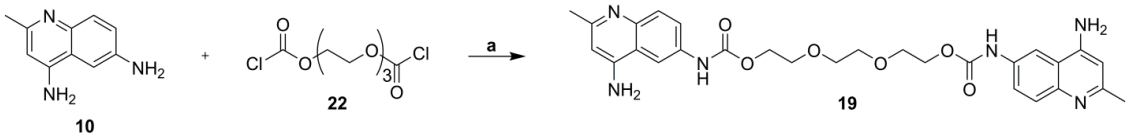

Scheme 4.4: Synthesis of **19**. *Reagents and Conditions:* (a) acetic acid, rt.

Compounds **18** and **19** also showed reduced activity in regards to FGF2 binding inhibition (**Figure 4.9**). The poor activity of **18** resulted from replacing the oxygen with a less electronegative sulfur atom impedes its biological activity. We saw similar reduced activity in our earlier studies (see Chapter 2) when the urea moiety was replaced with a thiourea. These results support the importance of the oxygen in the linker region of surfen-type compounds for their interaction with cell-surface HS. Furthermore, the reduced activity of **19** suggests that increasing the linker length, even while enhancing the hydrophilicity by adding multiple glycol units, is detrimental for binding to HS. We saw this similar effect in the extended analogs tested in Chapter 2. It seems that extending the length of surfen-type compounds hinders their ability to cooperatively bind to multiple GAG binding sites per polysaccharide. Future directions could include enhancing the number of hydrogen bonding sites on the surfen while maintaining the relative size and length.

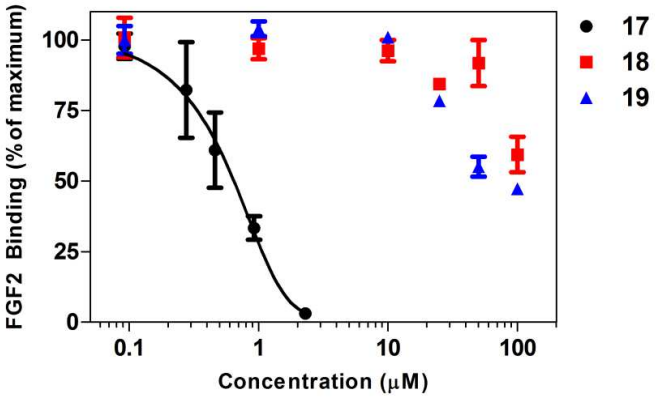

Figure 4.9: FGF2 binding inhibitory activity of diglycolyl surfen (**17**), trimesoyl surfen (**18**) and triQ surfen (**19**).

4.6 Future Directions

While a limited number of surfen analogs are discussed in this dissertation, one can imagine many other derivatives that could be synthesized to potentially improve on surfen's potency and utility as an antagonist of GAG-protein interactions. Surfen and the first generation of analogs synthesized here exhibit poor water solubility and their overall efficacy could be improved. DMSO stock solutions were necessary to solubilize the majority of these compounds, and the most potent analogs tested showed high nanomolar activity, at best. Both of these issues could interfere with their eventual therapeutic use in humans. Alterations could be made to surfen's structure to enhance its solubility properties while attempting to maintain or enhance biological activity. Methylation of the quinoline nitrogen with an alkylating agent, such as methyl iodide, could yield a more water soluble quaternary salt form of surfen (**23**).[71] Studies have shown that the introduction of a quaternary ammonium salt can enhance the water solubility properties of related heterocyclic compounds.[72-74] Although solubility could be improved, it would be necessary to explore whether these modifications could negatively affect biological activity. Alternatively, functionalizing the 2-methyl substituent of the aminoquinoline moieties of surfen (**24**) with longer hydrophilic groups (e.g. polyethylene glycol chains) could potentially yield more water soluble, biocompatible analogs while concurrently providing insight into the significance of the 2-methyl group for surfen's biological activity. One could further envision functionalizing the 2-methyl position with

"clickable" (e.g. azido or alkyne groups)[75] or peptide-coupling (amines or carboxylic acids) moieties to fluorescently-label surfen or amend its structure for other applications.

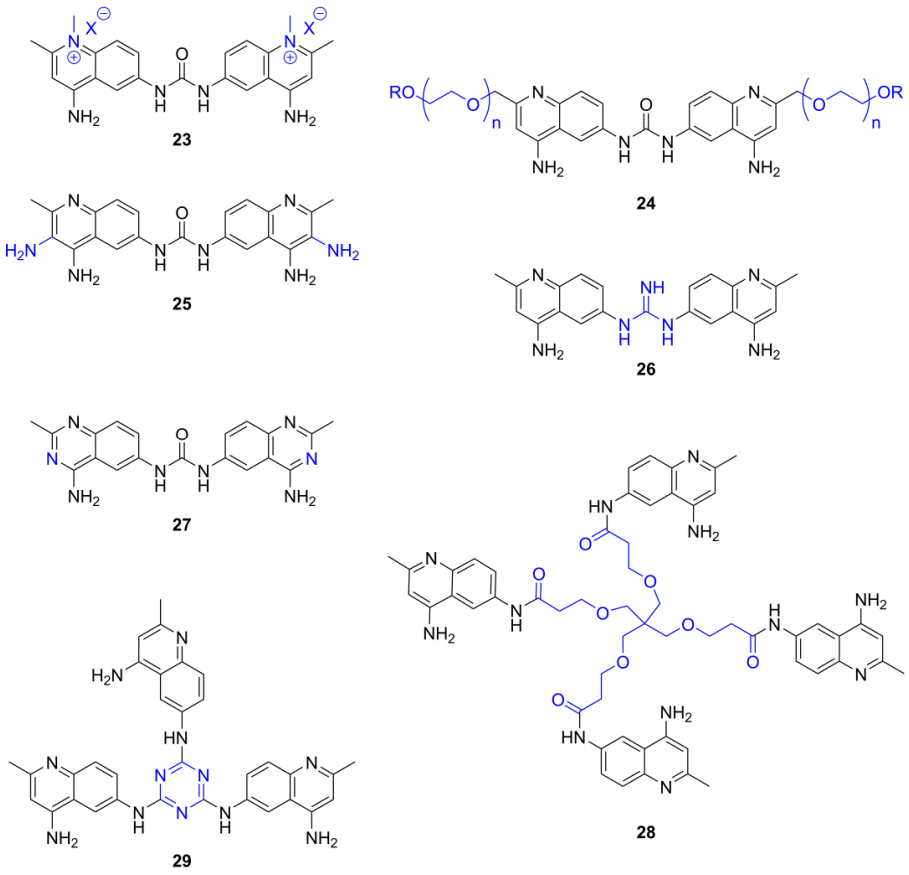

Figure 4.10: Potential surfen derivatives to improve biological activity. Modifications shown in blue.

In order to potentially improve surfen's interaction with the anionic GAG chains, an additional amino group could be introduced by replacing the quinoline ring systems with quinazolines (**25**) in order to provide an additional hydrogen bonding site.[76] Moreover, surfen's biological activity could be further improved by replacing the urea linker region with a highly basic ($pK_b \approx 0.5$) guanidine group (**26**).[71] Guanidinium cations, being protonated at physiological pH, have proven

to be superior to amino groups in their interaction with the anions and cell-surface HS.[77,78] Replacing the urea with a guanidine also adds an additional hydrogen bonding donor site to the linker region that could interact with the negatively charged sulfated and carboxylated regions of heparin and HS. In addition, converting the quinoline ring systems into quinazolines by inserting an additional nitrogen and hydrogen bonding site (**27**) could improve the biological activity.[79-81] As mentioned in the section above, multivalent surfen analogs could also be explored as more potent GAG antagonists. Preliminary studies with 4-aminoquinoline-based multivalent surfen analogs (section 4.5) demonstrated that the orientation and flexibility of the linker region could be essential for their inhibitory properties. While the compounds synthesized here were not superior to surfen in regards to FGF2 binding inhibition, other multivalent analogs could be synthesized to explore valency and the effects of altering the core linker region (**28, 29**).

Due to its unique “turn-on” fluorescence properties, one could envision many other potential applications for surfen as a fluorescent sensor. A recent study revealed surfen to be a potent nontoxic inhibitor of polyphosphate, a highly anionic linear biomolecule important in the inflammatory process.[82] Due to the high density of negatively-charged phosphate groups, it is possible that surfen could display similar turn-on fluorescence properties in the presence of polyphosphate as exhibited with anionic heparin. Other groups have applied fluorescent heparin[83] and DNA[84] sensors to the detection of polyphosphate in microbial and mammalian cell cultures. Likewise, surfen could potentially be

applied as a polyphosphate probe. Moreover, surfen could possibly be used as a fluorescent probe for amyloid peptides, such as SEVI and β-amyloid fibrils. Previous studies have proposed the binding of surfen to SEVI amyloid fibrils.[51] Surfen-amyloid interactions could be investigated further through exploiting its unique turn-on fluorescence properties. It is possible that surfen could fluorescently discriminate between different types of amyloid deposits depending on their structure and their aggregation state. This would have potential use in diagnosing and monitoring disorders involving distinct amyloid deposits, such as Alzheimer's and prion disease.

4.7 Experimental

Materials

Unless otherwise specified, materials purchased from commercial suppliers were used without further purification. Surfen (bis-2-methyl-4-amino-quinolyl-6-carbamide) was obtained from the Open Chemical Repository in the Developmental Therapeutic Program of the National Cancer Institute (NSC12155). All other anhydrous solvents and reagents were purchased from Sigma-Aldrich, with the exception of Solutol HS 15 (BASF Corp., Germany). NMR solvents were purchased from Cambridge Isotope Laboratories (Andover, MA). *Human* Biotin-LC-β-Amyloid (1-40) was purchased from AnaSpec Inc. (San Jose, CA). Basic FGF2 (E. Coli recombinant) was purchased from Peprotech, and the sulfo-NHS-LC-Biotin linker was purchased from Thermo Scientific. PBS (Dulbecco's phosphate buffered saline), F12 Media, Cell Dissociation Buffer

(PBS-based, Enzyme Free), and streptavidin-Cy5 were purchased from Life Technologies (Carlsbad, CA). FACS buffer (Isotonic solution 0.85% w/v, phosphate buffered pH 7.1–7.3) were purchased from BD Biosciences. Trypsin/EDTA was purchased from VWR (Mediatech). Tissue culture plates (20 mm) were from BD Falcon (BD Biosciences). Fondaparinux sodium (Arixtra®, 5 mg/mL) was obtained from the manufacturer.

Instrumentation

NMR spectra were recorded on Varian Mercury 300 and 400 MHz, and Varian VX 500 MHz spectrometers. Mass spectra were recorded at the UCSD Chemistry and Biochemistry Mass Spectrometry Facility, utilizing an Agilent 6230 HR-ESI-TOF mass spectrometer. Flow cytometry studies were performed on a BD FACSCalibur. Absorbance measurements for the factor Xa assay were performed on a VersaMax microplate reader (Molecular Devices) using Softmax Pro software. Confocal laser scanning microscopy was performed using a Nikon A1R inverted fluorescence microscope with z-stepping motor. Images were processed and analyzed using Nikon Imaging Software Elements and ImageJ (NIH).

Aβ (1-40) binding inhibition

Wild-type CHO cells (ATCC CCL-61) were grown in F12 growth medium supplemented with 10% (v/v) fetal bovine serum, 100 µg/ml of streptomycin sulfate, and 100 units/ml of penicillin G. Cells were grown to confluence, lifted with Cell Dissociation Buffer, washed with PBS buffer, and pre-incubated with

specific concentrations of surfen analog in PBS/0.1% BSA on ice for 10 min. Next, biotin-Aβ (1-40) (50 μg ml^{-1}, 1:1000) was added and incubated for 1 hour on ice. Cells were washed, and bound biotin-Aβ (1-40) was detected using streptavidin-Cy5 (1:1000, PharMingen) and flow cytometry (FACSCalibur, BD Biosciences). Crude data was interpreted using FlowJo Analytical Software (Tree Star Inc.). Protein binding was quantified by the geometric mean fluorescence intensity. Results are represented as the extent of binding compared with a sample incubated in the absence of surfen analog. These values were plotted and further analyzed using GraphPad Prism v5.0.

P4R5 X-gal chromogenic assay (collaboration with UCSD CFAR core)

P4R5 indicator cells were plated in 48-well plates (2 x 10^4 cells per well) in DMEM growth medium supplemented with 10% (v/v) fetal bovine serum, 100 μg/ml of streptomycin, 100 units/ml of penicillin, 1 μg/ml of puromycin, and 300 μg/ml of glutamine. Cells were grown overnight, infected with 100 μl of HIV virus (DMEM media contains 20 μg/ml of DEAE-Dextran instead of puromycin), and incubated at 37°C for 2 hours. Next, 400 μl of surfen solutions (1-100 μM) were added to the appropriate wells and the plates were incubated at 37°C for 2 days. Subsequently, the media was removed, the cells were fixed (1% formaldehyde, 0.2% glutaraldehyde in PBS) for 5 min. After washing with PBS, 300 μl of staining solution (0.2 M potassium ferrocyanide, 0.2 M potassium ferricyanide, 2 M $MgCl_2$, 40 mg/ml X-gal, PBS) was added to each well and the cells were incubated for 3 hours before analysis.

PBMC drug susceptibility assay (collaboration with UCSD CFAR core)

Healthy donor PBMC cells (4 x 10^6 cells/ml) were grown in RPMI 1640 media supplemented with 10% FCS, 1% glutamine, 100 units/ml of penicillin, 100 µg/ml of streptomycin, 10 units/ml of IL-2, 3 µg/ml PHA, and 2 µg/ml polybrene. The cells were infected with 4 x 10^3 TCID50/ml of virus (MOI = 0.001) and incubated at 37°C for 2-3 hours. Next, the cells were washed with PBS, centrifuged at 300 *g* for 10 min, and the supernatant was carefully removed. Cells were resuspended in fresh RPMI media, separated into wells containing various concentrations of inhibitor (surfen, AZT, or NVP), and incubated at 37°C for 7 days. Finally, the supernatant was harvested from each well and stored in 96-well plates at -20°C for p24 ELISA analysis.

In *vivo* heparin neutralization (Solutol HS 15 excipient)

Wild-type mice (8 weeks old, weight ~20-30 g) were divided into a control group (n=3) and an oxalyl surfen-treated group (n=3). Thirty minutes before fondaparinux administration, blood was collected by tail bleeding in 3.2% sodium citrate tubes (9:1 blood to citrate ratio). Each mouse received a subcutaneous injection of fondaparinux (0.5 mg/kg, PBS). Next, mice received an intravenous injection (via tail vein) of 30% Solutol solution (control) or oxalyl surfen (1.6, 4, 8, or 16 mg/kg, in 30% Solutol HS 15) 10 min after fondaparinux administration. Five min after administration of the reversal agent, blood was collected via submandibular bleeds into 3.2% sodium citrate tubes. Plasma was collected immediately (2200 *g* for 15 min) and stored at -80°C. A fondaparinux anti-FXa

colorimetric assay was used to analyze the neutralization effect of oxalyl surfen (**5**) at various concentrations. Their activity was compared to a fondaparinux control without reversal agent as described above. The change in the absorption at 405 nm for each sample was compared with a standard calibration curve to determine the amount of heparin present. The basis of this assay is to analyze the amount of fondaparinux remaining in plasma by indirectly measuring the residual activity of FXa. Heparinized plasma (3 μL) was mixed with antithrombin, forming an AT-heparin complex. The amount of fondaparinux remaining in plasma was plotted against the reversal agent dosage.

Fluorescence microscopy

CHO-K1 and pgsA-745 cells (40,000 cells/well) were grown for 24 hours in glass chamber slides (Lab-Tek® II, 4-well) equipped with a glass bottom coverslip. Cells were washed with PBS, treated with serum-free media (0.7 v% DMSO) containing surfen (10 μM), and incubated at 37°C for 15 minutes under an atmosphere of 5% CO_2. Cells were then washed with PBS, fixed with 4% paraformaldehyde (in 0.1M phosphate buffer) for 20 minutes at room temperature, then washed again with PBS before visualization. The DAPI channel (UV diode laser) with a blue/cyan filter was used to visualize surfen internalization.

Fluorescence microscopy experiments with live CHO cells were visualized immediately after addition of surfen (10 μM in serum-free media). Fluorescence images were taken every 20 seconds for 30 minutes. The fluorescence intensity

(average of multiple cells in viewing window) at each time point was plotted against time to study surfen internalization (**Figure 4.11**).

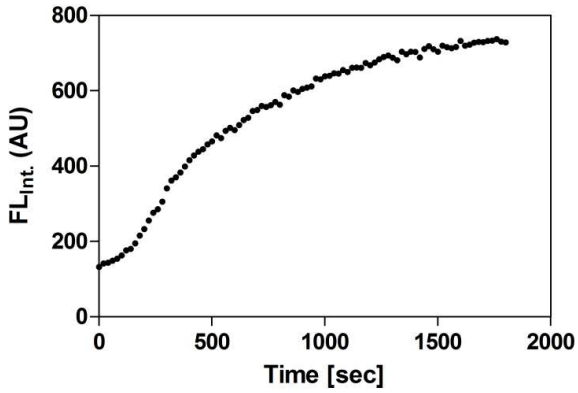

Figure 4.11: Cellular internalization of surfen over time. Results are plotted as the mean fluorescence intensity values at each time point of two separate experiments.

Synthesis of surfen analogs

1,1,1-Tris(cyanoethoxymethyl)ethane (**14**), 1,1,1-tris(carboxyethoxymethyl) ethane (**15**), and 1,1,1-tris(chlorocarbonylethoxymethyl)ethane (**16**) were synthesized according to previously published procedures.[68-70]

Compound 9. 4-6-diamino-2-methyl-quinoline (150 mg, 0.87 mmol) was dissolved in dry DMF (1.5 ml) under argon. Triethylamine (121 µl, 0.87 mmol) was added and the solution was cooled to 0°C on ice. Trimesoyl chloride (58 mg, 0.22 mmol) was dissolved in dry DMF in a separate flask under argon and was slowly added dropwise to the cooled solution. The mixture was stirred overnight and allowed to return to room temperature. A solid precipitate formed overnight. The crude product was filtered and dried overnight on high vacuum.

Subsequently, the crude product was dissolved in water (0.1% TFA) and purified by reverse phase HPLC [0 – 50% ACN in water (0.1% TFA) over 30 mins, flow rate is 3 mL / min, eluted after 23 min], then lyophilized. ^{1}H NMR (400 MHz, DMSO-d_6) δ 11.14 (s, 3H), 8.86 (s, 3H), 8.80 (brd, 8H), 8.12 (d, *J* = 7.4 Hz, 3H), 7.88 (d, *J* = 9.1 Hz, 3H), 6.62 (s, 3H), 2.60 (s, 9H). ESI-MS calculated for $C_{39}H_{33}N_9O_3$ $[M+H]^+$ 676.28; observed $[M+H]^+$ 676.31.

Compound 12. 1,1,1-Tris(chlorocarbonylethoxymethyl)ethane (**16**) (29 mg, 0.074 mmol) was dissolved in dry DMF under argon and potassium carbonate (46.2 mg, 0.33 mmol) was added to the mixture. In a separate flask, 4,6-diamino-2-methylquinoline (64 mg, 0.37 mmol) was dissolved in dry DMF then was added slowly dropwise to the solution. The reaction was stirred at room temperature overnight then was rotoevaporated to dryness, dissolved in methanol, and stirred in the prescence of DOWEX 50WX8-100 ion exchange resin for 2 hours to remove left over potassium carbonate salts. The solution was filtered, rotoevaporated, dissolved in 0.1% TFA, then purified using reverse-phase HPLC (5-40% ACN 0.1% TFA over 30 minutes, peak at 23.4 min.). ^{1}H NMR (300 MHz, D_2O) δ 7.66 (s, 3H), 7.27 (dd, *J* = 20.8, 8.0 Hz, 6H), 6.19 (s, 3H), 3.81 (t, *J* = 4.9 Hz, 6H), 3.52 (s, 6H), 2.60 (t, *J* = 4.2 Hz, 6H), 2.35 (s, 9H), 0.98 (s, 3H). ESI-MS calculated for $C_{44}H_{51}N_9O_6$ $[M+H]^+$ 802.40; observed $[M+H]^+$ 802.46.

Compound 18. 4-6-diamino-2-methyl-quinoline (63 mg, 0.36 mmol) was dissolved in glacial acetic acid (0.3 ml). 2,2'-thiodiacetyl chloride (22 µl, 0.18 mmol) was slowly added dropwise to the solution. A heavy precipitate formed,

and the mixture was stirred for 1 hour at room temperature. Diethyl ether (3 ml) was added to the reaction mixture, and the solid was filtered and washed with diethyl ether. The hydrochloride salt was dissolved in 4 ml of warm water, the solution cooled to room temperature, and made basic with 37% NaOH. The precipitated solid was filtered, washed with water, and dried on high vacuum overnight. Recrystallization was accomplished by dissolving the solid in a minimum amount of hot DMF, filtering, and adding diethyl ether until the solution became turbid. The solution was placed in the refrigerator at 4°C until a crystalline product formed. The crystals were collected by filtration, washed with ether, and dried under high vacuum. Product: tan solid (44 mg, 0.096 mmol, 53%). ^{1}H NMR (400 MHz, DMSO-d_6) δ 10.26 (s, 2H), 8.22 (s, 2H), 7.62 (brd, 4H), 6.43 (s, 2H), 6.39 (brd, 4H), 3.59 (s, 4H), 2.38 (s, 6H). ^{13}C NMR (125 MHz, DMSO-d_6) δ 167.51, 157.13, 151.12, 145.62, 133.68, 128.68, 123.32, 117.26, 111.44, 102.54, 35.89, 24.76. HR-ESI-MS calculated for $C_{24}H_{25}N_6O_2S$ $[M+H]^+$ 461.1754, found 461.1757.

Compound 19. 4-6-diamino-2-methyl-quinoline (34.7 mg, 0.20 mmol) was dissolved in glacial acetic acid (0.4 ml) under argon. Tri(ethylene glycol) bis(chloroformate) (21 µl, 0.10 mmol) was slowly added dropwise to the solution. A heavy precipitate formed, and the mixture was stirred for 1 hour at room temperature. Diethyl ether (3 ml) was added to the reaction mixture, and the solid was filtered and washed with diethyl ether. The hydrochloride salt was dissolved in 2 ml of warm water, cooled to room temperature, and made basic with 37%

NaOH. The precipitated solid was filtered, washed with water, and dried on high vacuum overnight. Product: tan solid (39.5 mg, 0.072 mmol, 72%). ^{1}H NMR (500 MHz, DMSO-d_6) δ 9.80 (s, 2H), 8.06 (s, 2H), 7.58 (d, J = 9.0 Hz, 2H), 7.48 (dd, J = 9.0, 1.6 Hz, 2H), 6.41 (s, 2H), 6.38 (brd, 4H), 4.23 (t, J = 4.0 Hz, 4H), 3.68 (t, J = 4.0 Hz, 4H), 3.60 (s, 4H), 2.37 (s, 6H).^{13}C NMR (125 MHz, DMSO-d_6): δ 156.69, 153.82, 151.01, 145.08, 133.97, 128.59, 123.00, 117.35, 110.01, 102.51, 69.85, 69.78, 68.79, 63.60, 24.66. HR-ESI-MS calculated for $C_{28}H_{33}N_6O_6$ $[M+H]^+$ 549.2456, found 549.2458.

Compound 21. 2,2′-Thiodiacetic acid was dissolved in dry benzene (7 ml) (CARCINOGENIC!) and three drops of dry pyridine were added. Next, oxalyl chloride (0.86 ml, 9.99 mmol) was slowly added dropwise to the solution. The reaction mixture was allowed to react at room temperature for 24 hrs, then the solution was filtered and evaporated under vacuum in the presence of benzene. The crude liquid product was dried overnight on high vacuum. The resulting diacid chloride was used immediately in the following reaction without further purification. (Synthesis of **21** was adapted from a previously published procedure.[85])

4.8 References

(1) Querfurth, H. W.; LaFerla, F. M. *N Engl J Med* **2010**, *362*, 329.

(2) Bredesen, D. *Molecular Neurodegeneration* **2009**, *4*, 27.

(3) Mondragón-Rodríguez, S.; Perry, G.; Zhu, X.; Boehm, J. *International Journal of Alzheimer's Disease* **2012**, *2012*, 7.

(4) Hardy, J. *Curr Alzheimer Res* **2006**, *3*, 71.

(5) Murray, M.; Kouri, N.; Lin, W.-L.; Jack, C.; Dickson, D.; Vemuri, P. *Alzheimer's Research & Therapy* **2014**, *6*, 1.

(6) Reitz, C. *International Journal of Alzheimer's Disease* **2012**, *2012*, 11.

(7) Pimplikar, S. W. *The international journal of biochemistry & cell biology* **2009**, *41*, 1261.

(8) Walsh, D. M.; Selkoe, D. J. *Journal of Neurochemistry* **2007**, *101*, 1172.

(9) Shankar, G.; Walsh, D. *Molecular Neurodegeneration* **2009**, *4*, 48.

(10) Choi, S. H.; Kim, Y. H.; Hebisch, M.; Sliwinski, C.; Lee, S.; D/'Avanzo, C.; Chen, H.; Hooli, B.; Asselin, C.; Muffat, J.; Klee, J. B.; Zhang, C.; Wainger, B. J.; Peitz, M.; Kovacs, D. M.; Woolf, C. J.; Wagner, S. L.; Tanzi, R. E.; Kim, D. Y. *Nature* **2014**, *515*, 274.

(11) Wilcock, D. M.; Gharkholonarehe, N.; Van Nostrand, W. E.; Davis, J.; Vitek, M. P.; Colton, C. A. *J Neurosci* **2009**, *29*, 7957.

(12) Henley, D. B.; May, P. C.; Dean, R. A.; Siemers, E. R. *Expert Opinion on Pharmacotherapy* **2009**, *10*, 1657.

(13) Fischer, C.; Zultanski, S. L.; Zhou, H.; Methot, J. L.; Brown, W. C.; Mampreian, D. M.; Schell, A. J.; Shah, S.; Nuthall, H.; Hughes, B. L.; Smotrov, N.; Kenific, C. M.; Cruz, J. C.; Walker, D.; Bouthillette, M.; Nikov, G. N.; Savage, D. F.; Jeliazkova-Mecheva, V. V.; Diaz, D.; Szewczak, A. A.; Bays, N.; Middleton, R. E.; Munoz, B.; Shearman, M. S. *Bioorganic & Medicinal Chemistry Letters* **2011**, *21*, 4083.

(14) Xin, Z.; Peng, H.; Zhang, A.; Talreja, T.; Kumaravel, G.; Xu, L.; Rohde, E.; Jung, M.-y.; Shackett, M. N.; Kocisko, D.; Chollate, S.; Dunah, A. W.; Snodgrass-Belt, P. A.; Moore Arnold, H.; Taveras, A. G.; Rhodes, K. J.; Scannevin, R. H. *Bioorganic & Medicinal Chemistry Letters* **2011**, *21*, 7277.

(15) Faux, N. G.; Ritchie, C. W.; Gunn, A.; Rembach, A.; Tsatsanis, A.; Bedo, J.; Harrison, J.; Lannfelt, L.; Blennow, K.; Zetterberg, H.; Ingelsson, M.; Masters, C. L.; Tanzi, R. E.; Cummings, J. L.; Herd, C. M.; Bush, A. I. *J Alzheimers Dis* **2010**, *20*, 509.

(16) Hawkes, C. A.; Ng, V.; McLaurin, J. *Drug Development Research* **2009**, *70*, 111.

(17) Lorenzo, A.; Yankner, B. A. *Proceedings of the National Academy of Sciences* **1994**, *91*, 12243.

(18) Cummings, J. L.; Morstorf, T.; Zhong, K. *Alzheimers Res Ther* **2014**, *6*, 37.

(19) Kanekiyo, T.; Zhang, J.; Liu, Q.; Liu, C.-C.; Zhang, L.; Bu, G. *The Journal of Neuroscience* **2011**, *31*, 1644.

(20) Patey, S. J. *Drug News Perspect* **2006**, *19*, 411.

(21) Brunden, K. R.; Richter-Cook, N. J.; Chaturvedi, N.; Frederickson, R. C. A. *Journal of Neurochemistry* **1993**, *61*, 2147.

(22) Sandwall, E.; O'Callaghan, P.; Zhang, X.; Lindahl, U.; Lannfelt, L.; Li, J.-P. *Glycobiology* **2010**, *20*, 533.

(23) Bruinsma, I. B.; te Riet, L.; Gevers, T.; ten Dam, G. B.; van Kuppevelt, T. H.; David, G.; Kusters, B.; de Waal, R. M.; Verbeek, M. M. *Acta Neuropathol* **2010**, *119*, 211.

(24) Gupta-Bansal, R.; Frederickson, R. C.; Brunden, K. R. *J Biol Chem* **1995**, *270*, 18666.

(25) Shaffer, L. M.; Dority, M. D.; Gupta-Bansal, R.; Frederickson, R. C. A.; Younkin, S. G.; Brunden, K. R. *Neurobiology of Aging* **1995**, *16*, 737.

(26) Lindahl, B.; Westling, C.; Gimenez-Gallego, G.; Lindahl, U.; Salmivirta, M. *J Biol Chem* **1999**, *274*, 30631.

(27) Bergamaschini, L.; Rossi, E.; Vergani, C.; De Simoni, M. G. *ScientificWorldJournal* **2009**, *9*, 891.

(28) Schworer, R.; Zubkova, O. V.; Turnbull, J. E.; Tyler, P. C. *Chemistry* **2013**, *19*, 6817.

(29) Woods, A. G.; Cribbs, D. H.; Whittemore, E. R.; Cotman, C. W. *Brain Res* **1995**, *697*, 53.

(30) Wright, T. M. *Drugs Today (Barc)* **2006**, *42*, 291.

(31) Ma, Q.; Cornelli, U.; Hanin, I.; Jeske, W. P.; Linhardt, R. J.; Walenga, J. M.; Fareed, J.; Lee, J. M. *Current pharmaceutical design* **2007**, *13*, 1607.

(32) Kisilevsky, R.; Lemieux, L. J.; Fraser, P. E.; Kong, X.; Hultin, P. G.; Szarek, W. A. *Nat Med* **1995**, *1*, 143.

(33) Leveugle, B.; Scanameo, A.; Ding, W.; Fillit, H. *Neuroreport* **1994**, *5*, 1389.

(34) Harris, N.; Kogan, F. Y.; Il'kova, G.; Juhas, S.; Lahmy, O.; Gregor, Y. I.; Koppel, J.; Zhuk, R.; Gregor, P. *Biochim Biophys Acta* **2014**, *1840*, 245.

(35) Zsila, F.; Gedeon, G. *Biochemical and Biophysical Research Communications* **2006**, *346*, 1267.

(36) Roan, N. R.; Sowinski, S.; Munch, J.; Kirchhoff, F.; Greene, W. C. *J Biol Chem* **2010**, *285*, 1861.

(37) UNAIDS 2014; Vol. 2015.

(38) Arts, E. J.; Hazuda, D. J. *Cold Spring Harbor Perspectives in Medicine* **2012**, *2*.

(39) Clavel, F.; Hance, A. J. *New England Journal of Medicine* **2004**, *350*, 1023.

(40) Hosseinipour, M. C.; Gupta, R. K.; Van Zyl, G.; Eron, J. J.; Nachega, J. B. *Journal of Infectious Diseases* **2013**, *207*, S49.

(41) Pirmohamed, M.; James, S.; Meakin, S.; Green, C.; Scott, A. K.; Walley, T. J.; Farrar, K.; Park, B. K.; Breckenridge, A. M. *BMJ : British Medical Journal* **2004**, *329*, 15.

(42) Chaponda, M.; Pirmohamed, M. *British Journal of Clinical Pharmacology* **2011**, *71*, 659.

(43) Smith, D. M.; Richman, D. D.; Little, S. J. *Journal of Infectious Diseases* **2005**, *192*, 438.

(44) Patel, M.; Yanagishita, M.; Roderiquez, G.; Bou-Habib, D. C.; Oravecz, T.; Hascall, V. C.; Norcross, M. A. *AIDS Research and Human Retroviruses* **1993**, *9*, 167.

(45) Vivès, R. R.; Imberty, A.; Sattentau, Q. J.; Lortat-Jacob, H. *J Biol Chem* **2005**, *280*, 21353.

(46) Connell, B. J.; Lortat-Jacob, H. *Front Immunol* **2013**, *4*, 385.

(47) Harrop, H. A.; Rider, C. C. *Glycobiology* **1998**, *8*, 131.

(48) Pearce-Pratt, R.; Phillips, D. M. *Biol Reprod* **1996**, *54*, 173.

(49) Nakashima, H.; Yoshida, O.; Baba, M.; De Clercq, E.; Yamamoto, N. *Antiviral Res* **1989**, *11*, 233.

(50) Schuksz, M.; Fuster, M. M.; Brown, J. R.; Crawford, B. E.; Ditto, D. P.; Lawrence, R.; Glass, C. A.; Wang, L.; Tor, Y.; Esko, J. D. *Proceedings of the National Academy of Sciences of the United States of America* **2008**, *105*, 13075.

(51) Roan, N. R.; Sowinski, S.; Muench, J.; Kirchhoff, F.; Greene, W. C. *Journal of Biological Chemistry* **2010**, *285*, 1861.

(52) Akrigg, A.; Wilkinson, G. W.; Angliss, S.; Greenaway, P. J. *AIDS* **1991**, *5*, 153.

(53) Burn, S. F. *Methods Mol Biol* **2012**, *886*, 241.

(54) Cihlar, T.; Ray, A. S. *Antiviral Research* **2010**, *85*, 39.

(55) Bardsley-Elliot, A.; Perry, C. M. *Paediatr Drugs* **2000**, *2*, 373.

(56) Tersmette, M.; Winkel, I. N.; Groenink, M.; Gruters, R. A.; Spence, R. P.; Saman, E.; van der Groen, G.; Miedema, F.; Huisman, J. G. *Virology* **1989**, *171*, 149.

(57) Galvao, J.; Davis, B.; Tilley, M.; Normando, E.; Duchen, M. R.; Cordeiro, M. F. *FASEB J* **2014**, *28*, 1317.

(58) Singla, A. K.; Garg, A.; Aggarwal, D. *International Journal of Pharmaceutics* **2002**, *235*, 179.

(59) Liu, R. *Water-Insoluble Drug Formulation*; Taylor & Francis, 2000.

(60) Kurkov, S. V.; Loftsson, T. *International Journal of Pharmaceutics* **2013**, *453*, 167.

(61) Coon, J. S.; Knudson, W.; Clodfelter, K.; Lu, B.; Weinstein, R. S. *Cancer Research* **1991**, *51*, 897.

(62) Suzuki, T.; Fujikura, K.; Higashiyama, T.; Takata, K. *Journal of Histochemistry & Cytochemistry* **1997**, *45*, 49.

(63) Schuksz, M. 2009.

(64) Bai, X.; Wei, G.; Sinha, A.; Esko, J. D. *Journal of Biological Chemistry* **1999**, *274*, 13017.

(65) Fuchs, J. E.; Spitzer, G. M.; Javed, A.; Biela, A.; Kreutz, C.; Wellenzohn, B.; Liedl, K. R. *Journal of Chemical Information and Modeling* **2011**, *51*, 2223.

(66) Dix, A. V.; Fischer, L.; Sarrazin, S.; Redgate, C. P. H.; Esko, J. D.; Tor, Y. *Chembiochem* **2010**, *11*, 2302.

(67) Kawamura, K. S.; Sung, M.; Bolewska-Pedyczak, E.; Gariépy, J. *Biochemistry* **2006**, *45*, 1116.

(68) Sun, Y.; Martell, A. E. *Tetrahedron* **1990**, *46*, 2725.

(69) Dupraz, A.; Guy, P.; Dupuy, C. *Tetrahedron Letters* **1996**, *37*, 1237.

(70) Weizman, H.; Ardon, O.; Mester, B.; Libman, J.; Dwir, O.; Hadar, Y.; Chen, Y.; Shanzer, A. *Journal of the American Chemical Society* **1996**, *118*, 12368.

(71) Morley, J. S.; Simpson, J. C. E. *Journal of the Chemical Society (Resumed)* **1952**, 2617.

(72) Zu, Y.-g.; Li, Q.-y.; Fu, Y.-j.; Wang, W. *Bioorganic & Medicinal Chemistry Letters* **2004**, *14*, 4023.

(73) Peiffer, G.; Chhan, S.; Bendayan, A.; Waegell, B.; Zahra, J.-P. *Journal of Molecular Catalysis* **1990**, *59*, 1.

(74) Fritz, S.; Hans, H.; Google Patents: 1936.

(75) Kolb, H. C.; Finn, M. G.; Sharpless, K. B. *Angewandte Chemie International Edition* **2001**, *40*, 2004.

(76) Heinrich, J.; Google Patents: 1937.

(77) Wexselblatt, E.; Esko, J. D.; Tor, Y. *The Journal of Organic Chemistry* **2014**, *79*, 6766.

(78) Pantos, A.; Tsogas, I.; Paleos, C. M. *Biochimica et Biophysica Acta (BBA) - Biomembranes* **2008**, *1778*, 811.

(79) Berg, S. S.; Parnell, E. W. *Journal of the Chemical Society (Resumed)* **1961**, 5275.

(80) Davoll, J.; Johnson, A. M.; Davies, H. J.; Bird, O. D.; Clarke, J.; Elslager, E. F. *J Med Chem* **1972**, *15*, 812.

(81) Hagan, R. L.; Hynes, J. B.; Pimsler, M.; Kisliuk, R. L. *Biochem Pharmacol* **1995**, *50*, 803.

(82) Smith, S. A.; Choi, S. H.; Collins, J. N. R.; Travers, R. J.; Cooley, B. C.; Morrissey, J. H. *Inhibition of polyphosphate as a novel strategy for preventing thrombosis and inflammation*, 2012; Vol. 120.

(83) Angelova, P. R.; Agrawalla, B. K.; Elustondo, P. A.; Gordon, J.; Shiba, T.; Abramov, A. Y.; Chang, Y.-T.; Pavlov, E. V. *ACS Chemical Biology* **2014**, *9*, 2101.

(84) Kulakova, A. N.; Hobbs, D.; Smithen, M.; Pavlov, E.; Gilbert, J. A.; Quinn, J. P.; McGrath, J. W. *Environmental Science & Technology* **2011**, *45*, 7799.

(85) Lodi, T.; Marchelli, R.; Dossena, A.; Dradi, E.; Casnati, G. *Tetrahedron* **1982**, *38*, 2055.